Syntheses and Bioactivities of Targeted and Conformationally Restrained Paclitaxel and Discodermolide Analogs

Chao Yang

Dissertation submitted to the faculty of the
Virginia Polytechnic Institute and State University
In the partial fulfillment of the requirement for the degree of

Doctor of Philosophy
In
Chemistry

Dr. David G. I. Kingston, Chairman
Dr. Karen Brewer
Dr. Paul R. Carlier
Dr. Felicia. Etzkorn
Dr. Harry W. Gibson

August 26 2008
Blacksburg, Virginia

Keywords: Taxol, drug targeting, , thio-taxol, tubulin-binding conformation, , T-taxol conformation, macrocyclic taxoids, discodermolide

Syntheses and Bioactivities of Targeted and Conformationally Restrained Paclitaxel and Discodermolide Analogs

Chao Yang

Abstract

Paclitaxel was isolated from the bark of *Taxus brevifolia* in the late 1960s. It exerts its biological effect by promoting tubulin polymerization and stabilizing the resulting microtubules. Paclitaxel has become one of the most important current drugs for the treatment of breast and ovarian cancers.

Studies aimed at understanding the biologically active conformation of paclitaxel bound on β–tubulin are described. In this work, the synthesis of isotopically labeled taxol analogs is described and the REDOR studies of this compound complexed to tubulin agrees with the hypothesis that palictaxel adopts T-taxol conformation. Based on T-taxol conformation, macrocyclic analogs of taxol have been prepared and their biological activities were evaluated. The results show a direct evidence to support T-taxol conformation.

(+) Discodermolide is a polyketide isolated from the Caribbean deep sea sponge *Discodermia dissoluta* in 1990. Similar to paclitaxel, discodermolide interacts with tubulin and stabilizes the microtubule *in vivo*. Studies aimed at understanding the biologically active conformation of discodermolide bound on β–tubulin are described. In this work, the synthesis of fluorescent labeled discodermolide analogs is described and their biological activities were evaluated. Synthetic approaches to fluorescent labeled and isotopically labeled discodermolide analogs discodermolide are also described.

Table of Contents

1. Introduction……..……..... 1

1.1 Cancer Overview…….…… 1

1.2 The mechanism of action of PTX….……4

1.3 Discodermolide…… 7

1.4 Overview of dissertation…….. 7

1.5 References…….. 8

2. Syntheses of thio-containing paclitaxel analogs for drug targeting through colloidal gold…… 13

2.1 Introduction…….……. 13

2.2 Structure-activity relationships……. 15

2.3 Syntheses of thio-containing taxol analogs……. 17

2.4 Biotinylated analogues of PTX……. 22

2.5 Experimental section ……. 23

2.6 References ……. 28

3. Synthesis of isotopically labeled paclitaxel analogs for REDOR (Rotational–Echo Double Resonance) NMR…… 37

3.1 Introduction…… 37

3.1.1 Structure of paclitaxel on the tubulin polymer…… 37

3.1.2 REDOR NMR and its application for the determination of paclitaxel structure…41

3.2 Synthetic chemistry…… 45

3.3 Biological evaluation and REDOR determined separation…….. 51

3.4 Conclusion……..…….. 52

3.5 Experimental section ……. 53

3.6 References…….. 71

4. Conformationally constrained paclitaxel analogs…… 77

4.1 Introduction…… 77

4.2 Synthesis of macrocyclic bridged PTX derivatives…… 82

4.3 Biological Activity…….. 90

4.4 Conclusion …….. 91

4.5 Experimental section ……..91

4.6 References…….118

5. Introduction to discodermolide……121

5.1 Isolation and structure of discodermolide……..121

5.2 Bioactivity of discodermolide……..… ..122

5.3 Structure-activity Relationships (SAR)…… …… 124

5.4 Synthesis of discodermolide……. 127

5.4.1 Schreiber Synthesis of Discodermolide……...128

5.4.2 Smith Synthesis of Discodermolide…….133

5.4.3 Myles Synthesis of Discodermolide…….139

5.4.4 Marshall Synthesis of Discodermolide…. ……...143

5.4.5 Paterson Synthesis of Discodermolide…….128

5.4.6 Summary……...152

5.5 References……...153

6. Synthesis of fluorescently labeled discodermolide analogs…….159

6.1 Introduction…….....159

6.2 Design and synthesis of simplified fluorescently labeled discodermolide analogs……160

6.3 Biological evaluation of simplified discodermolide analogs……..166

6.4 Design and synthesis towards fluorescent labeled discodermolide analogs……167

6.5 Experimental section ……..174

6.6 References……..179

7. Approaches to the synthesis of isotopically labeled discodermolide analogs for REDOR NMR and bridged discodermolide analogs for bioevaluation……..…… 183

7.1 Design of isotopically labeled discodermolide analogs…… 183

7.2 Summary of the synthesis of isotopically labeled discodermolide derivatives……..189

7.3 Design of bridged discodermolide analogs…….189

7.4 Summary of progress on the synthesis of bridged discodermolide derivatives……..193

7.5 Experimental section ……..…….193

7.6 References……..197

List of Figures

Figure 1.1 Structure of anticancer drugs …….. 3
Figure 1.2 Mechanism of paclitaxel……. 5
Figure 1.3 Structure of discodermolide …….…. 7
Figure 2.1 Disulfide prodrugs of paclitaxel ……. 14
Figure 2.2 SAR of paclitaxel …… 16
Figure 2.3 C2'-SH and C7-SH paclitaxel derivatives……. 17
Figure 3.1 Structure of 3.1 and 3.2 …… 43
Figure 3.2 Structures of isotopically labeled paclitaxel analogs……... 45
Figure 3.3 Structures of isotopically labeled paclitaxel analogs……... 52
Figure 4.1 Structure of bridged PTX analogs ……... 78
Figure 4.2 Structure of bridged PTX analogs based on REDOR-Taxol conformer…….78
Figure 4.3 Structure of bridged PTX analogs based on T-Taxol conformer…… 79
Figure 4.4 Structure of tether linker PTX analogs based on T-Taxol conformer…… 80
Figure 4.5 Structure of tether linker PTX analogs based on T-Taxol conformer…….81
Figure 4.6 Structure of macrocyclic PTX analogs based on T-Taxol conformer…… 81
Figure 5.1 Structure of discodermolide …… ….121
Figure 7.1 Isotopically labeled discodermolide analogs ……....183
Figure 7.2 Bridged discodermolide analogs ……...190
Figure 7.3 Structure of discodermolide ……..190
Figure 7.4 Structure of 7.32 ……190
Figure 7.5 Structure of 7.33 ……190

List of Tables

Table 3.1 Interatomic distances from REDOR NMR experiments and PTX modeling…… 44

Table 3.2 Biological evaluation of REDOR PTX analogs……..…. 51

Table 3.3 Interatomic distances for different PTX conformations and experimental distances determined by REDOR-NMR for PTX on tubulin for compound 3.4…….52

Table 3.3 Summary of interatomic distances for different PTX conformations and experimental distances determined by REDOR-NMR for PTX on tubulin ……. 52

Table 4.1 Cytotoxicity and tubulin polymerization activity of macrocyclic paclitaxel analogues …….. 90

Table 4.2 Bioactivity of bridged taxoids against paclitaxel and epothilone A resistant cell lines ……... 90

Table 6.1 Antiproliferative and tubulin-assembly activities of compounds **6.21a** and **6.21b**. …….166

List of Abbreviations

CAN	=	Ceric ammonium nitrate
10-DAB	=	10-Deacetylbaccatin III
DCC	=	Dicyclohexyl Carbodiimide
EDC	=	1-[3-(Dimethylammino)propyl]-3-ethylcarbodiimide hydrochloride
DMF	=	*N, N'*-Dimethylformamide
PMP	=	*para*-Methoxylphenyl
LHMDS	=	Lithium hexamethyldisilazide
RCM	=	Ring-closing metathesis
TIPS	=	Triisopropyl
TBS	=	*tert*-Butyldimethylsilyl
TES	=	Triethylsilyl
DMS	=	Dimethylsilyl
Bn	=	Benzyl
Bz	=	Benzoyl
DMAP	=	4-Dimethylamminopyridine
THF	=	Tetrahydrofuran
MAP	=	Microtubule associated protein
SAR	=	Structure activity relationships
PTLC	=	Preparative thin layer chromatography
TLC	=	Thin layer chromatography
LAH	=	Lithium aluminum hydride
cAu	=	Colloidal gold nanoparticles

Chapter 1 Introduction

1.1 Cancer Overview

Cancer is a term that applies to many diseases characterized by uncontrolled growth and the spread of abnormal cells. If the spread is not controlled, it can lead to death. All cancers are characterized by the malfunction of genes that control cell growth and division. However, most cancers (over 90%) are not caused by inherited genes, but result from mutations to normal genes caused by environmental or other factors.[1] Cancer can occur in anyone, and the risk increases with age; about 76% of cancer cases occur in adults 55 and older.[1] It was estimated that 1.4 million new cancer cases were detected in 2006 in the US, and over half a million Americans were expected to die from cancer in the same year.[1] Cancer accounts for one of every four deaths in the US, and is the second most common cause of death in the US after heart disease.[1] The National Cancer Institute estimates overall costs for cancer at $209.9 billion in 2005.[1] Among all cancers, breast cancer is the leading cancer diagnosed in woman, and the second leading cause of cancer death in women. Over 200,000 new cases of invasive women breast cancer (31%) are expected to occur in the US during 2006 and 40,000 deaths (15%) are expected.[1] Prostate cancer is the leading cause of cancer diagnosed in men in the US during 2006, with an estimated 234,460 new cases diagnosed and 27,350 deaths expected.[1]

It is known that exposure to external factors, such as tobacco, chemicals, radiation, and infectious organisms, might cause mutations of genes ten or more years later.[1] Cancer might also be caused by internal factors such as inherited mutations, hormones, immune conditions, and metabolic mutations. Both external and internal factors might act together or in sequence to initiate or promote cancer.

The associations between modifiable lifestyle factors or environmental exposure and specific cancers gives promise for cancer prevention.[2] It has been estimated that at least half of all cancer deaths could be prevented. For example, a high portion of diagnosed cancers are related to tobacco use, physical inactivity, obesity, and poor nutrition, all of which can be prevented. Greater use of established screening tests could prevent many cancer deaths. Additional examples of modifiable cancer risk factors include alcohol consumption and infections.

In general, the treatment of cancer can involve surgery, radiation, chemotherapy, hormone therapy, gene therapy and biological therapy. Chemotherapy is a type of cancer treatment that uses drugs to stop or slow the growth of cancer cells. It can be used alone or along with surgery, radiation or biological therapy. But it can also cause side effects by damaging healthy cells that divide quickly. These side effects often get better or go away after chemotherapy ends.[3]

Cytotoxic agents, such as cisplatin, doxorubicin, methotrexate, and paclitaxel (Figure 1.1) are widely used as anticancer drugs. Among these elite drugs, paclitaxel (PTX) is the most successful in the market because of its excellent clinical activities against breast cancer.[4]

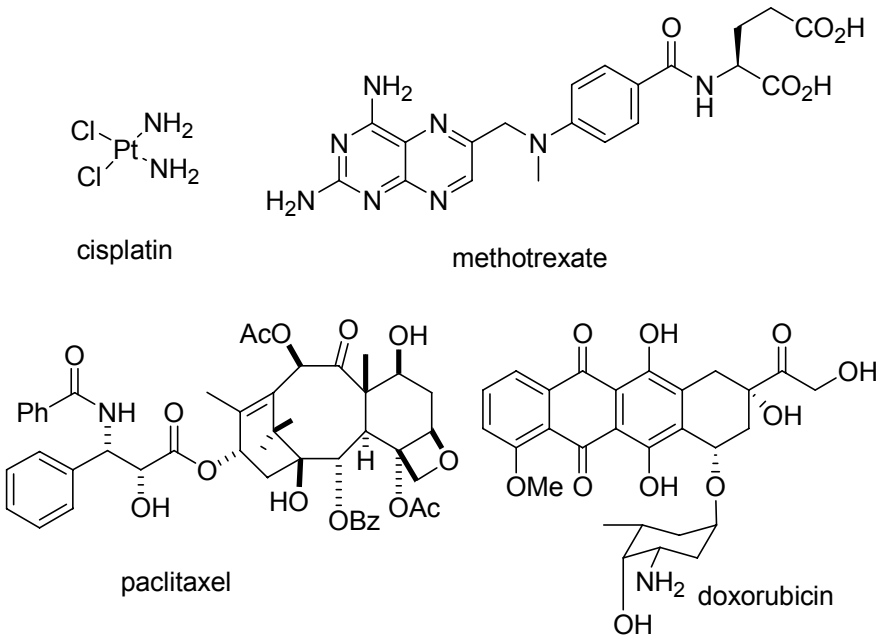

Figure 1.1 anticancer drugs

PTX belongs to the family of taxane diterpenoids, which has over 300 identified members.[5] The bioactivities of PTX were first noticed in 1962 when extracts of the stem and bark of *Taxus brevifolia* Nutt. showed cytotoxic activity to KB cells.[6] Although PTX was isolated in 1967, the structure was not published until 1971.[6] The initial studies indicated that PTX showed modest activities both in cell culture and also *in vivo* against various leukemias and the Walker 256 carcinosarcoma. Since it was highly insoluble in water, the formulation problem was clearly a big issue, and it presented a big supply problem due to a low isolated yield (0.02% w/w) from the bark of a rare and slow-growing tree.[7] Fortunately the turning point came in the early 1970's when the National Cancer Institute (NCI) introduced some new *in vivo* bioassays, and PTX proved to be strongly active against a B16 melanoma.[8] Moreover, the solubility problem was successfully solved by a formulation in ethanol and Cremophor EL, a polyethoxylated caster oil.

In 1979, it was reported[9] that PTX had a completely new mechanism of action, in which it intervenes in the equilibrium between tubulin and microtubules during cell division[10] by promoting the assembly of α- and β-tubulin into microtubules. The mechanism will be explained in detail below.

PTX went into Phase I clinical trials in 1983, and into Phase II trials in 1985, in which it proved to be clinically active against ovarian cancer[11] and breast cancer.[12] The Food and Drug Administration (FDA) approved PTX for the treatment of ovarian cancer in 1992 and for breast cancer in 1994.[13] Currently PTX and its semi-synthetic analog docetaxel are now used (either as single agents or in combination with other drugs such as cisplatin) as anticancer drugs in the treatment of a variety of solid tumours,[13] but their poor water solubility and side effects limit their clinical usefulness. Those side effects include hair loss, decrease in white blood cells (which may cause susceptibility to infections), nausea, vomiting, diarrhea, an acute pulmonary reaction, and numbness of the fingers and toes.[14-16] The solubility problem was solved by intravenous administration of paclitaxel with a non-aqueous carrier containing Cremophor EL, which causes allergic reactions in some cases.[16] This problem was circumvented by lengthening the time of administration and by premedication.

1.2 The mechanism of action of PTX

Paclitaxel promotes the polymerization of tubulin into microtubules and stabilizes them, leading to cell death by apoptosis (Figure 1.2). In the cell cycle the mitotic spindle, composed of microtubules and some proteins, must be created for the chromosomes to separate, and after that it must be destroyed. Therefore, many anticancer

chemotherapeutic drugs are designed to interfere with this subcellular target.[17] This discovery spurred great interest among researchers, and spurred efforts to overcome the problems associated with paclitaxel.

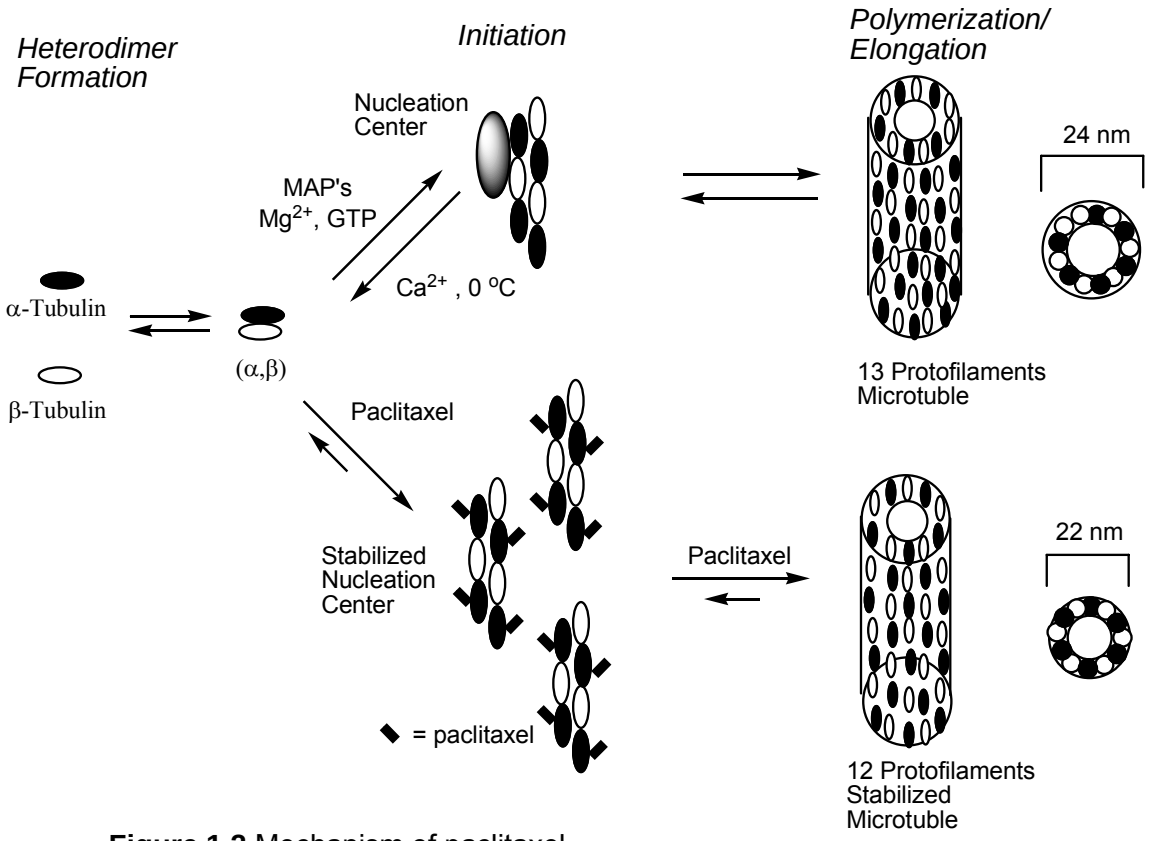

Figure 1.2 Mechanism of paclitaxel

Microtubules are long, hollow cylinders with an outer diameter of 25 nm, and an inner diameter of about 15 nm, formed by polymerization of α- and β-tubulin dimers.[10] α-Tubulin and β-tubulin are structurally similar but distinct proteins with molecular weight about 50,000, and there is about 35-40% homology between them.[18] In the presence of guanosine 5'-triphosphate (GTP) and magnesium ions, α-tubulin and β-tubulin form a dimer with a dissociation constant of about 10^{-6} mol/L.[18] Each α-tubulin and β-tubulin molecule associates with one GTP molecule.[10] The dimers then start to

form a nucleation center for further polymerization to form protofilaments.[10] Continuous growth occurs both along and perpendicular to the axis of the initial protofilaments in a slightly staggered manner, and the edge filaments meet together to form a microtubule with a left-handed helix.[18] A normal microtubule is formed by 13 protofilaments.[19] In a cell, the formation and decomposition of microtubules are at equilibrium, with constant loss and gain of tubulin subunits at both ends. The formation and decomposition of microtubules are totally reversible processes during a normal cell cycle.[20,21] Microtubule-targeted chemotherapeutic anticancer drugs act by interfering with the exchange of tubulin subunits between the microtubules and the free tubulin in the mitotic spindle. There are two types of drugs defined by this mechanism.[22,23] One class of cytotoxic agent, which includes colchicine, vinblastine and vincristine, prevents the polymerization of microtubules.[10] These compounds bind to tubulin and prevent microtubule polymerization, resulting in the rapid disappearance of the mitotic spindle and leading many abnormally dividing cells to die.[24] In contrast, members of the other class of cytotoxic agents, including paclitaxel, epothilone, and discodermolide, promote the polymerization of microtubules.[25] Microtubule polymerization-promoting agents shift the tubulin-microtubule equilibrium towards the formation of microtubules by decreasing both the critical concentration of tubulin for polymerization and the induction time for polymerization.

In the presence of paclitaxel, the microtubules formed are quite different from those formed under normal conditions. Compared with normal microtubules, they are thinner with a mean diameter of 22 nm rather than 24 nm, and they are composed of 12

protofilaments, instead of 13.[26] The binding site of paclitaxel is found to be on the β-tubulin subunit.[10,27]

1.3 Discodermolide

Discodermolide is a natural product isolated from marine sponge (Figure 1.3).[28] It is more potent than PTX in most cell lines, including PTX-resistant cell lines.[29,30] Similar in mechanism of action to PTX, discodermolide stabilizes the microtubules more potently than PTX.[31] Intriguingly, unlike other tubulin-promoting agents, discodermolide demonstrates synergistic effects in enhancement of cell death and induction of mitotic arrest in combination with PTX.[32] The encouraging biological profile of discodermolide makes it a promising microtubule targeting agent for the treatment of cancer. The bioactivity, structure-activity relationships and synthesis will be addressed in detail in Chapter 5.

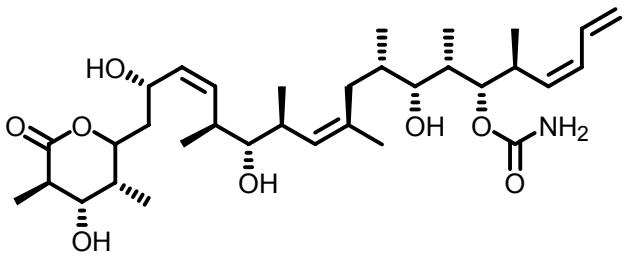

Figure 1.3 Structure of discodermolide

1.4 Overview of dissertation

This dissertation consists of two major parts, linked by the common theme of the study of tubulin polymerizing agents. The first part is about paclitaxel derivatives,

including a new approach to targeting paclitaxel using gold nanoparticles (Chapter 2), an approach to understanding how paclitaxel binds to microtubules (Chapter 3), and by the synthesis of conformationally restricted analogs (Chapter 4). The second part consists of an introduction to discodermolide (Chapter 5), and approaches to studies of how discodermolide binds to microtubules, including the synthesis of fluorescent discodermolide derivatives (Chapter 6) and synthetic approaches to bridged discodermolide derivatives (Chapter 7).

References:

1. American Cancer Society. *Cancer Facts and Figures* **2006**. http://www.cancer.org/docroot/STT/content/STT_1x_Cancer_Facts__Figures_2007.asp accessed on 01/03/2008.
2. American Cancer Society. *Cancer Prevention and Early Detection Facts & Figures* **2007**. http://www.cancer.org/docroot/STT/content/STT_1x_Cancer_Prevention_and_Early_Detection_Facts_and_Figures_2005.asp accessed on 01/03/2008.
3. Mastalerz, H.; Zhang, G.; Kadow, J.; Fairchild, C.; Long, B.; Vyas, D. M. Synthesis of 7β-sulfur analogues of paclitaxel utilizing a novel epimerization of the 7α-thiol group. *Org. Lett.* **2001,** *3*, 1613-1615.
4. Metaferia, B. B.; Hoch, J.; Glass, T. E.; Bane, S. L.; Chatterjee, S. K.; Snyder, J. P.; Lakdawala, A.; Cornett, B.; Kingston, D. G. I. Synthesis and biological evaluation of novel macrocyclic paclitaxel analogues. *Org. Lett.* **2001,** *3*, 2461-2464.

5. Li, Y.; Poliks, B.; Cegelski, L.; Poliks, M.; Gryczynski, Z.; Piszczek, G.; Jagtap, P. G.; Studelska, D. R.; Kingston, D. G. I.; Schaefer, J.; Bane, S. Conformation of microtubule-bound paclitaxel determined by fluorescence spectroscopy and REDOR NMR. *Biochemistry* **2000,** *39*, 281-291.

6. Wani, M. C.; Taylor, H. L.; Wall, M. E.; Coggon, P.; McPhail, A. T. Plant antitumor agents VI. The isolation and structure of taxol, a novel antileukemic and antitumor agent from *Taxus brevifolia*. *J. Am. Chem. Soc.* **1971,** *93*, 2325-2327.

7. Baloglu, E.; Miller, M. L.; Cavanagh, E. E.; Marien, T. P.; Roller, E. E.; Chari, R. V. J. A facile one-pot synthesis of 7-triethylsilylbaccatin III. *Synlett* **2005,** *5*, 817-818.

8. Fuchs, D. A.; Johnson, R. K. Cytologic evidence that taxol, an antineoplastic agent from *Taxus brevifolia*, acts as a mitotic spindle poison. *Cancer Treat. Rep.* **1978,** *62*, 1219-1222.

9. Shiff, P. B.; Fant, J.; Horwitz, S. B. Promotion of microtubule assembly in vitro by taxol. *Nature* **1979,** *277*, 665-667.

10. Wilson, L.; Jordan, M. A. Microtubule dynamics: Taking aim at a moving target. *Chem. Biol.* **1995,** *2*, 569-573.

11. McGuire, W. P.; Rowinsky, E. K.; Rosenshein, N. B.; Grumbine, F. C.; Ettinger, D. S.; Armstrong, D. K.; Donehower, R. C. Taxol: A unique antineoplastic agent with significant activity in advanced ovarian epithelial neoplasms. *Ann. Intern. Med.* **1989,** *111*, 273-279.

12. Holmes, F. A.; Walters, R. S.; Theriault, R. L.; Forman, A. D.; Newton, L. K.; Raber, M. N.; Buzdar, A. U.; Frye, D. K.; Hortobagyi, G. N. Phase II trial of taxol, an active drug in the treatment of metastatic breast cancer. *J. Natl. Cancer Inst.* **1991,** *83*, 1797-1805.

13. Rowinsky, E. K.; Donehower, R. C. Paclitaxel (taxol). *N. Engl. J. Med.* **1995,** *332*, 1004.

14. Grem, J. L.; Tutsch, K. D.; Simon, K. J.; Alberti, D. B.; Willson, J. K.; Tormey, D. C.; Swaminathan, S.; Trump, D. L. Phase I study of taxol administered as a short infusion daily for 5 days. *Cancer Treat. Rep.* **1987,** *71*, 1179-1184.

15. Donehower, R. C.; Rowinsky, E. K.; Grochow, L. B.; Longnecker, S. M.; Ettinger, D. S. Phase I trial of taxol in patients with advanced cancer. *Cancer Treat. Rep.* **1987,** *71*, 1171-1177.

16. Rowinsky, E. K.; Burke, P. J.; Karp, J. E.; Tucker, R. W.; Ettinger, D. S.; Donehower, R. C. Phase I and pharmacodynamic study of taxol in refractory acute leukemias. *Cancer Res.* **1989,** *49*, 4640-4647.

17. Geney, R.; Sun, L.; Pera, P.; Bernacki, R. J.; Xia, S.; Horwitz, S. B.; Simmerling, C. L.; Ojima, I. Use of the tubulin bound paclitaxel conformation for structure-based rational drug design. *Chem. Biol.* **2005,** *12*, 339-348.

18. Purich, D. L.; Kristofferson, D. Microtubule assembly: A review of progress, principles, and perspectives. *Adv. Protein Chem.* **1984,** *36*, 132-133.

19. Olmsted, J. B. Non-motor microtubule-associated proteins. *Curr. Opin. Cell Biol.* **1991,** *3*, 52-58.

20. Andreu, J. M.; Bordas, J.; Diaz, J. F.; de Ancos, J. G.; Gil, R.; Medrano, F. J.; Nogales, E.; Pantos, E.; Towns-Andrews, E. Low resolution structure of microtubules in solution : Synchrotron x-ray scattering and electron microscopy of taxol-induced microtubules assembled from purified tubulin in comparison with glycerol and map-induced microtubules. *J. Mol. Biol.* **1992,** *226*, 169-184.

21. Haimo, L. T. l. Dynein decoration of microtubules - determination of polarity. *Methods Cell Bio.* **1982,** *24*, 189-206.

22. DeBrabander, M. Microtubule dynamics during the cell cycle: The effects of taxol and nocodazole on the microtubule system of Pt K2 cells at different stages of the mitotic cycle. *Int. Rev. Cytol.* **1986,** *101*, 215-274.

23. Inouse, S. Cell division and the mitotic spindle. *J. Cell. Biol.* **1981,** *91*, 131-147.

24. Salmon, E. D.; McKeel, M.; Hays, T. Rapid rate of tubulin dissociation from microtubules in the mitotic spindle in vivo measured by blocking polymerization with colchicine. *J. Cell. Biol.* **1984,** *99*, 1066-1075.

25. Rao, S.; Horwitz, S. B.; Ringel, I. Direct photoaffinity labeling of tubulin with taxol. *J. Natl. Cancer Inst.* **1992,** *84*, 785-788.

26. Diaz, J. F.; Valupesta, J. M.; Chacon, P.; Diakun, G.; Andreu, J. M.; *J. Biol. Chem.* **1998**, *273*, 33803

27. Schibler, M. J.; Huang, B. The *col*^{R}*4* and *col*^{R}*15* β-tubulin mutations in *Chlamydomonas reinhardtii* confer altered sensitivities to microtubule inhibitors and herbicides by enhancing microtubule stability. *J. Cell Biol.* **1991,** *113*, 605-614.

28. Gunasekera, S. P.; Gunasekera, M.; Longley, R. E. Discodermolide: A new bioactive polyhydroxylated lactone from the marine sponge *Discodermia dissoluta*. *J. Org. Chem.* **1990,** *55*, 4912-4915

29. Hung, D. T.; Nerenberg, J. B.; Schreiber, S. L. Distinct binding and cellular properties of synthetic (+)- and (-)-discodermolides. *Chem. Biol.* **1994,** *1*, 67-71.

30. ter Haar, E.; Kowalski, R. J.; Hamel, E.; Lin, C. M.; Longley, R. E.; Gunasekera, S. P.; Rosenkranz, H. S.; Day, B. W. Discodermolide, a cytotoxic marine agent that stabilizes microtubules more potently than taxol. *Biochemistry* **1996,** *35*, 243.

31. Kowalski, R. J.; Giannakakou, P.; Gunasekera, S. P.; Longley, R. E.; Day, B. W.; Hamel, E. The microtubule-stabilizing agent discodermolide competitively inhibits the binding of paclitaxel (taxol) to tubulin polymers, enhances tubulin nucleation reactions more potently than paclitaxel, and inhibits the growth of paclitaxel-resistant cells. *Mol. Pharmacol.* **1997,** *52*, 613-622.

32. Martello, L. A.; McDaid, H. M.; Regl, D. L.; Yang, C. P. H.; Meng, D.; Pettus, T. R. R.; Kaufman, M. D.; Arimoto, H.; Danishefsky, S. J.; Smith, A. B. I.; Horwitz, S. B. Taxol and discodermolide represent a synergistic drug combination in human carcinoma cell lines. *Clin. Canc. Res.* **2000,** *6*, 1978-1987.

Chapter 2. Syntheses of thio-containing paclitaxel analogs for drug targeting through colloidal gold

2.1 Introduction

The field of drug delivery is advancing rapidly. By controlling the precise level and/or location of a drug in the body, side effects are reduced, lower doses can often be used, and new therapies are possible.[1] Due to abnormal vasculature, solid tumors often have demonstrated regions of hypoxia, which leads to a deficiency of oxygen and nutrients.[2] Hypoxia is present in many cancers including cervical cancer, squamous cell carcinoma of the head and neck, and breast and prostate cancer.[2] Targeting hypoxia would be an effective means of cancer therapeutics.[2] Bioreductive drugs are compounds that elicit their cytotoxicity through reductive activation by biological enzymes, which occur only or preferentially in the absence of oxygen. These drugs have the potential to improve the outcome of therapy due to the nature of hypoxia. Mitomycin,[3] tirapazamine[4] and AQ4N[5] are such drugs in clinical use or in clinical trials.

Due to its low water solubility, paclitaxel (PTX) is administered in Cremophor EL®, which might cause allergic reactions to some patients. Many efforts have addressed the preparation of water soluble prodrugs of paclitaxel.[6-8] Colloidal gold nanoparticals (cAu) have been developed as a vector for tumor targeted drug delivery in which Tumor Necrosis Factor (TNF) was delivered to solid tumors.[9,10] Thus, TNF acts a tumor targeting ligand as well as a therapeutic agent. Hence, if paclitaxel can bind to cAu preinstalled with TNF, the PTX-gold conjugate would deliver the PTX to solid tumor cells. In order to form a PTX-gold conjugate, a functional group with a high affinity for

gold must be introduced to paclitaxel, as well a linker connecting PTX with the functional group. It has been well established that thiol groups have an excellent affinity towards gold, and this characteristic makes the thiol group a promising candidate for the anchor. A series of disulfide-containing PTX derivatives have been extensively inverstigated.[11,12] These studies demonstrated that a disulfide bond can be cleaved under reductive conditions and PTX released, and that the compounds are stable in human serum.

Furthermore, a series of unsymmetrical disulfide prodrugs of paclitaxel, as shown in Figure 2.1**,** have been developed by scientists at Bristol-Myers Squibb.[13] An activated 2-pyridyl disulfide displayed a promising anchoring property.[13] The most fascinating feature of these compounds is that PTX is released through a "self-immolating" mechanism. Disulfide linkers can be cleaved in the cell where glutathione and other thiols are present in relatively high concentration. The resulting sulfur anion can attack the ester carbonyl group at the C-2' position to form a cyclic 3,3-dimethyldihydrothiophen-2(3H)-one, which leads to the release of free PTX. The geminal dimethyl group on the α−carbon facilitates cyclization of the intermediate thiol in the linker, while offering stability toward serum esterases as well.

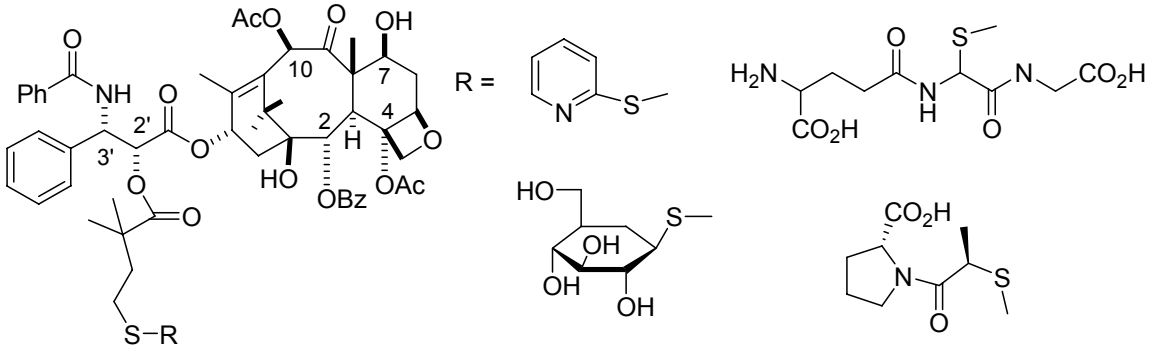

Figure 2.1 Disulfide prodrugs of paclitaxel[13]

As a starting approach, it was planned to esterify the C-7 and C-10 hydroxyl group with an ω–(2-pyridyldisulfide)carboxylic acid. Previous SAR studies had shown that modifications on these positions would have a relatively minor impact on the bioactivity of PTX. According to these studies, the most reactive hydroxyl group in PTX is the C2′-OH, followed by the C7- and C10-OH groups; the 1-OH group is inert to ester formation under normal conditions.[14] Direct acylation of PTX would generate only or preferentially C2′-acyl derivatives. In order to prepare C-7 and C-10 derivatives, the C2′-hydroxyl group must first be protected as its *tert*-butyldimethylsilyl ether. In general, modifications of the C2´-hydroxyl group of PTX lead to diminished cytotoxicity, unless the derivatizing groups can be cleaved by enzymatic or other mechanisms.[9] PTX-C2'-esters and carbonate-based PTX prodrugs have been reported to release PTX *in vivo* and *in vitro*.[13,15-17]

2.2 Structure-activity relationships

Structure-activity relationship (SAR) studies on drugs can provide useful information about interactions of drugs with their receptors, the role of certain functional groups and conformations in the action, and the essential structural requirements for the biological activity of drug.

The SAR of paclitaxel has been extensively investigated.[18] PTX can be divided into three main regions, the northern hemisphere, the southern hemisphere and the side chain (Figure 2.2). PTX can tolerate structural modification of the northern hemisphere. In contrast to the northern hemisphere, both the southern hemisphere and the side chain are essential for activity and are very sensitive to change.

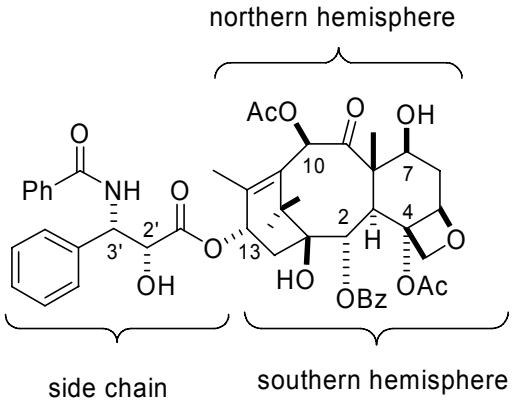

Figure 2.2 SAR of paclitaxel

Side chain. Insertion of a methylene group between the C1' and C2' positions lowers the activity dramatically.[19] The stereochemistry at C-2' and C-3' has a moderate effect on the activity.[20] A hydroxyl group or an easily cleaved 2'-hydroxyl ester is required at the C2' position.[20,21] A large group is required at the C3' position. Various PTX analogs with substituted phenyl groups at the C3' position demonstrated similar but slightly decreased activity.[22] Some large alkyl groups at the C3' position, such as isobutyl or isobutenyl groups proved to enhance activity.[23] However small alkyl groups such as a methyl group cause a significant loss in bioactivity.[20] The *N*-acyl group is required for activity, and structural modifications at this position can result a small increase in activity in some acyl analogs.[20,22]

The northern hemisphere. Hydroxylation of paclitaxel at the C6 position resulted in 30-fold decrease of bioactivity.[24] Modifications on the C7 position, such as acylation or dehydroxylation, usually have little effect on bioactivity.[23,25-27] However, oxidation of the C7-hydroxyl group to a ketone led to dramatic loss of bioactivity; because 7-oxotaxol is unstable and an oxetane-ring opening reaction was observed.[28] Conversion of the C9-keto group into a hydroxyl group proved to retain bioactivity.[29] Modifications on C10 had little effect on the bioactivity.[30] Modification of the double bond at the C11-C12 position

decreased the bioactivity slightly.[31] Modifications of PTX at C19 had a moderate effect on the bioactivity.[32]

The southern hemisphere. Small structural changes in the southern hemisphere can make large changes in the bioactivity of PTX. Deoxygenation at the C1 position led to a slight loss in activity.[33] The benzoyloxy group and the stereochemistry at the C2 position are required for full bioactivity.[34,35] But *meta*-substituted benzoyloxy analogs were more active than PTX itself.[36] The acetyl group at the C4 position is important for bioactivity,[19,37] and other C4 acylated analogs were generally less active than PTX.[38,39] However, it was reported that some groups such as a methyl carbonate at C4 enhanced the bioactivity.[40] The oxetane ring is an essential structure to maintain the bioactivity. PTX analogs with opened oxetane rings were dramatically less active in both cytotoxicity and microtubule assembly assays.[28,41] The stereochemistry at the C13 position is essential to the bioactivity.[42] Hydroxylation at the C14 position was found to have little effect on bioactivity.[43]

2.3 Syntheses of thio-containing taxol analogs

C2′-SH[44] and C7-SH[45] PTX derivatives, as shown in Figure 2.3, have been reported in the literature, but neither of them has the potential to be a candidate for linking to gold because the conjugate would release PTX derivatives, instead of PTX.

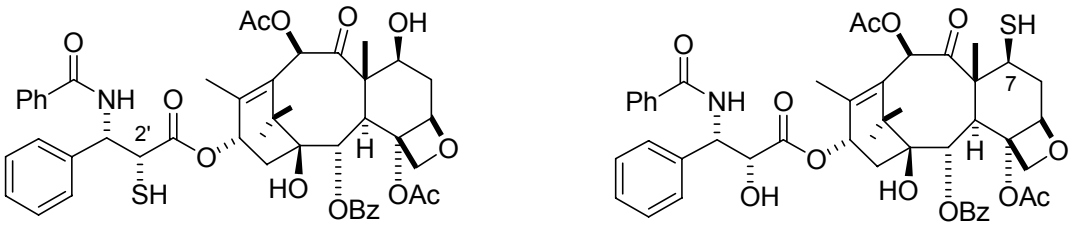

Figure 2.3 C2'-SH and C7-SH paclitaxel derivatives

A series of C7 and C10 PTX ester analogs with different chain lengths from the 7-O and 10-O position of PTX to the terminal SH group have been prepared and evaluated in our group.[46] It is well known that a thiol group can be endcapped with a 2-thiopyridyl group by reaction with dipyridyl disulfide. It seemed feasible to prepare a series of thiopyridyl PTX esters with terminal 2-thiopyridyl disulfide groups by simply coupling a PTX ester with 2-dipyridyl disulfide. The corresponding disulfide-PTX esters can bind to cAu nano particles, which could deliver the PTX into cells, thus enabling the release of PTX by endogenous esterase activity.[13]

The synthesis of thiol-containing PTX analogs is outlined in Scheme 2.1. The known 2′-TBS PTX was esterified at the C-7 position with iodoacetic acid, employing a carbodiimide-based coupling protocol to yield PTX analog **2.1**. Deprotection of the silyl group by 5% HCl, followed by an S_N2 substitution with NaSH in the presence of 15-crown-5, afforded the polar thiol **2.2**. Coupling **2.2** with 2,2′-dipyridyl disulfide under standard conditions failed to give the 2-thiopyridyl disulfide analog **2.3**.

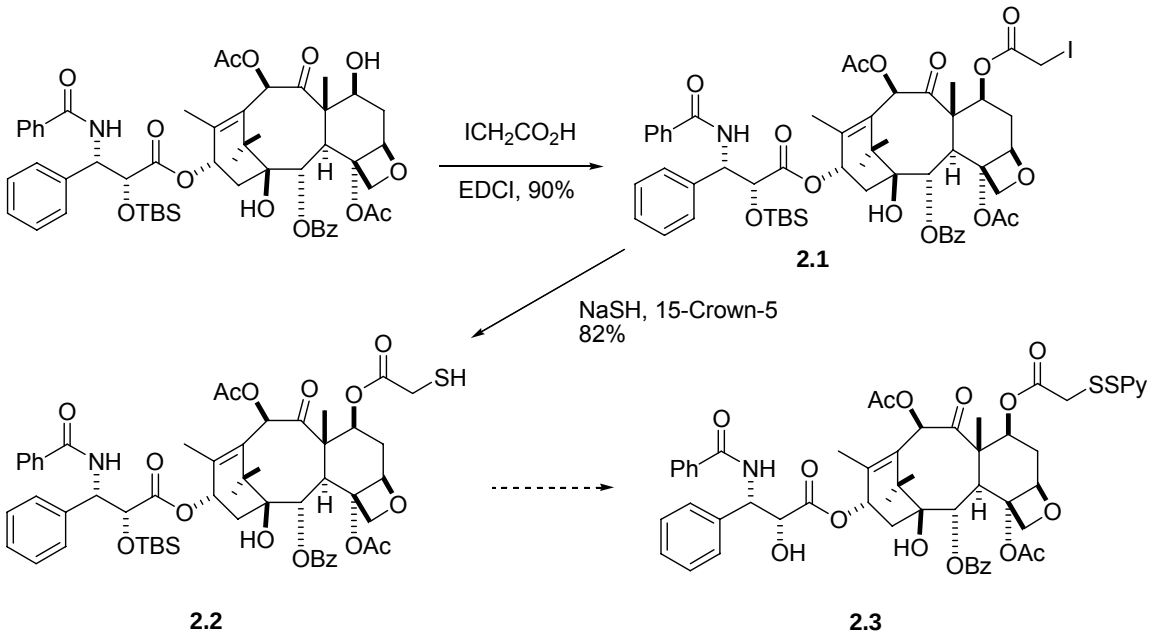

Scheme 2.1 Synthetic plan for disulfide PTX

The short distance between the bulky PTX moiety and the thiol group might be the main reason for the failure. If this is the case, the 2-thiopyridyl disulfide group should be installed on the terminal mercapto acid first, followed by the esterification of PTX. The synthesis of the disulfide linker is shown in Scheme 2.2. Commercially available 3-mercaptopropionic acid and 16-mercaptohexadecanoic acid were converted to the corresponding 2-thiolpyridyl disulfide acids **2.4** and **2.5**,[46] respectively. With the same procedure, 2-mercaptoethanol and 1-amino-2-ethanethiol were transformed with 2,2′-dithiodipyridine to the corresponding activated disulfide alcohol **2.6**[47] and amine **2.7**.[1]

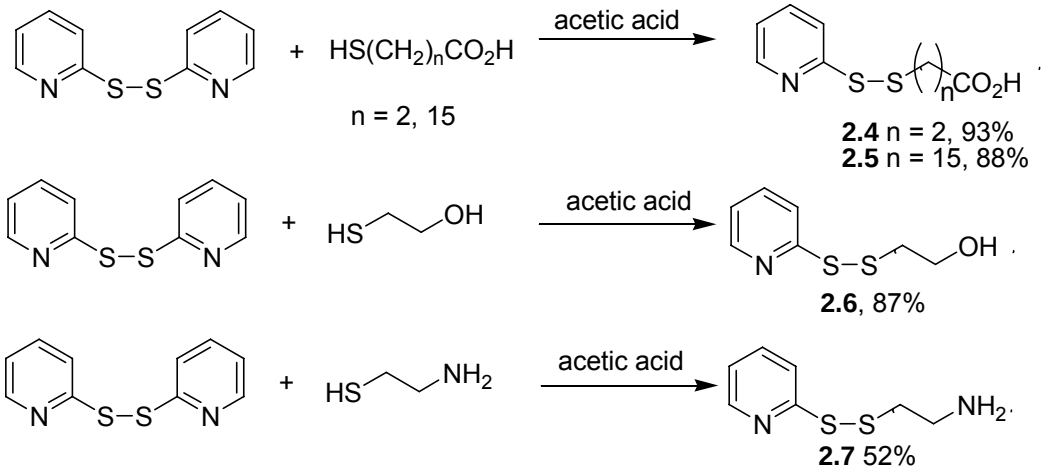

Scheme 2.2 Synthesis of 2-thiolpyridyl disulfide linkers

Coupling **2.4** and **2.5** with PTX at the C2′-position generated the corresponding C2′-PTX esters **2.8** and **2.9,** respectively (Scheme 2.3). Coupling PTX with succinic anhydride led to **2.10**, which was esterified with **2.6** in the present of EDC and DMAP to afford **2.11** as shown in Scheme 2.4.

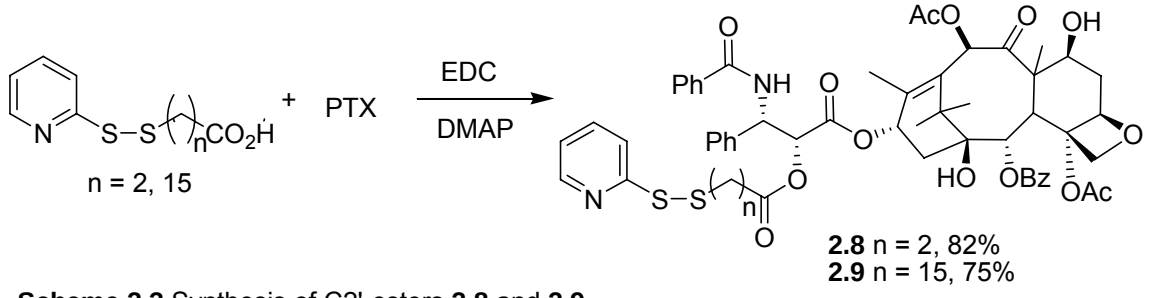

Scheme 2.3 Synthesis of C2'-esters **2.8** and **2.9**

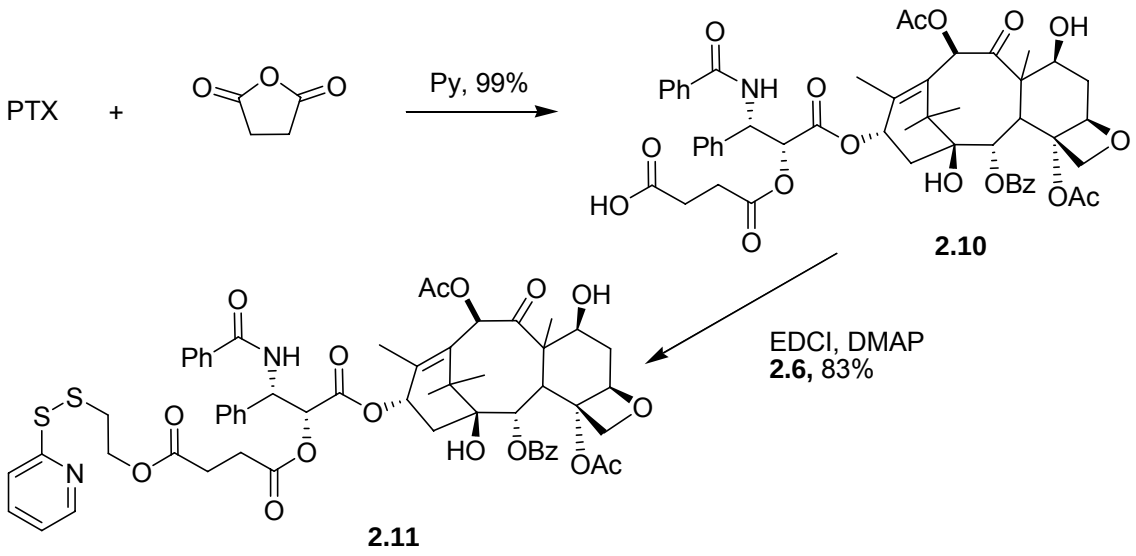

Scheme 2.4 Synthesis of C2'-PTX disulfide esters

It was also interesting to expand the scope of "self-immolating" linkers. Instead of a bulky α,α–dimethylcarbonyl group, we planned to use a carbamate group as a linker to PTX at the C7 and C10 positions.[12,17,48] Although the carbamate group is a relatively stable linkage, it was thought that it might be susceptible to immolation as shown in Scheme 2.5. The synthesis of the C2′-carbamate linked PTX conjugate was hampered because of the instability of the C2′-acyl bond,[49] but the C7- and C10- carbonates could be prepared as described below.

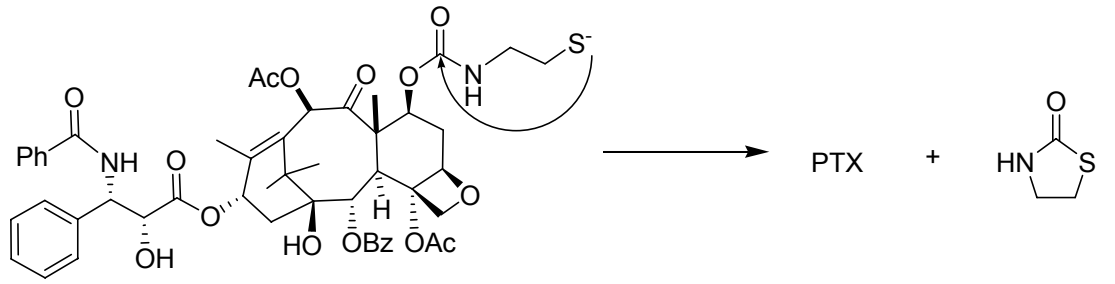

Scheme 2.5 Proposed mechanism of releasing PTX by a self-immolating carbamate linker

The known C2′-TBS C7-imidazolide PTX **2.12** and C2′-TBS C10-imidazolide PTX **2.13** were prepared as described in the literature.[17] Coupling the thiol amine **2.7** with **2.12** and **2.13**, followed by removal of TBS protecting group, afforded the corresponding C7 and C10 carbamate PTX conjugates **2.14** and **2.15**, respectively as shown in Scheme 2.6.

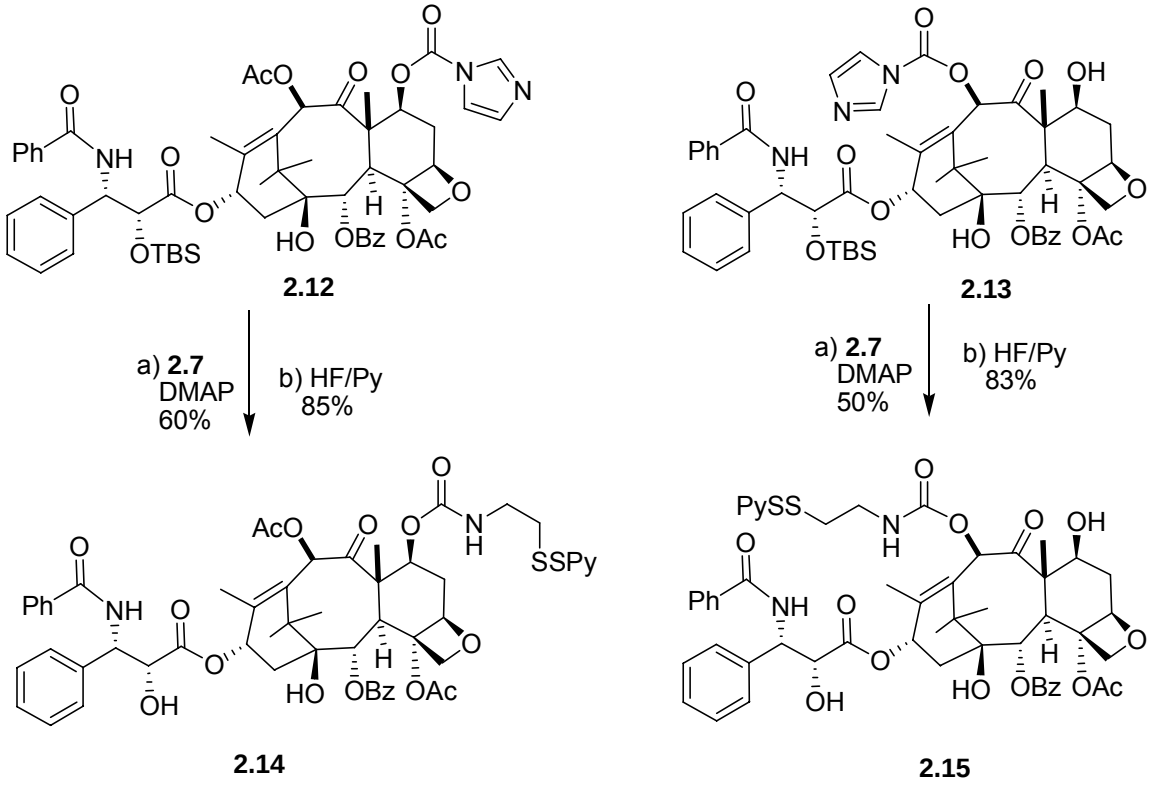

Scheme 2.6 Synthesis of self-immolating PTX analogs

Both compounds were tested for self-immolation. The disulfide bond was cleaved in the present of glutathione at rt, but no paclitaxel was released over an extended period of 1 day. Therefore, the carbamate linkage was dropped as a candidate for self-immolation.

2.4 Biotinylated analogues of PTX

It has been established that the biotin moiety has a strong noncovalent interaction with avidin or streptavidin.[45,50] Moreover, the affinity of biotin for avidin is related to the distance between the biotin moiety and the core of the molecule.[51] Biotin derivatives have been used in tumor targeting.[52] Interestingly, biotinylated docetaxel derivatives with a 6-aminocaproyl linker displayed significant loss of activity *in vivo* while maintaining activity *in vitro*.[53] Efforts on the synthesis of a shorter linker were fruitless because of the instability of docetaxel intermediates.[54] Nevertheless, a C7-biotinylated PTX analog with a 3-aminopropanoyl linker has been reported and showed improved cell permeability. We decided to synthesize the same compound for further investigation.

The synthesis of a C7-biotinylated PTX is shown in Scheme 2.7. The known C2′-TES-PTX was esterifed with N-(4-methoxytrityl)-β-alanine in the presence of EDCI and DMAP to afford C7-ester **2.16**. Detritylation and desilylation of **2.16** by acetic acid in THF/water mixture at 50 °C for 1.5 days generated the corresponding C7-(β-alanyl) PTX **2.17** in low yield. An alternative method of deprotection might be reduction.[55] Coupling of **2.17** with commercially available biotinyl-*N*-hydroxysuccinimide in the presence of *N*-ethylmorpholine completed the synthesis of the known target biotinylated paclitaxel derivative **2.18** in 62% yield. The ^{1}H NMR spectrum matched the literature value. [54]

The biotinylated paclitaxel derivative **2.18** was sent to CytoImmune Inc. for biological evaluation.

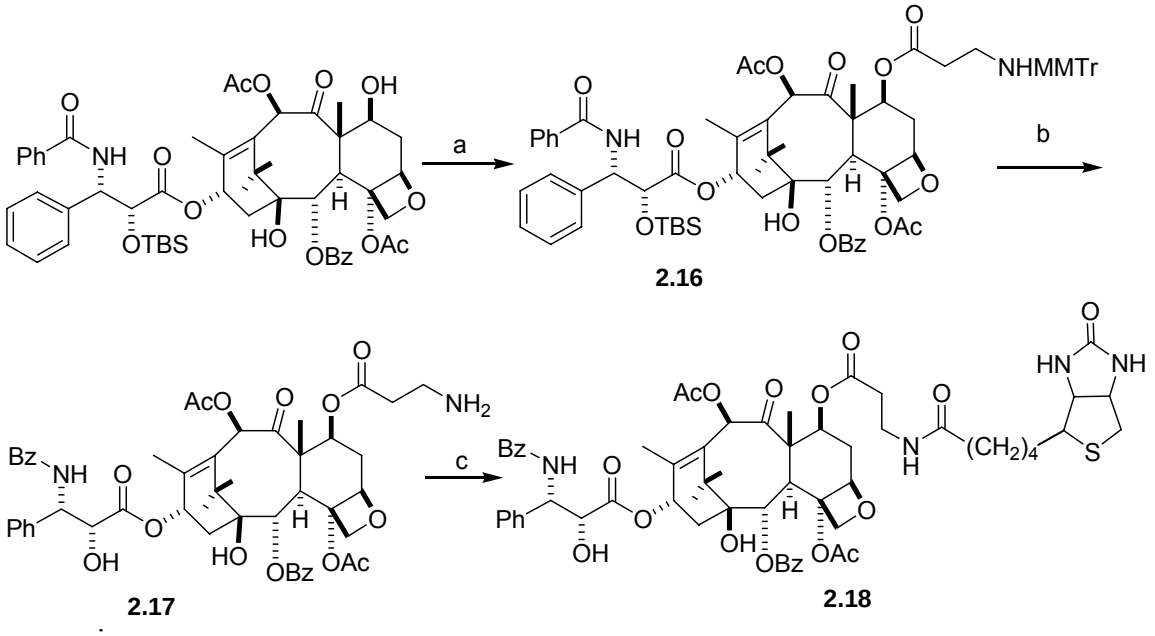

a) NHMMTr$(CH_2)_2CO_2H$, EDCI, DMAP 85% b) AcOH 50% c) biotinyl-N-hydroxysuccinimide 62%

Scheme 2.7 Synthesis of biotinylated PTX

2.5 Experimental section

General Experimental Methods. All reagents and solvents received from commercial sources were used without further purification. ^{1}H and ^{13}C NMR spectra were obtained in $CDCl_3$ on Varian Unity or Varian Inova spectrometers at 400 MHz or a JEOL Eclipse spectrometer at 500 MHz. High-resolution FAB mass spectra were obtained on a JEOL HX-110 instrument. Compounds were purified by chromatography on silica gel columns using EtOAc/hexane unless specified. Compounds (**2.4**-**2.7**, **2.10**, **2.12**, **2.13**, and **2.16**-**2.18**) have all been prepared by other investigators. These compounds were resynthesized as described below. All these compounds had NMR and mass spectra that matched the literature value, so these data are not reported here.

3-(2-pyridinyldithio)propanic acid (2.4). At rt, a solution of 3-mercaptopropionic acid (0.1 mL, 1.15 mmol) in MeOH (1 mL) was added dropwise to a solution of 2, 2′-dithiodipyridine (0.5 g, 2.23 mmol) in MeOH (2 mL) containing glacial acid (0.05 mL). After 3 hr, the solution was concentrated. This crude residue was purified on a silica column to afford oil **2.4** (0.23 g, 93%).[57]

16-(2-pyridinyldithio) hexadecanoic acid (2.5). At rt, a solution of 2, 2′-dipyridyl disulfide (0.5 g, 2.24 mmol) in 5 mL of ethyl acetate was added to 16-mercaptohexadecanoic acid (0.35 g, 1.1 mmol) and acetic acid (0.1 mL) in ethyl acetate (5 mL). After 1 day, the solution was concentrated. The residue was purified on a silica gel column to afford wax **2.5** (0.4 g, 88%).[58]

2-(2-pyridinyldithio) ethanol (2.6). At rt, 2-mercaptoethanol (0.1 mL, 1.44 mmol) was added to a solution of 2′-aldrithiol (0.45 g, 2.05 mmol) in 5 mL methanol with HOAc (20 μl). After 12 h, the solvent was removed. The residue was purified by silica gel to give oil **2.6** (248 mg, 87%).[59]

2-(2-pyridinyldithio) ethanamine (2.7). At rt, 2-mercaptoethylamine hydrochloride (1.1 g, 9.7 mmol) in MeOH (7.5 mL) was added dropwise to a solution of 2, 2′-dipyridyl disulfide (3.3 g, 1.5 mmol) in MeOH (15 mL) and glacial acetic acid (0.7 mL). After 3 days, the mixture was concentrated. The residue was purified on silica gel column to give oil **2.7** (0.9 g, 52%).[60]

2'-paclitaxel 3-(2-pyridinyldithio)propanoate (2.8). At rt, a solution of paclitaxel (45 mg, 0.053 mmol), **2.4** (13 mg, 0.12 mmol) and DMAP (cat.) in DCM (5 mL) was treated with EDCI (30 mg, 0.16 mmol). After 12 h, the reaction was quenched with water. The layer was separated and the aqueous phase was extracted with EtOAc. The combined

organic layer was washed with water, brine, dried over Na_2SO_4, filtered and concentrated. The residue was purified on PTLC to give glassy **2.8** (46 mg, 82%). ^{1}H NMR ($CDCl_3$) δ 1.13 (3H, s), 1.2 (3H, s), 1.68 (3H, s), 1.79 (1H, m), 1.86 (1H, m), 1.89 (1H, m), 1.92 (3H, brs), 2.16 (1H, m), 2.22 (3H, s), 2.34-2.40 (1H, m), 2.45 (3H, s), 2.52-2.58 (2H, m), 2.89 (2H, t, *J* = 7.2 Hz), 3.00 (2H, t, *J* = 6.4 Hz), 3.81 (1H, d, *J* = 6.8 Hz), 4.20 (1H, d, *J* = 8.4 Hz), 4.35 (1H, d, *J* = 8.4 Hz), 4.44 (1H, m), 4.97 (1H, d, *J* = 8.0 Hz), 5.52 (1H, d, *J* = 3.2 Hz), 5.68 (1H, d, *J* = 7.2 Hz), 5.98 (1H, dd, *J*= 9.2, 3.2 Hz), 6.25 (1H, t, *J* = 8.8 Hz), 6.29 (1H, s), 6.98 (1H, d, *J* = 9.2 Hz), 7.05-7.08 (1H, m), 7.32-7.44 (7H, Ar), 7.48-7.54 (3H, Ar), 7.59-7.65 (3H, Ar),7.72-7.75 (2H, m, Ar), 8.13 (2H, m, Ar); 8.42 (1H, m, Ar); ^{13}C NMR ($CDCl_3$) δ 9.6, 14.8, 20.8, 22.0, 22.7, 26.8, 33.0, 33.3, 35.5, 43.1, 45.6, 52.7, 58.5, 71.9, 72.1, 74.3, 75.0, 75.6, 76.4, 79.1, 81.0, 84.4, 94.8, 119.9, 120.96, 126.5, 127.1, 128.5, 128.68, 128.70, 129.11, 129.13, 130.2, 132.0, 132.8, 133.5, 133.7, 136.8, 137.2, 142.6, 149.7, 167.0, 167.1, 167.8, 169.8, 170.7, 171.2, 203.8; HRFABMS: found *m/z* 1233.5334; Calcd for $C_{68}H_{85}N_2O_{15}S_2$ $[M+H]^+$ *m/z* 1233.5391, Δ = 4.6 ppm.

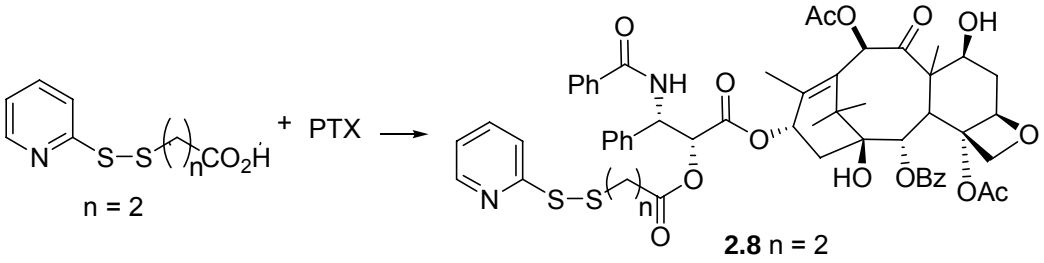

2'-paclitaxel 16-(2-pyridinyldithio)hexadecanoate (2.9). At rt, a solution of paclitaxel (32 mg, 0.037 mmol), **2.5** (17 mg, 0.04 mmol) and DMAP (cat.) in DCM (3 mL) was treated with EDCI (50 mg, 0.26 mmol). After 12h, the reaction was quenched with water. The layer was separated and the aqueous phase was extracted with EtOAc. The combined organic layer was washed with water, brine, dried over Na_2SO_4, filtered and concentrated.

The residue was purified on PTLC to give glassy **2.9** (30 mg, 75%). ^{1}H NMR ($CDCl_3$) δ 1.17 (3H, s), 1.27 (25H, bs), 1.41 (2H, m), 1.61 (2H, m), 1.71 (1H, m), 1.72 (3H, s), 1.80 (1H, m), 1.92 (1H,m), 1.98 (3H, brs), 2.19 (1H, m), 2.26 (3H, s), 2.36-2.46 (3H, m), 2.49 (3H, s), 2.58 (1H, m), 2.83 (2H, t, *J* = 7.2 Hz), 3.85 (1H, d, *J* = 6.8 Hz), 4.23 (1H, d, *J* = 8.2 Hz), 4.35 (1H, d, *J* = 8 Hz), 4.48 (1H, dd, *J* = 10.8, 6.8 Hz), 4.97 (1H, dd, *J* = 9.6, 2.0 Hz), 5.54 (1H, d, *J* = 3.2 Hz), 5.71 (1H, d, *J* = 7.2 Hz), 5.98 (1H, dd, *J*= 9.2, 3.2 Hz), 6.30 (1H, t, *J* = 9.2 Hz), 6.33 (1H, s), 6.94 (1H, d, *J* = 9.2 Hz), 7.11-7.14 (1H, m), 7.30-7.47 (7H, Ar), 7.52-7.57 (3H, Ar), 7.63-7.72 (2H, Ar),7.76-7.80 (3H, m, Ar), 8.17 (2H, m, Ar); 8.50 (1H, m, Ar); ^{13}CNMR ($CDCl_3$) δ 9.6, 14.8, 20.8, 22.1, 22.7, 24.7, 26.8, 28.4, 28.9, 29.1, 29.2, 29.36, 29.4, 29.5,29.57, 29.58, 33.7, 35.5, 39.0, 43.1, 45.5, 52.8, 58.5, 71.7, 72.1, 73.8, 75.1, 75.6, 76.4, 79.2, 81.0, 84.4, 119.7, 120.5, 126.5, 127.0, 128.4, 128.68, 128.7, 129.0, 129.1, 130.2, 131.9, 132.7, 133.6, 137.1, 137.3, 142.8, 149.1, 160.6, 167.0, 168.1, 169.7, 171.2, 172.7, 203.8; HRFABMS: found *m/z* 1233.5334; Calcd for $C_{68}H_{85}N_2O_{15}S_2$ $[M+H]^+$ *m/z* 1233.5391, Δ = 4.6 ppm.

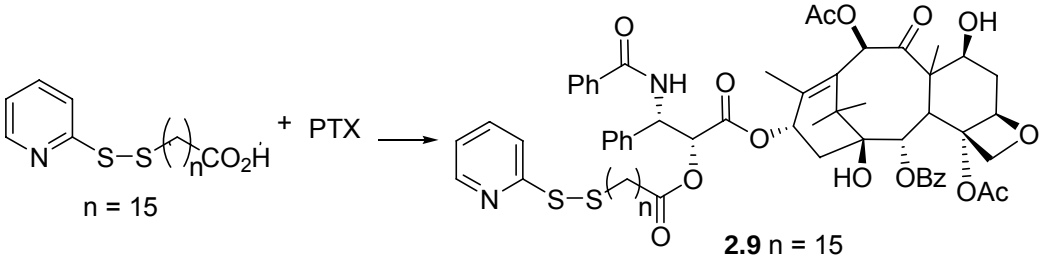

2'-succinyl paclitaxel (2.10). At rt, 0.14 g, (1.4 mmol) of succinic anhydride was added to a solution of 0.056 g (0.066 mmol) of paclitaxel in 2 mL of pyridine After 3 h, the solvent was evaporated. The residue was treated with 5 mL of water, stirred for 1h, and filtered. The precipitate was purified on PTLC to give **2.10** (0.07 g, 99%).[61]

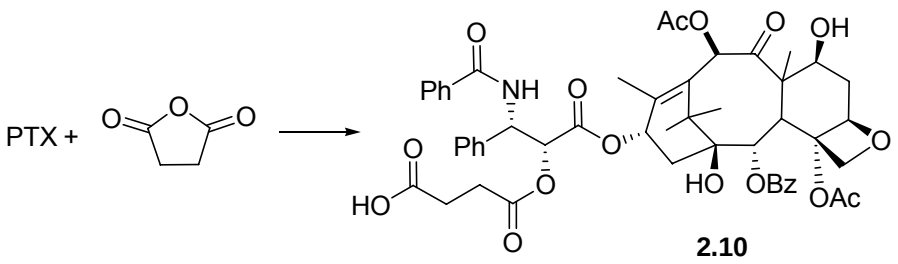

2'-paclitaxel 2-(2-pyridinyldithio)ethoxylsuccinate (2.11). At rt, a solution of **2.10** (72 mg, 0.075 mmol), **2.6** (72 mg, 0.17 mmol) and DMAP (cat.) in DCM (4 mL) was treated with EDCI (120mg, 0.62 mmol). After 12h, the reaction was quenched with water. The layer was separated and the aqueous phase was extracted with EtOAc. The combined organic layer was washed with water, brine, dried over Na_2SO_4, filtered and concentrated. The residue was purified on PTLC to give **2.11** (70 mg, 83%). ^{1}H NMR ($CDCl_3$) δ 1.14 (3H, s), 1.24 (3H, s), 1.69 (3H, s), 1.80 (1H, m), 1.93 (3H, br s), 2.16 (1H, m), 2.22 (3H, s), 2.38 (1H, m), 2.45 (3H, s), 2.57 (1H, m), 2.60 (2H, m), 2.73 (2H, m), 2.92 (2H, t, *J* = 6.4Hz), 3.81 (1H, d, *J* = 7.2 Hz), 4.20-4.23 (3H, overlap), 4.31 (1H, d, *J* = 8.2 Hz), 4.44 (1H, m), 4.97 (1H, app. d, *J* = 8.8 Hz), 5.49 (1H, d, *J* = 3.2 Hz), 5.69 (1H, d, *J* = 7.2 Hz), 5.99 (1H, dd, *J*= 9.2, 2.8 Hz), 6.25 (1H, t, *J* = 9.0 Hz), 6.30 (1H, s), 7.10 (2H, m), 7.26-7.44 (7H, Ar), 7.46-7.53 (3H, Ar), 7.58-7.64 (3H, Ar),7.78 (2H, m, Ar), 8.15 (2H, m, Ar), 8.40 (1H, m, Ar); ^{13}C NMR ($CDCl_3$) δ 9.6, 14.8, 20.8, 22.2, 22.7, 26.8, 29.0, 29.1, 35.57, 35.58, 36.9, 43.2, 45.5, 52.6, 58.5, 62.6, 71.8, 72.1, 74.3, 75.1, 75.6, 76.4, 79.1, 81.0, 84.4, 119.7, 120.9, 126.5, 127.2, 128.4, 128.6, 128.7, 129.0, 129.2, 130.2, 131.9, 132.8, 133.5, 133.6, 136.9, 137.1, 142.7, 149.7, 167.0, 167.2, 167.8, 170.0, 171.0, 171.2, 171.8, 203.8; HRFABMS: found *m/z* 1123.3602; Calcd for $C_{58}H_{63}N_2O_{17}S_2$ $[M+H]^+$ *m/z* 1123.3568, Δ = 3.0 ppm.

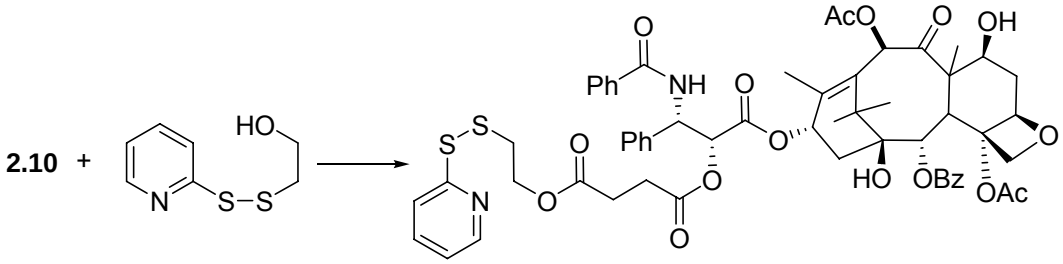

2.11

Compounds **2.14-2.17** were prepared as described in the literature.[54]

References:

1. Zugates, G. T.; Anderson, D. G.; Little, S. R.; Lawhorn, I. E. B.; Langer, R. Synthesis of poly(β-amino ester)s with thiol-reactive side chains for DNA delivery. *J. Am. Chem. Soc.* **2006,** *128*, 12726 -12734.
2. Wouters, B. G.; Weppler, S. A.; Koritzinsky, M.; Landuyt, W.; Nuyts, S.; Theys, J.; Chiu, R. K.; Lambin, P. Hypoxia as a target for combined modality treatments. *Eur. J. Cancer* **2002,** *38*, 240-257.
3. Tomasz, M. Mitomycin C: Small, fast, and deadly (but very selective). *Chem. Biol.* **1995,** *2*, 575-579.
4. Brown, J. M. SR 4233 (tirapazamine): A new anticancer drug exploiting hypoxia in solid tumours. *Br. J. Cancer* **1993,** *67*, 1163-1170.
5. McKeown, S. R.; Hejmadi, M. V.; McIntyre, I. A.; McAleer, J. J.; Patterson, L. H. Aq4n: An alkylaminoanthraquinone N-oxide showing bioreductive potential and positive interaction with radiation *in vivo*. *Br. J. Cancer* **1995,** *72*, 76-81.
6. Hayashi, Y.; Skwarczynski, M.; Hamada, Y.; Sohma, Y.; Kimura, T.; Kiso, Y. A novel approach of water-soluble paclitaxel prodrug with no auxiliary and no byproduct: Design and synthesis of isotaxel *J. Med. Chem.* **2003,** *46*, 3782 -3784.

7. Kumar, S. K.; Williams, S. A.; Isaacs, J. T.; Denmeade, S. R.; Khan, S. R. Modulating paclitaxel bioavailability for targeting prostate cancer. *Bioorg. Med. Chem.* **2007,** *15*, 4973-4984.

8. Skwarczynski, M.; Sohma, Y.; Noguchi, M.; Kimura, M.; Hayashi, Y.; Hamada, Y.; Kimura, T.; Kiso, Y. No auxiliary, no byproduct strategy for water-soluble prodrugs of taxoids: Scope and limitation of O-N intramolecular acyl and acyloxy migration reactions. *J. Med. Chem.* **2005,** *48*, 2655-2666.

9. Paciotti, G. F.; Kingston, D. G. I.; Tamarkin, L. Colloidal gold nanoparticles: A novel nanoparticle platform for developing multifunctional tumor-targeted drug delivery vectors. *Drug Deliv. Res.* **2006,** *67*, 47-54.

10. Paciotti, G. F. M., Lonnie; Weinreich, David; Goia, Dan; Pavel, Nicolae; McLaughlin, Richard E.; Tamarkin, Lawrence. Colloidal gold: A novel nanoparticle vector for tumor directed drug delivery. *Drug Deliv.* **2004,** *11*, 169-183.

11. Ojima, I.; Geng, X.; Wu, X.; Qu, C.; Borella, C. P.; Xie, H.; Wilhelm, S. D.; Leece, B. A.; Bartle, L. M.; Goldmacher, V. S.; Chari, R. V. J. Tumor-specific novel taxoid-monoclonal antibody conjugates. *J. Med. Chem.* **2002,** *45*, 5620-5623.

12. Miller, M. L.; Roller, E. E.; Zhao, R. Y.; Leece, B. A.; Baloglu, E.; Goldmacher, V. S.; Chari, R. V. Synthesis of taxoids with improved cytotoxicity and solubility for use in tumor-specific delivery. *J. Med. Chem.* **2004,** *47*, 4802-4805.

13. Vrudhula, V. M.; MacMaster, J. F.; Li, Z.; Kerr, D. E.; Senter, P. D. Reductively activated disulfide prodrugs of paclitaxel. *Bioorg. Med. Chem. Lett.* **2002,** *12*, 3591-3594.

14. Deutsch, H. M.; Glinski, J. A.; Hernandez, M.; Haugwitz, R. D.; Narayanan, V. L.; Suffness, M.; Zalkow, L. H. Synthesis of congeners and prodrugs. 3. Water-soluble prodrugs of taxol with potent antitumor activity. *J. Med. Chem.* **1989,** *32*, 788-792.

15. Ueda, Y.; Matiskella, J. D.; Mikkilineni, A. B.; Farina, V.; Knipe, J. O.; Rose, W. C.; Casazza, A. M.; Vyas, D. M. Novel, water-soluble phosphate derivatives of 2′-ethoxy carbonylpaclitaxel as potential prodrugs of paclitaxel: Synthesis and antitumor evaluation. *Bioorg. Med. Chem. Lett.* **1995,** *5*, 247-252.

16. Zakharian, T. Y.; Seryshev, A.; Sitharaman, B.; Gilbert, B. E.; Knight, V.; Wilson, L. J. A fullerene-paclitaxel chemotherapeutic: Synthesis, characterization, and study of biological activity in tissue culture. *J. Am. Chem. Soc.* **2005,** *127*, 12508-12509.

17. Aspland, S. E.; Ballatore, C.; Castillo, R.; Desharnais, J.; Eustaquio, T.; Goelet, P.; Guo, Z.; Li, Q.; Nelson, D.; Sun, C.; Castellino, A. J.; Newman, M. J. Kinase-mediated trapping of bi-functional conjugates of paclitaxel or vinblastine with thymidine in cancer cells. *Bioorg. Med. Chem. Lett.* **2006,** *16*, 5194-5198.

18. Kingston, D. G. I., History and chemistry, In *Taxol in Cancer Treatment,* McGuire, W. P.; Rowinsky, R. K., eds. Marcel Dekker: New York, 1995; p 21-27.

19. Datta, A.; Jayasinghe, L.; Georg, G. I. 4-Deacetyltaxol and 10-acetyl-4-deacetyltaxotere: Synthesis and biological evaluation. *J. Med. Chem.* **1994,** *37*, 4258-4260.

20. Gueritte-Voegelein, F.; Guenard, D.; Lavelle, F.; Goff, M.-T. L.; Mangatal, L.; Potier, P. Relationships between the structure of taxol analogues and their antimitotic activity. *J. Med. Chem.* **1991,** *34*, 992-998.

21. Denis, J. N.; Greene, A. E.; Serra, A. A.; Luche, M. J. An efficient, enantioselective synthesis of the taxol side chain. *J. Org. Chem.* **1986,** *51*, 46-50.

22. Georg, G. I.; Cheruvallath, Z. S.; Himes, R. H.; Mejillano, M. R.; Burke, C. T. Synthesis of biologically active taxol analogs with modified phenylisoserine side chains. *J. Med. Chem.* **1992,** *35*, 4230-4237.

23. Chaudhary, A. G.; Rimoldi, J. M.; Kingston, D. G. I. Modified taxols. 10. Preparation of 7-deoxytaxol, a highly bioactive taxol derivative, and interconversion of taxol and 7-epi-taxol. *J. Org. Chem.* **1993,** *58*, 3798-3799.

24. Harris, J. W.; Katki, A.; Anderson, L. W.; Chmurny, G. N.; Paukstelis, J. V.; Collins, J. M. Isolation, structural determination, and biological activity of 6 α-hydroxytaxol, the principal human metabolite of Taxol. *J. Med. Chem.* **1994,** *37*, 706-709.

25. Lataste, H.; Senilh, V.; Wright, M.; Guenard, D.; Potier, P. Relationships between the structures of taxol and baccatine III derivatives and their in vitro action on the disassembly of mammalian brain and physarum amoebal microtubules *Proc. Natl. Acad. Sci., USA* **1984,** *81*, 4090-4094.

26. Mathew, A. E. M., Magdalena R.; Nath, Jyoti P.; Himes, Richard H.; Stella, Valentino J. Synthesis and evaluation of some water-soluble prodrugs and derivatives of taxol with antitumor activity. *J. Med. Chem.* **1992,** *35*, 145-51.

27. Chen, S. H.; Huang, S.; Kant, J.; Fairchlid, C.; Wei, J.; Farina, V. Synthesis of 7-deoxy- and 7,10-dideoxytaxol via radical intermediates. *J. Org. Chem.* **1993,** *58*, 5028-5029.

28. Magri, N. F.; Kingston, D. G. I. Modified taxols. 2. Oxidation products of taxol. *J. Org. Chem.* **1986,** *51*, 797-802.

29. Datta, A. H., Michael; Georg, Gunda I. Selective deesterification studies on taxanes: Simple and efficient hydrazinolysis of C-10 and C-13 ester functionalities. *J. Org. Chem.* **1995,** *60*, 761-3.

30. Kant, J.; O'Keeffe, W. S.; Chen, S. H.; Farina, V.; Fairchild, C.; Johnston, K.; Kadow, J. F.; Long, B. H.; Vyas, D. A chemoselective approach to functionalize the C-10 position of 10-deacetylbaccatin III. Synthesis and biological properties of novel C-10 taxol analogs. *Tetrahedron Lett.* **1994,** *35*, 5543-5546.

31. Chen, S. H.; Fairchild, C.; Mamber, S. W.; Farina, V. Taxol structure-activity relationships: Synthesis and biological evaluation of 10-deoxytaxol. *J. Org. Chem.* **1993,** *58*, 2927-2928.

32. Chen, S. H.; Huang, S.; Wei, J.; Farina, V. Serendipitous synthesis of a cyclopropane-containing taxol analog via anchimeric participation of an unactivated angular methyl group. *J. Org. Chem.* **1993,** *58*, 4520-4521.

33. Kingston, D. G. I.; Chordia, M. D.; Jagtap, P. G. Synthesis and biological evaluation of 1-deoxypaclitaxel analogues. *J. Org. Chem.* **1999,** *64*, 1814-1822.

34. Chordia, D. M.; Kingston, D. G. I. Synthesis and biological evaluation of 2-epi-paclitaxel. *J. Org. Chem.* **1996,** *61*, 799-801.

35. Chen, S. H.; Wei, J.; Farina, V. Taxol structure-activity relationships: Synthesis and biological evaluation of 2-deoxytaxol. *Tetrahedron Lett.* **1993,** *34*, 3205-3206.

36. Chaudhary, A. G.; Gharpure, M. M.; Rimoldi, J. M.; Chordia, M. D.; Gunatilaka, A. A. L.; Kingston, D. G. I.; Grover, S.; Lin, C. M.; Hamel, E. Unexpectedly facile hydrolysis of the 2-benzoate group of taxol and syntheses of analogs with increased activities. *J. Am. Chem. Soc.* **1994,** *116*, 4097-4098.

37. Neidigh, K. A.; Gharpure, M. M.; Rimoldi, J. M.; Kingston, D. G. I.; Jiang, Y. Q.; Hamel, E. Synthesis and biological evaluation of 4-deacetylpaclitaxel. *Tetrahedron Lett.* **1994,** *35*, 6839-6842.

38. Chen, S. H.; Fairchild, C.; Long, B. H. Synthesis and biological evaluation of novel c-4 aziridine-bearing paclitaxel (taxol) analogs. *J. Med. Chem.* **1995,** *38*, 2263-2267.

39. Chen, S. H.; Kadow, J. F.; Farina, V.; Fairchild, C.; Johnston, K. First syntheses of novel paclitaxel (taxol) analogs modified at the C4-position. *J. Org. Chem.* **1994,** *59*, 6156-6158.

40. Chen, S. H.; Wei, J. M.; Long, B. H.; Fairchild, C. A.; Carboni, J.; Mamber, S. W.; Rose, W. C.; Johnston, K.; Casazza, A. M.; Kadow, J. F.; Farina, V.; Vyas, D. M.; Doyle, T. W. Novel C-4 paclitaxel (Taxol®) analogs: Potent antitumor agents. *Bioorg. Med. Chem. Lett.* **1995,** *5*, 2741-2746.

41. Samaranayake, G.; Magri, N. F.; Jitrangsri, C.; Kingston, D. G. I. Modified taxols. 5. Reaction of taxol with electrophilic reagents and preparation of a rearranged taxol derivative with tubulin assembly activity. *J. Org. Chem.* **1991,** *56*, 5114-5119.

42. Hoemann, M. Z.; Vander Velde, D.; Aube, J.; Georg, G. I. Synthesis of 13-epi-taxol via a transannular delivery of a borohydride reagent. *J. Org. Chem.* **1995,** *60*, 2918-2921.

43. Ojima, I.; Kuduk, S. D.; Chakravarty, S.; Ourevitch, M.; Begue, J.-P. A novel approach to the study of solution structures and dynamic behavior of paclitaxel and docetaxel using fluorine-containing analogs as probes. *J. Am. Chem. Soc.* **1997,** *119*, 5519-5527.

44. Qi, X.; Lee, S.-H.; Yoon, J.; Lee, Y.-S. Synthesis of novel taxoid analogue containing sulfur group on C-13 side-chain: 2′-deoxy-2′-epi-mercaptopaclitaxel. *Tetrahedron* **2003,** *59*, 7409-7412.

45. Mastalerz, H.; Zhang, G.; Kadow, J.; Fairchild, C.; Long, B.; Vyas, D. M. Synthesis of 7β-sulfur analogues of paclitaxel utilizing a novel epimerization of the 7α-thiol group. *Org. Lett.* **2001,** *3*, 1613-1615.

46. Liu, C. Syntheses and Bioactivities of Targeted and Conformationally Restrained Taxol Analogs. Ph.D. Thesis, Virginia Polytechnic Institute and State University, Blacksburg, 2003.

47. Coyle, L. C.; Danilov, Y. N.; Juliano, R. L.; Regen, S. L. Chemisorbed phospholipid monolayers on gold: Well-defined and stable phospholipid surfaces for cell adhesion studies. *Chem. Mater.* **1989,** *1*, 606-610.

48. Jones, L. R.; Goun, E. A.; Shinde, R.; Rothbard, J. B.; Contag, C. H.; Wender, P. A. Releasable luciferin-transporter conjugates: Tools for the real-time analysis of cellular uptake and release *J. Am. Chem. Soc.* **2006,** *128*, 6526 -6527.

49. Greenwald, R. B.; Pendri, A.; Bolikal, D. Highly water soluble taxol derivatives: 7-polyethylene glycol carbamates and carbonates. *J. Org. Chem.* **1995,** *60*, 331-336.

50. Battaglia, A.; Guerrini, A.; Baldelli, E.; Fontana, G.; Varchi, G.; Samorı, C.; Bombardelli, E. Synthesis of 7- and 10-spermine conjugates of paclitaxel and 10-deacetyl-paclitaxel as potential prodrugs. *Tetrahedron Lett.* **2006,** *47*, 2667-2670.

51. Hofmann, K.; Kiso, Y. An approach to the targeted attachment of peptides and proteins to solid supports. *Proc. Natl. Acad. Sci. U.S.A.* **1976,** *73*, 3516-3518.

52. Hofmann, K.; Titus, G.; Montibeller, J. A.; Finn, F. M. Avidin binding of carboxyl-substituted biotin and analogues. *Biochemistry* **1982,** *21*, 978-984.

53. Yao, Z.; Zhang, M.; Sakahara, H.; Saga, T.; Arano, Y.; Konishi, J. Avidin targeting of intraperitoneal tumor xenografts. *J. Natl. Cancer Inst.* **1998,** *90*, 25-29.

54. Dubois, J.; Goff, M.-T. L.; Voegelein, F. G.; Gue´nard, D.; Tollen, Y.; Wright, M. Fluorescent and biotinylated analogues of docetaxeh synthesis and biological evaluation. *Bioorg. Med. Chem. Lett.* **1995,** *3*, 1357-1368.

55. Sambaiah, T.; King, K.-Y.; Tsay, S.-C.; Mei, N.-W.; Lai, Y.-K.; Lieu, C.-H.; Hwu, J. R. Synthesis and immunofluorescence assay of a new biotinylated paclitaxel. *Eur. J. Med. Chem.* **2002,** *37*, 349-353.

56. Guy, R. K.; Scott, Z. A.; Sloboda, R. D.; Nicolaou, K. C. Fluorescent taxoids. *Chem. Biol.* **1996,** *3*, 1021-1031.

57. Samukov, V. A simple preparation of 3-(2-pyridyldithio)propionic acid. *Synth. Comm.* **1998,** *28*, 3213-3217.

58. Coyle, L. C.; Danilov, Y. N.; Juliano, R. L.; Regen, S. L. Chemisorbed phospholipid monolayers on gold: Well-defined and stable phospholipid surfaces for cell adhesion studies. *Chem. Mat.* **1989,** *1*, 606-10.

59. Wiseman, R. L.; Johnson, S. M.; Kelker, M. S.; Foss, T.; Wilson, I. A.; Kelly, J. W. Kinetic stabilization of an oligomeric protein by a single ligand binding event. *J. Am. Chem. Soc.* **2005,** *127*, 5540-5551.

60. Zugates, G. T.; Anderson, D. G.; Little, S. R.; Lawhorn, I. E. B.; Langer, R. Synthesis of poly(β-amino ester)s with thiol-reactive side chains for DNA delivery. *J. Am. Chem. Soc.* **2006,** *128*, 12726-12734.

61. Liu, D.-Z.; Sinchaikul, S.; Reddy, P. V. G.; Chang, M.-Y.; Chen, S.-T. Synthesis of 2'-paclitaxel methyl 2-glucopyranosyl succinate for specific targeted delivery to cancer cells. *Bioorg. Med. Chem. Lett.* **2007,** *17*, 617-620.

Chapter 3 Synthesis of isotopically labeled paclitaxel analogs for REDOR (Rotational–Echo Double Resonance) NMR

3.1 Introduction

This chapter describers the synthesis of isotopically labeled paclitaxel derivatives and their use in the REDOR NMRdetermination of the tubulin-bound structure of paclitaxel. REDOR NMR will be explained in section **3.1.2**.

3.1.1 Structure of paclitaxel on the tubulin polymer

Compared with remarkable achievements in biological activity and SARs, the structural studies of the paclitaxel-tubulin interaction are much less advanced, primarily because of the limitations of available techniques. Although the taxane skeleton is a rigid cyclic ring system, rotatable groups at C2, C4, C10, and especially the side chain at C13, impart a high degree of freedom and make paclitaxel a conformationally mobile molecule. Therefore, the paclitaxel molecule could in principle adopt a large number of possible conformations on the tubulin polymer. In theory, X-ray crystallography would be a direct method to determine the binding conformation of paclitaxel on the microtubule complex. Unfortunately polymeric microtubules are not amenable to this approach. It was found however that zinc cations induce tubulin to assemble into two-dimensional sheets, in which protofilaments are similar to those in microtubules, despite being associated in an antiparallel fashion.[1] Elegant studies succeeded in establishing the three-dimensional structure of tubulin from electron crystallography (EC) of two-dimensional crystalline sheets.[2] The resolution of the EC structure of tubulin dimer bound to PTX was initially at 6.5 Å,[2,3] but further work reduced this to 3.5 Å.[4] Even though this

"high" resolution EC structure shows the location of the PTX binding site on tubulin, it still lacks the atomic resolution necessary to define the detailed conformation of paclitaxel in the tubulin binding pocket.[5]

NMR is a powerful tool to investigate the conformations of molecule in solution or in the solid state. It was found that the solution conformation of PTX, in nonploar solvents such as chloroform and dichloromethane, is similar to that in the crystal structure.[6] Dubois *et al.* investigated the conformation of docetaxel by ^{1}H NMR analysis of docetaxel and its analogues in nonpolar solvents. In their study, the interproton distances were calculated by quantitative NOE experiments. The NMR results indicated there is an association between the benzoate group at C2 and the *N*-benzoyl or *N*-carboxy group at C3'. Based on the above observations, they suggested that paclitaxel and docetaxel in the tubulin polymer might adopt a 'nonpolar' conformation, instead of the conformation of docetaxel on the solid state.[7] Molecular modeling studies also suggested that the nonpolar conformer possessed a lower energy than the solid state conformer. Therefore the 'nonpolar' conformer was proposed as the bioactive tubulin-binding conformation. A solvated molecular modeling study by Williams *et al*.[8] indicated that paclitaxel might adopt different conformations depending on the solvent, and identified four conformations as particularly low in energy; the 'nonpolar' conformer is favored in an aprotic environment. This 'nonpolar' model hypothesis is supported by other modeling studies.[9]

Shortly thereafter, an alternative hypothesis was proposed by Vander Velde *et al*.[10] In contrast to the previous NMR studies of docetaxel in nonpolar organic solvents, NOESY and ROESY spectra of paclitaxel and docetaxel were acquired in 75%

DMSO/25% water. The NMR results showed significant differences from the spectra taken in nonpoplar solvents. The polar side chain *N*-amino or *N*-carbonyloxy groups were located outside of the hydrophobic cluster, and the hydrophobic collapse involved C2-benzoyl, C3' phenyl and C4 acetyl groups. This 'polar' conformer is consistent with results from solvated molecular modeling studies as one of the low-energy conformations. It was suggested that the environment of the binding site has a crucial role in inducing conformational changes. A study on fluorine-containing paclitaxel and docetaxel analogs supported the 'polar' conformer as the dominant structure in the tubulin binding site.[11] The same conclusion was drawn from photoaffinity studies[12] by docking the 'polar' conformation into tubulin.

As mentioned before, the polymeric and noncrystalline nature of the PTX-microtubule complex prevent the determination of the PTX conformation on microtubules by X-ray crystallography.[13] However, an electron crystallographically refined structure (1JFF) was derived from the structure of the tubulin dimer at 3.5 Å resolution by electron crystallography of PTX-stabilized zinc-induced tubulin sheets.[4]

Simultaneously, Snyder *et al*. proposed a binding conformation of PTX on β-tubulin by docking 26 experimentally observed unbound PTX conformers into the zinc-sheet EC density map.[14] Unlike the 'polar' and 'nonpolar' conformers, the conformation uncovered by this work had a unique feature in which the benzoyl group at the C2 position is nearly equidistant from the N-benzoyl group and the phenyl group at the C3′ position. Because of the T-shape of the molecule as viewed from C2, it is called the T-Taxol conformation. Although it is consistent with the observed EC density, the validity of the T-Taxol model was questioned.[15,16]

REDOR NMR is an important technique for the experimental determination of internuclear distance a ligand bound to solid proteins such as microtubules. Earlier experiments by the Kingston group in collaborations with Drs. Bane and Schaefer led to the determinations of internuclear distances from the side chain to the C2 benzoyloxy group in tubulin-bound PTX.[17] Restrained by these geometric requirements,[17] a conformationally modified T-Taxol structure (REDOR-Taxol) was proposed as the bioactive form by Ojima.[5] Sixteen conformations generated from a Monte Carlo conformational analysis were docked into β-tubulin. The conformer best matching the REDOR-NMR geometric requirements was selected as the tubulin bound PTX structure,[18] and named REDOR-Taxol. REDOR-Taxol is very similar to T-Taxol, and the main difference between them is in the C13 side chain from C1′-C3′, where REDOR-Taxol exhibits a slight distortion of the C2 side chain. Due to the low resolution of the tubulin-PTX complex density map, it was not possible to distinguish the T-Taxol and REDOR-Taxol models.[5]

In practice, the determination of solution conformation is much more complex, because the structures and relative populations of several conformers in fast exchange cannot be determined by NMR data only. Since the relative populations of the different conformations could be directly derived from their relative energy content, computational modeling is a crucial method to help us understand the conformations. On the other hand, the accuracy of these computations is not sufficient to provide unique solutions. Therefore, computational studies are often assisted by NMR data, often derived from NOE data[19,20] and *J*-couplings.[21] Previous conformational studies were frequently hampered by a long list of different conformers as potential candidates. Calculation of the

distributions of each conformer is limited and many efforts are being made to address this problem. Among these different approaches, NMR analysis of molecular flexibility in solution (NAMFIS) can provide information on the probable population either of a single conformer or of a set of conformers sharing a common feature.[22]

Initially, NAMFIS analysis of PTX in chloroform yielded eight conformations, many of which had been undetected by previous studies.[14] Among them, the "nonpolar" form is the most populated form (35%) and the "polar form", routinely observed in DMSO-d_6/D_2O and CD_3OD, is the fifth most populated conformer (4%).[14] In the later study,[23] NAMFIS analysis, combining the later NMR populations and the full 514 conformer data set, identified eight conformations, with predicted populations ranging from 2 to 35% ($\Delta\Delta G$= 0-1.7 kcal/mol). Two 'nonpolar' forms comprise 40% of the total population and extended conformers account for 60%. Interestingly, no "polar" forms appeared in the second NAMFIS analysis.[23] Remarkably, the T-Taxol conformation population is only 5%, but it is clearly within reasonable energetic limits for binding to tubulin.[24] It is important to point out that the conformations derived from both NOE and molecular modeling studies are the low-energy conformers, instead of the bioactive one literally. However, it is reasonable that low-energy experimental conformational minima are prime conformations for protein-bound molecules.[25]

3.1.2 REDOR NMR and its application for the determination of paclitaxel structure

The mechanism of paclitaxel anti-cancer activity is promotion of microtubule polymerization by binding to α,β-tubulin. Thus the antitumor activity of PTX is closely related to its tubulin binding activity.[26] Therefore, the conformation of PTX bound to

tubulin should be the bioactive conformation of PTX. Due to the mobility of its side chain, there are numerous PTX conformers in solution; however, there might be only one dominant tubulin-binding conformer of PTX. To date, various conformations of PTX while bound to tubulin have been proposed:[18] "non-polar",[27] "polar",[10] electron crystallography (EC) structure (1JFF),[28] T-Taxol,[29] and REDOR-Taxol.[5] Obviously, the best way to distinguish these conformations is by direct observation of PTX bound on tubulin, which is hampered because of either the polymeric nature of microtubule or insufficient resolution. Therefore, indirect measurements are the only amenable approach to this issue.

REDOR (Rotational–Echo Double Resonance) NMR is a solid state, magic angle-spinning NMR technique to solve structures of biological macromolecules, such as proteins and enzyme–bound substrates by providing accurate internuclear distances.[30] REDOR NMR is performed by measurement of the heteronuclear dipolar coupling between isolated pairs of labeled nuclei. This technique is a useful supplemental method for X–ray and neutron diffraction methods, especially when an X-ray crystal structure cannot be obtained.

Dipolar interaction is an interaction between the magnetic moment of any nuclei and a non–zero nuclear spin. Due to reorientational motion, the dipolar coupling averages to zero in liquid. However, in a crystalline powder or amorphous solid, the dipolar coupling is not zero because reorientational motion is limited. The dipolar coupling (D) between two NMR active nuclei is inversely proportional to the cube of the internuclear distance r, i.e. $D \approx 1/r^3$.[31]

In a solid sample with dipolar coupling between two unlike nuclei such as ^{13}C and ^{15}N, two ^{15}N π pulses per period are inserted to prevent the C rotational spin echoes from reaching full intensity. The first N π pulse occurs either at half the rotor period or at one seventh the rotor period and the second π pulse in each rotor period always occurs at the end of the period. Two REDOR signal intensities of the nucleus ^{13}C are obtained; S′ with a π pulse and S without a π pulse from the ^{13}C-NMR spectrum, respectively. The ratio between the REDOR signal intensity difference (ΔS=S-S′) and the normal rotational echo signal intensity S, i.e. ΔS/S, is used to calculate the dipolar coupling *D* between two nuclei, which in turn is converted to intermolecular distances.[32]

Earlier REDOR studies of tubulin–bound labeled paclitaxel analogs demonstrated the feasibility of the method to measure internuclear distances while paclitaxel is bound to tubulin. Labeled paclitaxels **3.1** and **3.2** were prepared, (Figure 3.1). Simultaneous ^{13}C-^{19}F double REDOR experiments were performed on **3.1**, from which distances of 10.3 Å for the C2-F – C3′ and 9.8 Å for the C2-F –benzamide carbonyl were derived. A distance of 6.5 Å was also determined for the F-F distance of **3.2**, although this result was obtained by a different method and has not yet been published with full experimental details.[11]

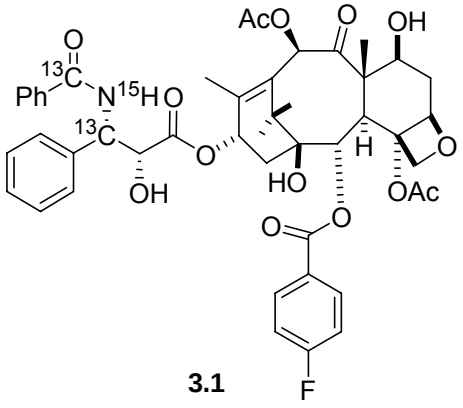

3.1

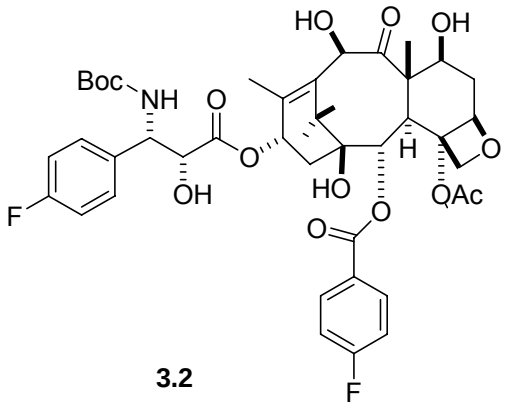

3.2

Figure 3.1 Structure of **3.1** and **3.2**

The interatomic separations determined by these REDOR NMR experiments are listed in Table 3.1, along with the interatomic distances for the five paclitaxel conformations proposed for its binding to tubulin.

Table 3.1 Interatomic distances from REDOR NMR experiments and PTX modeling[17]

	distance (Å) [13,17]					
Separation	polar model	nonpolar model	Ojima model	1JFF model	T-PTX model	REDOR observed
C2-C3′	9.6	8.5	9.4	9.3	9.9	10.3
C2-**C**ONH	10.4	6.2	10.0	8.1	9.1	9.8

It is clear from these data that the electron crystallographically refined structure 1JFF model[28,29] and the nonpolar model do not agree with the observed REDOR distances, with differences from the experimental data by as much as 3.6 Å for the nonpolar model and 1.7 Å for the 1JFF model. These data do not however distinguish clearly among the other three models.

It was thus necessary to design and prepare other labeled paclitaxel derivatives to distinguish among these three conformations. Comparison of the three remaining candidate conformations showed that they differed most clearly in two key distances. The first distance is between the methyl group of the C4-acetate and the *para*-position of the C3′-phenyl group. And the second is between the *para*-positions of the C3′-phenyl and the C2-benzoyl groups.

In work carried out by another member of the group,[13] compound **3.3** was prepared to provide a way of determining the distance between the *para*-position of the C2-benzoate and the C3′-phenyl group. This determination was only partly successful because of difficulties with the REDOR experiment, and only a distance of greater than 8 Å was assigned to the D-F separation of **3.3**. A distance of 7.8 Å was determined for the F-CD_3 separation.

The crucial C4-acetate to C3′-phenyl separation required a different compound, and compounds **3.4** and **3.5** were designed to achieve this determination. Compound **3.6** was also designed in an attempt to obtain a better REDOR measurement for the C3′-phenyl to C2-benzoyl distance.

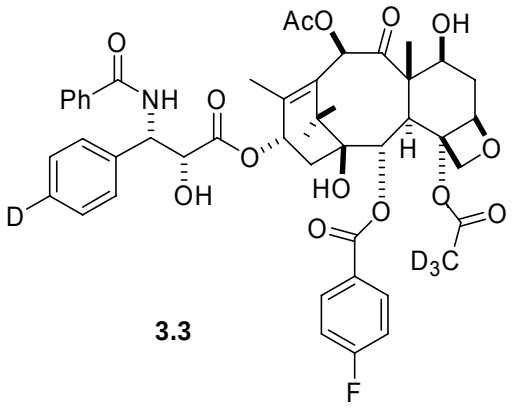

3.3

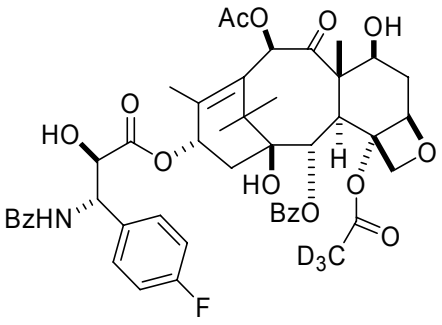

3.4

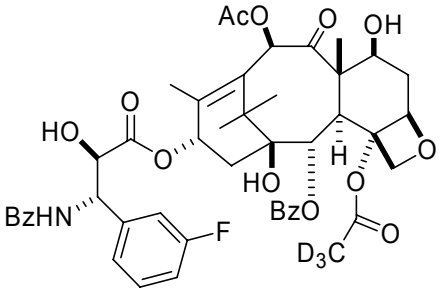

3.5

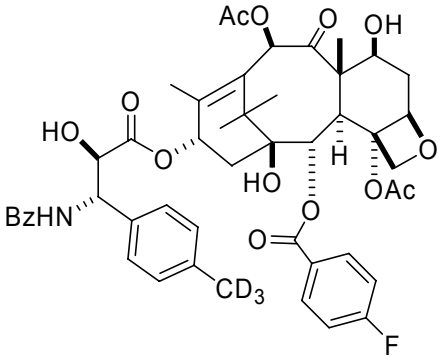

3.6

Figure 3.2 Structures of isotopically labeled paclitaxel analogs

3.2 Synthetic chemistry

The retrosynthesis of compounds **3.4** and **3.5** is given in Scheme 3.1. The major disconnection gave two main fragments for the synthesis, the β-lactam part **3.7** and baccatin core **3.8**. The coupling of **3.7** and **3.8** could be accomplished by known Holton protocol. [23]

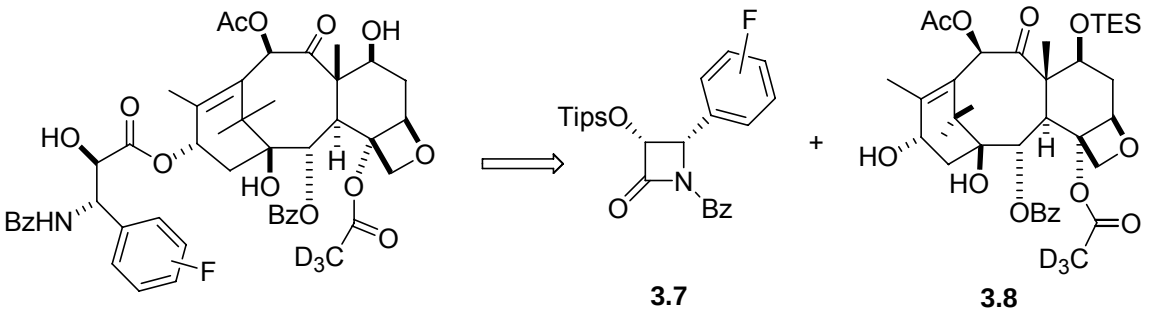

Scheme 3.1 Retrosynthetic analysis of labeled paclitaxel analogs

The synthesis of the β-lactam side chain started from commercially available 3- and 4-fluorobenzaldehydes by application of literature procedures[33,34] as shown in Scheme 3.2. The aldehydes reacted with *p*-anisidine to form the corresponding imine intermediates. Staudinger [2 + 2] cyclocondensation of the imines with ketene generated in situ from acetoxyacetyl chloride gave the racemic β-lactams **3.9a** and **3.9b**. Kinetic resolution of the racemic β-lactam with Lipase–PS–Amano enzyme yielded the acetates of the desired (+)-enantiomers **3.10a** and **3.10b**, along with the corresponding undesired (-)-alcohols. Deacetylation under basic conditions, followed by protection of the secondary alcohol as its triisopropylsilyl ether, then deprotection of the PMP group by CAN gave β-lactams **3.11a** and **3.11b**, which were benzoylated to give the desired labeled side chain precursors **3.12a** and **3.12b**.

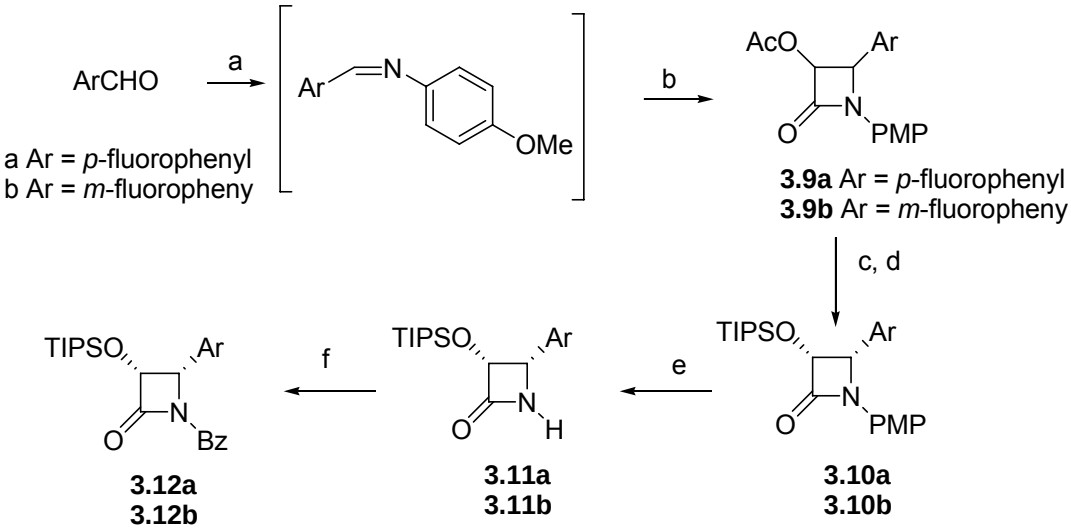

a) anisidine; b) $CH_3CO_2CH_2COCl$, Et_3N, 75%; c) lipase, 80%, 1 M KOH aq. 98%; d) TIPSCl, Im, 84%; e) CAN, 67%; f) BzCl, 87%

Scheme 3.2 Synthesis of labeled β–lactams

The forward synthesis sequence of the baccatin III portion starting from the natural product 10-deacetylbaccatin III (10-DAB, **3.13**) is shown in Scheme 3.3. TES protection of the C7, C10 and C13–hydroxyl groups, followed by DMS protection of the C1 hydroxyl group gave silyl protected baccatin **3.14**, which was treated with Red–Al® to give the C–4 deacetate **3.15**. Reacetylation of the C4 hydroxyl group of **3.15** using deuterated acetyl chloride gave the desired CD_3 labeled **3.16.** Global deprotection of all silyl groups was followed by selective acetylation of the C10 hydroxyl group to give the C10 acetyl intermediate **3.17** and selective protection of the C7 hydroxyl group by TES completed the synthesis of the labeled baccatin unit **3.18**.

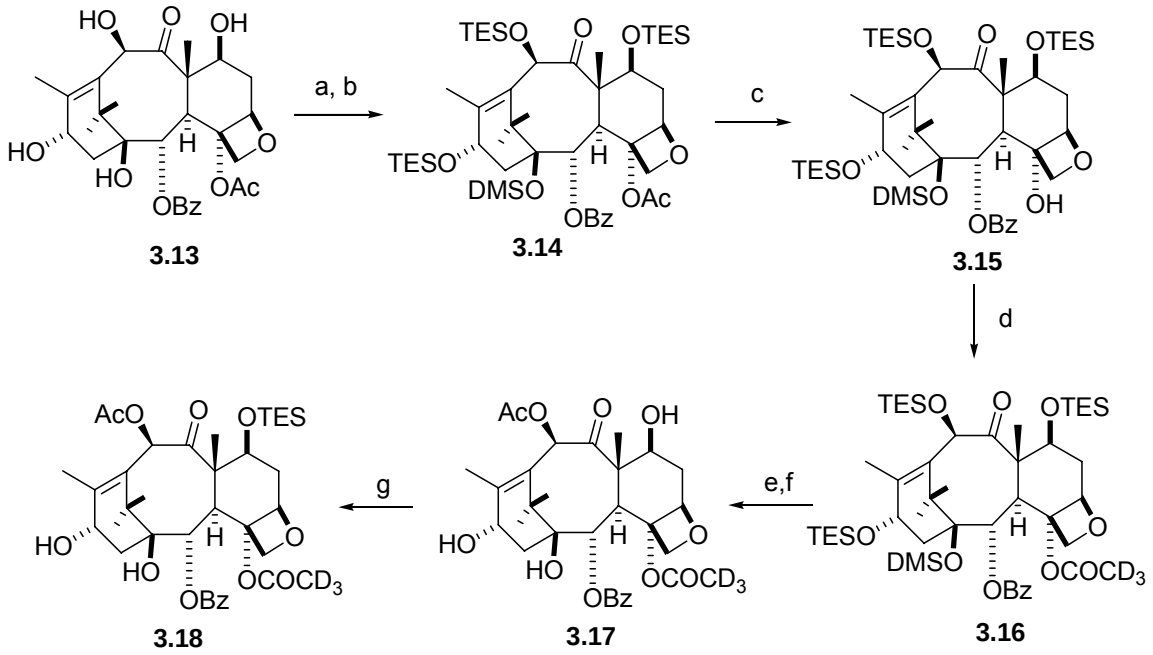

a) TESCl, Im, 88%; b) DMSCl, Im, 91%; c) Red Al, 78%; d) LHMDS, CD_3COCl, 60%; e)HF/py; f) Ac_2O, $CeCl_3$, two steps 75% g) TESCl, Im, 93%

Scheme 3.3 Synthesis of labeled baccatin III core

Coupling of β–lactams **3.12a** and **3.12b** with the baccatin core **3.18** was achieved by treatment with LHMDS. Finally, global deprotection with HF/pyridine completed the synthesis of isotopically labeled paclitaxel analogs **3.4** and **3.5**, as shown in Scheme 3.4.

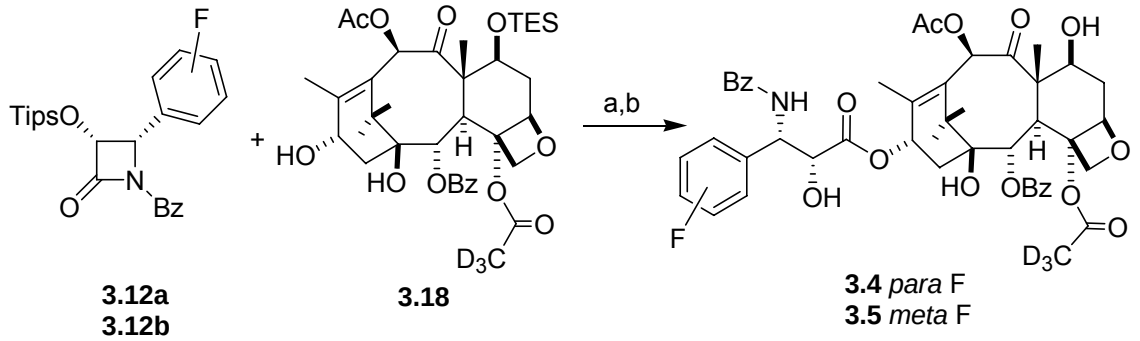

a) LHMDS b) HF/py, 74%

Scheme 3.4 Completion of paclitaxel analogs synthesis

The synthesis of the β–lactam sidechain for compound **3.6** started from commercially available 4-d_3-methylbenzaldehyde as shown in Scheme 3.5. A procedure similar to that just described was performed to give the racemic β–lactam **3.19**. Kinetic resolution, then deacetylation under basic conditions, followed by protection of the secondary alcohol as its triisopropylsilyl ether, deprotection of the PMP group by CAN, and benzoylation gave the desired labeled sidechain **3.20**.

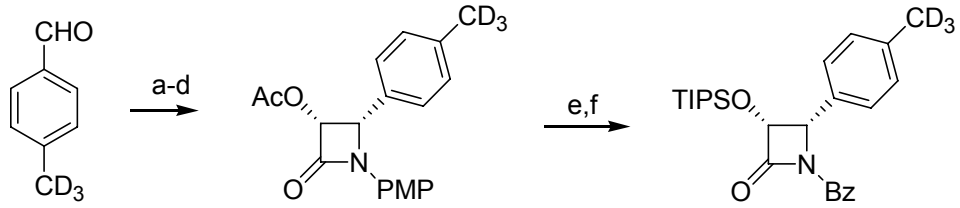

3.19 **3.20**

a) anisidine; b) $CH_3CO_2CH_2COCl$, Et_3N, 72%; c) lipase. 92%, 1 M KOH aq. 96%;
d) TIPSCl, Im, 84%; e) CAN, 55%; f) BzCl, 98%

Scheme 3.5 Synthesis of labeled β-lactams

The synthetic sequence for the baccatin III portion of compound **3.6** starting from the natural product 10-deacetylbaccatin III (10–DAB, **3.13**), as shown in Scheme 3.6. Protection of the C7, C10 and C13 hydroxyl groups as their TES ethers, followed by Red–Al® reduction gave the silyl protected C-2 debenzoylated baccatin III derivatives **3.21**. Acylation of the C2-hydroxy group with EDCI and 4-fluorobenzoyl chloride gave the 2-debenzoyl-2-(4-fluorobenzoyl)-baccatin III **3.22**. Global deprotection of all silyl groups with HF/py gave the deprotected baccatin III **3.23**. Selective acetylation of the C10 hydroxyl group with acetic anhydride and $CeCl_3$ gave the C10 acetate intermediate **3.24**. Selective protection of the C7 hydroxyl group by TES completed the synthesis of the labeled baccatin core **3.25**.

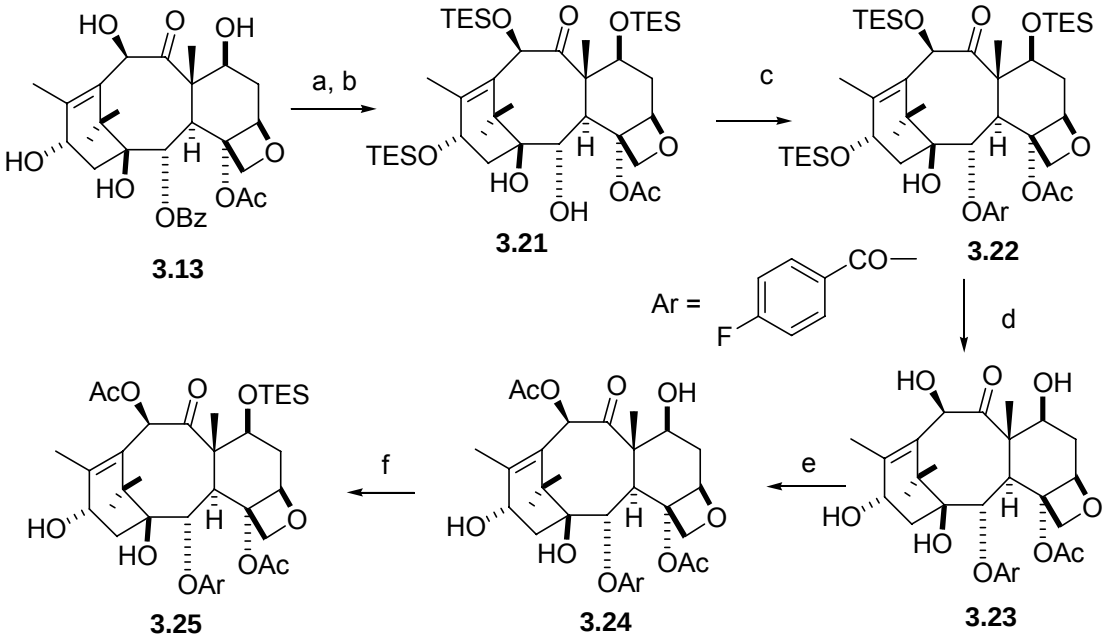

a) TESCl, Im, 92%; b) Red Al, 72%; c) EDCI, ArCl, 73%; d) HF/py, 94%; e) Ac_2O, $CeCl_3$, 90%; f) TESCl, Im, 80%

Scheme 3.6 Synthesis of labeled baccatin III core

Coupling of β-lactam **3.20** with the baccatin core **3.25** in the presence of LHMDS, followed by global deprotection with HF/py completed the synthesis of isotopically labeled paclitaxel analog **3.6**, as shown in Scheme 3.7.

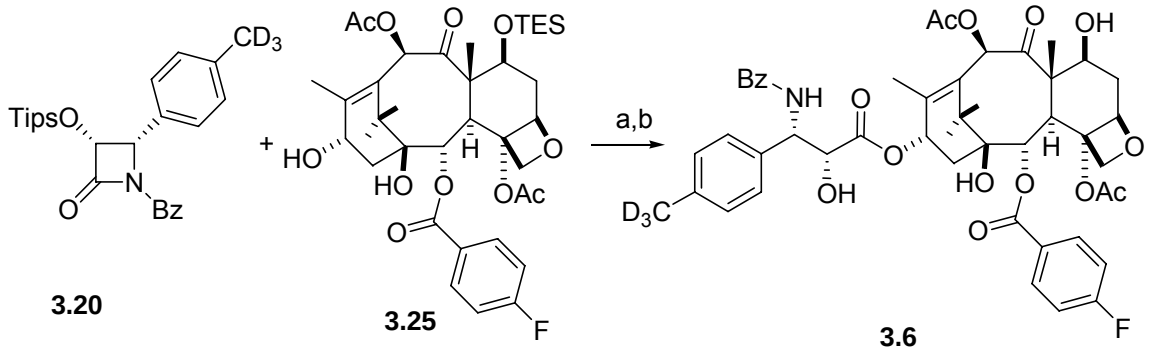

a) LHMDS, 54%; b) HF/py, 87%

Scheme 3.7 Completion of paclitaxel analogs synthesis

3.3 Biological evaluation and REDOR determined separation

For a paclitaxel analog to be a valid model for paclitaxel for REDOR NMR studies, it must have comparable tubulin-assembly activities to paclitaxel itself. The three analogs were thus subjected to evaluation in a tubulin-assembly assay by Dr. Susan Bane at SUNY Binghamton. The results, together with cytotoxicities in the A2780 assay, are shown in Table 3.2.

Table 3.2 Biological evaluation of REDOR PTX analogs[13]

Compound	Paclitaxel	**3.4**	**3.5**	**3.6**
Tubulin assembly activity, ED_{50}, μM	1.7 ± 0.4	2.6 ± 0.5	18	280
A2780 cytotoxicity IC_{50}, μM	0.023	0.047	ND	ND

ND: not determined

REDOR analog **3.4** has similar cytoxicity and tubulin assembly activity to paclitaxel, while compounds **3.5** and **3.6** were both significantly less active as tubulin-assembly agents than paclitaxel. The reason of loss activity is unclear. Compound **3.4** was thus selected for REDOR NMR analysis because it has similar actitive as PTX.

A REDOR NMR experiment on compound **3.4** was carried out by Dr. Susan Bane and Dr. Jacob Schaefer. The interatomic distances from this experiment are listed in Table 3.3, and a summary of all the REDOR NMR data is listed in Table 3.4. The distances were used as direct evidences to distinguish the bioactive conformation.

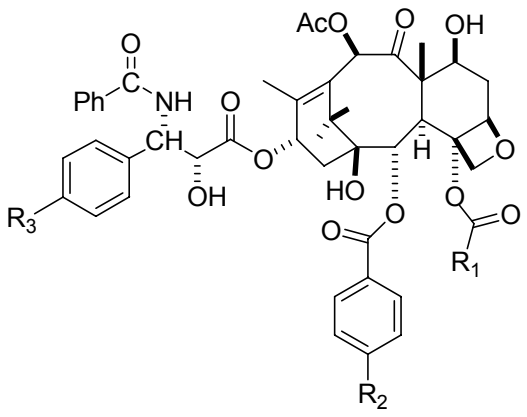

Figure 3.3 Structures of isotopically labeled paclitaxel analogs

Table 3.3 Interatomic distances for different PTX conformations and experimental distances determined by REDOR-NMR for PTX on tubulin for compound 3.4[13]

	distance (Å)					
separation	polar model	nonpolar model	Ojima model	1JFF model	T-PTX model	REDOR observed
R_2-R_3	4.5	12.5	13.1	11.6	12.2	>8±0.5
R_1-R_3	5.5	7.2	6.4	7.2	6.6	6.3±0.5

Table 3.4 Summary of interatomic distances for different PTX conformations and experimental distances determined by REDOR-NMR for PTX on tubulin[13]

		distance (Å)					
compound	Separation	polar model	nonpolar model	Ojima model	1JFF model	T-PTX model	REDOR observed
3.3	R_1-R_2	7.4	8.0	7.3	6.5	7.9	7.8±0.5
3.1	R_2-CH	9.6	8.5	9.4	9.3	9.9	10.3±0.5
3.1	R_2-C	10.4	6.2	10.0	8.1	9.1	9.8±0.5
3.4	R_2-R_3	4.5	12.5	13.1	11.6	12.2	>8±0.5
3.4	R_1-R_3	5.5	7.2	6.4	7.2	6.6	6.3±0.5

3.4 Conclusion

The polar, nonpolar and 1JFF conformations are ruled out as the PTX binding conformation on tubulin by these REDOR experiments. The polar model calculates the R_2-R_3 distance to be 4.5 Å, while the experimental value is >8 Å. The nonpolar model

calculates the R_2-C distance to be 6.2 Å, while the experimental value is 9.8 Å. The 1JFF model calculates the R_2-C distance to be 8.1 Å, while the experimental value is 9.8 Å. In addition the Ojima model is less consistent with the REDOR results than is the T-Taxol conformation. The Ojima model calculates the R_2-CH distance to be 9.4 Å, while the experimental value is 10.3 Å. It is thus concluded that the T-taxol model is the only one that correctly predicts the observed REDOR NMR distances, and is the most probable tubulin binding conformation of paclitaxel.

3.5 Experimental section

General Experimental Methods. All reagents and solvents received from commercial sources were used without further purification. ^{1}H and ^{13}C NMR spectra were obtained in $CDCl_3$ on Varian Unity or Varian Inova spectrometers at 400 MHz or a JEOL Eclipse spectrometer at 500 MHz. High-resolution FAB mass spectra were obtained on a JEOL HX-110 instrument. Compounds were purified by chromatography on silica gel using EtOAc/hexanes unless specified.

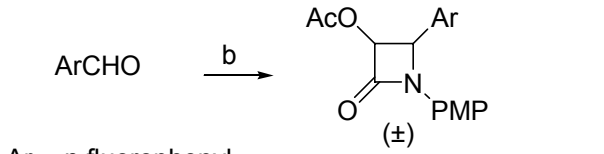

***(3RS + 3S4R)*-1-(*p*-methoxyphenyl)-3-acetoxyl-4-(*p*-fluorophenyl)-azetidin-2-one (3.9).** At rt, *p*–anisidine (1.45 g, 11.8 mmol) was added to a solution of *p*–fluorobenzaldehyde (1.4 g, 11.5 mmol) in dichloromethane (45 mL) and a large excess of anhydrous $MgSO_4$ and the slurry stirred at rt for 12 h. The yellowish slurry was filtered and the crude imine was taken to the next step without purification. To the crude imine

dissolved in anhydrous dichloromethane (45 mL) was added Hünig's base (6.2 mL) and cooled to -78 °C. Acetoxyacetyl chloride (1.5 mL, 14 mmol) was added to this solution dropwise and the mixture was allowed to warm up to rt slowly and stirred for 12 h. The dark crude mixture was concentrated and purified on a silica gel column to afford β–lactam **3.9** (2.5 g, 75%). ^{1}H NMR: δ 1.73 (s, 3H), 3.76 (s, 3H), 5.33 (d, *J* = 4.4 Hz, 1H), 5.41 (d, *J* = 4.8, 1H), 6.81 *(d, J* = 8.8 Hz, 2H), 7.05 (m, 2H), 7.28 (m, 4H), ^{13}C NMR δ 20.08, 55.28, 61.06, 76.62, 114.69, 115.74, 115.95, 119.00, 129.92, 156.93, 161.35, 169.44; HRFABMS: found *m/z* 329.1044, Calcd for $C_{18}H_{16}NFO_4$ $(M+H)^+$, *m/z* 329.1063. Δ = 5.6 ppm.

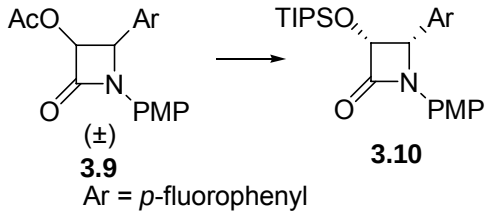

(3*R*,4*S*)-1-(*p*-methoxyphenyl)-3-triisopropylsilyloxy-4-(*p*-fluorophenyl)-azetidin-2-one (3.10). The racemic β–lactam (2.5 g, 7.6 mmol) was dissolved in 60 mL CH_3CN, and to this solution a phosphate buffer at pH 7.2 (120 mL) was added and stirred vigorously. Immobilized Lipase PS Amano enzyme (2.5 g) was added and the mixture stirred for 7 days. The progress of the reaction was monitored by TLC, and after completion the solution was extracted with EtOAc. The organic phase was washed with H_2O and brine, dried over Na_2SO_4, and concentrated. Purification by column chromatography gave (3*R*,4*S*)-1-(*p*-methoxyphenyl)-4-(*p*-fluorophenyl)-3-acetoxyl-azetidin-2-one (1 g, 80%). A solution of acetoxy β– lactam (1 g, 3.0 mmol) in THF (70 mL) was added slowly to a 1 M KOH solution (80 mL) at 0 ºC. The solution was stirred 45 min at this temperature and the mixture was extracted with EtOAc. The organic phase was washed with H_2O and brine,

dried over Na_2SO_4, and concentrated. Purification by column chromatography gave (3*R*,4*S*)-1-(*p*-methoxyphenyl)-4-(*p*-fluorophenyl)-3-hydroxyl-azetidin-2-one (0.93g, 98%). At rt, imidazole (0.65 g, 9.6 mmol) and triisopropylsilyl chloride (0.9 mL, 4.2 mmol) were added to a solution of (3*R*,4*S*)-1-(*p*-methoxyphenyl)-4-(*p*-fluorophenyl)-3-hydroxyl-azetidin-2-one (0.93 g, 3.0 mmol) in 5.5 mL of DMF, and the mixture was stirred at RT overnight. The reaction mixture was diluted with EtOAc, quenched with $NaHCO_3$, and extracted with EtOAc. The organic phase was washed with H_2O and brine, dried over Na_2SO_4, and concentrated. Column chromatography of the crude product gave β-lactam **3.10** (1.3 g, 84%).

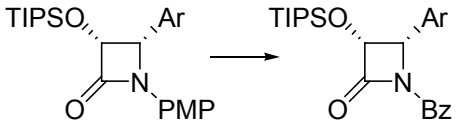

3.10 **3.12**

Ar = *p*-fluorophenyl

(3*R*,4*S*)-1-benzoyl-4-(*p*-fluorophenyl)-3-triisopropylsilyloxy-β-lactam (3.12). A solution of ceric ammonium nitrate (CAN) (1.5 g, 2.7 mmol) in 8 mL H_2O was added dropwise to a solution of β-lactam **3.10** (0.43 g, 0.97 mmol) in 20 mL CH_3CN at -5 ^oC. The reaction mixture was stirred for 45 min and monitored by TLC, diluted with EtOAc and washed with H_2O, a saturated solution of sodium metabisulfite and saturated $NaHCO_3$, dried over Na_2SO_4, and concentrated. The crude product was purified on a silica gel column to give the PMP deprotected oil β-lactam **3.11** (250 mg, 67%). To a solution of the deprotected β–lactam **3.11** (230 mg) in 12 mL CH_2Cl_2 at 0 ºC was added a catalytic amount of DMAP, 0.3 mL triethylamine, and 0.25 mL benzoyl chloride. The mixture was then warmed to rt with monitoring by TLC; after 3 h it was diluted with EtOAc and worked up in the usual way. The product was purified by silica gel chromatography to give the final

β-lactam oil **3.12** (275 mg, 87%). ^{1}H NMR: δ 0.93 (m, 18H), 1.01 (m, 3H), 5.23 (d, *J* = 6 Hz, 1H), 5.41 (d, *J* = 6 Hz, 1H), 7.07 (m, 2H), 7.39 (m, 2H), 7.49 (m, 2H), 7.58 (m, 1H), 8.04 (d, *J* = 8 Hz, 2H), ^{13}C NMR δ 11.89, 17.58, 17.68, 60.7, 76.74, 115.28, 115.50, 128.42, 129.98, 130.01, 130.10, 130.21, 130.29, 132.18, 133.67, 161.87, 164.33, 165.48, 166.45; HRFABMS: found *m/z* 442.2236, Calcd for $C_{25}H_{33}NO_3SiF$ $(M+H)^+$ *m/z* 442.2214. Δ = 4.9 ppm.

4-Deacetyl–1–dimethylsilyl-7,10,13-tris(triethylsilyl)-10-deacetylbaccatin III 3.15: This compound was synthesized from commercially available 10-deacetylbaccatin III by the literature method.[35]

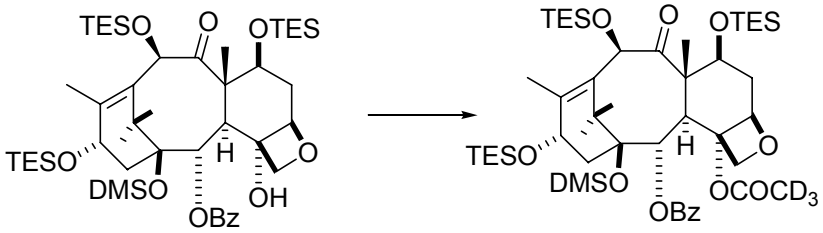

3.15 **3.16**

4-deacetyl-4-(*d*$_3$–acetyl)-1-dimethylsilyl-7,10,13-tris(triethylsilyl)-10-deacetyl baccatin III (3.16). A solution of 400 mg (0.44 mmol) of the 4-deacetylbaccatin III **3.15** in 10 mL THF at 0 °C was treated with 1 M LiHMDS (0.6 mL) followed by acetyl–*d*$_3$–chloride (0.15 mL, 2.1 mmol). The mixture was stirred for 3 h with monitoring by TLC, and then quenched with saturated aq. NH_4Cl. The reaction mixture was extracted with EtOAc and washed with H_2O and brine. The combined organic layer was dried over anhydrous Na_2SO_4 and concentrated under reduced pressure. Purification of the crude residue by silica gel column gave **3.16** (300 mg, 60%). ^{1}H NMR: δ –0.28 (d, *J* = 2.8, 3H), 0.05 (d, *J* = 2.8, 3H), 0.65 (m, 18H), 0.92 (m, 27H), 1.13 (s, 3H), 1.22 (s, 3H), 1.70 (s,3H),

1.98 (m, 1H), 2.00 (s, 3H), 2.24 (m, 1H), 2.38 (m, 1H), 2.45 (m, 1H), 3.85 (1H, d, *J* = 6.9 Hz), 4.24 (1H, *d, J* = 8.3 Hz), 4.27 (1H, d, *J* = 8.3 Hz), 4.41 (1H, *J* = 10.6, 6.6 Hz), 4.91 (1H, dd, *J* = 9.6, 2.0 Hz), 4.99 (1H, *t, J* = 8.4 Hz), 5.08-5.17 (2H, overlapped), 5.18 (1H, s), 5.74 (1H, d, *J* = 6.9 Hz), 5.84-5.95 (1H, m), 7.49 (t, *J* = 8, 2H), 7.62 (m, 1H), 8.18 (m, 2H), ^{13}C NMR δ 0.18, 0.53, 5.43, 5.99, 6.12, 7.12, 7.15, 10.58 14.68, 21.57, 27.48, 37.55, 39.51, 44.24, 46.84, 58.42, 68.59, 72.88, 75.91, 76.05, 76.98, 81.20, 82.27, 84.27, 115.81, 116.03, 128.59, 130.27, 130.72, 133.31, 136.19, 138.78, 165.53, 205.75; HRFABMS: found *m/z* 948.5419, Calcd for $C_{49}H_{82}D_3FO_{10}Si_4$ $(M+H)^+$, *m/z* 948.5408. Δ = 1.1 ppm.

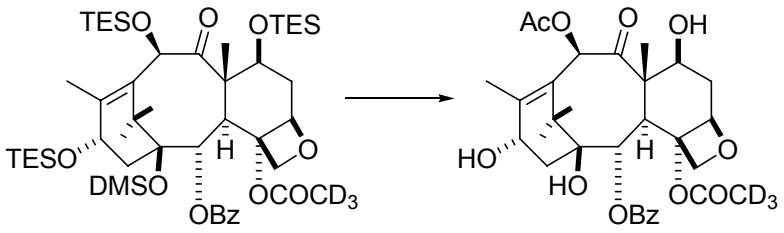

3.16 **3.17**

4-deacetyl-4-(*d*$_3$–acetyl) baccatin III (3.17). At 0 ºC, 2 mL HF/pyridine was added to a solution of **3.16** (300 mg, 0.3 mmol) in 20 mL of THF and the solution was warmed to rt and stirred overnight. The reaction mixture was diluted with EtOAc and washed with aq. $NaHCO_3$. The organic layer was washed with H_2O and brine, dried over anhydrous Na_2SO_4, and concentrated under reduced pressure. The residue was purified by PTLC to afford 4-deacetyl-4-(*d*$_3$–acetyl)-10-deacetylbaccatin III. To a solution of 4-deacetyl-4-(*d*$_3$–acetyl)-10-deacetylbaccatin in 1.5 mL of THF was added a catalytic amount of $CeCl_3$ and the solution was stirred at rt for 20 min. Acetic anhydride was added and the solution was stirred for 4 h. The mixture was diluted with EtOAc, quenched with aq. $NaHCO_3$ and washed with H_2O and brine. The organic phase was dried over anhydrous Na_2SO_4,

concentrated, and purified by preparative TLC to give **3.17** (147 mg, 75%). ^{1}H NMR: δ 1.08 (s, 3H), 1.63 (s, 3H), 1.85 (m, 1H), 2.02 (s, 3H), 2.20 (s, 3H), 2.25 (m, 2H), 2.56 (m, 3H), 3.84 (d, *J* = 6.8 Hz, 1H), 4.14 (d, *J* = 7.6 Hz, 1H), 4.25 (d, *J* = 8.4 Hz, 1H), 4.42 (m, 1H), 4.83 (t, *J* = 6.8 Hz, 1H), 4.96 (d, 7.6 Hz, 1H), 5.59 (d, *J* = 7.2 Hz, 1H), 6.31 (s, 1H), 7.45 (t, *J* = 9.2 Hz, 2H), 7.60 (t, *J* = 7.2 Hz, 2H), 8.10 (m, 2H); ^{13}C NMR: δ 9.67, 15.82, 21.14, 21.16, 27.14, 35.80, 38.92, 42.89, 46.37, 58.84, 67.98, 72.51, 75.15, 76.49, 76.64, 79.24, 80.87, 84.67, 128.86, 129.56, 130.30, 131.81, 132.89, 146.92, 167.21, 171.62, 204.48; HRFABMS: found *m/z* 590.2697, Calcd for $C_{31}H_{36}D_3O_{11}$ $(M+H)^+$, *m/z* 590.2681. Δ = 2.7 ppm.

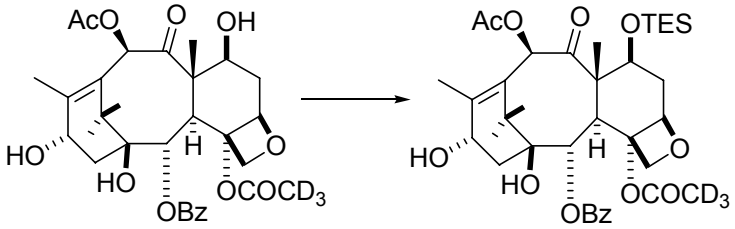

3.17 **3.18**

4-deacetyl-4-(*d*$_3$–acetyl)-7-triethylsilylbaccatin III (3.18). A solution of 4–(*d*$_3$–acetyl)–baccatin III **3.17** (147 mg, 0.25 mmol) in 6 mL of dry DMF was treated with imidazole (159 mg, 2.3 mmol) and chlorotriethylsilane (210 mg, 1.2 mmol) and the mixture was stirred at rt for 30 min with monitoring by TLC. The reaction mixture was quenched with MeOH saturated with $NaHCO_3$ and stirred for 10 min. The mixture was diluted and extracted with EtOAc, which was washed with H_2O and brine. The organic phase was concentrated and purified by preparative silica gel TLC to give **3.18** (165 mg, 93%). ^{1}H NMR δ 0.59 (m, 16H), 0.87 (t, *J* = 8Hz, 9H), 1.04 (s, 3H), 1.20 (s, 4H), 1.58 (s, 3H), 1.68 (s, 3H), 1.87 (m, 1H), 2.05 (m, 1H), 2.18 (s, 3H), 2.19 (m, 1H), 2.55 (m, 1H), 3.88 (d, *J* = 8 Hz, 1H), 4.15 (d, *J* = 8 Hz, 1H), 4.31 (d, *J* = 8 Hz, 1H), 4.48 (dd, *J* = 6.8, 4 Hz, 1H),

4.84 (m, 1H), 4.96 (d, J = 9.6 Hz, 1H), 5.64 (d, J = 7.2 Hz, 1H), 6.46 (s, 1H), 7.48 (t, J = 7.6 Hz, 2H), 7.60 (t, J = 7.2 Hz, 2H), 8.11 (m, 2H). ^{13}C NMR δ 5.50, 6.97, 10.16, 15.17, 20.31, 21.17, 27.03, 37.45 38.50, 42.99, 47.48, 58.87, 68.13, 72.57, 74.95, 76.02, 76.74, 78.94, 81.04, 84.45, 128.81, 129.61, 130.32, 132.88, 133.84, 144.24, 167.32, 169.60, 170.98, 202.47; HRFABMS: found *m/z* 704.3568, Calcd for $C_{37}H_{50}D_3O_{11}Si$ $(M+H)^+$, *m/z* 704.3545. Δ = 3.2 ppm.

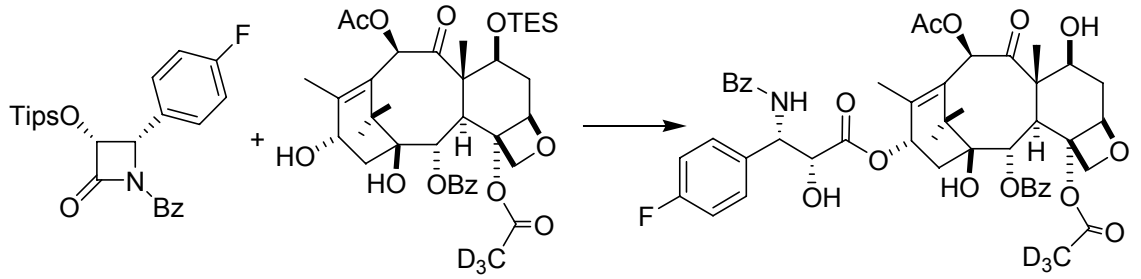

3.12 **3.18** **3.4**

3'-dephenyl-3'-(*p*–fluorophenyl)-4-deacetyl-4-(*d*$_3$-acetyl)-paclitaxel (3.4). A solution of 57 mg (0.13 mmol) β–lactam **3.12** and 19 mg (0.027 mmol) 4–(*d*$_3$–acetyl)–7–triethylsilylbaccatin III **3.18** in 2 mL THF was treated slowly with 0.06 mL LiHMDS at -45 °C and stirred for 4 h, with monitoring by TLC. The reaction was quenched with sat. NH_4Cl, and extracted with EtOAc. Usual work-up gave crude product which was purified by preparative TLC to give 2'-*O*-(triisopropyl)-3'-(*p*-fluorophenyl)-7-*O*-triethylsilyl-4-deacetyl-4-(*d*$_3$-acetyl)-paclitaxel (30 mg). To this compound in 14 mL of THF was added 1 mL HF/pyridine (large excess) and the solution was warmed to rt and stirred overnight. The reaction mixture was diluted with EtOAc and washed with aq. $NaHCO_3$. The organic layer was washed with H_2O and brine, dried over anhydrous Na_2SO_4, and concentrated under reduced pressure. Purification by preparative TLC gave **3.4** (20 mg, 74%). ^{1}H NMR: δ 1.14 (s, 3H), 1.23 (s, 3H), 1.25 (bs, 3H), 1.68 (s, 3H), 1.79 (s, 3H), 1.88 (m, 1H), 2.23 (s, 1H), 2.32 (m, 2H),

2.49-2.58 (m, 2H), 3.77 (bs, 1H), 3.79 (d, *J* = 7.2 Hz, 1H), 4.19 (d, *J* = 8.4 Hz, 1H), 4.30 (d, *J* = 8.4 Hz, 1H), 4.39 (m, 1H), 4.76 (d, *J* = 2.4 Hz, 1H), 4.94 (d, *J* = 9.6 Hz, 1H), 5.69 (d, *J* = 7.2 Hz, 1H), 5.81 (dd, *J* = *2*.4, 8.8 Hz, 1H), 6.30 (t, *J* = 8.4 Hz, 1H), 6.27 (s, 1H), 7.04 (d, *J* = 8.8 Hz, 1H), 7.09 (t, *J* = 8.4 Hz, 2H), 7.39 (t, *J* = 7.6 Hz, 2H), 7.46-7.52 (m, 5H), 7.61 (m, 1H), 7.72 (m, 2H), 8.12 (m, 2H); ^{13}C NMR δ 9.78, 15.13, 21.08, 21.93, 27.10, 35.88, 43.39, 45.89, 54.45, 58.86, 72.44, 72.60, 73.29, 75.11, 75.78, 76.74, 77.46, 79.21, 81.43, 84.60, 115.99, 116.20, 127.27, 128.95, 128.98, 129.12, 129.20, 129.32, 130.42, 132.29, 133.54, 133.69, 133.98, 134.22, 134.25, 142.00, 161.51, 163.98, 167.17, 167.24, 171.46, 172.70, 203.80; HRFABMS: found *m/z* 875.3466, Calcd for $C_{47}H_{48}D_3FNO_{14}$ $(M+H)^+$, *m/z* 875.3482. Δ = 1.8 ppm.

***(3R,4S* + *3S,4R)*-1-(*p*-methoxyphenyl)-3-acetoxyl-4-(*p*-d_3-methyl-phenyl)-azetidin-2-one.** At rt, *p*–anisidine (2 g, 16 mmol) was added to a solution of the *p*-trideuteromethylbenzdaldehyde[36] (2 g, 15 mmol) in CH_2Cl_2 (70 mL) and a large excess of anhydrous $MgSO_4$ (pre-activated at 100 °C for 2 hours) and the mixture was stirred at rt for 12 h. The yellowish slurry was filtered and concentrated under reduced pressure, and the CH_2Cl_2 solution of the crude imine was taken to the next step without purification. The CH_2Cl_2 solution was treated with triethylamine (13 mL) and cooled to -78 ^oC.

Acetoxyacetyl chloride (3.0 mL, 28 mmol) was added dropwise to this solution and the thick reaction mixture was allowed slowly to warm up to rt and stirred for 12 h. The dark crude reaction mixture was concentrated and purified twice by silica gel column chromatography to give (3.7 g, 72%) as colorless needles. ^{1}H NMR ($CDCl_3$): δ 5 7.28 (2H, d, *J* = 8.0 Hz), 7.06 (2H, d, *J* = 8.4 Hz), 6.88-6.82 (overlapped, 4H), 6.10 (1H, d, *J* = 4.0 Hz), 5.15 (1H, d, *J* = 4.0 Hz), 3.62 (3H, s), 2.03 (3H, s); ^{13}C NMR: δ 171.2, 161.9, 156.6, 136.8, 130.2, 128.6, 127.8, 125.2, 117.8, 114.1, 80.4, 62.5, 55.4, 20.8; HRFABMS: found *m/z* 329.1578, Calcd for $C_{19}H_{16}D_3NO_4$ $(M+H)^+$, *m/z* 329.1581, Δ = -1.0 ppm.

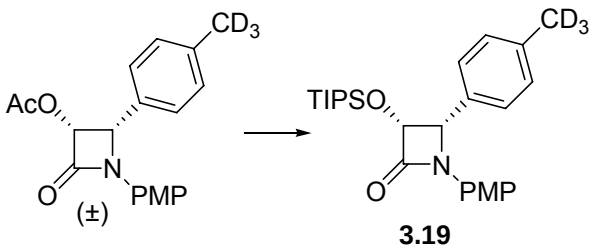

3.19

(3*R*,4*S*)-1-(*p*-methoxyphenyl)-3-3-triisopropylsilyloxy-4-(*p*-trideuteriomethyl-phenyl)-azetidin-2-one (3.19). The above racemic β-lactam (3.0 g, 9.1 mmol) was dissolved in MeCN and a phosphate buffer at pH 7.2 (45 mL) was mixed and stirred vigorously. Immobilized Lipase PS enzyme (Amano) (3.4 g) was added and the mixture was stirred for 7 days. Reaction progress was monitored by TLC, and after completion of the reaction, the lipase was filtered off and the solution was diluted with 100 mL of water and extracted with EtOAc. The combined organic layers were washed with water and brine and then dried over anhydrous Na_2SO_4. Purification by column chromatography gave enantiomerically pure **3.19** (1.5 g, 50% yield) as colorless crystals. $[\alpha]_D^{25}$ = +16.8° ($CHCl_3$, c = 0.32). NMR data were identical to those of racemic β-lactam mixture above.

The solution of enantiomerically pure β-lactam (1.5 g, 4.5 mmol) in THF (50 mL) was added slowly to 50 mL 1 M aqueous KOH solution at 0 ^{o}C. The solution was stirred for 45 min. After the reaction was completed, the reaction mixture was extracted with EtOAc and the organic part was washed with water and brine, and then dried over anhydrous Na_2SO_4. After removal of solvent and drying under vacuum, the product of this reaction (1.38 g, 96%) was used directly for the next step without purification. The crude product was dissolved in 10 mL of DMF, imidazole (1.64 g, 24 mmol) and triisopropyl chloride (2.38 mL, 2.18 g, 12 mmol) were added, and the mixture was stirred at rt for 3 h. The reaction mixture worked up in the usual way. Column chromatography (EtOAc:hexane, 2:8) on silica gel gave silyl protected β–lactam **3.19** (1.83 g, 84.5%) as a white solid. ^{1}H NMR ($CDCl_3$): δ 7.27 (2H, d, *J* = 8.0 Hz), 7.18 (2H, *d, J* = 8.4 Hz), 7.05 (2H, d, *J* = 8.4 Hz), 6.84 (2H, d, *J* = 8.0 Hz), 5.42 (1H, d, *J* = 4.0 Hz), 5.15 (1H, d, *J* = 4.0 Hz), 3.58 (3H, s), 0.94-0.87 (overlapped, 21H); ^{13}C NMR: δ 165.6, 156.5, 137.6, 130.2, 128.6, 127.8, 125.2, 117.1, 115.2, 79.7, 61.4, 55.4, 17.5, 11.8; HRFABMS: found *m/z* 443.2829, Calcd for $C_{26}H_{35}D_3NO_3Si$ $(M+H)^+$, *m/z* 443.2809, Δ = +4.4 ppm.

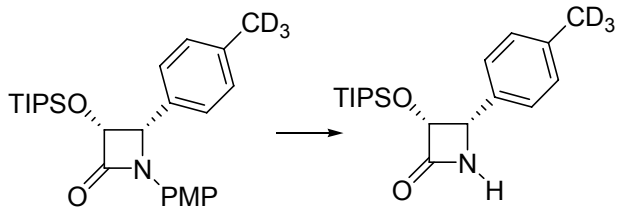

3.19

(3*R*,4*S*)-3-triisopropylsilyloxy-4-(*p*-trideuteriomethylphenyl)-azetidin-2-one. A solution of CAN (1.36 g, 2.5 mmol) in 15 mL water was added dropwise to a solution of **3.19** (0.52 g, 1.2 mmol) in CH_3CN (25 mL) at -5 ^{o}C. The reaction mixture was stirred for 45 min until TLC indicated the consumption of the starting material. Then the mixture was diluted with EtOAc and washed with saturated aqueous $NaHCO_3$, water, saturated

sodium metabisulfite and brine, and then the organic layer was dried over Na_2SO_4. The crude product was chromatographed on silica gel to give the deprotected β-lactam oil (213 mg, 55% yield). ^{1}H NMR: δ 7.19 (2H, d, *J* = 8.0 Hz), 7.11 (2H, d, *J* = 8.0 Hz), 5.08 (m, 1H), 4.72 (d, 1H, *J* = 5.5 Hz), 0.94-0.86 (overlapped, 21H); ^{13}C NMR: δ 170.6, 137.6, 133.4, 128.6, 128.2, 79.7, 59.7, 17.5, 11.8; HRFABMS: found *m/z* 337.2384, Calcd for $C_{19}H_{29}D_3NO_2Si$ $(M+H)^+$ *m/z* 337.2391, Δ = -2.1 ppm.

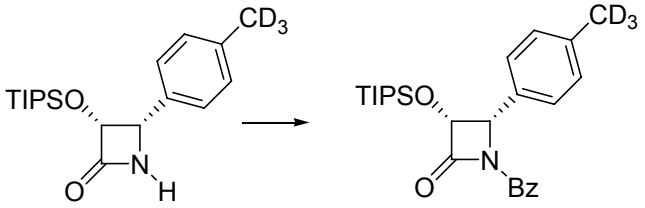

3.20

(3*R*,4*S*)-1-benzoyl-3-triisopropylsilyloxy-4-(*p*-trideuteriomethylphenyl)-azetidin-2-one (3.20). To a solution of deprotected β-lactam (182 mg, 0.54 mmol) in anhydrous CH_2Cl_2 (1 mL) at 0 ^{o}C, triethylamine (190 µl) and benzoyl chloride (92 µl, 0.79 mmol) were added. The mixture was then stirred at rt for 3 h, diluted with EtOAc, washed with saturated aqueous $NaHCO_3$ and brine, and dried over Na_2SO_4. The crude product was purified by chromatography to give the β–lactam **3.20** oil (234 mg, 98% yield). $[\alpha]_D^{25}$ = +86.4° ($CHCl_3$, c = 0.17); ^{1}H NMR: δ 8.05 (dd, 2H, *J* = 8.0, 1.5 Hz), 7.59 (m,1H), 7.48 (2H, t, *J* =8.0 Hz), 7.31 (2H, dd, *J* = 8.5, 1.0 Hz), 7.17 (2H, dd, *J* = 8.5, 1.0 Hz), 5.41 (1H, d, *J* = 6.0 Hz), 5.23 (1H, d, *J* = 6.0 Hz), 0.98-0.88 (overlapped, 21H); ^{13}C NMR: δ 166.3, 165.7, 138.0, 133.3, 132.4, 131.0, 129.9, 128.9, 128.3, 128.2, 76.6, 61.2, 17.5, 17.4, 11.8 ppm; HRFABMS: found *m/z* 441.2664, Calcd for $C_{26}H_{33}D_3NO_3Si$ $(M+H)^+$, *m/z* 441.2653, Δ = 2.3 ppm.

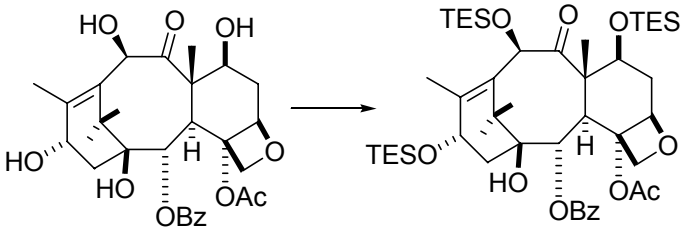

3.13

7,10,13-tris(triethylsilyl)-10-deacetylbaccatin III. To the solution of 10-deacetylbaccatin III **3.13** (800 mg, 1.8 mmol) in 5 mL of DMF was added imidazole (1.15 g, 17 mmol) and triethylsilyl chloride (1.5 mL, 8.6 mmol) and the mixture was stirred at rt for 3 h. The reaction mixture was diluted with EtOAc (50 mL) and the combined organic layer was washed with saturated aqueous $NaHCO_3$ and brine, and dried over Na_2SO_4. Column chromatography on silica gel gave compound tri-TES 10-DAB III (989 mg, 76%) as a white solid. ^{1}H NMR: δ 8.07 (2H, dd, *J* = 8.0, 1.5 Hz), 7.56 (1H, t, *J* = 8.0 Hz), 7.45(2H, t, *J* = 8.0 Hz) , 5.60(1H, d, *J* = 6.0 Hz), 5.17 (1H, s), 4.93 (1H, dd, *J* =9.0, 2.5 Hz), 4.42 (1H, dd, *J* = 7.5, 1.5 Hz), 4.26 (1H, d, *J* = 8.5 Hz), 4.11 (1H, dd, *J* = 9.0, 2.0 Hz), 4.08 (1H, dd, *J* = 9.5, 2.5 Hz), 3.83 (1H, d, *J* = 7.0 Hz), 2.48 (1H, m), 2.26 (3H, s), 2.01 (3H, s), 1.62 (3H, s), 1.17 (3H, s), 1.10 (3H, s), 0.98-0.96 (overlapped, 27H), 0.62-0.60 (overlapped, 18H); ^{13}C NMR: δ 209.0, 170.0, 167.2, 139.5, 133.5, 130.1, 128.6, 84.1, 80.9, 79.6, 76.8, 76.7, 75.8, 75.6, 72.7, 68.4, 58.3, 47.0, 43.1, 39.9, 37.4, 26.4, 22.4, 20.7, 14.6, 14.2, 10.5, 7.0-6.9 (overlapped), 5.75, 5.44, 5.12; HRFABMS: found *m/z* 887.5047, Calcd for $C_{47}H_{79}O_{10}Si_3$ $(M+H)^+$, *m/z* 887.4981, Δ = +7.4 ppm.

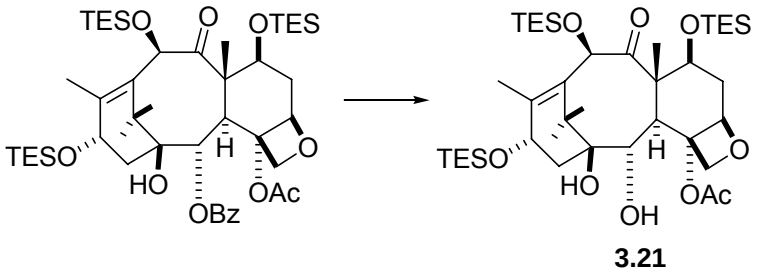

3.21

2-debenzoyl-7,10,13-tris(triethylsilyl)-10-deacetylbaccatin III (3.21). To a solution of tri-TES 10-DAB III (750 mg, 0.84 mmol) in anhydrous THF (15 mL) at -20 °C, Red-Al (4M in THF, 1.1 mL) was added dropwise under nitrogen. The reaction was stirred for 45 min until TLC showed the exhaustion of starting material. After quenching with a few drops of water, the reaction mixture was added to 50 mL of 1M sodium potassium tartrate and extracted with EtOAc. The organic part was washed with water and brine, and dried over Na_2SO_4. Column chromatography on silica gel gave compound **3.21** (484 mg, 72%). ^{1}H NMR δ 5.14 (1H, s), 4.72 (1H, d, *J* = 7.0 Hz), 4.63 (1H, dd, *J* = 9.5, 4.0 Hz), 4.42 (1H, dd, *J* = 7.5, 1.5 Hz), 4.56 (1H, d, *J* = 9.0 Hz), 4.11 (1H, m), 3.98 (1H, dd, *J* = 10.5, 6.0 Hz), 3.74(1H, dd, *J* =10.5, 5.5 Hz), 3.45 (1H, d, *J* = 10.5 Hz), 3.23 (1H, d, *J* = 6.0 Hz), 2.45-2.37 (3H, overlapped, m), 2.08 (3H, s), 1.98 (3H,s), 1.78 (3H, s), 1.04 (3H, s), 1.01 (3H, s), 0.97-0.94 (overlapped, 27H), 0.63-0.60 (overlapped, 18H); ^{13}C NMR δ 206.3, 169.7, 139.0, 136.0, 83.7, 82.0, 78.7, 78.0, 76.8, 75.8, 74.7, 72.7, 68.4, 58.2, 46.8, 42.5, 40.4, 37.4, 26.0, 22.4, 20.6, 14.5, 10.6, 6.9-6.8 (overlapped), 5.21, 5.13, 4.82.

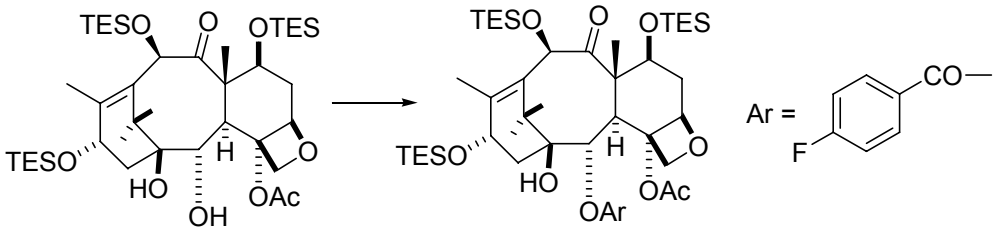

2-debenzoyl-2-(*p*–fluorobenzoyl)-7,10,13-tris(triethylsilyl)-10-deacetylbaccatin III (3.22). *N,N'*–diisopropylcarbodiimide (0.85 mL, 5.5 mmol) and DMAP (660 mg, 5.4 mmol) were added to a solution of *p*–fluorobenzoic acid (757 mg, 5.4 mmol) in dry toluene (10 mL)**,** the heterogenous mixture was stirred at rt for 0.5 h, then compound **3.21** (200 mg, 0.026 mmol) in 5 mL of toluene was added dropwise. The solution was stirred

for 10 min. at rt and heated to 55 °C for 24 h. The reaction mixture was diluted with EtOAc and washed with H_2O and $NaHCO_3$. The combined organic phase was washed with H_2O and brine, dried over anhydrous Na_2SO_4, and concentrated under reduced pressure. Column chromatography gave **3.22** (223 mg, 73%) as a white solid . ^{1}H NMR δ 8.08 (2H, dd, *J* = 8.5, 5.5 Hz), 7.07 (2H, dd, *J* = 8.5, 8.0 Hz), 5.65 (1H, d, *J* = 5.6 Hz) , 5.08 (1H, s), 4.96 (dd, *J* = 9.0, 2.5 Hz), 4.42 (1H, dd, *J* = 7.5, 1.5 Hz), 3.82 (1H, d, *J* = 7.0 Hz), 2.83 (overlapped, m, 2H), 2.18 (m, 2H), 2.14 (3H, s), 1.90 (3H, s), 1.63 (m, 1H), 1.53 (3H, s), 1.32 (3H, s), 1.20 (3H, s), 1.09 (3H, s), 0.98-0.92 (overlapped, 27H), 0.61-0.59 (overlapped, 18H); ^{13}C NMR δ 206.8, 171.3, 164.4, 159.6, 139.5, 137.9, 132.4, 132.3, 116.2, 116.0, 90.2, 86.6, 77.1, 73.2, 2.6, 70.9, 68.8, 55.8, 43.2, 41.0, 38.1, 25.4, 22.5, 21.1, 14.5, 10.8, 7.0, 5.8, 5.7, 5.4; HRFABMS: found *m/z* 903.4713, Calcd for $C_{47}H_{78}FO_{10}Si_3$ $(M+H)^+$, *m/z* 903.4730, Δ = -1.9 ppm.

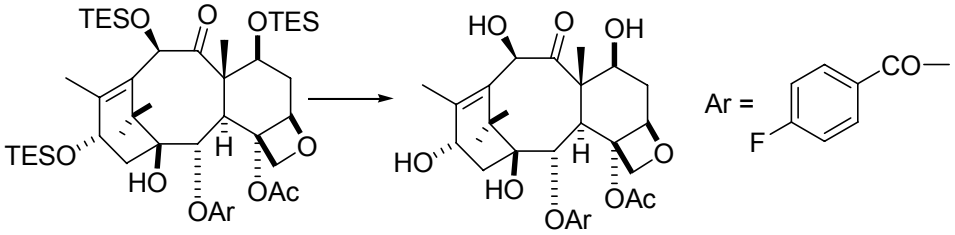

3.22 **3.23**

2-debenzoyl-2-(*p*–fluorobenzoyl)-10-deacetylbaccatin III (3.23). At 0 °C, HF/pyridine (70 wt%, 1.0 mL) was added to a solution of **3.22** (220 mg, 0.24 mmol) in 2.5 mL of THF and the solution was stirred at rt for 10 h. The reaction mixture was diluted with EtOAc and washed with aqueous $NaHCO_3$ solution. The organic layer was washed with water and brine, dried over anhydrous Na_2SO_4, and evaporated under reduced pressure. The residue was purified by chromatography on silica gel to yield **3.23** (128 mg, 94%) as colorless crystals. ^{1}H NMR: δ 8.08 (2H, dd, *J* = 8.5, 5.5 Hz), 7.14 (2H, dd, *J* = 8.5, 8.0

Hz), 5.58 (1H, d, *J* = 5.6 Hz), 4.95 (dd, *J* = 9.0, 2.5 Hz), 4.80 (1H, t, *J* = 7.5 Hz), 4.42 (1H, dd, *J* = 7.5, 1.5 Hz), 3.82 (1H, d, *J* = 7.0 Hz), 2.83 (overlapped, m, 2H), 2.18 (m, 2H), 2.14 (3H,s), 1.90 (3H, s), 1.63 (m, 2H), 1.32 (3H, s), 1.20 (3H, s), 1.09 (3H, s); ^{13}C NMR: δ 208.4, 170.6, 164.4, 158.7, 139.5, 137.9, 132.4, 132.3, 116.2, 116.0, 90.2, 86.6, 77.1, 73.2, 2.6, 70.9, 68.8, 55.8, 43.2, 41.0, 38.1, 25.4, 22.5, 21.1, 14.5, 10.5., 6.9, 5.8; HRFABMS: found *m/z* 563.2285, Calcd for $C_{29}H_{36}FO_{10}$ *m/z* 563.2293, Δ = -1.4 ppm.

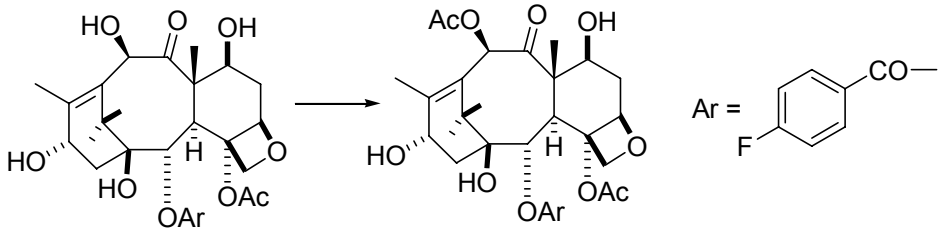

3.23 **3.24**

2-debenzoyl-2-(*p*-fluorobenzoyl)-baccatin III (3.24). To a solution of **3.23** (120 mg, 0.21 mmol) in 1 mL of anhydrous THF was added 5 mg of $CeCl_3$ at rt. The mixture was stirred for 5 min and then acetic anhydride (0.18 mL) was added and stirring continued at rt for 1 h. The reaction mixture was diluted with EtOAc. The organic layer was washed with saturated aqueous $NaHCO_3$, water and brine, and dried with Na_2SO_4. The residue was purified on silica gel chromatography to yield **3.24** (113 mg, 90%). ^{1}H NMR δ 8.09 (2H, dd, *J* = 8.5, 5.5 Hz), 7.12 (2H, ddd, *J* = 8.5 and 2.0), 6.30 (1H, s), 5.56 (1H, *d, J* = 7.0 Hz), 4.96 (dd, *J* = 9.5, 2.0 Hz), 4.85 (1H, *t, J* = 8.0), 4.45 (1H, dd, *J* = 7.5, 1.5 Hz), 4.24 (1H, *d, J* = 8.5 Hz), 4.12 (1H, *d, J* = 8.5 Hz), 3.84 (1H, *d, J* = 7.0 Hz), 3.75 (1H, br, s), 2.60-2.53 (overlapped, m, 3H), 2.24 (3H, s), 2.21 (3H, s), 2.02 (3H, s), 1.84 (m, 1H), 1.63 (3H, s), 1.08 (3H, s), 1.06 (3H, s); ^{13}C NMR δ 204.2, 171.4, 171.3, 170.6, 166.1, 165.2, 146.8, 132.8, 132.7, 131.7, 125.8, 125.7, 116.0, 115.8, 84.5, 80.8, 79.1, 76.4, 76.3, 75.2, 72.3, 67.8, 60.4, 58.7, 46.2, 42.7, 38.6, 35.6, 26.9, 22.6, 21.1, 21.0, 20.9, 15.6, 14.2, 9.47;

HRFABMS: found *m/z* 605.2384, Calcd for $C_{31}H_{38}FO_{11}$ $(M+H)^+$, *m/z* 605.2398, Δ = -2.4 ppm.

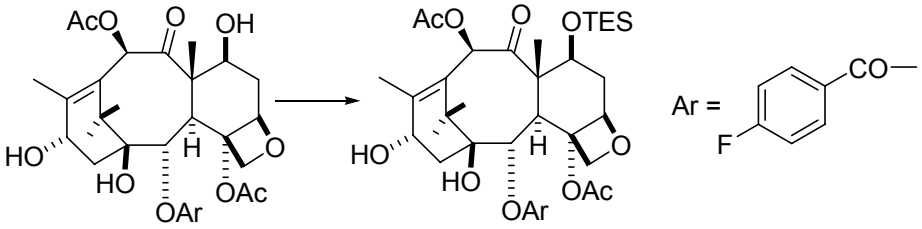

3.24 **3.25**

2-debenzoyl-2-(*p*–fluorobenzoyl)-7-(triethylsilyl)-baccatin III (3.25). To a solution of **3.24** (80 mg, 0.013 mmol) in DMF (4 mL) at 0 ^oC was added imidazole (27 mg, 0.4 mmol) and chlorotriethylsilane (40 μL, 0.2 mmol). The progress of the reaction was carefully monitored to avoid the side reaction on the C-13 hydroxyl group. After 2 h the reaction was completed and the mixture was diluted with 20 mL of EtOAc and quenched with saturated aqueous $NaHCO_3$. The organic layer was washed with saturated aqueous $NaHCO_3$, water and brine, and dried over Na_2SO_4. The crude product was purified by preparative silica gel TLC with to give **3.25** (82 mg, 80%) as a glassy solid. ^1H NMR: δ 8.11 (2H, dd, *J* = 8.5, 5.5 Hz), 7.14 (2H, dd, *J*= 8.5, 8.0 Hz), 6.47 (1H, s), 5.60 (1H, *d, J* = 7.0 Hz), 4.95 (dd, *J* = 9.0, 2.5 Hz), 4.82 (1H, t, *J* = 7.5 Hz), 4.46 (1H, dd, *J* =7.5, 1.5 Hz), 4.27 (1H, d, *J* = 8.0 Hz), 4.10 (1H, d, *J* = 8.0 Hz), 3.87 (1H, d, *J* = 7.0 Hz), 3.75 (1H, br, s), 2.53 (overlapped, m, 3H), 2.26 (3H, s), 2.18 (3H, s), 2.17 (3H, s), 1.84 (m, 1H), 1.66 (3H, s), 1.18 (3H, s), 1.03 (3H, s), 0.92-0.89 (9H, overlapped), 0.58-0.55 (6H, overlapped); ^{13}C NMR δ 204.2, 171.4, 171.3, 170.6, 166.1, 165.2, 146.8, 132.8, 132.7, 131.7, 125.8, 125.7, 116.0, 115.8, 84.5, 80.8, 79.1, 76.4, 76.3, 75.2, 72.3, 67.8, 60.4, 58.7,

46.2, 42.7, 38.6, 35.6, 26.9, 22.6, 21.1, 21.0, 20.9, 15.6, 14.2, 9.5, 7.0, 5.56; HRFABMS: found *m/z* 719.3266, Calcd for $C_{37}H_{52}FO_{11}Si$ $(M+H)^+$, *m/z* 719.3263, Δ = 0.5 ppm.

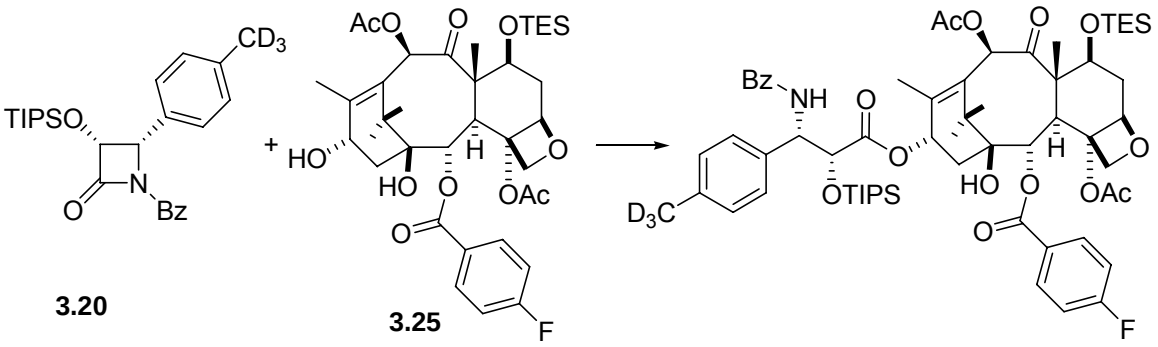

3´-dephenyl-3´-(*p*-trideuteriomethylphenyl)-2-(debenzoyl)-2(*p*-flurobenzoyl)-2´-(triisopropylsilyl)-7-(triethylsilyl)-paclitaxel. To a solution of **3.25** (19 mg, 0.026 mmol) in THF (1 mL) at -20 °C was added LHMDS (2.5 M in THF, 40 μl) and the mixture was stirred for 10 min. A solution of β-lactam **3.20** (13 mg, 0.16 mmol) in THF (1 mL) was added slowly. The reaction mixture was stirred for 4 h until TLC showed the complete reaction of the starting material. Then 1 mL of saturated aqueous NH_4Cl was added and the mixture was extracted with EtOAc. The organic layer was washed with water and brine and then dried under reduced pressure. The crude reaction product was purified on preparative TLC to give the protected labeled paclitaxel (14.5 mg, 54% yield). ^{1}H NMR: δ 8.15 (2H, dd, *J* = 8.5, 5.0 Hz), 7.72 (2H, dd, *J* = 8.0, 1.5 Hz), 7.37 (m, 2H), 7.21-7.16 (7H, overlapped), 6.44 (1H, s), 6.21 (1H, t, *J* = 8.0 Hz), 5.68 (1H, d, *J* = 7.0 Hz), 5.65 (1H, d, *J* = 7.0 Hz), 4.92 (2H, m), 4.48 (1H, dd, *J* = 10.5, 7.0 Hz), 4.27 (1H, d, *J* = 8.5 Hz), 4.19 (1H, d, *J* = 8.5 Hz), 3.83 (1H, d, *J* = 7.0 Hz), 2.53 (1H, m), 2.24 (3H, s), 2.18 (2H, m), 2.05 (3H, s), 1.92 (1H, m), 1.68 (3H, s), 1.21 (3H, s), 1.02 (3H, s), 0.92-

0.89 (30H, overlapped), 0.62-0.60 (6H, overlapped); ^{13}C NMR δ 204.2, 171.4, 171.3, 170.6, 166.1, 165.2, 146.8, 132.8, 132.7, 131.7, 125.8, 125.7, 116.0, 115.8, 84.5, 80.8, 79.1, 76.4, 76.3, 75.2, 72.3, 67.8, 60.4, 58.7, 46.2, 42.7, 38.6, 35.6, 26.9, 22.6, 21.1, 21.0, 20.9, 15.6, 14.2, 11.7, 9.47, 6.9, 5.5 ppm; HRFABMS: found *m/z* 1143.5867, Calcd for $C_{63}H_{84}D_3FNO_{14}Si_2$ $(M+H)^+$, *m/z* 1143.5888, **Δ =** -1.9 ppm.

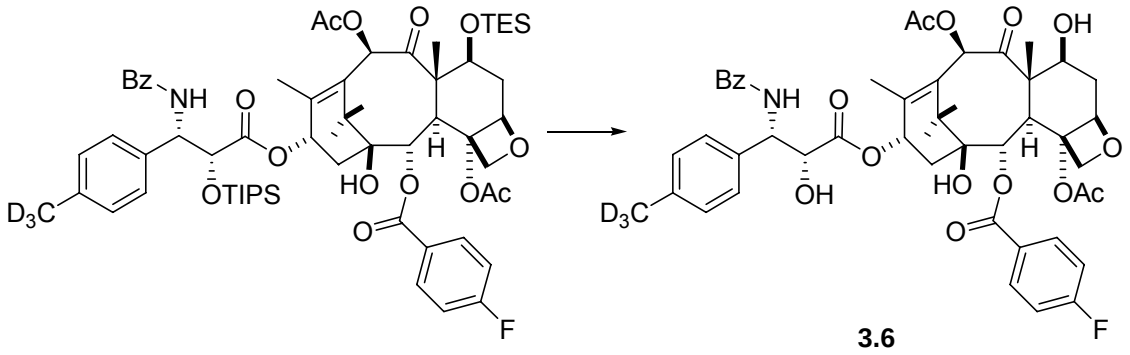

3.6

3´-dephenyl-3´-(*p*-trideuteriomethylphenyl)-2-(debenzoyl)-2-(*p*-flurobenzoyl)-paclitaxel (3.6). HF/pyridine (70 wt%, 1.5 mL, large excess) was added to a solution of the above protected labeled paclitaxel (11 mg, 0.01 mmol) in THF (1.0 mL) and the solution was stirred at rt for 3 h. The reaction mixture was diluted with EtOAc and washed with aqueous $NaHCO_3$ solution. The organic layer was washed with water and brine, dried over anhydrous Na_2SO_4, and concentrated under reduced pressure. The residue was purified by preparative TLC to afford the desired product **3.6** (8.5 mg, 87%). ^{1}H NMR δ 8.16 (2H, dd, *J* = 8.5, 5.0 Hz), 7.70 (2H, dd, *J* = 8.0, 1.5 Hz), 7.47 (m, 1H), 7.38 (4H, m), 7.22-7.16 (4H, overlapped), 6.88 (1H, d, *J* = 8.5 Hz), 6.26 (1H, s), 6.24 (1H, t, *J* = 8.0 Hz), 5.76 (1H, dd, *J* =7.0, 2.5 Hz), 5.64 (1H, d, *J* = 7.0 Hz), 4.94 (1H, dd, *J* = 9.0, 2.0 Hz), 4.78 (1H, s), 4.41 (1H, m), 4.28 (1H, d, *J* = 8.5 Hz), 4.18 (1H, d, *J* = 8.5 Hz), 3.80 (1H, d, *J* = 7.0 Hz), 3.51 (1H, m, br), 2.55 (1H, m), 2.44-2.40 (2H, m), 2.38 (3H, s), 2.24 (3H, s), 2.18 (2H, m), 1.92 (1H, m), 1.81 (3H, s), 1.63 (3H, s), 1.13 (3H, s),

1.06 (3H, s). ^{13}C NMR δ 203.7, 173.0, 171.4, 167.3, 166.1, 142.7, 133.8, 133.1, 133.0, 132.9, 132.1, 129.9, 128.8, 127.1, 126.9, 116.1, 116.0, 84.5, 81.2, 79.2, 75.6, 75.2, 73.2, 72.4, 72.2, 68.1, 58.7, 54.8, 45.6, 43.2, 35.8, 35.6, 26.9, 22.7, 20.9, 14.9, 9.65ppm; HRFABMS: found *m/z* 911.3443, Calcd for $C_{48}H_{49}D_3FNO_{14}Na$, $(M+Na)^+$, *m/z* 911.3459, **Δ=** -1.8 ppm.

References:

1. Nogales, E.; Wolf, S. G.; Zhang, S. X.; Downing, K. H. Preservation of 2-D crystals of tubulin for electron crystallography. *J. Struct. Biol.* **1995,** *115*, 199-208
2. Nogales, E.; Wolf, S. G.; Khan, I. A.; Luduena, R. F.; Downing, K. H. Structure of tubulin at 6.5 Å and location of the taxol-binding site. *Nature* **1995,** *375*, 424-427.
3. Nogales, E.; Wolf, S. G.; Downing, K. H. Visualizing the secondary structure of tubulin: Three dimensional map at 4 Å. *J. Struct. Biol.* **1997,** *118*, 119-127.
4. Lowe, J.; Li, H.; Downing, K. H.; Nogales, E. Refined structure of α,β-tubulin at 3.5 Å resolution. *J. Mol. Biol.* **2001,** *313*, 1045-1057.
5. Geney, R.; Sun, L.; Pera, P.; Bernacki, R. J.; Xia, S.; Horwitz, S. B.; Simmerling, C. L.; Ojima, I. Use of the tubulin bound paclitaxel conformation for structure-based rational drug design. *Chem. Biol.* **2005,** *12*, 339-348.
6. Falzone, C. J.; Benesi, A. J.; Lecomte, T. J. Characterization of taxol in methylene chloride by NMR spectroscopy. *Tetrahedron Lett.* **1992,** *33*, 1169-1172.

7. Gueritte-Voegelein, F.; Guenard, D.; Lavelle, F.; Goff, M.-T. L.; Mangatal, L.; Potier, P. Relationships between the structure of taxol analogues and their antimitotic activity. *J. Med. Chem.* **1991,** *34*, 992-998.

8. Williams, H. J.; Scott, A. I.; Dieden, R. A.; Swindell, C. S.; Chirlian, L. E.; Francl, M. M.; Heerding, J. M.; Krauss, N. E. NMR and molecular modeling study of the conformations of taxol and of its side chain methylester in aqueous and non-aqueous solution. *Tetrahedron* **1993,** *49*, 6545-6560.

9. Cachau, R. E.; Gussio, R.; Beutler, J. A.; Chmurny, G. N.; Hilton, B. D.; Muschik, G. M.; Erickson, J. W. Solution structure of taxol determined using a novel feedback-scaling procedure for noe-restrained molecular dynamics. *Supercomput. Appl. High Perform. Comput.* **1994,** *8*, 24-34.

10. Vander Velde, D. G.; Georg, G. I.; Grunewald, G. L.; Gunn, C. W.; Mitscher, L. A. "Hydrophobic collapse" Of taxol and taxotere solution conformations in mixtures of water and organic solvent *J. Am. Chem. Soc.* **1993,** *113*, 11650-11651.

11. Ojima, I.; Inoue, T.; Chakravarty, S. Enantiopure fluorine-containing taxoids: potent anticancer agents and versatile probes for biomedical problems. *J. Fluorine Chem.* **1999,** *97*, 3-10.

12. Rao, S.; He, L.; Chakravarty, S.; Ojima, I.; Orr, G. A.; Horwitz, S. B. Characterization of the taxol binding site on the microtubule. *J. Biol. Chem.* **1999,** *274*, 37990-37994.

13. Paik, Y.; Yang, C.; Metaferia, B.; Tang, S.; Bane, S.; Ravindra, R.; Shanker, N.; Alcaraz, A. A.; Johnson, S. A.; Schaefer, J.; O'Connor, R. D.; Cegelski, L.;

Snyder, J. P.; Kingston, D. G. I. Rotational-echo double-resonance NMR distancemeasurements for the tubulin-bound paclitaxel conformation. *J. Am. Chem. Soc.* **2007,** *129*, 361-370

14. Snyder, J. P.; Nevins, N.; Cicero, D. O.; Jansen, J. The conformations of taxol in chloroform. *J. Am. Chem. Soc.* **2000,** *122*, 724-725.

15. Ivery, T. G. M.; Le, T. Modeling the interaction of paclitaxel with β-tubulin. *Oncol. Res.* **2003,** *14*, 1-19.

16. Aspland, S. E.; Ballatore, C.; Castillo, R.; Desharnais, J.; Eustaquio, T.; Goelet, P.; Guo, Z.; Li, Q.; Nelson, D.; Sun, C.; Castellino, A. J.; Newman, M. J. Kinase-mediated trapping of bi-functional conjugates of paclitaxel or vinblastine with thymidine in cancer cells. *Bioorg. Med. Chem. Lett.* **2006,** *16*, 5194-5198.

17. Li, Y.; Poliks, B.; Cegelski, L.; Poliks, M.; Gryczynski, Z.; Piszczek, G.; Jagtap, P. G.; Studelska, D. R.; Kingston, D. G. I.; Schaefer, J.; Bane, S. Conformation of microtubule-bound paclitaxel determined by fluorescence spectroscopy and REDOR NMR. *Biochemistry* **2000,** *39*, 281-291.

18. Alcaraz, A. A.; Mehta, A. K.; Johnson, S. A.; Snyder, J. P. The T-taxol conformation. *J. Med. Chem.* **2006,** *49*, 2478-2488.

19. Fesik, S. W.; O'Donnell, J. O.; Gampe, R. T., Jr.; ; Olejniczak, E. T. Determining the structure of a glycopeptide Ac_2-Lys-D-Ala-D-Ala complex using NMR parameters and molecular modeling. *J. Am. Chem. Soc.* **1986,** *108*, 3165-3170.

20. Mierke, D. F.; Kurz, M.; Kessler, H. Peptide flexibility and calculations of an ensemble of molecules. *J. Am. Chem. Soc.* **1994,** *116*, 1042-1049.

21. Mierke, D. F.; Scheek, R. M.; Kessler, H. Coupling constant restraints in ensemble calculations. *Biopolymers* **1994,** *34*, 559-563.

22. Cicero, D. O.; Barbato, G.; Bazzo, R. NMR analysis of molecular flexibility in solution: A new method for the study of complex distributions of rapidly exchanging conformations. Application to a 13-residue peptide with an 8-residue loop. *J. Am. Chem. Soc.* **1995,** *117*, 1027-1033.

23. Metaferia, B. B.; Hoch, J.; Glass, T. E.; Bane, S. L.; Chatterjee, S. K.; Snyder, J. P.; Lakdawala, A.; Cornett, B.; Kingston, D. G. I. Synthesis and biological evaluation of novel macrocyclic paclitaxel analogues. *Org. Lett.* **2001,** *3*, 2461-2464.

24. Ganesh, T.; Guza, R. C.; Bane, S.; Ravindra, R.; Shanker, N.; Lakdawala, A. S.; Snyder, J. P.; Kingston, D. G. I. The bioactive taxol conformation on β-tubulin: Experimental evidence from highly active constrained analogs. *Proc. Natl. Acad. Sci. U.S.A.* **2004,** *101*, 10006-10011.

25. Klebe, G. Toward a more efficient handling of conformational flexibility in computer-assisted modelling of drug molecules. *Perspect. Drug Discovery Des.* **1995,** *3*, 85-105.

26. Ganesh, T.; Guza, R. C.; Bane, S.; Ravindra, R.; Shanker, N.; Lakdawala, A. S.; Snyder, J. P.; Kingston, D. G. I. The bioactive taxol conformation on β-tubulin: Experimental evidence from highly active constrained analogs. *Proc. Natl. Acad. Sci USA* **2004,** *101*, 10006-10011.

27. Gueritte-Voegelein, F.; Guenard, D.; Lavelle, F.; Goff, M.-T. L.; Mangatal, L.; Potier, P. Relationships between the structure of taxol analogues and their antimitotic activity. *J. Med. Chem.* **1991,** *34*, 992-998.

28. Lowe, J.; Li, H.; Downing, K. H.; Nogales, E. Refined structure of αβ-tubulin at 3.5 Å resolution. *J. Mol. Biol.* **2001,** *313*, 1045-1057.

29. Snyder, J. P.; Nettles, J. H.; Cornett, B.; Downing, K. H.; Nogales, E. The binding conformation of Taxol in β-tubulin: A model based on electron crystallographic density. *Proc. Natl. Acad. Sci. U.S.A.* **2001,** *98*, 5312-5316.

30. Beusen, D. D.; McDowell, L. M.; Slomczynska, U.; Schaefer, J. Solid-state nuclear magnetic resonance analysis of the conformation of an inhibitor bound to thermolysin. *J. Med. Chem.* **1995,** *38*, 2742-2747.

31. Gullion, T.; Schaefer, J. Detection of weak heteronuclear dipolar coupling by rotational-echo double-resonance nuclear magnetic resonance. *Adv. Magn. Reson.* **1989,** *13*, 58-82.

32. Gullion, T.; Schaefer, J. Rotational-echo double-resonance NMR. *J. Magn. Reson.* **1989,** *81*, 196-200.

33. Carr, J. A.; Al-Azemi, T. F.; Long, T. E.; Shim, J.-Y.; Coates, C. M.; Turos, E.; Bisht, K. S. Lipase catalyzed resolution of 4-aryl substituted ,β-lactams: effect of substitution on the 4-aryl ring. *Tetrahedron* **2003,** *59*, 9147-9160, and references cited therein.

34. Brieva, R.; Crich, J. Z.; Sih, C. J. Chemoenzymatic synthesis of the C-13 side chain of taxol: optically active 3-hydroxy-4-phenyl, β-lactam derivatives. *J. Org. Chem.* **1993,** *58*, 1068-1075.

35. Chen, S. H.; Kadow, J. F.; Farina, V. First syntheses of novel paclitaxel(taxol) analogs modified at the C4-position. *J. Org. Chem.* **1994,** *59*, 6156-6158.

36. Atkinson, J. G.; Csakvary, J. J.; Herbert, G. T.; Stuart, R. S. Exchange reactions of carboxylic acid salts. Facile preparation of α-deuteriocarboxylic acids. *J. Am. Chem. Soc.* **1968,** *90*, 498-499.

Chapter 4. Conformationally constrained paclitaxel analogs

4.1 Introduction

Studies of the tubulin bound conformation of paclitaxel are crucial because they unveil the bioactive structure of PTX for further rational drug design. Unfortunately, as mentioned before, the electron crystallography (EC) structure of the α,β–tubulin heterodimer bound to PTX[1] lacks the resolution to unambiguously ascertain the structure of PTX in the β–tubulin binding pocket.[2] To date, many PTX conformers have been proposed as the bioactive conformation.[3] The REDOR NMR studies[4,5] described in the previous chapter disproved most proposed conformers, leaving the T-Taxol conformation as the most probable one.

The ultimate approach to investigating the conformation of paclitaxel bound to tubulin is the biological evaluation of paclitaxel analogs with additional conformational restrictions.[6] If the conformationally constrained PTX derivatives mimic the bioactive conformation, they should show both tubulin polymerization and cytotoxic bioactivities equal to or greater than PTX itself, because introducing the conformational constraints would lower the conformational entropy loss upon binding.[2] Previous studies of the bioactive conformation have suggested 'nonpolar' or 'polar' models for the bioactive conformation. A number of elegant synthetic studies of constrained analogs designed to mimic these conformations have been achieved, including the synthesis of analogs with conformationally restricted side chains and studies of analogs with bridges linking the C–3' and C–2 phenyls with both shorter **4.1** and longer **4.2** linkers.

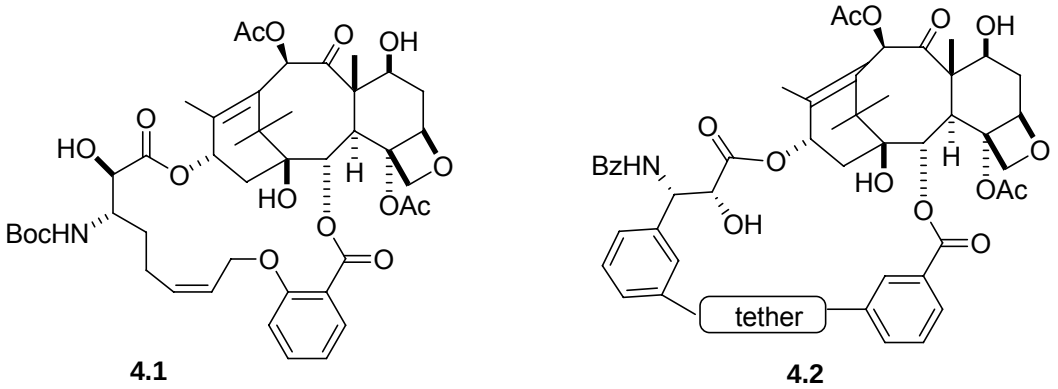

Figure 4.1 Structure of bridged PTX analogs

However, to date, most constrained analogues synthesized based on these models were either inactive or much less active than paclitaxel itself in both tubulin polymerization and cytotoxicity assays.[2] As mentioned above, REDOR NMR results suggest that neither the 'nonpolar' nor the 'polar' conformers represent the bioactive conformation of paclitaxel. The loss of activity when PTX is constrained to these conformers further confirms this conclusion.

Couple of PTX derivatives (Figure 4.2) were synthesized by Ojima based on the REDOR-Taxol conformation. The derivative with a bridge linking C14 and the C3' N-benzoyl group (**4.3b**) was more active than previous bridged compounds, but it was still 3-fold less active than paclitaxel in certain cell lines.[2] Compared with other conformationally constrained PTX analogs, it was a considerable improvement, but it failed to provide proof that REDOR-Taxol is the bioactive conformation.

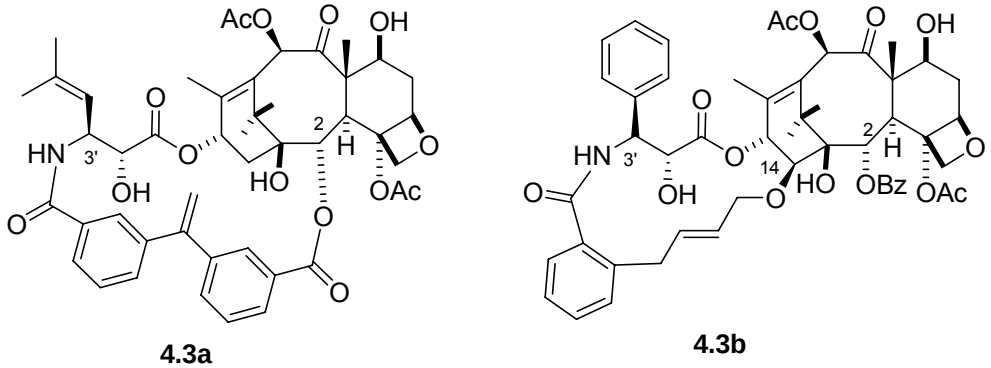

Figure 4.2 Structure of bridged PTX analogs based on REDOR-Taxol conformer

Some macrocyclic PTX derivatives designed to mimic the T-Taxol conformation have been synthesized in our group. According to molecular modeling of the T-Taxol conformer, the acetate group at the C4 position is 2.5-2.9 Å and 4.3-4.9 Å from the *ortho* and *meta* hydrogens of the C3' phenyl group, respectively.[6] Therefore, structural analysis forecast that a tether linking the C4 acetate and the C3' phenyl would reduce conformational mobility and lock the structure into the T-Taxol conformer. Initially, a series of macrocyclic PTX bislactone derivatives **4.4** was prepared to test the T-Taxol hypothesis.[7] Remarkably, all the bridged compounds were more cytotoxic than their corresponding open-chain analogs, although the desired macrocylic PTX lactones were less active than PTX. One reason might be the unstable nature of macrocyclic lactones, which are prone to rearrange to the corresponding inactive macrocyclic isomers **4.5**.[7]

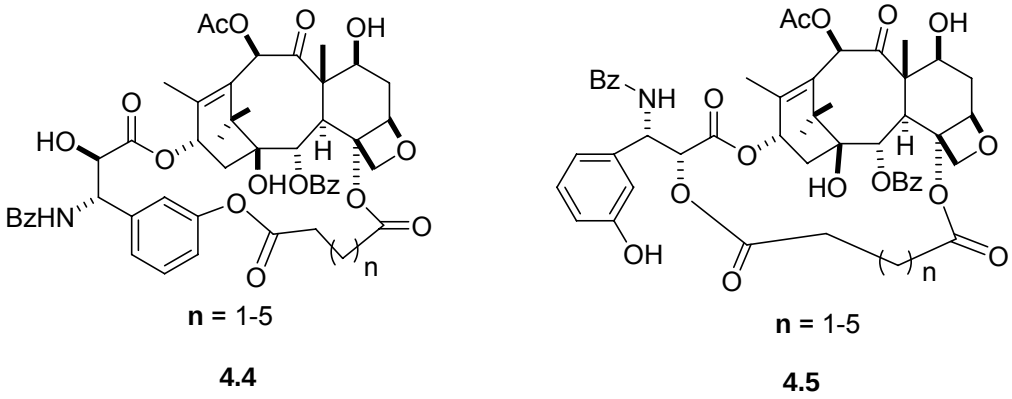

Figure 4.3 Structure of bridged PTX analogs based on T-Taxol conformer

To circumvent the lactone issue, it was decided to use an ether linkage. Two proof-of-principle PTX derivatives (**4.6**, **4.7** in Figure 4.4) connecting the *meta* position of C3' phenyl and the C4 methyl with three and five atom bridges were prepared. Surprisingly, both derivatives proved much less active than PTX.[8] However, NMR/NAMFIS analysis determined that only 5% of compound **4.7** adopted a T-Taxol

conformation in solution, comparable with PTX (4%). Further study revealed that there was a close contact between Phe-270 of the tubulin and the propene moiety of the *m*-phenyl tether linker. Due to lack of induced fit, these compounds were seated in the hydrophobic binding pocket higher than PTX.

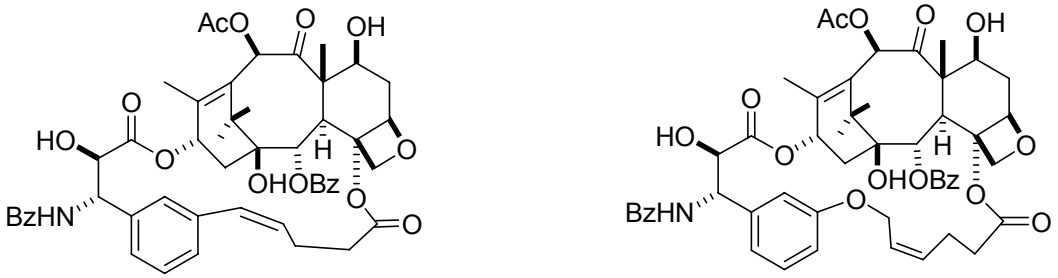

4.6 **4.7**

Figure 4.4 Structure of tether linker PTX analogs based on T-Taxol conformer

To minimize the ligand-protein interaction, modeling studies showed that the bridge should link the C4 acetate group with the C3' phenyl ring at the *ortho* position. A series of PTX derivatives (**4.9**, **4.10** in Figure 4.5) connecting the *ortho* position of C3' phenyl and C4 methyl with different chain lengths were prepared.[9] Among them, **4.9** was the most potent compound, and was about 20-fold more active than PTX itself (**4.9** with IC_{50} value of 0.18 nM; PTX with IC_{50} value of 4 nM). NMR/NAMFIS analysis indicated that >80% of the compound adopted the T-Taxol conformation in solution.[6] This study strongly supported the T-Taxol conformer as the bioactive conformation, and suggested that the additional 5-atom bridge linking C4 and *ortho* C3' phenyl locked the structure into the T-Taxol conformation and thus enhanced its bioactivity.

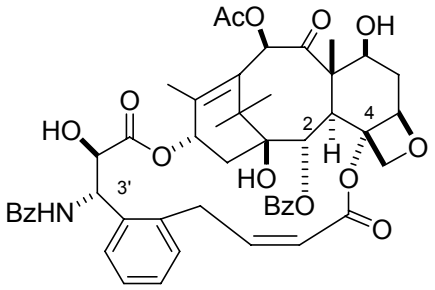

4.9

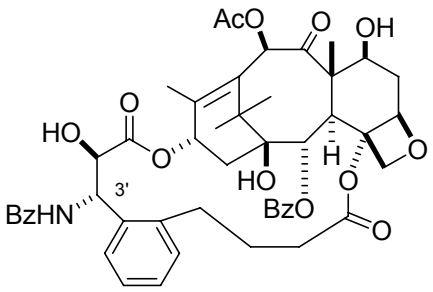

4.10

Figure 4.5 Structure of tether linker PTX analogs based on T-Taxol conformer

These studies indicated that binding from the *ortho*-position of the C3'-phenyl ring to the C4 acetate enhanced the activity of PTX significantly. Previous work by the Kingston group[4,10] and others[11,12] has shown that the activity of PTX could also be enhanced by replacement of the C2-benzoyl group with a C2-*m*-methoxybenzoyl group (with IC_{50} value of 0.19 nM; PTX with IC_{50} value of 2.1 nM against 1A9 cell line),[4] and also by replacement of the *N*-benzoyl group with a Boc group (with IC_{50} value of 0.17 nM; PTX with IC_{50} value of 0.27 nM against P388 cell line).[4] It was thus of interest to determine whether the activity enhancement also applied to bridged PTX derivatives.

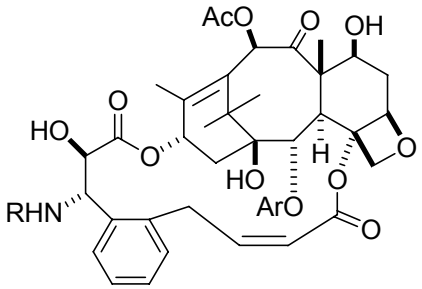

R = benzoyl, Boc
Ar = benzoyl
3-MeObenzoyl

4.11

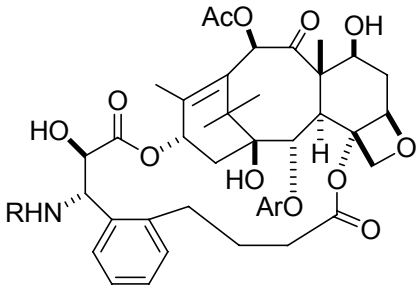

R = benzoyl, Boc
Ar = benzoyl
3-MeObenzoyl

4.12

Figure 4.6 Structure of macrocyclic PTX analogs based on T-Taxol conformer

4.2 Synthesis of macrocyclic bridged PTX derivatives

The synthesis of the macrocycles was planned to be accomplished by the well-established ring-closing olefin metathesis (RCM) method[13-15] in the crucial macrocyclization step.[12]

The retrosynthesis of compound **4.13** is given in Scheme 4.1. The major disconnection gave two main fragments for the synthesis; the lactam part **4.14** and the baccatin core **4.15.** The coupling of **4.14** and **4.15** could be accomplished by Holton's protocol.

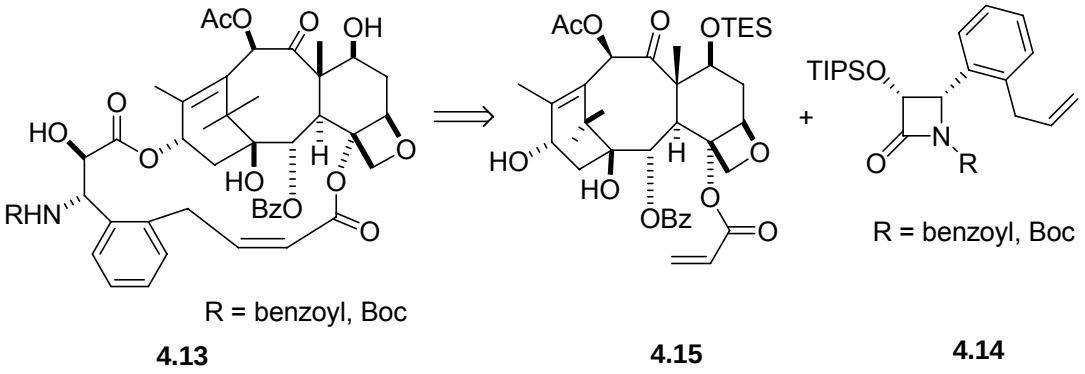

4.13 **4.15** **4.14**

Scheme 4.1 Retrosynthesis of **4.13**

The synthesis of the β–lactam sidechain started from commercially available 2–bromobenzaldehyde by application of literature procedures, as shown in Scheme 4.2. The aldehyde reacted with *p*–anisidine to form the corresponding imine intermediate. Staudinger [2 + 2] cyclocondensation of the imine with ketene generated in situ from acetoxyacetyl chloride gave the racemic β–lactam **4.16**. Kinetic resolution of the racemic β–lactam with Lipase–PS (Amano) enzyme yielded the acetate of the desired (+)-enantiomer **4.17**, along with the undesired (-)-alcohols. Deacetylation under basic conditions, followed by protection of the secondary alcohol as its triisopropylsilyl ether,

and Stille coupling with allyltributyltin produced **4.18**. Deprotection of the PMP group by CAN gave **4.19.** Benzoylation of **4.19** generated **4.20**, while Boc protection of **4.19** gave **4.21**.

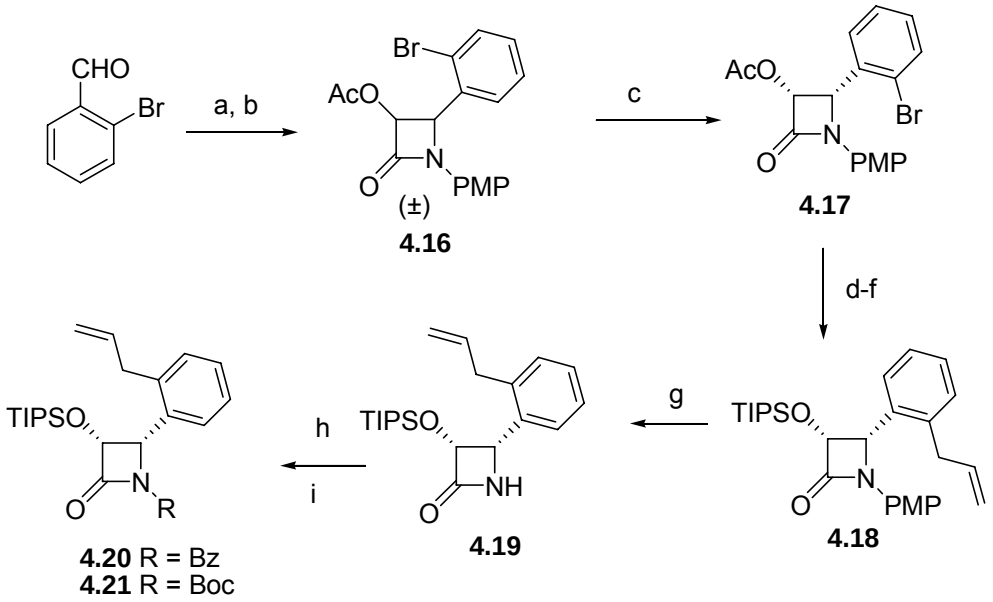

a) anisidine; b) $CH_3CO_2CH_2COCl$, Et_3N, 78%; c) lipase buffer, 80%; d) KOH, 91%; e) TIPSCl, Im; f) $allylBu_3Sn$, $Pd(PPh_3)_4$, 82%; g) CAN, 80%; h) BzCl, 86% **4.20**; i) $(Boc)_2O$, 86% **4.21**

Scheme 4.2 Synthesis of labeled β-lactams

The forward synthesis sequence starting from the natural product 10–deacetylbaccatin III (10–DAB, **4.22**) is shown in Scheme 4.3. TES protection of the C7, C10 and C13–hydroxyl groups, followed by DMS protection of the C1 hydroxyl group gave the silyl protected baccatin core **4.23**, which was treated with Red–Al® to give the C4 deacetyl compound **4.24**. Reacetylation of the C4 hydroxyl group of **4.24** using acryloyl chloride gave the desired derivative **4.25.** Global deprotection of all silyl groups was followed by selective acetylation of the C10 hydroxyl group to give the C10 acetyl intermediate **4.26**, and selective protection of the C7 hydroxyl group by TES completed the synthesis of the labeled baccatin core **4.15**.

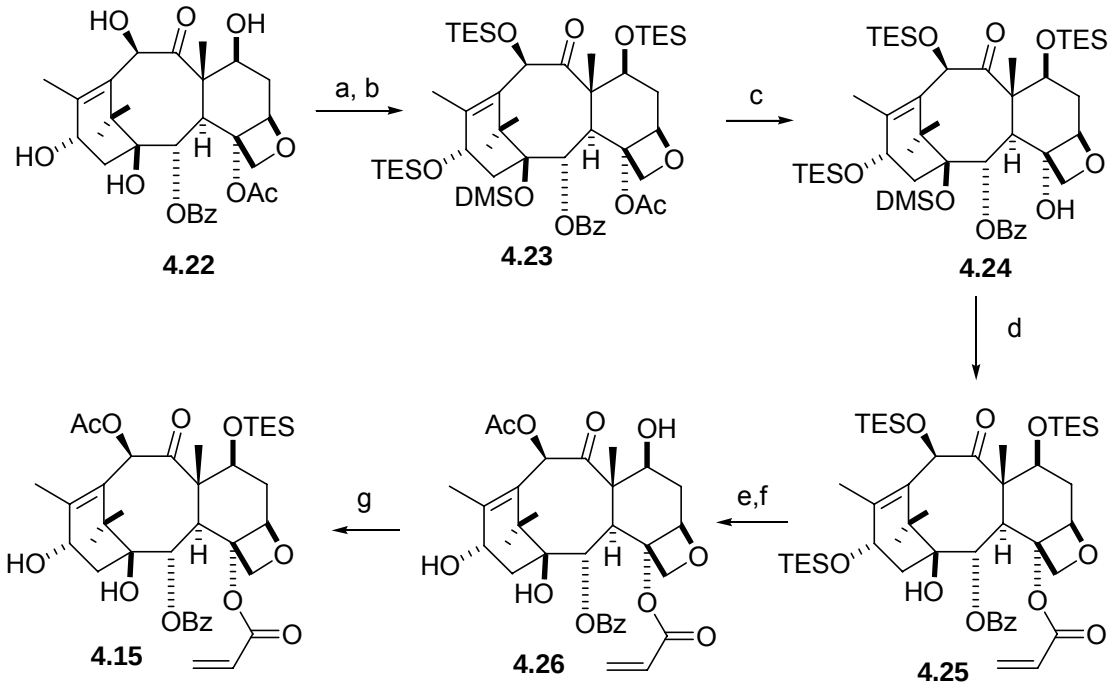

a) TESCl, Im, 90%; b) DMSCl, Im, 95%; c) Red-Al, 70%d) LHMDS, CH_2=CHCOCl, 50%; e) HF/py, 85%; f) Ac_2O, $CeCl_3$, 93%; g) TESCl, Im, 68%

Scheme 4.3 Synthesis of labeled baccatin core **4.15**

Coupling β–lactams **4.20** and **4.21** with the baccatin core **4.15** by LHMDS, followed by a global deprotection step with HF/py provided open-chain paclitaxel analogs **4.27** and **4.28** as shown in Scheme 4.4.

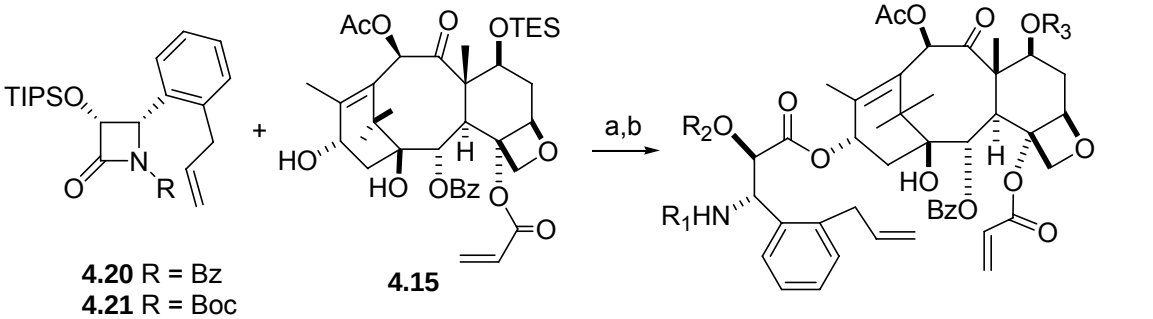

4.20 R = Bz
4.21 R = Boc

4.15

a) LHMDS, **4.27** 65%, **4.29** 86% b) HF/py **4.28** 90%, **4.30** 92%

4.27 R_1 = Bz, R_2 = TIPS, R_3 = TES
4.28 R_1 = Bz, R_2 = R_3 = H
4.29 R_1 = Boc, R_2 = TIPS, R_3 = TES
4.30 R_1 = Boc, R_2 = R_3 = H

Scheme 4.4 Completion of paclitaxel analogs synthesis

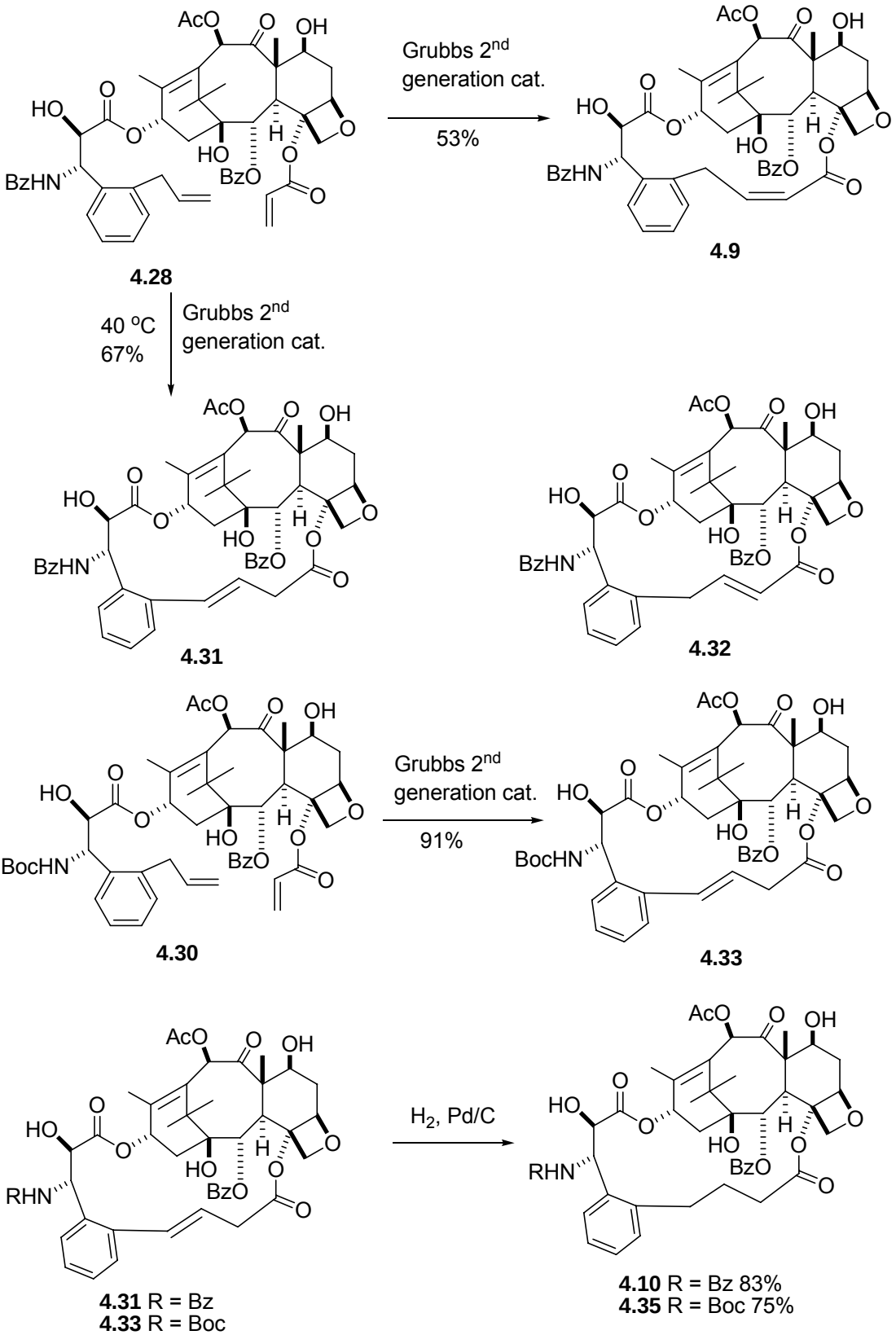

Scheme 4.5 RCM of open chain PTX derivatives

Ring-closing olefin metathesis (RCM) of **4.28** by Grubbs first generation catalyst gave no cyclic product. RCM of **4.28** by Grubbs second generation catalyst at rt gave *cis* cyclic product **4.9**; however, at elevated temperature it gave the *trans* cyclic isomer **4.31** instead of the expected isomer **4.32**. Surprisingly, RCM of **4.30** by Grubbs second generation catalyst gave solely isomer **4.33**, even at rt. Hydrogenation of **4.31** and **4.33** gave the corresponding dihydro derivatives **4.10** and **4.35**, respectively.

Previous work had indicated that a *m*-methoxy substituent on the C2-benzoyl group of paclitaxel increased its activity significantly. It was thus of interest to determine whether a similar substitution on the bridged compound **4.9** would enhance its activity, and compound **4.36** was designed to test this hypothesis.

The reterosynthesis of compound **4.36** is given in Scheme 4.6.

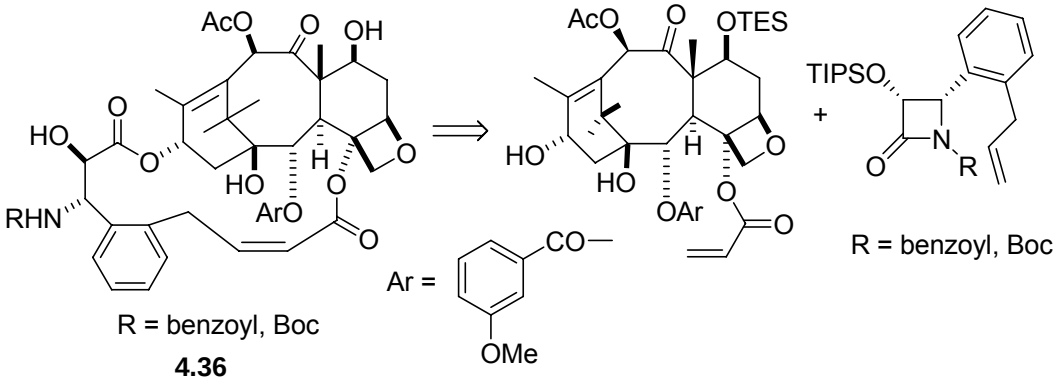

Scheme 4.6 Retrosynthesis of **4.36**

The synthetic sequence for **4.36** starting from the natural product 10–deacetylbaccatin III (10–DAB, **4.22**) is shown in Scheme 4.7. TES protection of the C7, C10 and C13 hydroxyl groups, followed by Red–Al® reduction, gave silyl protected C2 debenzoylated baccatin **4.37.** Rebenzoylation of the C2 hydroxy group with *m*-methoxybenzoic acid in the presence of EDC gave the 2-(3-methoxybenzoyl) baccatin III

4.38. DMS protection of the C1 hydroxyl group gave silyl protected baccatin core **4.39**, which was treated with Red–Al® to give the C4 deacetate **4.40**. Acylation of the C4 hydroxyl group of **4.40** using acryloyl chloride gave the desired derivative **4.41.** Global deprotection of all silyl groups was followed by selective acetylation of the C10 hydroxyl group to give the C10 acetate intermediate **4.42**, and selective protection of the C7 hydroxyl group by TES completed the synthesis of the labeled baccatin core **4.43**.

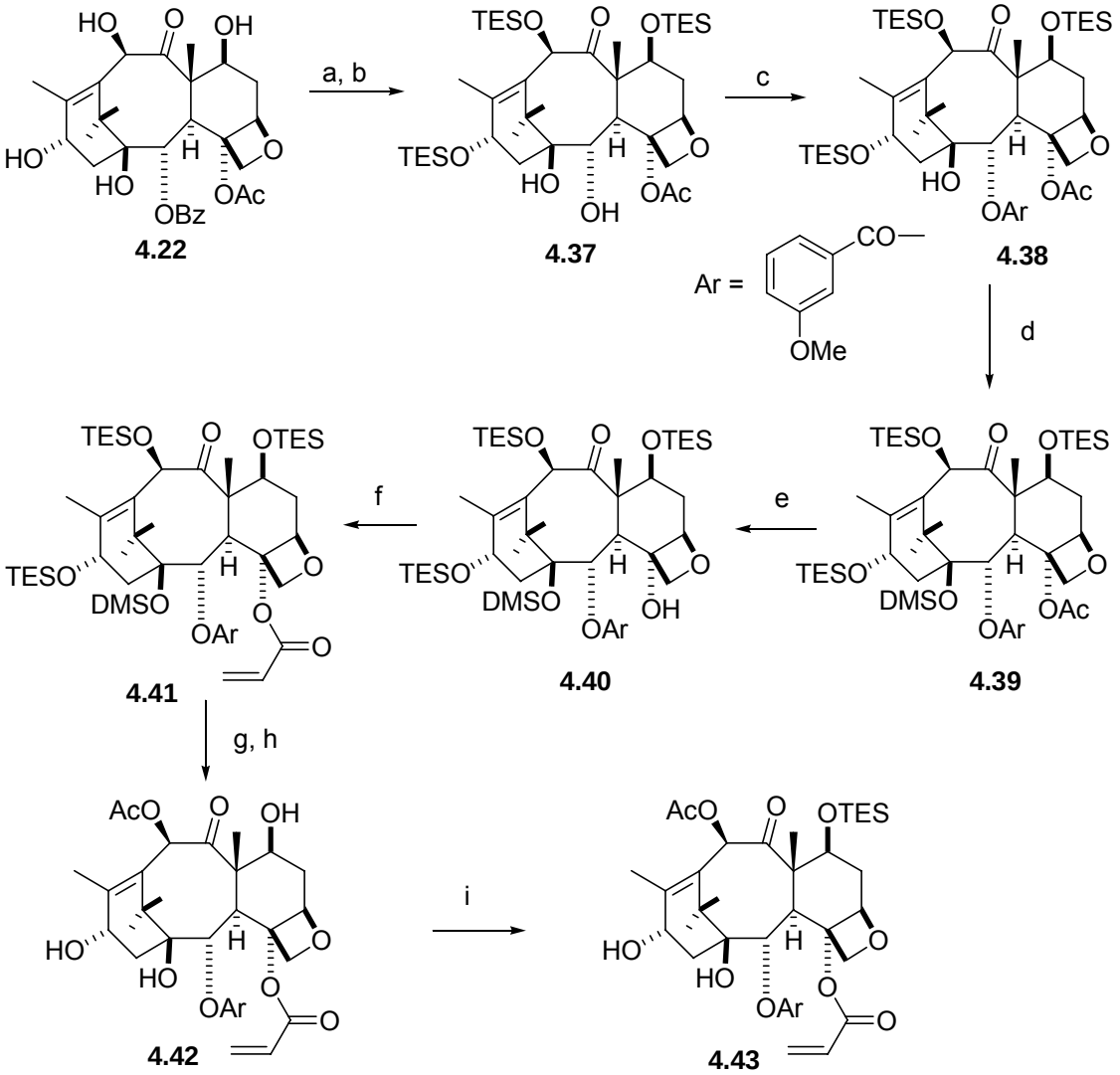

a) TESCl, Im, 76%; b)Red Al, 72%; c) EDCI, $ArCO_2H$, 73%; d) DMSCl, Im e) Red Al, 56%; f) LHMDS, acryloyl chloride, 35%; g) HF/py, 78%; h) Ac_2O, $CeCl_3$, 95%; i) TESCl, Im, 43%

Scheme 4.7 Synthesis of labeled baccatin core **4.43**

Coupling β–lactams **4.20** and **4.21** with the baccatin core **4.43** by LHMDS, followed by a global deprotection step with HF/py provided the open chain paclitaxel analogs **4.44** and **4.45**, as shown in Scheme 4.8.

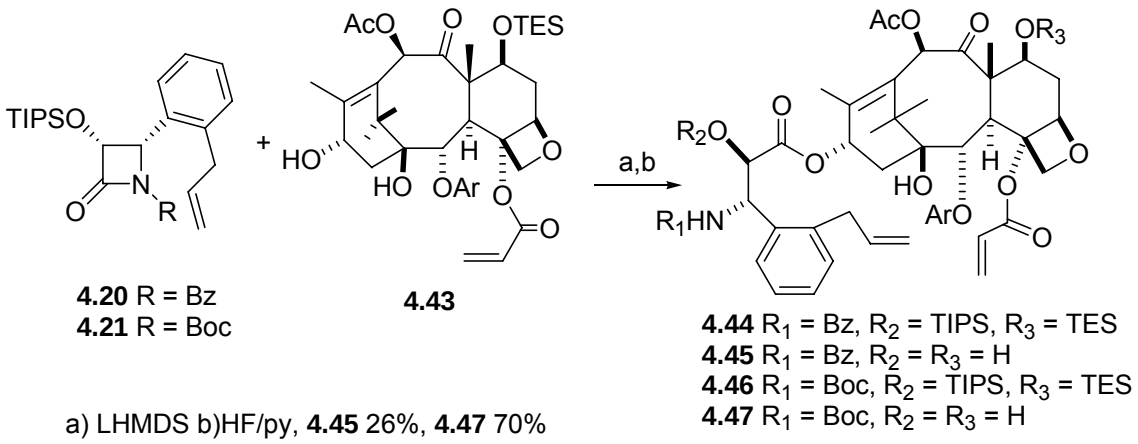

4.20 R = Bz
4.21 R = Boc

4.43

4.44 R_1 = Bz, R_2 = TIPS, R_3 = TES
4.45 R_1 = Bz, R_2 = R_3 = H
4.46 R_1 = Boc, R_2 = TIPS, R_3 = TES
4.47 R_1 = Boc, R_2 = R_3 = H

a) LHMDS b)HF/py, **4.45** 26%, **4.47** 70%

Scheme 4.8 Completion of paclitaxel analogs synthesis

RCM of **4.45** by Grubbs second generation catalyst at rt gave cyclic products **4.48** and **4.49**. Surprisingly, RCM of **4.47** by Grubbs second generation catalyst gave only isomer **4.50** at rt. Hydrogenation of **4.49** and **4.50** gave the corresponding dihydro derivatives **4.51** and **4.52**, respectively.

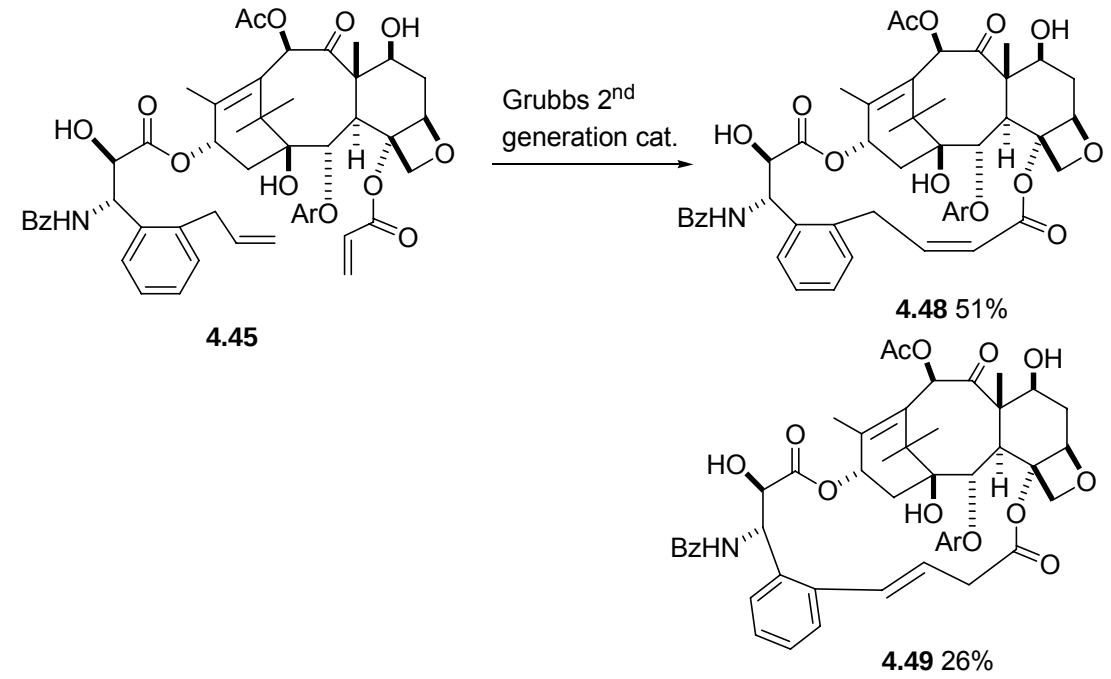

Scheme 4.9 Completion of paclitaxel analogs synthesis

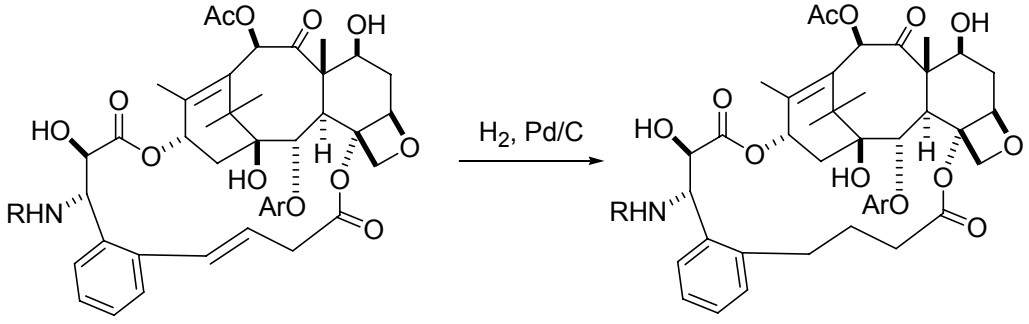

4.49 R = Bz
4.50 R = Boc

4.51 R = Bz 83%
4.52 R = Boc 72%

Scheme 4.10

4.3 Biological Activity

All the macrocyclic PTX derivatives were tested for bioactivity. The bioactivity evaluation data are listed in Tables 4.1 and Table 4.2.

Table 4.1 Cytotoxicity and tubulin polymerization activity of macrocyclic paclitaxel analogues

compound	IC_{50} value (nM)		tubulin polym (ED_{50}, μM)
	A2780	PC3	
PTX	15	5	0.5
4.9	0.3	2.5	0.3
4.31	0.5	3.1	0.33
4.33	1.4	3.2	0.49
4.10	0.5	2.4	0.21
4.35	0.65	1.5	0.18
4.48	17.7	8.2	0.22
4.49	23.7	6	0.57
4.50	6	11	0.35
4.51	23.1	ND	ND
4.52	0.49	1.3	0.22

Table 4.2 Bioactivity of bridged taxoids against paclitaxel and epothilone A resistant cell lines

compound	IC_{50} value (nM)			IC_{50} (nM)	
	1A9	1A9-PTX10 (Fβ270V)	PTX10/1A9	1A9-A8 (Tβ274I)	A8/1A9
PTX	4.8±4.5	157	20	21.5±11.5	4.5
4.9	0.32 ±0.35	0.13	1.8	0.27±0.08	0.84
4.32	0.07±0.02	1.03	12	0.44±0.19	6.3

1A9 is the parental drug-sensitive cell line, 1A9-PTX10 is the paclitaxel resistant clone with an acquired Fβ270V mutation, and 1A9-A8 is the epothilone A resistant clone with an acquired Tβ274I mutation which also confers cross-resistance to paclitaxel.

All the analogs show bioactivities equal to or greater than PTX itself. However, disappointingly all the derivatives were less active than the simple analog **4.9**. Since the derivatives are more difficult to make than **4.9**, **4.9** and its dihydro derivative **4.10** are the best candidates for *in vivo* testing to date.

Based on these results, a large scale synthesis of **4.9** was carried out to prepare material for *in vivo* evaluations. During this synthesis, formation of both **4.9** and **4.31** occurred during the RCM step. The inseparable mixture of products was thus converted

to the single dihydro derivative **4.10** to provide enough material for evaluations, and a total of 200 mg of **4.10** was prepared. An additional 140 mg of **4.9** was also prepared in a separate synthesis where isomerization did not occur in the RCM step.

Compound **4.10** was submitted to Dr. Ralph Bernacki at Roswell Park Memorial Institute for *in vivo* evaluations. This work showed that the compound had similar activity to that of paclitaxel against the DLD-1 human colon caranoma, but also showed significant toxicity. Further work is planned to determine whether the activity is improved in a different tumor system.

4.4 Conclusion

All of the macrocyclic PTX analogs show both tubulin polymerization and cytotoxic bioactivities equal to or greater than PTX itself. These results provided additional evidence to support T-Taxol conformer as the bioactive conformation. Among all the macrocyclic PTX analogs, **4.9** and **4.10** are the most active. Both derivatives were synthesized for *in vivo* evaluation, and further *in vivo* evaluations are planned.

4.5 Experimental section

General Experimental Methods. All reagents and solvents received from commercial sources were used without further purification. ^{1}H and ^{13}C NMR spectra were obtained in $CDCl_3$ on Varian Unity or Varian Inova spectrometers at 400 MHz or a JEOL Eclipse spectrometer at 500 MHz. High-resolution FAB mass spectra were obtained on a JEOL HX-110 instrument. Compounds were purified by chromatography on silica gel using EtOAc/hexane unless specified.

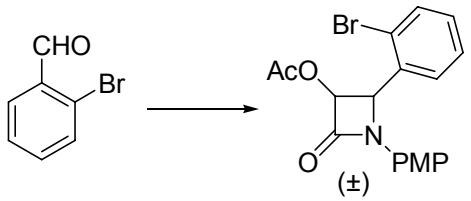

4.16

(3R,4S and 3S,4R)-1-(*p*-methoxyphenyl)-3-acetoxyl-4-(*o*-bromophenyl)-azetidin-2-one (4.16). At rt, *p*–anisidine (3.7 g, 30 mmol) was added to a solution of *o*–bromobenzaldehyde (3.5 mL, 30 mmol) in dichloromethane (170 mL) and a large excess of anhydrous $MgSO_4$. After 12 h, the yellowish slurry was filtered and the crude imine was taken to the next step without purification. To the crude imine dissolved in DCM was added Hünig's base (18 mL, 103 mmol) and the solution was cooled to -78 °C. Acetoxyacetyl chloride (4 mL, 37 mmol) was added to this solution dropwise and the reaction was allowed slowly to warm up to rt and stirred for 12 h. The dark crude mixture was concentrated and purified on a silica column to afford **4.16** (8 g, 78%). ^{1}H NMR (400 MHz, $CDCl_3$) δ 2.13 (3H, s), 3.77 (3H, s), 5.76 (1H, d, *J* = 5.0 Hz), 6.19 (1H, d, *J* = 5.0 Hz), 6.77 (d, 2H, *J* = 8.7 Hz), 6.99 (m, 1H), 7.19 (d, 2H, *J* = 8.7 Hz), 7.20 (m, 1H), 7.42 (m, 2H). ^{13}C NMR ($CDCl_3$): δ 169.5, 162.7, 160.0, 134.0, 133.6, 128.3, 128.2, 128.1, 127.0, 126.5, 117.0, 114.3, 81.9, 66.1, 55.2, 20.5

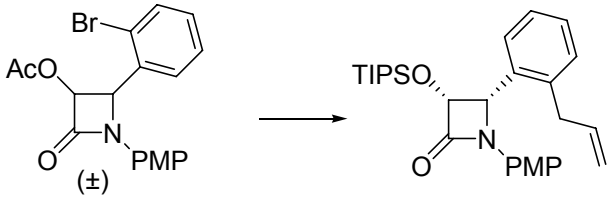

4.16 **4.18**

(3R,4S)-1-(*p*-methoxyphenyl)-3-triisopropylsilyloxy-4-(*o*-bromophenyl)-azetidin-2-one (4.18). The racemic β–lactam **4.16** (3 g, 7.7 mmol) was dissolved in CH_3CN (60

mL), and to this solution a pH 7.2 phosphate buffer (130 mL) was mixed vigorously. Immobilized Lipase PS Amano enzyme (2.6 g) was added and the mixture was stirred for 77 days. The progress of the reaction was monitored by TLC, and after the completion of the reaction the solution was extracted by EtOAc. The organic phase was washed with H_2O and brine, dried over Na_2SO_4, and concentrated. Purification by column chromatography gave acetoxy β-lactam **4.17** oil (1.2 g, 80%). The solution of acetoxy β-lactam **4.17** (1.1 g, 2.8 mmol) in THF (70 mL) was added slowly to a 1 M KOH (80 mL) solution at 0 ºC. The solution was stirred 45 min further at this temperature, and the mixture was extracted with EtOAc. The organic phase was washed with H_2O and brine, dried over Na_2SO_4, and concentrated. Purification by column chromatography gave hydroxy β-lactam (0.94 g, 91%). To a solution of hydroxy β-lactam (0.94 g, 2.7 mmol) in 5 mL of DMF was added imidazole (0.67 g, 9.8 mmol) and triisopropylsilyl chloride (0.7 mL, 3.3 mmol), and the mixture was stirred at rt overnight. The reaction mixture was diluted with EtOAc, quenched with $NaHCO_3$, and extracted with EtOAc. The organic phase was washed with H_2O and brine, dried over Na_2SO_4, and concentrated to give the TIPS protected β-lactam, which was used without purification. At rt, a solution of β-lactam (200 mg, 0.40 mmol), Ph_3P (150 mg, 0.57 mmol), $Pd_2(dba)_3$ (50 mg, 0.055 mmol) in dioxane (10 mL) was treated with allyl tributyl tin (200 mg). After 2 days at 80 ^oC, the mixture was diluted with EtOAc and filtered (product:starting materials = 1:1). The filtrate was washed with 0.005M KF, water and brine, dried over Na_2SO_4, and concentrated. Purification by column chromatography gave allyl β–lactam **4.18** oil (80 mg, 82% based on unrecovered starting materials). ^1H NMR (400 MHz, $CDCl_3$): δ 7.26 (2H, d, J = 5.2 Hz), 7.23 (1H, m), 7.21 (2H, m), 7.12-7.16 (1H, m), 6.79 (2H, d, J = 9.2 Hz), 5.99-6.09

(1H, m), 5.42 (1H, d, J = 5.2 Hz), 5.29 (1H, d, J = 5.2 Hz), 5.16 (1H, dd, J = 10, 0.8 Hz), 5.09 (1H, dd, J = 16.8, 3.2 Hz), 3.74 (3H, s), 3.55 (1H, dd, J = 16.4, 7.2 Hz), 3.45 (1H, ddt, J = 16, 6, 1.6 Hz), 1.00-1.01 (3H, m), 0.89-0.94 (18H, m). ^{13}C NMR (100 MHz): δ 165.7, 156.3, 137.9, 132.1, 131.2, 129.9, 129.2, 128.6, 128.2, 126.6, 118.9, 116.6, 114.5, 77.9, 55.6, 37.5, 17.82, 17.79, 12.3. HRFABMS: found *m/z* 464.2645, Calculated for $C_{28}H_{38}NO_3Si$ $(M+H)^+$ *m/z* 464.2621, (Δ= + 5.2 ppm).

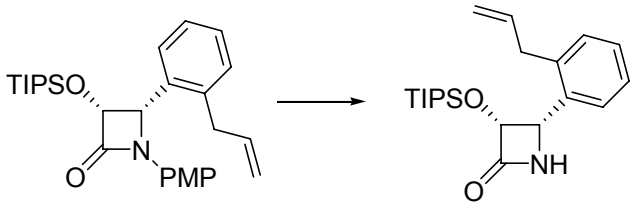

4.18 **4.19**

(3R,4S)-3-acetoxyl-4-(*o*-allylphenyl)-azetidin-2-one (4.19). A solution of ceric ammonium nitrate (CAN) (2 g, 3.6 mmol) in 12 mL H_2O was added dropwise to a solution of **4.18** (0.66 g, 1.4 mmol) in 28 mL CH_3CN at -5 ^oC. The reaction mixture was stirred for 45 min and monitored by TLC, diluted with EtOAc and washed with H_2O, a saturated solution of sodium metabisulfite and saturated $NaHCO_3$, dried over Na_2SO_4, and concentrated. The crude product was purified on a silica column to give the PMP deprotected β-lactam **4.19** oil (420 mg, 80%).

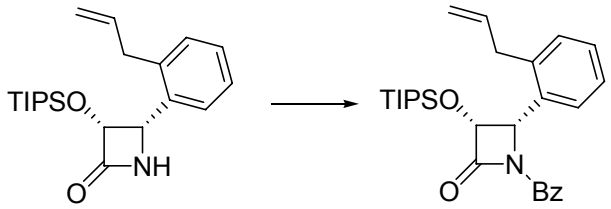

4.19 **4.20**

(3R,4S)-1-benzoyl-3-triisopropylsilyloxy-4-(*o*-allylphenyl)-azetidin-2-one (4.20). To a solution of the PMP deprotected β-lactam **4.19** (510 mg, 1.4 mmol) in 25 mL CH_2Cl_2 at 0 ºC was added a catalytic amount of DMAP (80 mg, 0.66 mmol), 0.6 mL (4.3 mmol)

triethylamine, and 0.5 mL (4.3 mmol) benzoyl chloride. The mixture was warmed to rt with monitoring by TLC; after 3 h it was diluted with EtOAc and washed with saturated $NaHCO_3$, and H_2O, dried over Na_2SO_4, and concentrated. The product was purified by silica gel chromatography to give the final β–lactam **4.20** oil (545 mg, 86%). $[\alpha]_D$: +183.4 (c 0.35, $CHCl_3$). ^1H NMR (400 MHz, $CDCl_3$): δ 8.0 (2H, d, J = 8 Hz), 7.60 (1H, t, J = 7.2 Hz), 7.49 (2H, t, J = 7.6 Hz), 7.37 (1H, m), 7.22 (3H, m), 6.05 (1H, m), 5.72 (1H, d, J = 6.4 Hz), 5.31 (1H, d, J = 6 Hz), 5.16 (1H, dd, J = 11.6, 1.2 Hz), 5.12 (1H, dd, J = 17, 1.6 Hz), 3.60 (2H, m), 1.0 (3H, m), 0.94 (18H, m). ^{13}C NMR (100 MHz): δ 166.4, 165.5, 138.5, 136.8, 133.5, 132.3, 132.1, 130.1, 129.8, 128.4, 128.3, 127.4, 126.3, 116.6, 76.7, 57.6, 37.6, 17.77, 17.74, 12.2. HRFABMS: found *m/z* 464.2645, Calculated for $C_{28}H_{38}NO_3Si$ $(M+H)^+$ *m/z* 464.2621, (Δ= + 5.2 ppm).

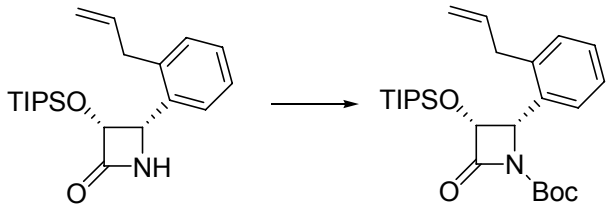

4.19 **4.21**

(3R,4S)-1-(*t*-butyloxycarbonyl)-3-triisopropylsilyloxy-4-(*o*-allylphenyl)-azetidin-2-one (4.21). To a solution of the PMP deprotected β-lactam **4.19** (150 mg, 0.42 mmol) in 8 mL CH_2Cl_2 at 0 ºC was added a catalytic amount of DMAP (30 mg, 0.024 mmol), 0.3 mL (2.1 mmol) triethylamine, and 0.3 mL (1.3 mmol) di-*tert*-butyl dicarbonate. The mixture was then warmed to rt with monitoring by TLC; after 3 h it was diluted with EtOAc and worked up in the usual way. The product was purified by silica chromatography to give the final β–lactam **4.21** oil (163 mg, 86%). ^1H NMR (400 MHz, $CDCl_3$): δ 7.28-7.30 (1H, m), 7.21-7.24 (2H, m), 7.14-7.17 (1H, m), 7.22 (3H, m), 5.93-6.03 (1H, m), 5.36 (1H, d, J = 5.6 Hz), 5.21 (1H, d, J = 6.0 Hz), 5.09 (1H, ddd, J = 10.0, 3.6, 1.2 Hz), 5.03 (1H, ddd,

J = 16.8, 3.6, 1.6 Hz), 3.44 (2H, m), 1.42 (9H, s), 0.96-1.02 (3H, m), 0.86-0.89 (18H, m). ^{13}C NMR (100 MHz): δ 166.5, 138.0, 136.8, 132.3, 129.8, 128.2, 127.4, 126.4, 116.5, 83.6, 77.8, 37.5, 20.1, 17.74, 17.70, 12.2. HRFABMS: found *m/z* 459.6885, Calculated for $C_{26}H_{41}NO_4Si$ $(M+H)^+$ *m/z* 459.6925, Δ = 8.7 ppm.

4-Deacetyl-1-dimethylsilyl-7,10,13-tris(triethylsilyl)-10-deacetylbaccatin III 4.24. This compound was synthesized from commercially available 10-deacetylbaccatin III by the literature method.[16]

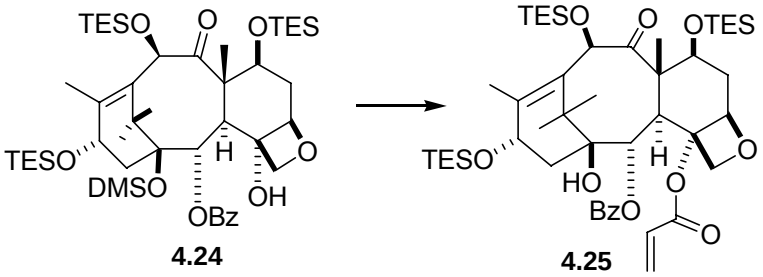

4-Deacetyl-4-acryloyl-1-dimethylsilyl-7,10,13-tris(triethylsilyl)-10-deacetylbaccatin III (4.25). At 0^o C, a solution of **4.24** (1 g, 1.1 mmol) in 6 mL THF at 0 °C was treated with 1 M LiHMDS (1.3 mL) followed by acryloyl chloride (0.15 mL, 1.8 mmol). After 3 h with monitoring by TLC, the mixture was quenched with saturated NH_4Cl. The reaction mixture was extracted with EtOAc and washed with H_2O and brine. The combined organic layers were dried over Na_2SO_4 and concentrated under reduced pressure. Purification of the crude residue by silica gel column gave **4.25** (550 mg, 50%). ^{1}H NMR (400 MHz, $CDCl_3$): δ 8.18 (2H, d, *J* = 8.4 Hz), 7.62 (1H, d, *J* = 7.2 Hz), 7.49 (2H, t, *J* = 8 Hz), 6.56 (1H, dd, *J* = 17.4, 1.2 Hz), 6.25 (1H, dd, *J* = 17.4, 10.5 Hz), 6.15 (1H, dd, *J* = 10.5, 1.17 Hz), 5.76 (1H, d, *J* = 7 Hz), 4.94 (2H, t, *J* = 9.5 Hz), 4.58 (1H, m), 4.48 (1H,

dd, *J* = 10, 6.6 Hz), 4.30 (2H, ABq, *J* = 11.2, 8.4 Hz), 3.98 (1H, d, *J* = 6.8 Hz), 2.55 (1H, m), 2.30 (2H, m), 2.00 (3H, s), 1.98 (1H, m), 1.70 (3H, s), 1.22 (3H, s), 1.13 (3H, s), 1.0 (27H, m), 0.65 (18H, m), 0.05 (3H, d, *J* = 2.7 Hz), -0.28 (3H, d, *J* = 2.7 Hz). ^{13}C NMR (100 MHz): δ 205.6, 165.3, 164.4, 138.9, 135.7, 133.1, 130.6, 130.3, 130.1, 130.0, 128.3, 84.1, 82.1, 81.3, 75.9, 75.7, 72.7, 68.2, 58.3, 46.6, 44.0, 39.3, 37.4, 27.3, 21.3, 14.5, 10.4, 7.0, 6.9, 6.0, 5.2, 4.9, 4.8, 0.4, 0.05, HRFABMS: found *m/z* 957.5202, Calculated for $C_{50}H_{85}O_{10}Si_4$ $(M+H)^+$ *m/z* 957.5220, Δ = 1.9 ppm.

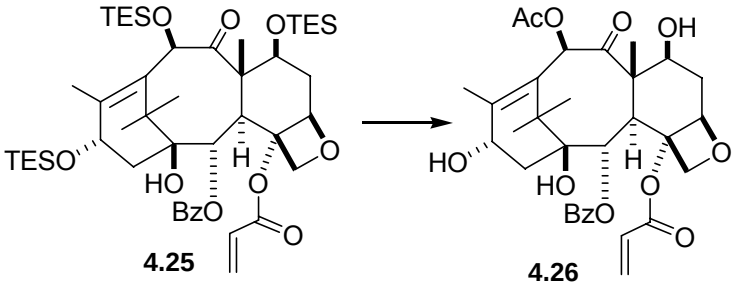

4-deacetyl-4-acryloyl baccatin III (4.26). At 0 ºC, HF/pyridine (5 mL) was added to a solution of **4.25** (0.95 g, 1.0 mmol) in THF (60 mL) and the solution was warmed to rt and stirred overnight. The reaction mixture was diluted with EtOAc and washed with aq. $NaHCO_3$. The layers were separated and the aqueous phase was extracted with EtOAc. The combined organic layers were washed with water, brine, dried over Na_2SO_4, filtered and concentrated to give crude 4-deacetyl-4-acryloyl-10-deacetylbaccatin III (470 mg, 85%). At rt, a solution of this crude product (470 mg, 0.84 mmol) in THF (20 mL) was treated with a catalytic amount of $CeCl_3$. After 20 min, the mixture was treated with acetic anhydride (1.5 mL, 16 mmol). After 4 h, the mixture was diluted with EtOAc, quenched with aq. $NaHCO_3$. The layers were separated and the aqueous phase was extracted with EtOAc. The combined organic layers were washed with water, brine, dried over Na_2SO_4, filtered and concentrated. The residue was purified by preparative TLC to

give **4.26** (470 mg, 93%). ^{1}H NMR (500 MHz, $CDCl_3$): δ 8.0 (2H, d, *J* = 8.4 Hz), 7.59 (1H, t, *J* = 7 Hz), 7.46 (2H, t, *J* = 8 Hz), 6.48 (1H, dd, *J* = 17.4, 1.2 Hz), 6.32 (1H, s), 6.27 (1H, dd, *J* = 17.4, 10.5 Hz), 6.00 (1H, dd, *J* = 17.4, 1.2 Hz), 5.62 (1H, d, *J* = 7 Hz), 4.96 (1H, dd *J* = 9.6, 2 Hz), 4.79 (1H, t, *J* = 7 Hz), 4.52 (1H, dd, *J* = 10.9, 6.8 Hz), 4.33 (1H, d, *J* = 8.4 Hz), 4.20 (1H, d, *J* = 8.5 Hz), 3.94 (1H, d, *J* = 6.8 Hz), 2.56 (1H, m), 2.20 (3H, s), 2.22-2.18 (1H, m), 2.03 (3H, s), 1.86 (1H, m), 1.67 (3H, s), 1.08 (3H, s), 1.07 (3H, s). ^{13}C NMR (125 MHz): δ 204.1, 186.2, 171.4, 167.0, 165.2, 146.6, 133.7, 131.7, 131.3, 130.1, 129.6, 128.6, 84.5, 81.2, 79.1, 76.5, 76.3, 75.0, 72.3, 68.0, 58.8, 46.1, 42.7, 39.2, 35.7, 27.0, 20.9, 15.5, 9.5. HRFABMS: found *m/z* 599.25018, Calculated for $C_{32}H_{39}O_{11}$ $(M+H)^+$ *m/z* 599.2492, Δ = 4.3 ppm.

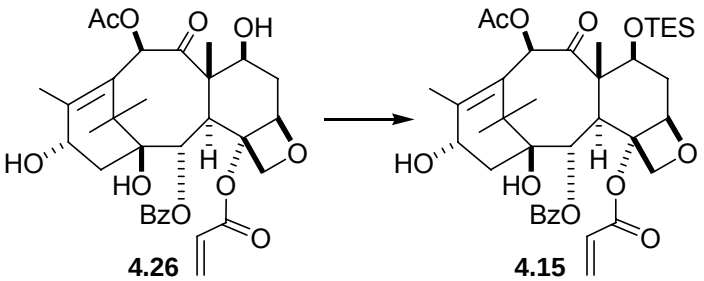

4-Deacetyl-4-acryloyl-7-(triethylsilyl) baccatin III (4.15). At 0 ^{o}C, a solution of **4.26** (157 mg, 0.26 mmol) in DCM (15 mL) was treated with imidazole (169 mg, 2.5 mmol) and chlorotriethylsilane (210 mg, 1.2 mmol). After 3 h, the reaction mixture was quenched with HCl. The layers were separated and the aqueous phase was extracted with EtOAc. The combined organic layers were washed with water, brine, dried over Na_2SO_4, filtered and concentrated. The residue was purified on silica gel to give **4.15** (120 mg, 68%). ^{1}H NMR (500 MHz, $CDCl_3$): δ 8.11 (2H, d, *J* = 7.1 Hz), 7.59 (1H, t, *J* = 7.2 Hz), 7.46 (2H, t, *J* = 7.2 Hz), 6.52 (1H, dd, *J* = 17.4, 1.2 Hz, 1H), 6.47 (1H, s), 6.28 (1H, dd, *J* = 17.4, 10.5 Hz), 6.01 (1H, dd, *J* = 17.4, 1.2 Hz), 5.64 (1H, d, *J* = 6.8 Hz), 4.94 (1H, d, *J*

= 7.7 Hz), 4.76 (1H, m), 4.53 (1H, dd, *J* = 10, 6.7 Hz), 4.33 (1H, d, *J* = 8.4 Hz), 4.20 (1H, d, *J* = 8.4 Hz), 3.94 (1H, d, *J* = 6.8 Hz), 2.55 (1H, m), 2.20 (3H, s), 2.22-2.10 (2H, m), 2.18 (3H, s), 1.90 (1H, m), 1.70 (3H, s), 1.18 (3H, s), 1.02 (3H, s), 0.91 (9H, t, *J* = 7.2 Hz), 0.60 (6H, m). ^{13}C NMR (125 MHz): δ 202.2, 169.4, 165.3, 144.0, 133.7, 131.2, 130.1, 129.8, 129.6, 128.6, 84.2, 81.3, 78.8, 76.6, 75.8, 74.8, 72.4, 68.1, 58.8, 47.2, 42.8, 38.9, 37.3, 26.9, 21.0, 20.1, 14.9, 10.0, 6.84, 5.36. HRFABMS: found *m/z* 713.33258, Calculated for $C_{38}H_{53}O_{11}Si$ $(M+H)^+$ *m/z* 713.3357, (Δ = 4.3 ppm).

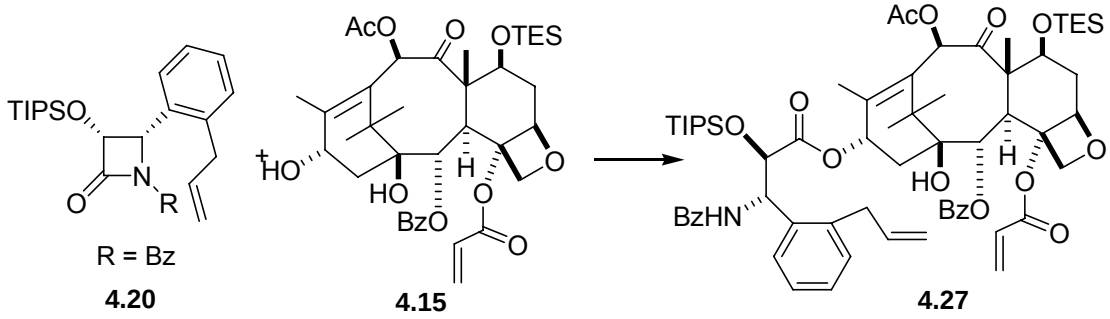

Protected Open Chain paclitaxel (4.27). At -45 °C, a solution of β–lactam **4.20** (90 mg, 0.19 mmol) and 4-acryloyl-7-triethylsilylbaccatin III **4.15** (69 mg, 0.097 mmol) in THF (20 mL) was treated slowly with LiHMDS (0.16 mL). After 4 h with monitoring by TLC, the reaction was quenched with NH_4Cl. The layers were separated and the aqueous phase was extracted with EtOAc. The combined organic layers were washed with water, brine, dried over Na_2SO_4, filtered and concentrated to give crude protected open chain paclitaxel **4.27** (50 mg, 65%). ^{1}H NMR (400 MHz, $CDCl_3$): δ 8.11 (2H, d, *J* = 8 Hz), 7.70 (2H, d, *J* = 7.6 Hz), 7.60 (1H, t, *J* = 7.6 Hz), 7.44-7.52 (4H, m), 7.38 (2H, t, *J* = 7.6 Hz), 7.24-7.31 (3H, m), 6.95 (1H, d, *J* = 9.2 Hz), 6.48 (1H, s), 6.44 (1H, d, *J* = 1.6 Hz), 6.32 (1H, d, *J* = 10 Hz), 6.28 (1H, d, *J* = 10 Hz), 6.0 (1H, m), 5.95 (1H, t, *J* = 9.6 Hz), 5.80 (1H, d, *J* = 9.6 Hz), 5.75 (1H, d, *J* = 7.2 Hz), 5.57 (1H, dd, *J* = 10, 1.6 Hz), 5.18 (1H, dd, *J* = 16.8, 1.6

Hz), 5.12 (1H, dd, *J* = 10, 1.6 Hz), 4.90 (1H, d, *J* = 7.6 Hz), 4.74 (1H, d, *J* = 1.6 Hz), 4.54 (1H, dd, *J* = 10.4, 6.4 Hz), 4.34 (1H, d, *J* = 8 Hz), 4.25 (1H, d, *J* = 8.4 Hz), 3.90 (1H, d, *J* = 7.2 Hz), 3.72 (1H, dd, *J* = 15, 6.4 Hz), 3.52 (1H, dd, *J* = 15.4, 6.8 Hz), 2.56 (1H, m), 2.40 (2H, m), 2.18 (3H, s), 2.03 (3H, s), 1.71 (3H, s), 1.23 (3H, s), 1.18 (3H, s), 1.00-1.07 (11H, m), 0.94 (9H, t, *J* = 8 Hz), 0.60 (6H, m). ^{13}C NMR (100 MHz): δ 202.8, 172.8, 169.5, 167.0, 165.0, 140.9, 137.4, 136.8, 136.2, 134.3, 133.7, 133.5, 132.0, 131.8, 130.29, 130.23, 129.7, 129.4, 128.8, 128.8, 128.5, 127.7, 127.6, 127.0, 126.8, 117.3, 84.4, 81.7, 78.9, 75.2, 74.4, 73.4, 72.3, 58.6, 52.4, 46.9, 43.5, 37.4, 37.1, 36.1, 26.6, 21.8, 21.0, 18.2, 18.1, 14.4, 13.0, 10.3, 6.9, 5.5. HRFABMS: found *m/z* 1198.5742, Calculated for $C_{60}H_{89}NO_{14}Si_2Na$ $(M+Na)^+$ *m/z* 1198.5719, Δ = 1.9 ppm.

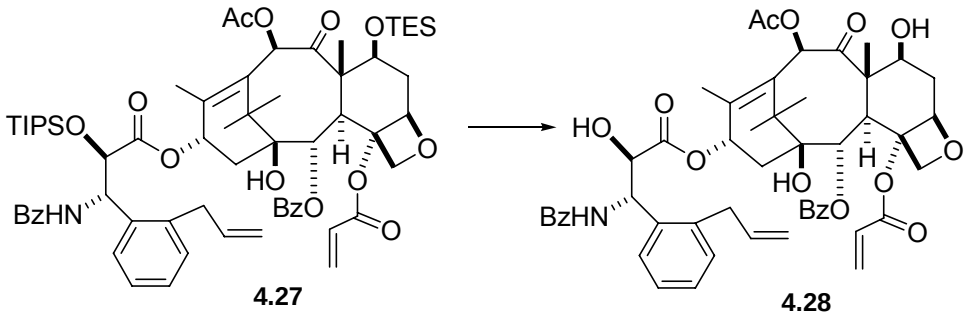

Open Chain paclitaxel (4.28). At 0 ^{o}C, HF/pyridine (0.6 mL) was added to a solution of **4.27** (15 mg, 0.013 mmol) in THF (14 mL) and the solution was warmed to RT and stirred overnight. The reaction mixture was diluted with EtOAc and quenched with $NaHCO_3$. The layers were separated and the aqueous phase was extracted with EtOAc. The combined organic layers were washed with water, brine, dried over Na_2SO_4, filtered and concentrated. Purification by PTLC gave **4.28** (11 mg, 90%). ^{1}H NMR (400 MHz, $CDCl_3$): δ 8.11 (2H, d, *J* = 8 Hz), 7.70 (2H, d, *J* = 7.6 Hz), 7.60 (1H, t, *J* = 7.6 Hz), 7.44-7.52 (4H, m), 7.38 (2H, t, *J* = 7.6 Hz), 7.24-7.31 (3H, m), 6.95 (1H, d, *J* = 9.2 Hz), 6.48 (1H, s), 6.44 (1H, d, *J* = 1.6 Hz), 6.32 (1H, d, *J* = 10 Hz), 6.28 (1H, d, *J* = 10 Hz), 6.0

(1H, m), 5.95 (1H, t, *J* = 9.6 Hz), 5.80 (1H, d, *J* = 9.6 Hz), 5.75 (1H, d, *J* = 7.2 Hz), 5.57 (1H, dd, *J* = 10, 1.6 Hz), 5.18 (1H, dd, *J* = 16.8, 1.6 Hz), 5.12 (1H, dd, *J* = 10, 1.6 Hz), 4.90 (1H, d, *J* = 7.6 Hz), 4.74 (1H, d, *J* = 1.6 Hz), 4.54 (1H, dd, *J* = 10.4, 6.4 Hz), 4.34 (1H, d, *J* = 8 Hz), 4.25 (1H, d, *J* = 8.4 Hz), 3.90 (1H, d, *J* = 7.2 Hz), 3.72 (1H, dd, *J* = 15, 6.4 Hz), 3.52 (1H, dd, *J* = 15.4, 6.8 Hz), 2.56 (1H, m), 2.40 (2H, m), 2.18 (3H, s), 2.03 (3H, s), 1.71 (3H, s), 1.23 (3H, s), 1.18 (3H, s), 1.00-1.07 (11H, m), 0.94 (9H, t, *J* = 8 Hz), 0.60 (6H, m). ^{13}C NMR (100 MHz): δ 202.8, 172.8, 169.5, 167.0, 165.0, 140.9, 137.4, 136.8, 136.2, 134.3, 133.7, 133.5, 132.0, 131.8, 130.29, 130.23, 129.7, 129.4, 128.8, 128.8, 128.5, 127.7, 127.6, 127.0, 126.8, 117.3, 84.4, 81.7, 78.9, 75.2, 74.4, 73.4, 72.3, 58.6, 52.4, 46.9, 43.5, 37.4, 37.1, 36.1, 26.6, 21.8, 21.0, 18.2, 18.1, 14.4, 13.0, 10.3, 6.9, 5.5. HRFABMS: found *m/z* 1198.5742, Calculated for $C_{60}H_{89}NO_{14}Si_2Na$ $(M+Na)^+$ *m/z* 1198.5719, Δ = 1.9 ppm.

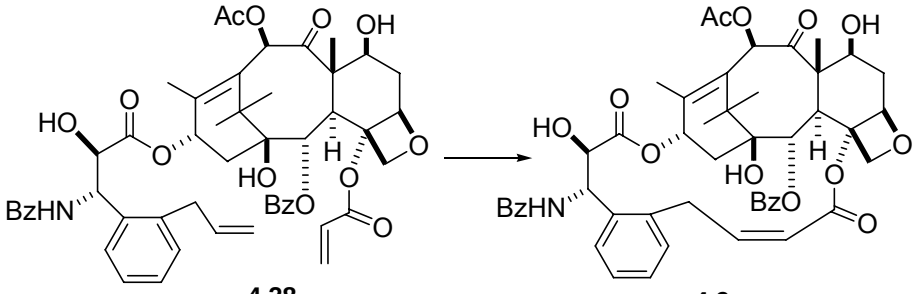

Bridged paclitaxel (4.9). At rt, a solution of **4.28** (38 mg, 0.042) in DCM (4 mL) was added to Grubbs second generation catalyst (10 mg, 0.011 mmol) in DCM (15 mL) for 3 h. After 12 h, the reaction mixture was concentrated and the residue was purified on PTLC to give **4.9** (20 mg, 53%). $[\alpha]_D$: -66.6 (c 0.09, $CHCl_3$). ^{1}H NMR (400 MHz, $CDCl_3$): δ 8.14 (d, *J* = 8Hz, 2H), 7.76 (d, *J* = 7.6Hz, 2H), 7.60 (t, *J* = 7.2Hz, 1H), 7.42-7.52 (m, 6H), 7.30 (m, 3H), 7.13 (d, *J* = 8Hz, 1H), 6.76 (td, *J* = 9.2, 2Hz, 1H), 6.49 (t, *J* =

8.8Hz 1H) 6.36 (s, 1H), 6.30 (dd, *J* = 11.4, 2Hz, 1H), 5.93 (d, *J* = 8 Hz, 1H), 5.73 (d, *J* = 6.8 Hz, 1H), 5.01 (d, *J* = 7.6Hz, 1H), 4.89 (dd, *J* = 19.2, 9.2Hz, 1H), 4.46 (d, *J* = 9.2Hz, 1H), 4.35 (s, 1H), 4.34 (d, *J* = 8.4Hz, 1H), 4.24 (d, *J* = 8Hz, 1H), 3.89 (d, *J* = 6.8Hz, 1H), 3.66 (td, *J* = 19.2, 2.8Hz, 1H), 3.25 (d, *J* = 2Hz, 1H), 2.66 (m, 1H), 2.48 (m, 2H), 2.24 (s, 3H), 2.24-2.26 (m 1H), 1.94-1.96 (m, 1H), 1.95 (s, 3H), 1.75 (s, 3H), 1.3 (s, 3H), 1.19(s, 3H). ^{13}C NMR (100 MHz): δ 203.8, 173.3, 171.4, 167.3, 166.8, 165.6, 153.2, 142.4, 138.6, 137.0, 134.0, 133.3, 132.1, 131.0, 130.5, 129.2, 129.0, 128.9, 128.6, 127.9, 127.3, 126.5, 120.5, 84.6, 81.3, 79.2, 75.7, 75.0, 72.9, 72.6, 72.2, 59.1, 51.0, 46.2, 43.6, 36.3, 35.6, 35.1, 27.2, 22.0, 21.0, 15.5, 9.7. HRFABMS: found *m/z* 878.3382, Calculated for $C_{49}H_{52}NO_{14}$ $(M+H)^+$ *m/z* 878.3388, Δ = 0.7 ppm.

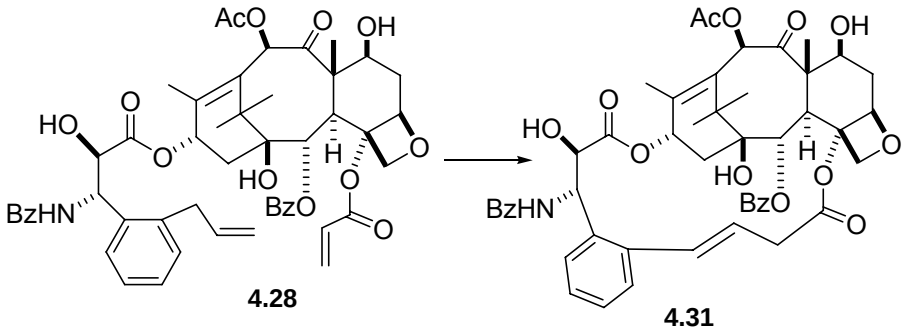

Bridged paclitaxel isomer (4.31). At 55 ^{o}C, a solution of **4.27** (20 mg, 0.022 mmol) in DCM (8 mL) was added to Grubbs second generation catalyst (5 mg, 0.006 mmol) in DCM (3 mL) and the mixture was stirred for 3h. The reaction mixture was concentrated and the residue was purified on PTLC to give **4.9** (4 mg) and **4.31** (9 mg, 67%). **4.31** ^{1}H NMR (400 MHz) δ 8.21 (2H, d, *J* = 7.6 Hz), 8.00 (1H, d, *J* = 7.6 Hz), 7.70 (2H, d, *J* = 7.6 Hz), 7.63 (1H, m), 7.60-7.40 (3H, m), 7.42-7.36 (5H, m), 7.22 (1H, d, *J* = 7.2 Hz), 6.72 (1H, d, *J* = 9.2 Hz), 6.33 (1H, t, *J* = 9.6 Hz), 6.29 (1H, s), 5.88 (1H, d, *J* = 16 Hz), 5.74 (1H, d, *J* = 6.8 Hz), 5.59 (1H, d, *J* = 16Hz), 4.97 (1H, d, *J* = 8.8 Hz), 4.61 (1H, bs), 4.45 (1H, dd, *J* = 10.6, 6.4 Hz), 4.38 (1H, d, *J* = 8.4 Hz), 4.29 (1H, d, *J* = 8.4 Hz), 4.26 (1H, d,

J = 4.8 Hz), 3.81 (1H, d, *J* = 6.8 Hz), 3.60 (1H, d, *J* = 19.2 Hz), 3.49 (1H, bs), 2.60 (2H, m), 2.46 (2H, m), 2.24 (3H, s), 2.21 (1H, m), 1.90 (1H, m), 1.82 (3H, s), 1.73 (3H, s), 1.25 (3H, s), 1.17 (3H, s). ^{13}C NMR (125 MHz) δ 203.9, 173.5, 171.4, 167.3, 166.9, 164.4, 149.3, 142.2, 140.0, 134.6, 133.9, 133.7, 133.5, 132.1, 131.4, 130.4, 129.7, 129.3, 128.9, 128.8, 128.1, 127.3, 123.4, 84.4, 80.8, 79.3, 76.6, 75.8, 75.5, 72.5, 72.4, 72.1, 58.1, 49.9, 46.1, 43.3, 37.4, 35.8, 35.7, 27.0, 21.8, 21.0, 15.2, 9.7. HRFABMS: found *m/z* 878.3362, Calcd for $C_{49}H_{52}NO_{14}$ $(M+H)^+$ *m/z* 878.3388, Δ = 3.0 ppm.

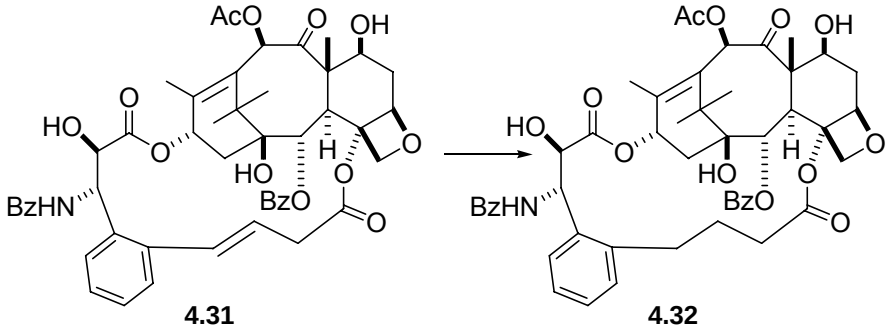

4.31 **4.32**

Dihydro bridged paclitaxel (4.10). At rt, a solution of **4.31** (6 mg, 0.0068 mmol) in methanol (5 mL) was treated with 10%Pd-C (10 mg) and hydrogenated at 50 psi overnight. The reaction mixture was filtered a through short plug of silica gel. The filtrate was concentrated and purified on PTLC to afford **4.32** (5 mg, 83%). ^{1}H NMR (400 MHz, $CDCl_3$): δ 8.16 (d, *J* = 8 Hz, 2H), 7.77(d, *J* = 7 Hz, 1H), 7.70(d, *J* = 7.4 Hz, 2H), 7.60 (t, *J* = 7.6 Hz, 1H), 7.5 (m, 3H), 7.38 (t, *J* = 8 Hz, 2H), 7.24-7.30 (m, 3H), 6.97 (d, *J* = 8.8 Hz, 1H), 6.53 (t, *J* = 8.4 Hz 1H) 6.28 (s, 1H), 5.95 (d, *J* = 8.8 Hz, 1H), 5.74 (d, *J* = 7.2 Hz, 1H), 4.95(d, *J* = 8 Hz, 1H), 4.57 (d, *J* = 2.4 Hz, 1H), 4.38 (dd, *J* = 10.4, 6.8 Hz, 1H), 4.32(d, *J* = 8.8 Hz, 1H), 4.22(d, *J* = 8.4 Hz, 1H), 3.74 (d, *J* = 7.2 Hz, 1H), 3.47 (d, *J* = 3.2 Hz, 1H), 3.22 (m, 1H), 3.05 (m, 1H), 2.76-2.90 (m, 2H), 2.25-2.45(m, 5H), 2.23 (s, 3H), 2.05 (m 1H), 1.98 (m, 1H), 1.83 (s, 3H), 1.71 (s, 3H), 1.34 (s, 3H), 1.18 (s, 3H). ^{13}C NMR (100 MHz): δ 203, 173.7, 172.3, 171.3, 167.1, 166.8, 142.2, 139.3, 138.7,

133.7, 133.6, 133.0, 131.9, 130.3, 130.1, 129.1, 128.8, 128.6, 128.4, 127.4, 127.1, 84.4, 80.9, 79.4, 75.4, 75.0, 73.1, 72.4, 72.2, 58.6, 49.4, 45.5, 43.4, 35.7, 35.0, 33.5,27.3, 26.0, 22.6, 20.8, 14.7, 9.6. HRFABMS: found *m/z* 902.3419, Calculated for $C_{49}H_{53}NO_{14}Na$: $(M+Na)^+$ *m/z* 902.3364, Δ = 6.1 ppm.

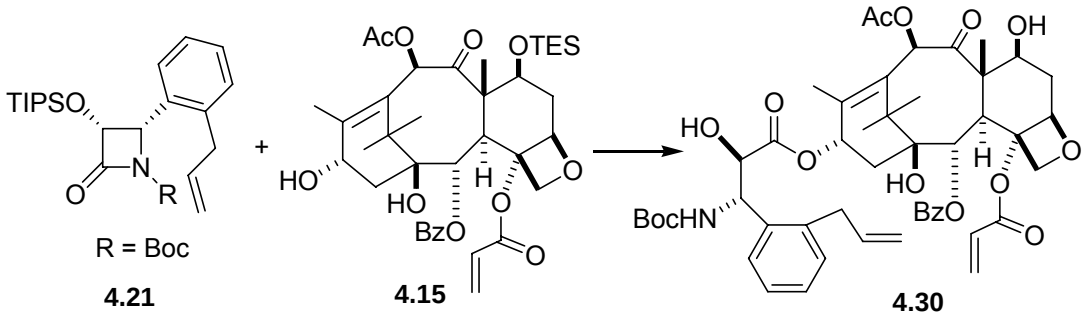

***N*-Debenzoyl-*N*-Boc open chain paclitaxel (4.30).** A solution of 56 mg (0.12 mmol) β–lactam **4.21** and 25 mg (0.035 mmol) 4–acryloyl–7–triethylsilylbaccatin III **4.15** in 7 mL THF was treated slowly with 0.06 mL LiHMDS at -45 °C and stirred for 4 h, with monitoring by TLC. The mixture was quenched with NH_4Cl, and extracted with EtOAc. Usual work-up gave crude product which was purified by preparative TLC to give 2'-*O*-(triisopropyl)-3'-(*o*-allylphenyl) -7-*O*-triethylsilyl-4-deacetyl-4-acryloyl-paclitaxel **4.29** (36 mg, 86%). At 0 ^oC, 0.2 mL HF/pyridine (large excess) was added to this compound (20 mg) in 4 mL of THF and the solution was warmed to RT and stirred overnight. The reaction mixture was diluted with EtOAc and washed with aq. $NaHCO_3$. The organic layers were washed with H_2O and brine, dried over anhydrous Na_2SO_4, and concentrated under reduced pressure to give **4.30** (16 mg, 92%). This product was used directly in the next step.

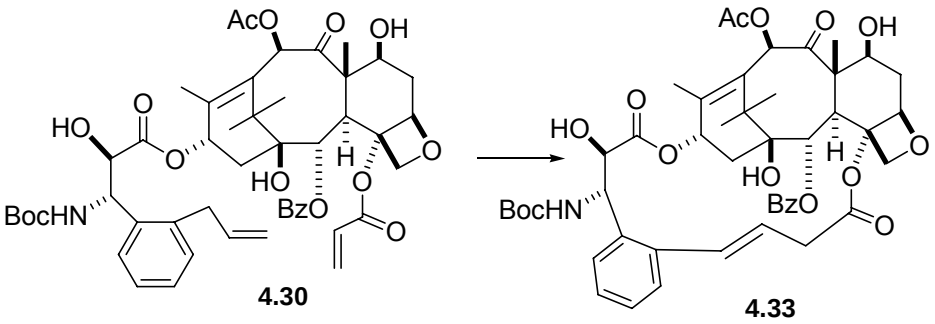

***N*-Debenzoyl-*N*-Boc bridged paclitaxel (4.33).** At rt, a solution of **4.30** (22 mg, 0.019 mmol) in DCM (8 mL) was added to Grubbs second generation catalyst (6.2 mg, 0.007 mmol) in DCM (4 mL) for 3 h. After 12 h, the reaction mixture was concentrated and the residue was purified on PTLC to give **4.33** (20 mg, 91%). ^{1}H NMR (400 MHz) δ 8.17 (2H, d, *J* = 7.2 Hz), 7.88 (2H, d, *J* = 7.6 Hz), 7.64 (1H, t, *J* = 6.8 Hz), 7.52 (3H, m), 7.38-7.30 (2H, m), 7.19 (1H, dd, *J* = 7.2, 1.6 Hz), 6.33 (1H, t, *J* = 8.4 Hz), 6.28 (1H, s), 6.15 (1H, t, *J* =5.5 Hz), 5.69 (1H, d, *J* = 7.2 Hz), 5.61 (1H, d, *J* = 16 Hz), 5.40 (1H, d, *J* = 9.6 Hz), 5.15 (1H, d, *J* = 10.0, Hz), 4.95 (1H, d, *J* = 8.0 Hz), 4.47 (1H, s), 4.44 (1H, dd, *J* = 10.8, 6.8 Hz), 4.34 (1H, d, *J* = 8.4 Hz), 4.26 (1H, d, *J* = 8.4 Hz), 4.15 (1H, m), 3.79 (1H, d, *J* = 7.2 Hz), 3.56 (1H, m), 3.39 (1H, bs), 2.56 (1H, m), 2.35 (1H, m), 2.24 (3H, s), 1.88 (1H, m), 1.82 (3H, s), 1.71 (3H, s), 1.65 (1H, m), 1.35 (9H, s), 1.27 (1H, m),1.25 (3H, s), 1.16 (3H, s). ^{13}C NMR (100 MHz) δ 204.0, 173.6, 171.5, 167.5, 164.5, 155.3, 149.3, 142.5, 140.4, 134.3, 133.9, 133.4, 131.3, 130.4, 129.9, 129.0, 128.9, 128.7, 128.1, 123.3, 84.4, 80.8, 80.1, 79.4, 77.4, 76.7, 75.9, 75.5, 72.5, 71.7, 58.8, 51.0, 46.2, 43.3, 37.5, 35.8, 35.6, 29.9, 28.4, 21.9, 21.1, 15.3, 9.7. HRFABMS: found *m/z* 874.3685, calcd for $C_{47}H_{56}NO_{15}$ $(M+H)^{+}$ *m/z* 874.3650, Δ = 4.0 ppm.

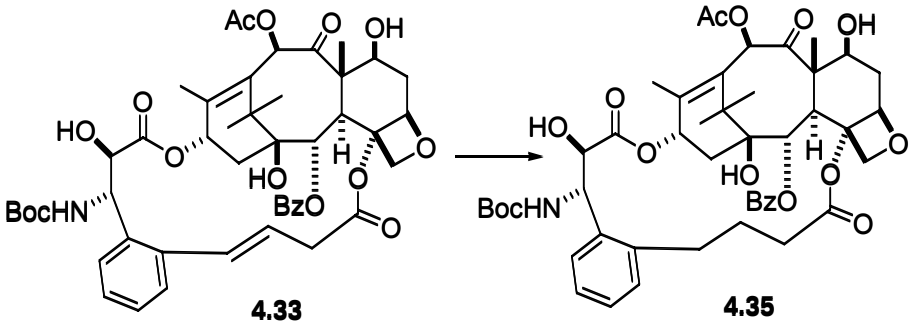

***N*-Debenzoyl-*N*-Boc dihydro bridged paclitaxel (4.35).** At rt, a solution of **4.33** (6 mg, 0.0069 mmol) in methanol (3 mL) was treated with 10% Pd-C (20 mg) and hydrogenated at 35 psi overnight. The reaction mixture was filtered through a short plug of silica gel.

The filtrate was concentrated and purified on PTLC to afford **4.35** (4.5 mg, 75%). ^{1}H NMR (400 MHz) δ 8.15 (2H, d, *J* = 7.6 Hz), 7.63 (2H, t, *J* = 5.6 Hz), 7.52 (2H, t, *J* = 7.6 Hz), 7.31-7.19 (3H, m), 6.52 (1H, t, *J* = 9.0 Hz), 6.27 (1H, s), 5.72 (1H, d, *J* = 7.2 Hz), 5.42 (2H, m), 4.93 (1H, d, *J* = 8.0 Hz), 4.44 (1H, d, *J* = 3.2 Hz), 4.37 (1H, dd, *J* = 10.8, 6.8 Hz), 4.30 (1H, d, *J* = 8.4 Hz), 4.19 (1H, d, *J* = 8.4 Hz), 3.73 (1H, d, *J* = 7.2 Hz), 3.35 (1H, bs) 3.11-2.98 (2H, m), 2.88-2.68 (2H, m), 2.56 (1H, m), 2.35 (1H, m), 2.23 (3H, s), 2.28-2.22 (1H, m), 2.11-1.98 (2H, m), 1.94-1.88 (1H, m), 1.82 (3H, s), 1.71 (3H, s), 1.35 (3H, s), 1.33 (9H, s), 1.18 (3H, s). ^{13}C NMR (100 MHz) δ 203.8, 174.0, 172.5, 171.5, 167.4, 155.3, 142.7, 139.1, 134.0, 133.0, 130.5, 130.2, 129.3, 129.0, 128.4, 127.4, 84.6, 81.1, 79.7, 7.4, 75.6, 75.2, 73.5, 72.6, 72.1, 58.8, 50.7, 45.8, 43.6, 35.9, 35.8, 33.7, 28.4, 27.4, 26.0, 22.7, 21.1, 14.9, 9.8. HRFABMS: found *m/z* 876.3795, Calcd for $C_{47}H_{58}NO_{15}$ $(M+H)^+$ *m/z* 876.3806, Δ = 1.3 ppm.

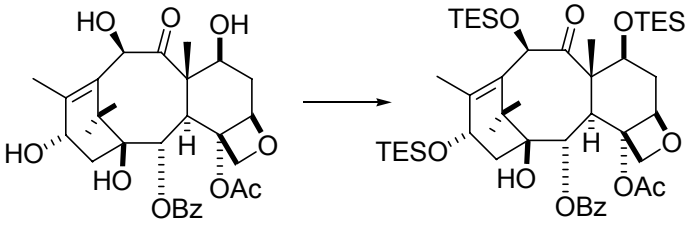

4.22

7,10,13-Tris(triethylsilyl)-10-deacetylbaccatin III. To the solution of 10-deacetylbaccatin III **4.22** (800 mg, 1.5 mmol) in 5 mL of DMF was added imidazole (1.15 g, 17 mmol) and triethylsilyl chloride (1.5 mL, 8.9 mmol) and the mixture stirred at rt for 3 h. The reaction mixture was diluted with EtOAc (50 mL) and the combined organic layers were washed with saturated aqueous $NaHCO_3$ and brine, and dried over Na_2SO_4. Column chromatography on silica gel gave compound 7,10,13-tris(triethylsilyl)-10-deacetylbaccatin III (989 mg, 76%) as a white solid. ^{1}H NMR: δ 8.07 (2H, dd, *J* = 8.0

and 1.5), 7.56 (1H, t, *J* = 8.0), 7.45(2H, t, *J* = 8.0) , 5.60(1H, d, *J* = 6.0), 5.17 (1H, s), 4.93 (1H, dd, *J* =9.0 and 2.5), 4.42 (1H, dd, *J* = 7.5 and 1.5), 4.26 (1H, d, *J* = 8.5), 4.11 (1H, dd, *J* = 9.0 and 2.0), 4.08 (1H, dd, *J* = 9.5 and 2.5), 3.83 (1H, d, *J* = 7.0), 2.48 (1H, m), 2.26 (3H, s), 2.01 (3H, s), 1.62 (3H, s), 1.17 (3H, s), 1.10 (3H, s), 0.98-0.96 (overlapped, 27H), 0.62-0.60 (overlapped, 18H); ^{13}C NMR: δ 209.0, 170.0, 167.2, 139.5, 133.5, 130.1, 128.6, 84.1, 80.9, 79.6, 76.8, 76.7, 75.8, 75.6, 72.7, 68.4, 58.3, 47.0, 43.1, 39.9, 37.4, 26.4, 22.4, 20.7, 14.6, 14.2, 10.5, 7.0-6.9 (overlapped), 5.75, 5.44, 5.12; HRFABMS: found *m/z* 887.5047, Calcd for $C_{47}H_{79}O_{10}Si_3$ $(M+H)^+$ *m/z* 887.4981, Δ = +7.4 ppm.

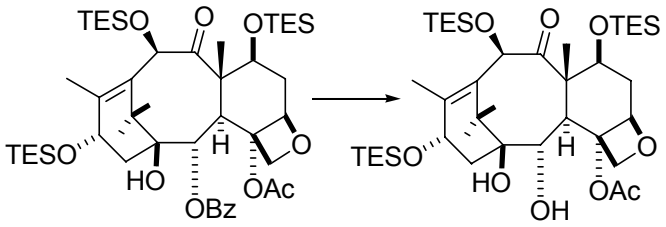

4.37

2-Debenzoyl-7,10,13-tris(triethylsilyl)-10-deacetylbaccatin III (4.37). To a solution of 7,10,13-tris(triethylsilyl)-10-deacetylbaccatin III (750 mg, 0.84 mmol) in anhydrous THF (15 mL) at -20 °C, Red-Al (4M in THF, 1.1 mL) was added dropwise under nitrogen. The reaction was stirred for 45 min until TLC showed the exhaustion of starting material. After quenching with a few drops of water, the reaction mixture was added to 50 mL of 1M sodium potassium tartrate and extracted with EtOAc. The organic part was washed with water and brine, and dried over Na_2SO_4. Column chromatography on silica gel gave compound **4.37** (484 mg, 72%). ^{1}H NMR δ 5.14 (1H, s), 4.72 (1H, d, *J* = 7.0 Hz), 4.63 (1H, dd, *J* = 9.5 and 4.0 Hz), 4.42 (1H, dd, *J* = 7.5 and 1.5 Hz), 4.56 (1H, d, *J* = 9.0 Hz), 4.11 (1H, m), 3.98 (1H, dd, *J* = 10.5, 6.0 Hz), 3.74(1H, dd, *J* =10.5, 5.5 Hz), 3.45 (1H, d, *J* = 10.5 Hz), 3.23 (1H, d, *J* = 6.0 Hz), 2.45-2.37 (3H, overlapped, m), 2.08 (3H, s), 1.98 (3H,s), 1.78 (3H, s), 1.04 (3H, s), 1.01 (3H, s), 0.97-0.94 (overlapped, 27H), 0.63-0.60

(overlapped, 18H); ^{13}C NMR δ 206.3, 169.7, 139.0, 136.0, 83.7, 82.0, 78.7, 78.0, 76.8, 75.8, 74.7, 72.7, 68.4, 58.2, 46.8, 42.5, 40.4, 37.4, 26.0, 22.4, 20.6, 14.5, 10.6, 6.9-6.8 (overlapped), 5.21, 5.13, 4.82.

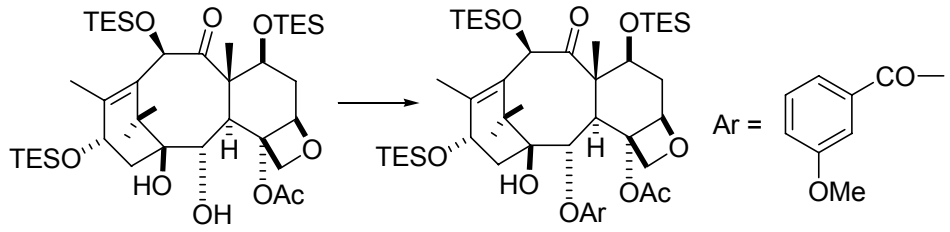

4.37 **4.38**

2-Debenzoyl-2(*m*-methoxybenzoyl)-7,10,13-tris(triethylsilyl)-10-deacetylbaccatin III (4.38). *N,N'*–Diisopropylcarbodiimide (0.85 mL, 5.5 mmol) and DMAP (660 mg, 5.4 mmol) were added to a solution of *m*–methoxybenzoic acid (757 mg, 5.0 mmol) in dry toluene (10 mL); the heterogenous mixture was stirred at rt for 0.5 h, and compound **4.36** (200 mg, 0.26 mmol), in 5 mL of toluene was added dropwise. The solution was stirred for 10 min. at rt and heated to 55 °C for 24 h. The reaction mixture was then diluted with EtOAc and washed with H_2O and $NaHCO_3$. The combined organic phase was washed with H_2O and brine, dried over anhydrous Na_2SO_4, and concentrated under reduced pressure. Column chromatography gave **4.37** (223 mg, 73% based on **4.36**) as a white solid. ^{1}H NMR: δ 7.69 (1H, d, *J* = 8.0 Hz), 7.63 (1H, m), 7.35 (1H, t, *J* = 8.0), 7.10 (1H, m) , 5.70 (1H, d, *J* = 6.0 Hz), 5.16 (1H, s), 4.95 (2H, m), 4.55 (1H, m), 4.37 (1H, dd, *J* = 7.5 and 1.5 Hz), 4.28 (1H, d, *J* = 6.0 Hz), 4.20 (1H, d, *J* = 6.4 Hz) , 3.86 (overlapped 4H), 2.50 (1H, m), 2.34 (1H, m), 2.26 (3H, s), 1.97 (3H, s), 1.88 (1H, m), 1.64 (3H, s), 1.18 (3H, s), 1.10 (3H, s), 0.98-0.96 (overlapped, 27H), 0.62-0.60 (overlapped, 18H); ^{13}C NMR: δ 207.0, 166.4, 165.7, 160.7, 140.0, 136.7, 132.8, 131.5, 130.7, 130.2, 123.3, 120.0, 116.0, 84.8, 82.7, 82.0, 77.4, 76.7, 76.3, 73.3, 68.8, 58.9, 55.9, 47.1, 44.5, 39.7, 37.8, 27.7, 21.7,

14.9, 10.7, 7.0-6.9 (overlapped), 6.2, 5.50, 5.06; HRFABMS: found *m/z* 917.50433, calcd for $C_{48}H_{81}O_{11}Si_3$ $(M+H)^+$ *m/z* 917.5087, $\Delta = 4.8$ ppm.

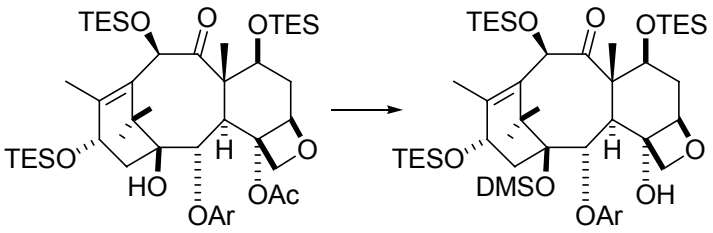

4.38 **4.40**

2-Debenzoyl-2-(*m*-methylbenzoyl)-4-deacetyl-1-dimethylsilyl-7,10,13-tris(triethylsilyl)-10-deacetylbaccatin III (4.40). Compound **4.40** was synthesized from **4.38** by the literature method.[16]

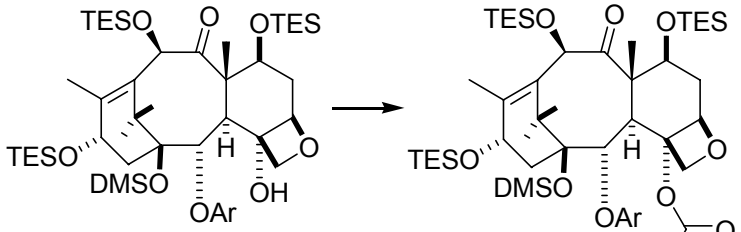

4.40 **4.41**

2-Debenzoyl-2-(*m*-methoxybenzoyl)-4-deacetyl-4-acryloyl-1-dimethylsilyl-7,10,13-tri(triethylsilyl)-10-deacetylbaccatin III (4.41). A solution of 400 mg **4.40** (270 mg, 0.28 mmol) in 6.5 mL THF at 0 °C was treated with 1 M LiHMDS (0.4 mL) followed by acryloyl chloride (0.045 mL, 0.55 mmol). The mixture was stirred for 3 h with monitoring by TLC, and then quenched with saturated aq. NH_4Cl. The reaction mixture was extracted with EtOAc and washed with H_2O and brine. The combined organic layers were dried over anhydrous Na_2SO_4 and concentrated under reduced pressure. Purification of the crude residue by silica column gave **4.41** (100 mg, 35%). ^{1}H NMR: δ 7.69 (1H, d, *J* = 8.0 Hz), 7.63 (1H, m), 7.35 (1H, t, *J* = 8.0), 7.10 (1H, m), 6.56 (1H, dd, *J* = 17.4, 1.2 Hz), 6.25 (1H, dd, *J* = 17.4, 10.5 Hz), 6.15 (1H, dd, *J* = 10.5, 1.17 Hz), 5.70 (1H, d, *J* = 7 Hz),

5.10 (1H, s), 4.86 (2H, m), 4.58 (1H, m), 4.42 (1H, dd, *J* = 10, 6.6 Hz), 4.30 (2H, ABq, *J* = 11.2, 8.4 Hz), 3.98 (1H, d, *J* = 6.8 Hz), 3.82 (3H, s), 2.58 (1H, m), 2.26 (2H, m), 2.00 (3H, s), 1.96 (1H, m), 1.67 (3H, s), 1.22 (3H, s), 1.08 (3H, s), 1.0 (27H, m), 0.65 (18H, m), 0.05 (3H, d, *J* = 2.7 Hz), -0.28 (3H, d, *J* = 2.7 Hz).; ^{13}C NMR: δ 207.0, 166.4, 165.7, 160.7, 140.0, 136.7, 132.8, 131.5, 130.7, 130.2, 123.3, 120.0, 116.0, 84.8, 82.7, 82.0, 77.4, 76.7, 76.3, 73.3, 68.8, 58.9, 55.9, 47.1, 44.5, 39.7, 37.8, 27.7, 21.7, 14.9, 10.7, 7.0-6.9 (overlapped), 6.2, 5.50, 5.06, 0.62, 0.29; HRFABMS: found *m/z* 975.53857, Calcd for $C_{50}H_{87}O_{11}Si_4$ $(M+H)^+$ *m/z* 975.5326, Δ = 6.2 ppm.

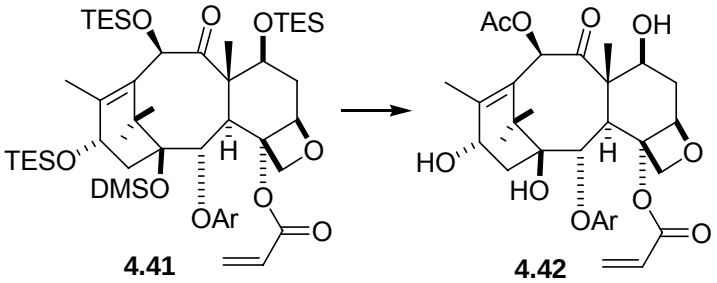

2-Debenzoyl-2-(*m*-methoxybenzoyl)-4-deacetyl-4-acryloyl-10-deacetylbaccatin III (4.42). At 0 ºC, HF/pyridine (0.6 mL) was added to a solution of **4.41** (100 mg, 0.10 mmol) in 8 mL of THF and the solution was warmed to rt and stirred overnight. The reaction mixture was diluted with EtOAc and washed with aq. $NaHCO_3$. The organic layers were washed with H_2O and brine, dried over anhydrous Na_2SO_4, and concentrated under reduced pressure. The residue was purified by PTLC to afford 2-debenzoyl-2-(*m*-methoxybenzoyl)-4-deacetyl-4-acryloyl-10-deacetylbaccatin III (45 mg, 78%). To a solution of above 4-deacetyl-4-acryloyl-10-deacetylbaccatin in 1.5 mL of THF was added a catalytic amount of $CeCl_3$ and the solution stirred at RT for 20 min. Acetic anhydride was then added and the solution stirred for 4 h. The mixture was then diluted with EtOAc, quenched with aq. $NaHCO_3$ and washed with H_2O and brine. The organic phase

was dried over anhydrous Na_2SO_4, concentrated, and purified by preparative TLC to give 2-debenzoyl-2-(*m*-methoxybenzoyl)-4-deacetyl-4-acryloyl baccatin III **4.42** (47 mg, 95%). ^{1}H NMR (400 MHz, $CDCl_3$): δ 7.66 (1H, d, *J* = 8.0 Hz), 7.60 (1H, m), 7.36 (1H, t, *J* = 8.0), 7.12 (1H, m), 6.50 (1H, dd, *J* = 17.4, 1.2 Hz), 6.32 (1H, s), 6.27 (1H, dd, *J* = 17.4, 10.5 Hz), 5.99 (1H, dd, *J* = 17.4, 1.2 Hz), 5.60 (1H, d, *J* = 7 Hz), 4.96 (1H, dd *J* = 9.6, 2 Hz), 4.78 (1H, t, *J* = 7 Hz), 4.52 (1H, dd, *J* = 10.9, 6.8 Hz), 4.36 (1H, d, *J* = 8.4 Hz), 4.18 (1H, d, *J* = 8.5 Hz), 3.94 (1H, d, *J* = 6.8 Hz), 3.86 (3H, s), 2.60 (2H, m), 2.20 (3H, s), 2.22-2.18 (2H, m), 2.02 (3H, s), 1.80-1.86 (2H, m), 1.67 (3H, s), 1.08 (3H, s), 1.07 (3H, s). ^{13}C NMR (100 MHz): δ 205.5, 172.6, 168.0, 166.4, 160.8, 147.7, 132.6, 132.4, 131.6, 130.6, 130.4, 123.2, 120.3, 116.2, 85.1, 81.8, 79.7, 77.8, 76.9, 75.7, 72.9, 68.5, 59.3, 56.0, 46.5, 43.1, 39.7, 36.0, 27.3, 21.2, 15.8, 9.7. HRFABMS: found *m/z* 629.2502, Calculated for $C_{33}H_{41}O_{12}$ $(M+H)^+$ *m/z* 629.2492, Δ = 1.6 ppm.

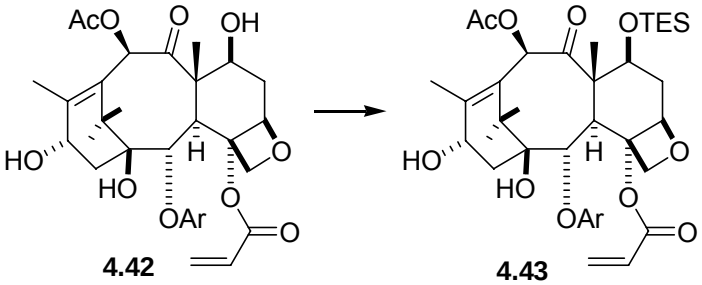

2-Debenzoyl-2-(*m*-methoxybenzoyl)-4-deacetyl-4-acryloyl-7-triethylsilylbaccatin III (4.43). The 4-acryloyl-baccatin III derivative **4.42** (47 mg, 0.075 mmol) was dissolved in 5 mL of DCM and treated with imidazole (79 mg, 1.2 mmol) and chlorotriethylsilane (0.10 mL, 0.5 mmol) and the mixture stirred at rt for 30 min with monitoring by TLC. The reaction mixture was quenched with MeOH saturated with $NaHCO_3$ and stirred for 10 min. The mixture was diluted and extracted with EtOAc, washed with H_2O and brine. The organic phase was concentrated and purified by preparative silica TLC to give 4-

acryloyl-7-triethylsilylbaccatin III **4.43** (28 mg, 43%). HRFABMS found *m/z* 743.34589, Calcd for $C_{39}H_{55}O_{12}Si$ $(M+H)^+$ *m/z* 743.3463, Δ = 0.5 ppm.

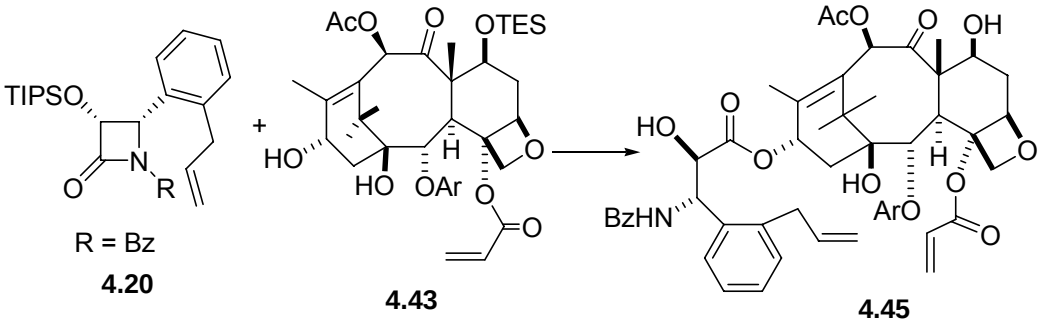

Paclitaxel derivative (4.45). A solution of β-lactam **4.20** (50 mg, 0.11 mmol) and baccatin **4.43** (24 mg, 0.0032 mmol) in THF (7 mL) was treated slowly with 1 M LiHMDS (0.06 mL) at -45 °C and stirred for 4 h, with monitoring by TLC. The mixture was quenched with sat. NH_4Cl, and extracted with EtOAc. The organic phase was washed with H_2O and brine, dried over Na_2SO_4, and concentrated. The residue was purified by preparative TLC to give silyl protected N-benzoyl-2-(*m*-methoxybenzoyl) paclitaxel **4.44** (20 mg, 51%). HRFABMS: found *m/z* 1206.6038, Calcd for $C_{67}H_{92}NO_{15}Si_2$ $(M+H)^+$ *m/z* 1206.6006, Δ = 2.7 ppm. At 0 ^oC, HF/pyridine (0.1 mL) was added to this compound (5 mg, 0.0041 mmol) in 2.2 mL of THF and the solution was warmed to rt and stirred overnight. The reaction mixture was diluted with EtOAc and washed with aq. $NaHCO_3$. The organic layers were washed with H_2O and brine, dried over anhydrous Na_2SO_4, and concentrated under reduced pressure. This crude compound N-benzoyl-2-(*m*-methoxybenzoyl) paclitaxel **4.45** (2 mg, 52%) was used directly in the next step.

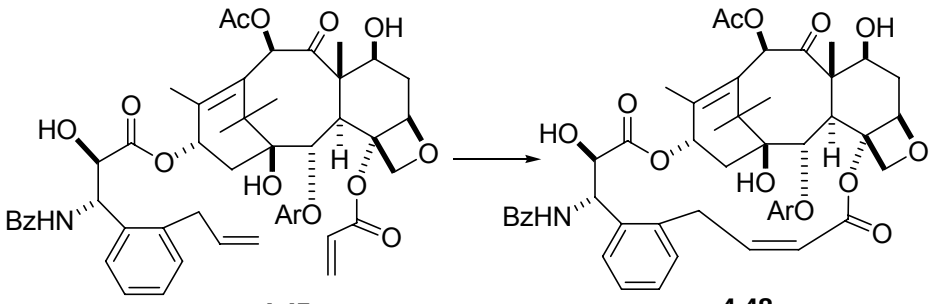

2-Debenzoyl-2-(*m*-methoxybenzoyl) bridged paclitaxel (4.48) and (4.49). At rt, a solution of **4.45** (10 mg, 0.011 mmol) in DCM (4 mL) was added to Grubbs second generation catalyst (2 mg, 0.0023 mmol) in DCM (2 mL) for 3h. After 12 h, the reaction mixture was concentrated and the residue was purified on PTLC to give **4.48** (2.5 mg, 25%) and **4.49** (5 mg, 50%).

Compound **4.48** (*cis* isomer): ^{1}H NMR (400 MHz) δ 7.76 (2H, d, *J* = 8.0 Hz), 7.6 (1H, m), 7.52 (1H, t, *J* = 7.2 Hz), 7.46-7.37 (4H, m), 7.31 (3H, m), 7.13 (2H, d, *J* = 8.4 Hz), 6.74 (1H, t, *J* = 10.4 Hz), 6.50 (1H, t, *J* = 9.0 Hz), 6.36 (1H, s), 6.28 (1H, d, *J* = 11.6 Hz), 5.93 (1H, d, *J* = 8.4 Hz), 5.73 (1H, d, *J* = 6.8 Hz), 5.03 (1H, d, *J* = 8.0 Hz), 4.86 (1H, dd, *J* = 10.8, 7.2 Hz), 4.44 (1H, s) 4.37 (1H, d, *J* = 8.0 Hz), 4.25 (1H, d, *J* = 8.4 Hz), 3.89 (1H, d, *J* = 6.8 Hz), 3.86 (3H, s), 3.65 (1H, d, *J* = 18.8 Hz), 2.69-2.61 (1H, m), 2.25 (3H, s), 2.23 (1H, m), 1.96 (1H, m), 1.95 (3H, s), 1.76 (3H, s), 1.30 (3H, s), 1.19 (3H, s). ^{13}C NMR (100 MHz) δ 203.9, 173.3, 171.5, 167.3, 166.7, 165.6, 159.9, 153.3, 142.4, 138.6, 137.0, 134.0 133.3, 132.2, 131.0, 130.4, 130.1, 128.9, 128.6, 127.9, 127.3, 126.5, 122.9, 120.8, 120.5, 114.6, 84.6, 81.3, 79.1, 77.2, 75.8, 75.1, 73.0, 72.6, 72.1, 58.2, 55.8, 51.0, 46.2, 43.6, 36.3, 35.7, 35.1, 29.9, 27.3, 22.0, 21.1, 15.5, 9.7; HRFABMS: found *m/z* 908.3516, Calcd for $C_{50}H_{54}NO_{15}^{+}$ *m/z* 908.3493, Δ = 2.5 ppm.

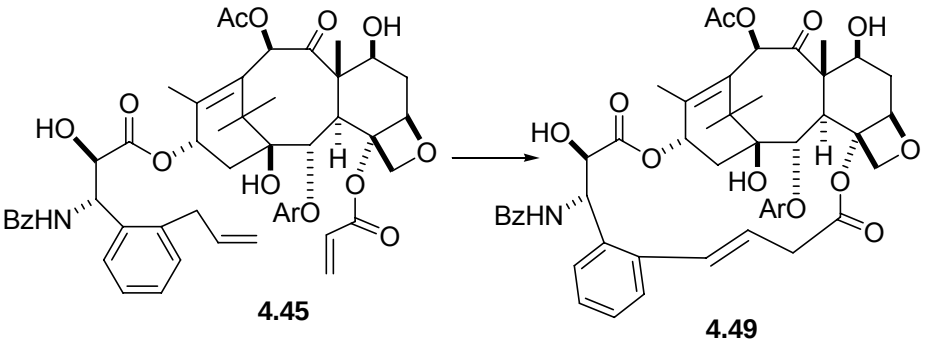

Compound **4.49** (*trans* isomer): ^{1}H NMR (400 MHz) δ 8.00 (1H, d, *J* = 7.6 Hz), 7.80 (1H, d, *J* = 7.6 Hz), 7.73-7.65 (3H, m), 7.50-7.35 (6H, m), 7.20 (1H, m), 7.16 (1H, m), 6.69 (1H, d, *J* = 9.2 Hz), 6.33 (1H, t, *J* = 9.4 Hz), 6.29 (1H, s), 5.85 (1H, d, *J* = 9.2 Hz), 5.72 (1H, dd, *J* = 7.2 Hz), 5.55 (1H, d, *J* = 16.0 Hz), 4.97 (1H, d, *J* = 7.6 Hz), 4.59 (1H, s), 4.44 (1H, dd, *J* = 10.8, 6.8 Hz), 4.41 (1H, d, *J* = 8.0 Hz), 4.28 (1H, d, *J* = 8.2 Hz), 3.87 (3H, s), 3.80 (1H, d, *J* = 6.8 Hz), 3.58 (1H, d, *J* = 19.2 Hz), 3.50 (1H, brs), 2.62-2.42 (3H, m), 2.24 (3H, s), 1.98-1.80 (2H, m), 1.83 (3H, s), 1.72 (3H, s), 1.26 (1H, m), 1.24 (3H, s), 1.16 (3H, s). ^{13}C NMR (100 MHz) δ 204.0, 173.6, 171.5, 167.1, 167.0, 164.5, 160.0, 149.4, 142.3, 140.0, 134.6, 133.8, 133.7, 133.6, 132.0, 131.5, 131.0, 130.0, 129.4, 129.0, 128.9, 128.1, 127.3, 123.3, 122.7, 119.5, 115.8, 84.4, 80.9, 77.4, 76.9, 75.9, 75.5, 58.9, 55.8, 50.1, 46.2, 43.4, 37.4, 35.8, 35.7, 27.0, 21.8, 21.1, 15.3, 9.7; HRFABMS: found *m/z* 908.3516, Calcd for $C_{50}H_{54}NO_{15}$ $(M+H)^{+}$ *m/z* 908.3493, Δ = 2.5 ppm.

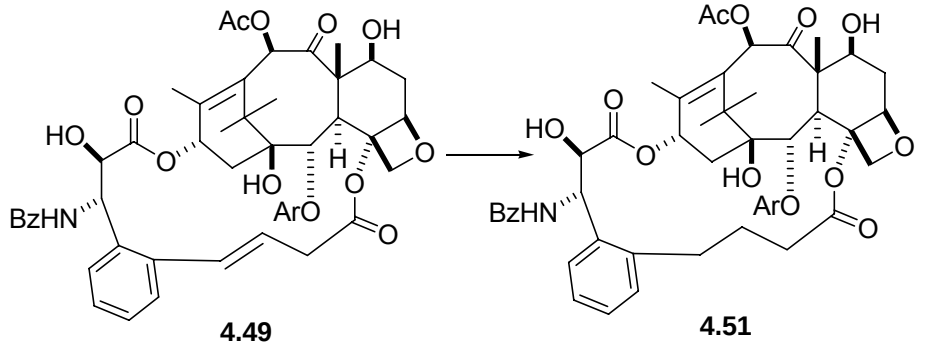

2-Debenzoyl-2-(*m*-methoxybenzoyl) dihydro bridged paclitaxel (4.51). At rt, a solution of **4.49** (6 mg, 0.0066 mmol) in methanol (5 mL) was treated with 10% Pd-C (10 mg) and hydrogenated at 50 psi overnight. The reaction mixture was filtered through a short plug of silica gel. The filtrate was concentrated and purified on PTLC to afford **4.51** (5 mg, 83%).[1]H NMR (400 MHz) δ 7.77 (1H, d, *J* = 7.2 Hz), 7.66-7.63 (2H, m), 7.50-7.36 (4H, m), 7.31-7.15 (3H, m), 6.95 (1H, d, *J* = 8.8Hz), 6.53 (1H, t, *J* = 8.6 Hz), 6.27 (1H, s), 5.94 (1H, d, *J* = 8.8 Hz), 5.74 (1H, d, *J* = 7.2 Hz), 4.96 (1H, d, *J* = 8.0 Hz), 4.56 (1H, bs), 4.40-4.33 (2H, m), 4.23 (1H, d, *J* = 8.4 Hz), 3.90 (3H, s), 3.73 (1H, d, *J* = 6.8 Hz), 3.11-2.96 (2H, m), 2.86-2.68 (2H, m), 2.56 (1H, m), 2.35 (1H, m), 2.28-2.24 (1H, m), 2.24 (3H, s), 2.11-1.98 (2H, m), 1.94-1.88 (1H, m), 1.82 (3H, s), 1.72 (3H, s), 1.34 (3H, s), 1.18 (3H, s). [13]C NMR (100 MHz) δ 203.8, 174.0, 172.4, 171.5, 167.2, 167.0, 160.0, 142.5, 139.4, 138.9, 133.8, 133.2, 130.5, 130.3, 130.1, 128.9, 128.8, 128.6, 127.7, 127.3, 122.9, 120.7, 114.6, 84.6, 81.1, 79.6, 77.4, 75.6, 75.3, 73.4, 72.6, 72.4, 58.8, 55.7, 50.7, 49.5, 45.7, 43.6, 40.0, 35.4, 33.8, 30.0, 27.5, 25.9, 22.8, 21.1, 14.9, 9.8.

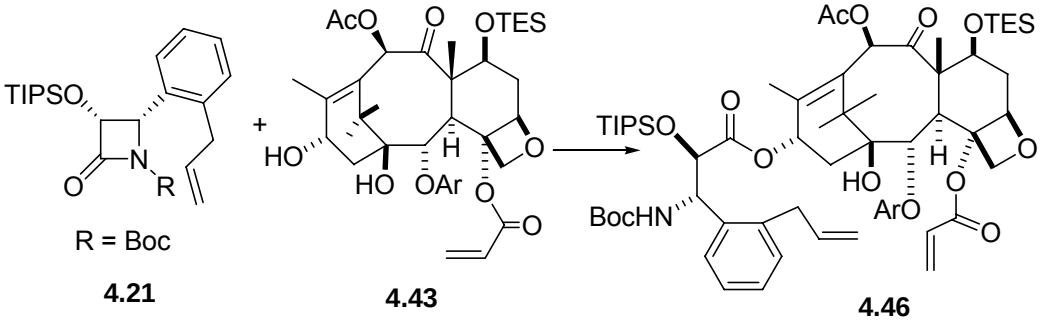

Silylated *N*-Boc-2-(*m*-methoxybenzoyl) paclitaxel (4.46). A solution of 58 mg (0.13 mmol) β–lactam **4.21** and 4-acryloyl-7-triethylsilylbaccatin III **4.43** (28 mg, 0.038 mmol) in 2 mL THF was treated slowly with 1M LiHMDS (0.06 mL) at -45 °C and stirred for 4 h, with monitoring by TLC. The reaction was quenched with sat. NH_4Cl, and extracted with

EtOAc. Usual work-up gave crude product which was purified by preparative TLC to give silyl protected N-Boc-2-(*m*-methoxybenzoyl) paclitaxel **4.46** (34 mg, 80%). HRFABMS: found *m/z* 1202.6338, Calcd for $C_{65}H_{96}NO_{16}Si_2$ $(M+H)^+$ *m/z* 1202.6268, Δ = 5.8 ppm.

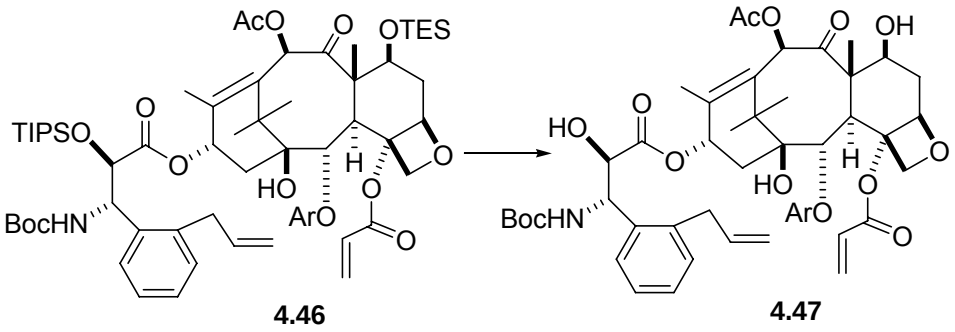

4.46 **4.47**

***N*-Boc-2-(*m*-methoxybenzoyl) paclitaxel (4.47).** At 0 ^oC, HF/pyridine (0.1 mL) was added to **4.46** (9 mg, 0.0075 mmol) in 2 mL of THF and the solution was warmed to RT and stirred overnight. The reaction mixture was diluted with EtOAc and washed with aq. $NaHCO_3$. The organic layer was washed with H_2O and brine, dried over anhydrous Na_2SO_4, and concentrated under reduced pressure. Purification by preparative TLC gave **4.47** (6.2 mg, 88%).

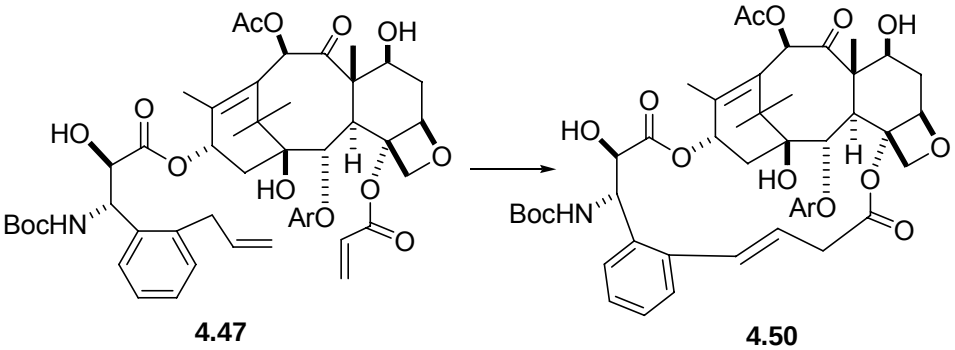

4.47 **4.50**

***N*-Debenzoyl-*N*-Boc-2-debenzoyl-2-(*m*-methoxybenzoyl) bridged paclitaxel (4.50).** At rt, a solution of **4.47** (18 mg, 0.019 mmol) in DCM (8 mL) was added to Grubbs second generation catalyst (5.8 mg, 0.0059 mmol) in DCM (4 mL) for 3 h. After 12 h, the reaction mixture was concentrated and the residue was purified on PTLC to give **4.50** (10

mg, 56%). ^{1}H NMR (400 MHz) δ 7.88 (1H, d, *J* = 7.2 Hz), 7.76 (1H, d, *J* = 7.6 Hz), 7.70 (1H, dd, *J* = 1.6, 2.4 Hz), 7.60 (1H, dd, *J* = 3.6, 5.6 Hz), 7.56 (1H, dd, *J* = 3.6, 5.6 Hz), 7.43 (1H, t, *J* = 8.0 Hz) 7.38-7.30 (2H, m), 7.19-7.14 (2H, m), 6.32 (t, *J* = 9.0 Hz), 6.28 (1H, s), 5.69 (1H, d, *J* = 7.2 Hz), 5.57 (1H, d, *J* = 16.0 Hz), 5.36 (1H, d, *J* = 9.6 Hz), 5.13 (1H, d, *J* = 9.6 Hz), 4.96 (1H, d, *J* = 8.0 Hz), 4.46 (1H, s), 4.43 (1H, dd, *J* = 6.8, 10.8 Hz), 4.32 (1H, d, *J*= 8.4 Hz), 4.25 (1H, d, *J* = 8.4 Hz), 4.14 (1H, m), 3.89 (3H, s), 3.78 (1H, d, *J* = 7.2 Hz), 3.55 (1H, d, *J* = 19.2 Hz), 3.39 (1H, bs), 2.58-2.48 (3H, m), 2.35 (2H, m), 2.34 (3H, s), 1.86 (2H, m), 1.81 (3H, s), 1.70 (3H, s), 1.34 (9H, s), 1.25 (3H, s), 1.15 (3H, s). ^{13}C NMR (100 MHz) δ 204.0, 173.6, 171.4, 167.3, 164.5, 160.0, 155.3, 149.4, 142.5, 140.4, 134.3, 133.4, 131.3, 131.0, 129.0, 128.8, 128.1, 123.2, 122.6, 119.6, 115.6, 84.4, 80.8, 80.1, 79.3, 77.4, 76.7, 75.9, 75.5, 72.5, 71.7, 58.8, 55.8, 51.0, 46.2, 43.3, 37.4, 35.8, 35.5, 28.4, 27.0, 21.8, 21.1, 15.3, 9.7. HRFABMS: found *m/z* 904.3729, calcd for $C_{48}H_{58}NO_{16}$ $(M+H)^{+}$ *m/z* 904.3756, Δ = 2.9 ppm.

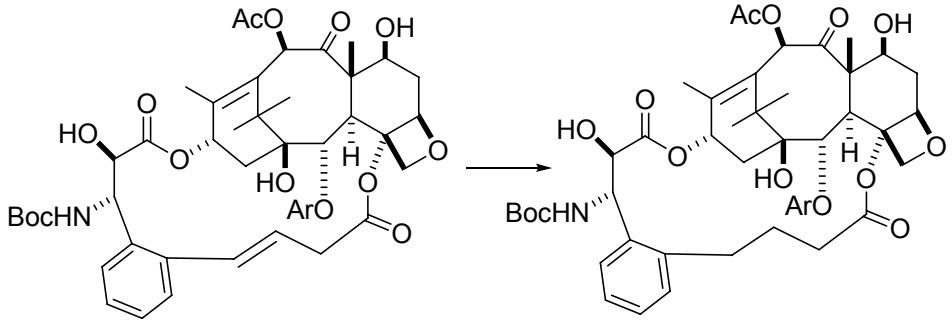

***N*-Boc-2-(*m*-methoxybenzoyl) dihydro bridged paclitaxel (4.52).** At rt, a solution of **4.50** (5.2 mg, 0.058 mmol) in methanol (3.5 mL) was treated with 10%Pd-C (10 mg) and hydrogenated at 35 psi for overnight. The reaction mixture was filtered through a short plug of silica gel. The filtrate was concentrated and purified on PTLC to afford **4.52** (3.6 mg, 72%). ^{1}H NMR (400 MHz) δ 7.76 (1H, d, *J* = 7.6 Hz), 7.66-7.63 (2H, m), 7.43 (1H, t,

J = 8.0 Hz), 7.31-7.15 (5H, m), 6.52 (1H, t, *J* = 9.2 Hz), 6.27 (1H, s), 5.72 (1H, d, *J* = 7.2 Hz), 5.42 (2H, m), 4.95 (1H, d, *J* = 7.6 Hz), 4.43 (1H, bs), 4.38 (1H, dd, *J* = 10.8, 6.8 Hz), 4.34 (1H, d, *J* = 8.0 Hz), 4.20 (1H, d, *J* = 8.0 Hz), 3.90 (3H, s), 3.73 (1H, d, *J* = 6.8 Hz), 3.35 (1H, bs) 3.11-2.96 (2H, m), 2.86-2.68 (2H, m), 2.56 (1H, m), 2.35 (1H, m), 2.28-2.24 (1H, m), 2.24 (3H, s), 2.11-1.98 (2H, m), 1.94-1.88 (1H, m), 1.82 (3H, s), 1.71 (3H, s), 1.35 (3H, s), 1.32 (9H, s), 1.18 (3H, s). ^{13}C NMR (100 MHz) δ 203.8, 174.0, 172.5, 171.5, 167.3, 160.0, 155.3, 142.7, 139.2, 139.0, 133.0, 130.5, 130.2, 130.1, 128.4, 127.6, 127.5, 122.9, 120.7, 114.6, 84.6, 81.1, 80.2, 79.7, 77.4, 75.6, 75.3, 73.5, 72.6, 72.1, 58.8, 55.7, 50.7, 45.8, 43.6, 35.9, 35.8, 35.3, 33.7, 28.4, 27.4, 25.9, 22.7, 21.1, 14.9, 9.8. HRFABMS found *m/z* 928.3690, calcd for $C_{48}H_{59}NO_{16}Na$ $(M+Na)^+$ *m/z* 928.3732, Δ = 6.3 ppm.

References:

1. Loewe, J.; Li, H.; Downing, K. H.; Nogales, E. Refined structure of α,β-tubulin at 3.5 Å resolution. *J. Mol. Biol.* **2001,** *313*, 1045-1057.
2. Geney, R.; Sun, L.; Pera, P.; Bernacki, R. J.; Xia, S.; Horwitz, S. B.; Simmerling, C. L.; Ojima, I. Use of the tubulin bound paclitaxel conformation for structure-based rational drug design. *Chem. Biol.* **2005,** *12*, 339-348.
3. Alcaraz, A. A.; Mehta, A. K.; Johnson, S. A.; Snyder, J. P. The T-taxol conformation. *J. Med. Chem.* **2006,** *49*, 2478-2488.

4. Kingston, D. G. I.; Chaudhary, A. G.; Chordia, M. D.; Gharpure, M.; Gunatilaka, A. A. L.; Higgs, P. I.; Rimoldi, J. M.; Samala, L.; Jagtap, P. G.; Giannakakou, P.; Jiang, Y. Q.; Lin, C. M.; Hamel, E.; Long, B. H.; Fairchild, C. R.; Johnston, K. A. Synthesis and biological evaluation of 2-acyl analogs of paclitaxel (taxol). *J. Med. Chem.* **1998,** *41*, 3715-3726.

5. Paik, Y.; Yang, C.; Metaferia, B.; Tang, S.; Bane, S.; Ravindra, R.; Shanker, N.; Alcaraz, A. A.; Snyder, J. P.; Schaefer, J.; O'Connor, R. D.; Cegelski, L.; Kingston, D. G. I. REDOR NMR distance measurements for the tubulin-bound paclitaxel conformation. *J. Am. Chem. Soc.* **2007,** *129*, 361-370.

6. Ganesh, T.; Guza, R. C.; Bane, S.; Ravindra, R.; Shanker, N.; Lakdawala, A. S.; Snyder, J. P.; Kingston, D. G. I. The bioactive Taxol conformation on β-tubulin: Experimental evidence from highly active constrained analogs. *Proc. Natl. Acad. Sci. U.S.A.* **2004,** *101*, 10006-10011.

7. Liu, C.; Schilling, J. K.; Ravindra, R.; Bane, S.; Kingston, D. G. I. Syntheses and bioactivities of macrocyclic paclitaxel bis-lactones. *Bioorg. Med. Chem.* **2004,** *12*, 6147-6161.

8. Metaferia, B. B.; Hoch, J.; Glass, T. E.; Bane, S. L.; Chatterjee, S. K.; Snyder, J. P.; Lakdawala, A.; Cornett, B.; Kingston, D. G. I. Synthesis and biological evaluation of novel macrocyclic paclitaxel analogues. *Org. Lett.* **2001,** *3*, 2461-2464.

9. Ganesh, T.; Yang, C.; Norris, A.; Glass, T.; Bane, S.; Ravindra, R.; Banerjee, A.; Metaferia, B.; Thomas, S. L.; Giannakakou, P.; Alcaraz, A. A.; Lakdawala, A. S.; Snyder, J. P.; Kingston, D. G. I. Evaluation of the tubulin-bound paclitaxel

conformation: synthesis, biology and SAR studies of C-4 to C-3' bridged paclitaxel analogs. *J. Med. Chem.* **2007,** *50*, 713-725.

10. Chaudhary, A. G.; Gharpure, M. M.; Rimoldi, J. M.; Chordia, M. D.; Kingston, D. G. I.; Grover, S.; Lin, C. M.; Hamel, E.; Gunatilaka, A. A. L. Unexpectedly facile hydrolysis of the 2-benzoate group of taxol and syntheses of analogs with increased activities. *J. Am. Chem. Soc.* **1994,** *116*, 4097-4098.
11. Uoto, K.; Mitsui, I.; Terasawa, H.; Soga, T. First synthesis and cytotoxic activity of novel docetaxel analogs modified at the c18-position. *Bioorg. Med. Chem. Lett.* **1997,** *7*, 2991-2996.
12. Ojima, I.; Fumero-Oderda, C. L.; Kuduk, S. D.; Ma, Z.; Kirikae, F.; Kirikae, T. Structure-activity relationship study of taxoids for their ability to activate murine macrophages as well as inhibit the growth of macrophage-like cells. *Bioorg. Med. Chem.* **2003,** *11*, 2867-2888.
13. Fürstner, A. Olefin metathesis and beyond. *Angew. Chem. Int. Ed.* **2000,** *39*, 3012 -3043.
14. Grubbs, R. H.; Chang, S. Recent advances in olefin metathesis and its applications in organic synthesis. *Tetrahedron* **1998,** *54*, 4413-4450 and references cited therein.
15. Trnka, T. M.; Grubbs, R. H. The development of $L_2X_2Ru{=}CHR$ olefin metathesis catalysts: An organometallic success story. *Acc. Chem. Res.* **2001,** *34*, 18-29.
16. Chen, S. H.; Kadow, J. F.; Farina, V. First syntheses of novel paclitaxel(taxol) analogs modified at the C4-position. *J. Org. Chem.* **1994,** *59*, 6156-6158.

Chapter 5 Introduction to discodermolide

5.1. Isolation and structure of discodermolide

(+) Discodermolide is a polyketide isolated by Gunasekera *et al*.[1-3] from the Caribbean deep sea sponge *Discodermia dissoluta* in 1990. The sponge samples were exhaustively extracted and purified to provide crystalline discodermolide, ($C_{33}H_{55}NO_8$), in 0.002% w/w isolated yield from the frozen sponge. The structure of discodermolide was determined by extensive spectroscopic studies and single crystal X-ray crystallography, and is shown in Figure 5.1. The absolute configuration was confirmed by Schreiber in 1993 through total synthesis. It features 13 stereogenic centres, a tetrasubstituted δ-lactone, one di- and one tri-substituted (*Z*)-alkene, a carbamate subunit and a terminal (*Z*)-diene. Studies on the conformation of discodermolide in both the solid state and in solution suggest that it adopts a U-shaped conformation to minimize strain and steric interactions,[4] but this hypothesis is still controversial.[5]

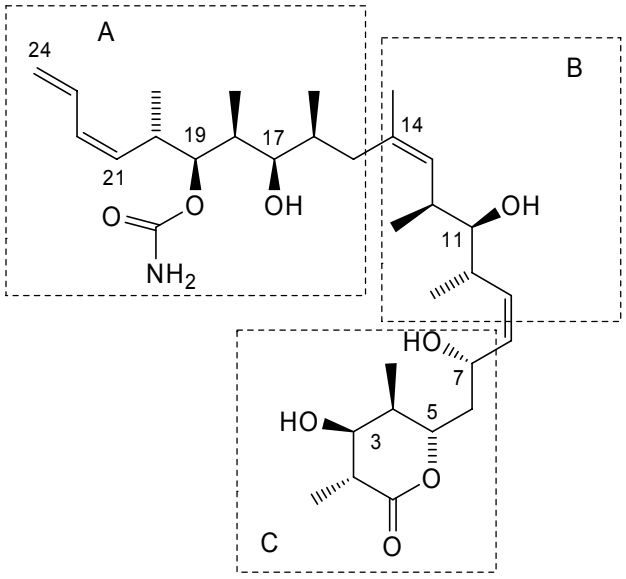

Figure 5.1 Structure of discodermolide

5.2. Bioactivity of discodermolide

Initially, discodermolide was isolated as a potent immunosuppressive as well as antifungal agent.[6-8] The *in vitro* studies showed that discodermolide suppressed the proliferation of splenocytes in the murine two-way mixed lymphocyte reaction (MLR) and concanavalin A stimulated cultures, with IC_{50} values of 0.24 μM and 0.19 μM, respectively. It also suppressed the proliferation of human peripheral blood leukocytes (PBL) in the two-way MLR, and Con A and phytohemagglutinin mitogenesis, with IC_{50} values of 5.6 μM, 28 μM, and 30 μM, respectively. Additionally, discodermolide inhibited the phorbol 12-myristate 13-acetate (PMA)/ionomycin induced proliferation of pure, murine T cells with IC_{50} values of 9.0 nM, and suppresses graft-versus-host disease in transplanted mice.[7] In the subsequent *in vivo* immunosuppression studies, it was suggested that *in vivo* discodermolide acted through a specific mechanism of immunosuppression different from that of general immunosuppressive agents.[8]

However, the most noticeable feature of discodermolide is its outstanding cytotoxicity. Discodermolide inhibited incorporation of tritiated thymidine into DNA with IC_{50} values of 7 nM.[6] Further biological screening showed that it had potent cytotoxicity in human and murine cell lines with IC_{50} values of 3-80 nM.[9] It was found that (+)-discodermolide induced cell arrest at the G_2/M phase[6], while synthetic (-)–discodermolide blocked the cell cycle at the S phase; both eventually led to cell death by apoptosis. Interestingly, the arresting phases in the cell cycle were totally different for the two enantiomers, indicating that they acted through distinct mechanisms. Further studies[10] on the arresting mechanism revealed that (+)-discodermolide had no effects on the expression of cyclin B at the beginning of cell cycle. However, in the presence of

(+)– discodermolide the subsequent degradation of cyclin B at anaphase of mitosis was considerably delayed. During this prolonged period, the cells had the same morphology as mitotic cells and finally re-adhered instead of completing mitosis as usual. The re-adhered cells were mostly micronucleated and larger in size than the control cells.

Similar to paclitaxel (PTX), and the epothilones, discodermolide interacts with tubulin and stabilizes the microtubule *in vivo*. Furthermore, it was found that discodermolide promoted the polymerization of microtubules more potently than PTX,[11] and the microtubules formed by discodermolide were more stable than those formed by PTX.[10] However, these microtubules had a different morphology. Electron microscopy (EM) studies revealed that discodermolide produces large numbers of much shorter microtubules (0.53-0.59 μm) than those produced by PTX (0.70-1.69 μm), which indicates that discodermolide has a major effect on microtubule nucleation.[11]

Studies on the binding of [^{3}H] discodermolide to microtubules showed that discodermolide could bind to tubulin dimer at 1:1 stoichiometry. Additionally, discodermolide strongly inhibited the binding of [^{3}H] PTX to preformed microtubules in a drug binding competition, while PTX only weakly inhibited the binding of [^{3}H] discodermolide to polymer. On the contrary, (-)-discodermolide was not a competitive inhibitor for binding of ^{3}H(+)-discodermolide to microtubules, which suggested that these two synthetic enantiomers arrested the cell cycle at different stages by interacting with distinct cellular targets. Those results indicate that discodermolide and PTX bound to mutually exclusive sites on microtubules. The critical concentrations of tubulin for assembly with discodermolide were much lower than those with PTX, which also

indicates that discodermolide displayed better binding affinity to microtubules than PTX.[11]

Remarkably, the growth of paclitaxel-resistant ovarian and colon carcinoma cells can be inhibited by discodermolide at nanomolar concentrations.[10] In contrast to the epothilones and eleutherobin, discodermolide does not substitute for PTX in a PTX-resistant carcinoma cell line that requires low concentrations of PTX for normal growth.

Surprisingly, the cytotoxicity of discodermolide is enhanced 20-fold in the presence of a low concentration of PTX.[12] Discodermolide and PTX also synergistically inhibit overall microtubule dynamic properties in living cells, blocking the cell cycle at the G_2/M phase, and promoting apoptosis more effectively.[13]

5.3. Structure-activity Relationships (SAR)

Both the crystal and recent solution structures of (+)-discodermolide[14] demonstrated that the molecule arranges the C1-C19 region into a U-shaped conformation, bringing the lactone and the C19 side chain in close proximity. The molecule of discodermolide can be divided into three regions as shown in Figure 5.1, and each region will be addressed individually below.

A region

A series of C19 carbamate-substitued analogs have been extensively investigated. Interestingly, potent cytotoxicity requires the original structure in the NCI/ADR multidrug-resistant cell line, but modifications are tolerated in drug-sensitive cell lines.[4,10,15] The introduction of an acetoxy group at C19 in place of the carbamate reduces the antimitotic activity of discodermolide. However, analogs with a series of carbamate

derivatives at the C19 position had potent cytotoxicity in drug-sensitive cell lines but lost activity in drug resistant cell lines.[4] This indicated that the C19 carbamate moiety is necessary, but relatively tolerant to modifications, at least for drug sensitive cell lines.[16,17]

Acetylation of the hydroxyl group at the C17 position severely reduced the cytotoxicity of the molecule. Epimerization of the C17 hydroxyl group caused the final molecule to be inactive. Together these results indicated the essential role of the hydroxyl group at C17 in maintaining the favorable stereochemistry of the pharmacophore, possibly through a hydrogen bonding interaction with the neighboring carbamate group. The absence of the C16 methyl group resulted in little or no loss of activity. On the contrary, inversion of the absolute configuration at C16 led to reduced cytotoxicity, indicating that C16 stereochemistry was essential for biological activity of discodermolide. Changes in the C17-C20 region of the discodermolide backbone resulted in almost complete loss of activity. The terminal conjugated diene system makes little contribution to the cytotoxicity.[10,18] The diene unit can be reduced to an alkyl group or replaced with a bulky group without loss of activity.[16]

B olefin region

The C13-C14 double bond is crucial for the cytotoxicity. Hydrogenation of this double bond leads to complete loss of activity, which suggests the U-shaped conformation of C1-C19 region is essential for activity. Biological evaluation of C14-nor-methyldiscodermolide shows that removal of the C14-methyl results in only a slight reduction in tubulin polymerization and cytoxicity, but loss of activity against the NCI/ADR multidrug-resistant cell line. Similar to discodermolide, the truncated analog competes with PTX for preformed microtubles. Interestingly, the microtubules assembled

in the present of C14-nor-methyldiscodermolide are 12-fold longer than those formed by discodermolide. Later, two C13-C14 cyclopropane analogs of discodermolide were synthesized and evaluated.[19] Both analogs retained nanomolar cytoxicity against the drug-sensitive cell line but were relatively inactive against the multidrug-resistant cell line. In a further study of the structure and function of the C13-C14 region, several C14-nor-methyl discodermolide derivatives were synthesized with further modifications on other regions of discodermolide. These analogs displayed loss of cytoxicity against drug-sensitive cell lines to different extents, but the general trend was loss of cytotoxicity against the multidrug-resistant cell lines. It is concluded[19] that the C13-C14 (Z)-double bond partly controls the folding of the discodermolide molecule to an optimum conformation in order to fit into the binding site. Inversion of stereochemistry at C11 strongly reduced the bioactivity of the overall molecule.

C region

The C3 hydroxyl group was proven not to be essential for cytotoxicity. Acetylation at the C3 hydroxyl group had little effect on the cytotoxicity of discodermolide, but a silyl group at C3 resulted in a remarkable loss of cytotoxicity.[20] The absence of the hydroxyl group at C3 resulted in an increase of bioactivity,[12,21] and the elimination of the C2 methyl and C3 hydroxyl groups enhanced the activity 10-fold.[21] Those simplified congeners were potent both *in vitro* and *in vivo*.[21] Additionally, thiophenylation at C1 showed no effects on the biological potency.[10] Sequential removal of functionality from the lactone moiety had little effect on the antiproliferative activity against drug sensitive cell lines,[22] but activity was modified to different extents against the NCI/ADR multidrug-resistant cell lines. Replacement of the 6-ring lactone by certain

5-membered ring substituents at the C7 position remarkably enhances the activity.[23] This suggested that discodermolide has a large tolerance for modifications on the lactone moiety. However, analogs with the lactone replaced by various aryl groups[24] or acyl groups[25] and elimination of the C7 hydroxyl group led to significant loss of activity.[26] Alkylation and acylation of the C7 hydroxyl group resulted in compounds with similar cytotoxicity.[20,27] Interestingly, discodermolide was discovered to be more effective in polymerizing purified tubulin than the compound with the C7 hydroxyl group acetylated, indicating either that acetylated discodermolide at C7 is more cell-membrane permeable, or that acetylation at the C7 hydroxyl group induced additional cytotoxic qualities not present in the original discodermolide molecule. Inversion of stereochemistry at C7 and C5 led to significant loss of activity,[28] and elimination of the C7 hydroxyl group[26] also resulted in loss of activity. Replacement of the entire C1-C7 unit with a series of substituted benzyl derivatives showed considerably reduced activity; however, substitution of the C1-C7 unit with coumarin derivatives retains equivalent activity.[22] It is concluded that the lactone region can be replaced by an aromatic unit if it maintains the appropriate orientation.[22]

5.4. Synthesis of discodermolide

While the clinical supply of the anti-cancer agent Taxol was severely limited by its scarce natural resources, this problem was eventually resolved by semi-synthesis from 10-deacetylbaccatin III, which is obtained by extracting the needles of the European yew tree. Unfortunately, this approach is not possible for discodermolide, even though as a polyketide, it is possibly produced by a symbiotic microorganism associated with the

sponge source. Therefore, the supply problem for discodermolide is severe and could be solved at present only by total synthesis, rather than semi-synthesis as for Taxol. Consequently, its synthesis has attracted considerable attention, resulting in numerous partial syntheses and several total syntheses. The total synthesis of discodermolide by six groups will be briefly reviewed as follows.

5.4.1 Schreiber Synthesis of Discodermolide[10,29]

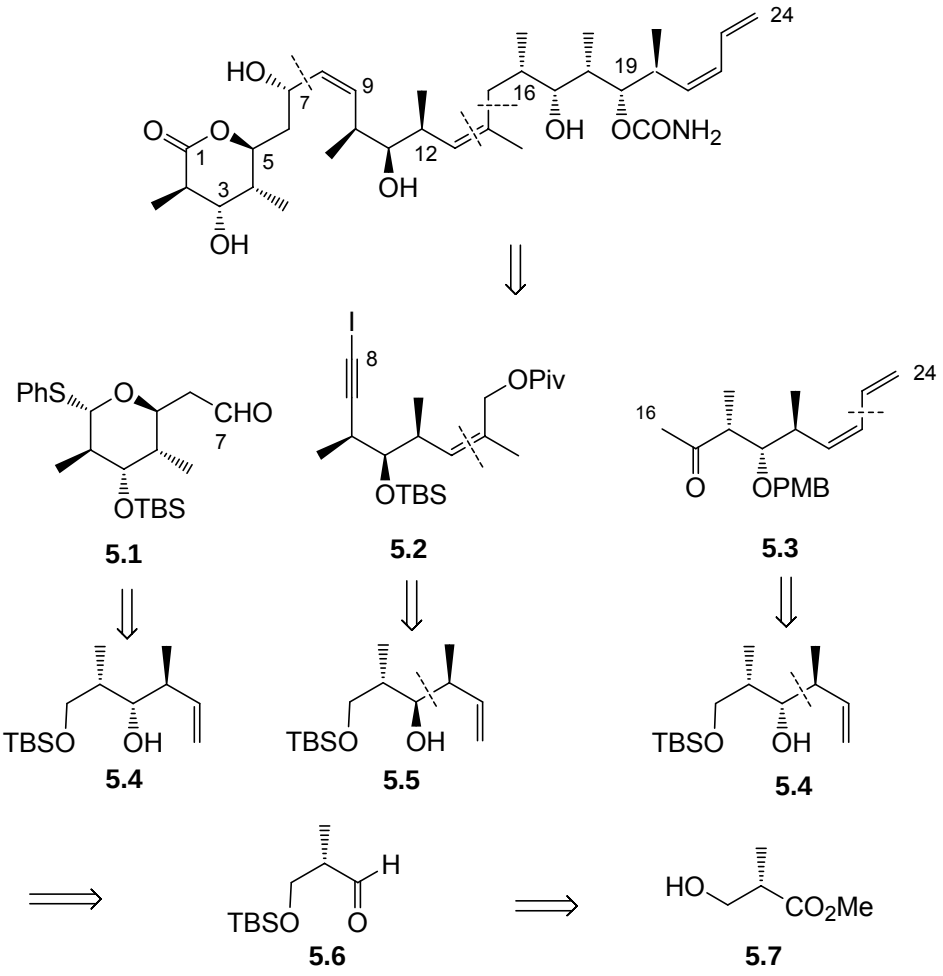

Scheme 5.1 Retrosynthesis of discodermolide by Schreiber group

In 1993, Schreiber *et al.* disclosed their total synthesis of *ent*-(-)-discodermolide, which served to establish the absolute configuration. In their later work, they achieved the first synthesis of the natural antipode (+)-discodermolide, using essentially the same route performed in the correct enantiomeric series, along with several analogues designed to study their tubulin-binding and microtubule-stabilizing properties.

Scheme 5.1 shows Schreiber's retrosynthesis. In their synthetic route to (+)-discodermolide, three key segments **5.1** (C1-C7), **5.2** (C8-C15), and **5.3** (C16-C24) were employed, with key couplings at C7-C8 based on a Nozaki-Kishi addition and C15-C16 by enolate alkylation, respectively.

The Roche ester[7] **5.7** was protected by TBS and selectively reduced to the corresponding aldehyde **5.6**, which was then subjected to two separate Roush asymmetric crotylation reactions[7] to give two homoallylic alcohols **5.4** and **5.5**, (Scheme 5.2).

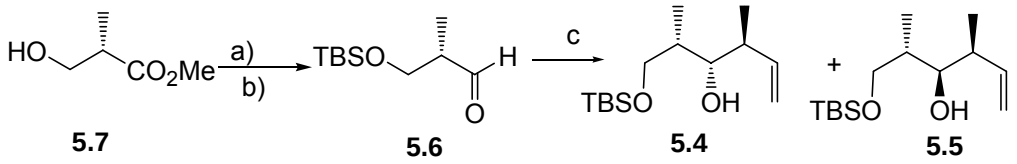

5.7 **5.6** **5.4** **5.5**

a) TBSCl; b) DIBAl c) $BrCHCH_3CH{=}CH_2$

Scheme 5.2

PMB protection of alcohol **5.4,** followed by ozonolysis and a Wittig olefination, gave vinyl iodide **5.8**, which was subject to a second Wittig olefination to give terminal diene **5.9** as shown in Scheme 5.3. Diene **5.9** was converted to diene **5.3** in three steps. Alternatively ozonolysis of alcohol **5.4,** followed by a Wittig olefination, gave the *trans* enoate **5.10**. Subsequently an intramolecular Michael addition of the hemiacetal formed from **5.10** and benzaldehyde provided **5.11** with complete stereoselectivity. A further five

steps performed on the acetal completed the synthesis of the C1-C7 segment thioacetal **5.1** [β:α =2:1], which served as a precursor to the δ-lactone as shown in Scheme 5.3.

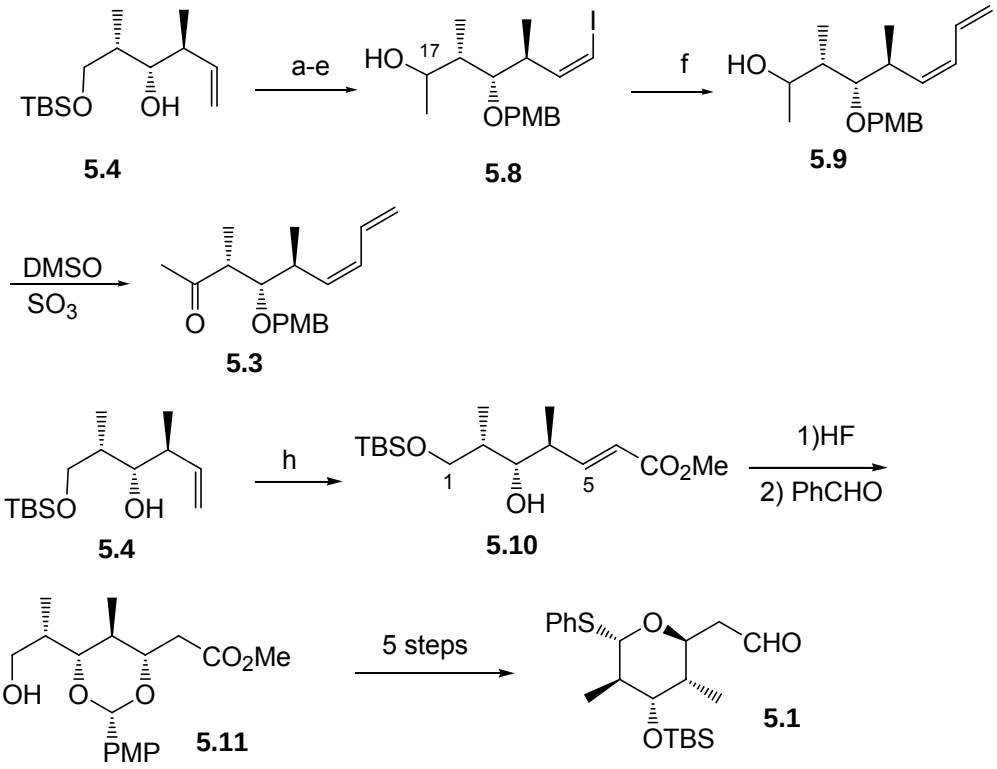

a) PMBBr; b) O_3, c) MeMgBr, d) DMSO, SO_3; e) Ph_3PCH_2I f) $CH_2CHZnBr$; g) O_3; h) Ph_3PCHCO_2Me

Scheme 5.3

The second unit was prepared by ozonolysis of the TBS protected alcohol **5.5**, followed by Still-Gennari olefination to give (*Z*) alkene [(*Z*):(*E*) > 20:1] **5.12**. This ester was reduced to the alcohol and protected with pivalic acid. Selective deprotection of TBS and oxidation to the corresponding aldehyde followed by the Wittig protocol gave terminal alkyne **5.18** as shown in Scheme 5.4; this alkyne was then converted to the iodoacetylene **5.7**.

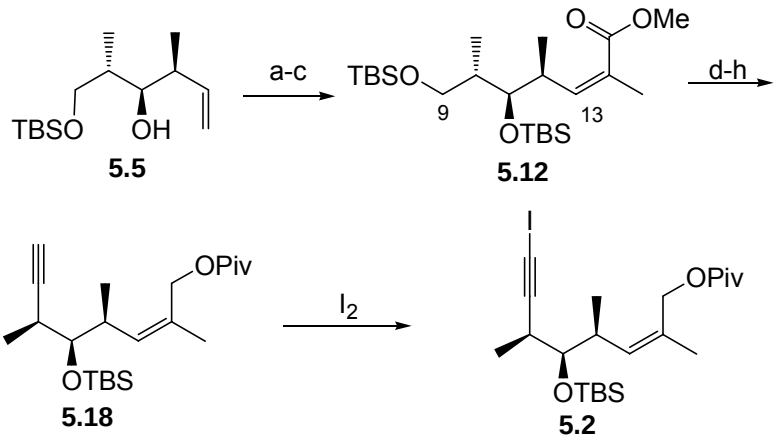

a) TBSCl, b) O_3, c) $Ph_3PCHMeCO_2Me$ d)LAH, e) PivCl, f) HF
g) DMSO, SO_3, h) Ph_3PCHN_2

Scheme 5.4

Coupling of the iodoacetylene **5.2** with aldehyde **5.1** in a Nozaki-Kishi reaction in the presence of $CrCl_2/NiCl_2$ gave propargylic alcohol **5.13** with *dr* = 2:1 at C7 (Scheme 5.5). The stereoselectivity is not satisfactory; however, the undesired diastereomer, can be recycled by oxidation followed by selective reduction.

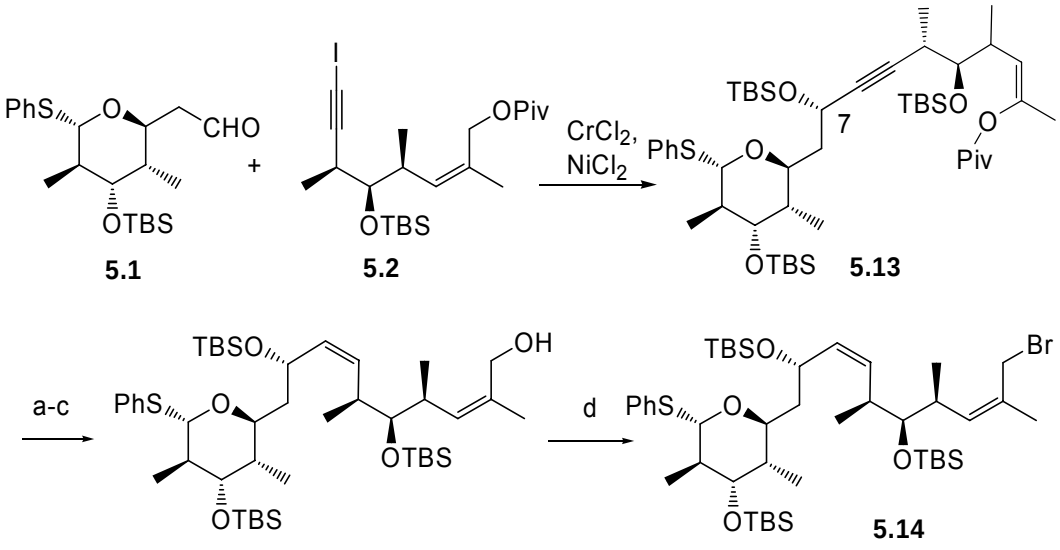

a) H_2, Pd b) TBSCl, c) DABAl, d) MsCl, LiBr

Scheme 5.5

Bromide **5.14** was coupled with methyl ketone **5.3** via the lithium enolate, followed by conversion of the thiophenyl acetal to a lactone, to give **5.15** (Scheme 5.6). DDQ oxidation of **5.15**, followed by carbamation gave **5.16**, and global deprotection completed the synthesis of discodermolide (**1**), with an overall yield of 4.3% over 24 steps in the longest linear sequence.

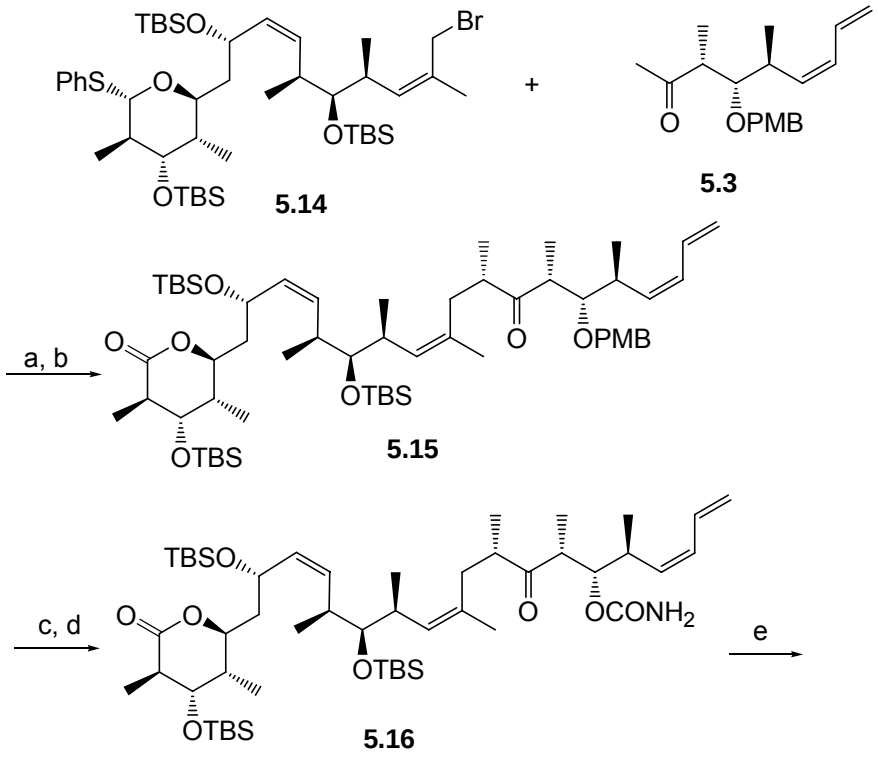

a) LDA b) $HgCl_2$, Jones' reagent, c) DDQ d) Cl_3CONO, e) *p*-TsOH

Scheme 5.6

The absolute stereochemistry of discodermolide was assigned unambiguously, and the first structure-activity relationship study was carried out using those simplified analogs. Surprisingly, the unnatural antipode is also cytotoxic and causes cell cycle arrest in the S-phase.

5.4.2 Smith Synthesis of Discodermolide[30-32]

Smith III *et al.* first achieved the total synthesis of discodermolide and subsequently developed a second-generation approach to provide discodermolide itself in 1995. Their synthetic route to discodermolide involved two key fragment couplings at C8-C9 and C14-C15 using a Wittig olefination and a Negishi cross-coupling reaction, respectively. Scheme 5.7 shows the restrosynthesis.

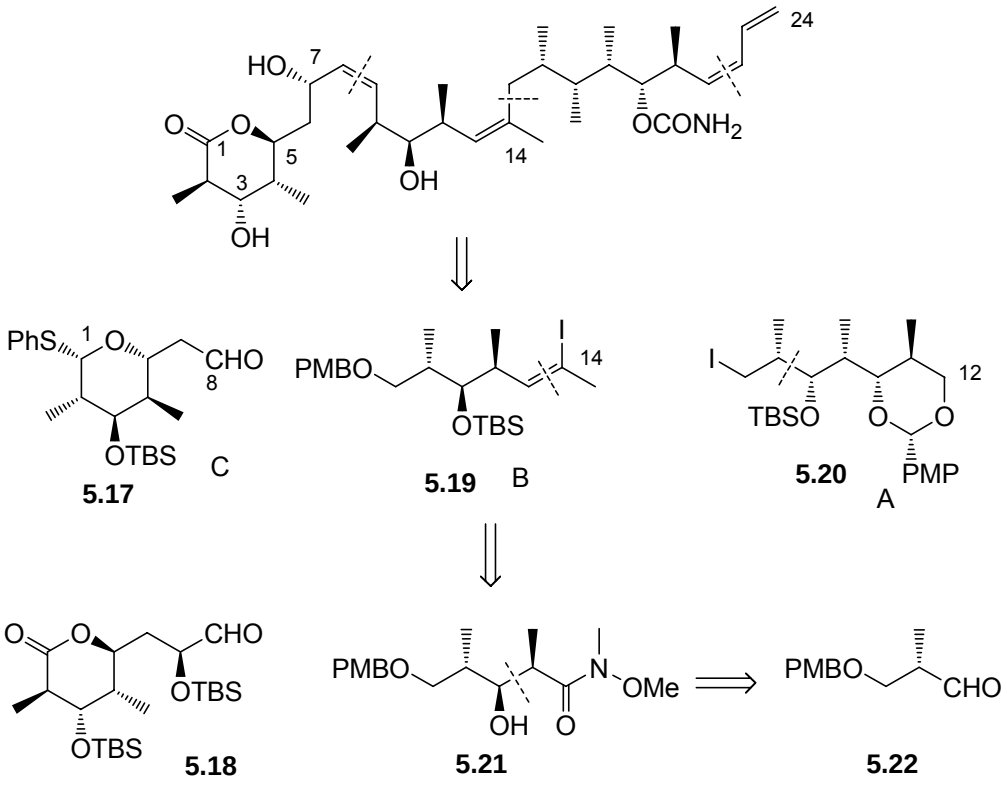

Scheme 5.7 Restrosynthesis of discodermolide by the Smith group

The modifications to their original route were focused on the introduction of the terminal (*Z*)-diene unit by a Yamamoto olefination and the replacement of thioacetal aldehyde **5.17** with δ-lactone aldehyde **5.18** for the C1-C8 segment. The segments **5.19** (C9-C14) and **5.20** (C15-C21) were adopted in both syntheses without modification.

In their second-generation route, all three segments were derived from the common precursor **5.21**, which incorporates the repeating stereotriad sequence of discodermolide.

In the second generation synthesis, commercially available Roche ester **5.17** was protected by PMB and converted to aldehyde **5.22**, which was then subjected to Evans aldol *syn*-selective conditions with propionyl-(*R*)-oxazolidinone **5.23**. Conversion to the corresponding Weinreb amide gave the common precursor **5.21**, which served as the building block of the synthesis as shown in Scheme 5.8.

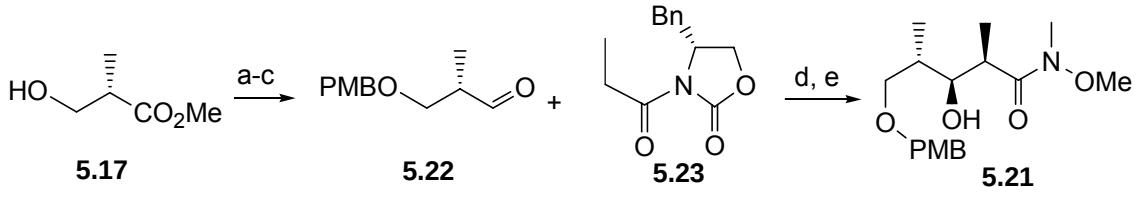

5.17 **5.22** **5.23** **5.21**

a) PMBBr; b) LAH; c) DMSO, SO_3; d) Bu_2BOTf e) HNMeOMe

Scheme 5.8

Protection of the common precursor as its TBS ether, followed by reduction with DIBAL and reaction of the resulting aldehyde **5.24** gave fragment B **5.19** by the Zhao-Wittig olefination protocol with variable selectivity [(*Z*)/(*E*) = 8:1 to 17:1] (Scheme 5.9). Alternatively oxidation of the common precursor **5.21** with DDQ gave a cyclic acetal, and reduction with DIBAL gave an aldehyde, which was coupled with the same acyloxazolidinone by means of a second Evans aldol *syn*-addition to give **5.25**. This compound was converted to fragment A **5.20** by reduction and iodination.

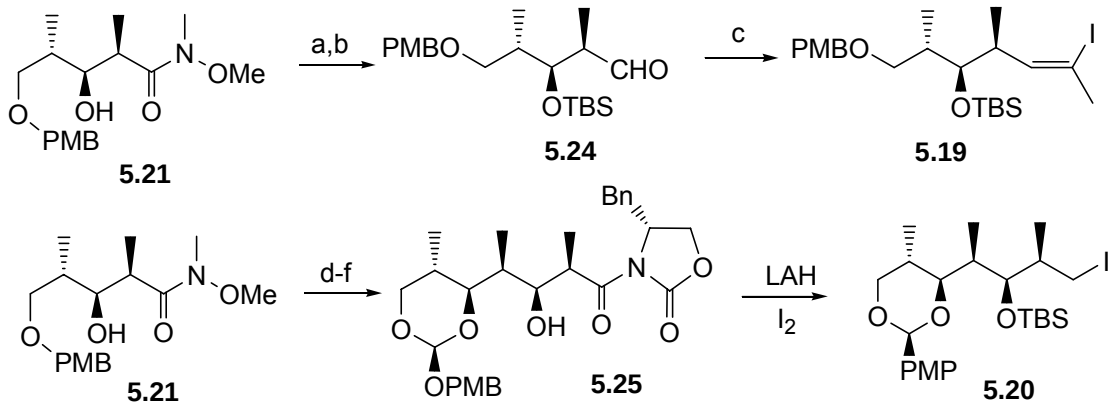

a)TBSCl, b)DIBAL c)Ph_3CH_2CHIMe d) DDQ, e) DIBAL f) BuBOTf, 2-35

Scheme 5.9

The synthesis of the C1-C8 segment also started with the common precursor **5.21**, which was converted to the aldehyde **5.26** by protection as its TBS ether, hydrogenolysis, and oxidation. This aldehyde was converted to the enone **5.27** by a remarkable anti-Felkin addition with a diene, followed by δ-lactonization under acidic condition. Stereoselective reduction at C7 by K-Selectride with *dr* = 9:1, followed by TBS protection and ozonolysis gave fragment C (Scheme 5.10).

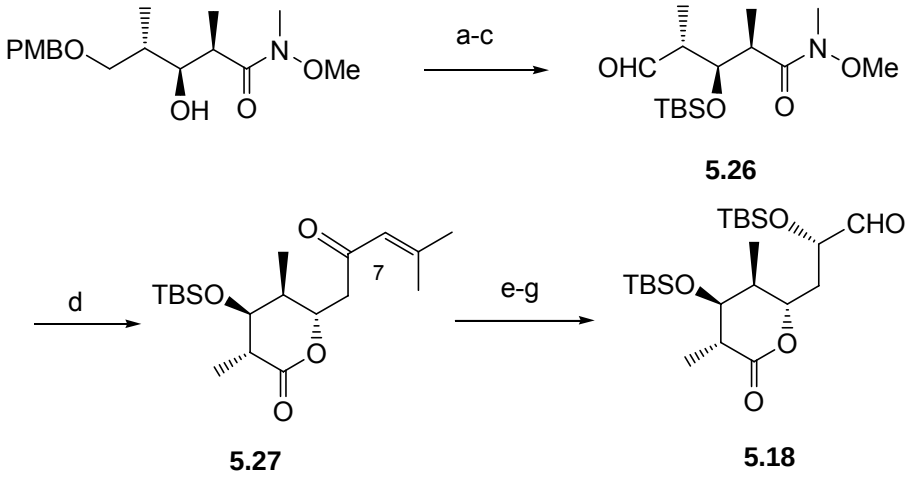

a) TBSCl, b) H_2 /Pd; c) DMSO, SO_3 d) CH_2=COTBSCCH=CMe_2 e) $NaBH_4$; f) TBSCl g) O_3

Scheme 5.10

The C9-C21 segment **5.28** was completed by coupling fragment A **5.19** and fragment B **5.20** by the Negishi protocol (Scheme 5.11). The PMB protecting group was then selectively removed with DDQ and replaced by a trityl group, and the acetal was reduced to give the primary alcohol **5.28b**.

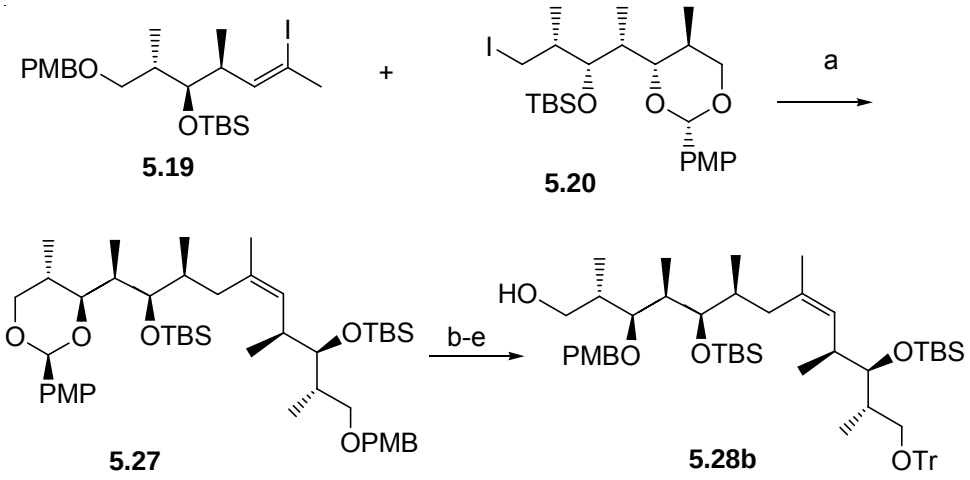

a) $Pd(PPh_3)_4$ b) DDQ c) TriCl d) DIBAL e) I_2, PPh_3

Scheme 5.11

Oxidation to an aldehyde and conversion to the terminal diene unit proceeded by a Wittig olefination protocol (Scheme 5.12). Deprotection of the trityl group and iodination gave intermediate **5.29**. Subsequent (*Z*)-selective Wittig coupling of fragment C **5.18** with the Wittig salt of intermediate **5.29** gave **5.30** [(*Z*)/(*E*) = 15:1 to 24:1] as shown in Scheme 5.12. However, conversion of intermediate **5.29** to the corresponding phosphonium salt required ultrahigh pressure (12.8 kBar) and a long time (6 days). Deprotection of PMB, followed by carbamation and global deprotection were performed to complete the synthesis of discodermolide.

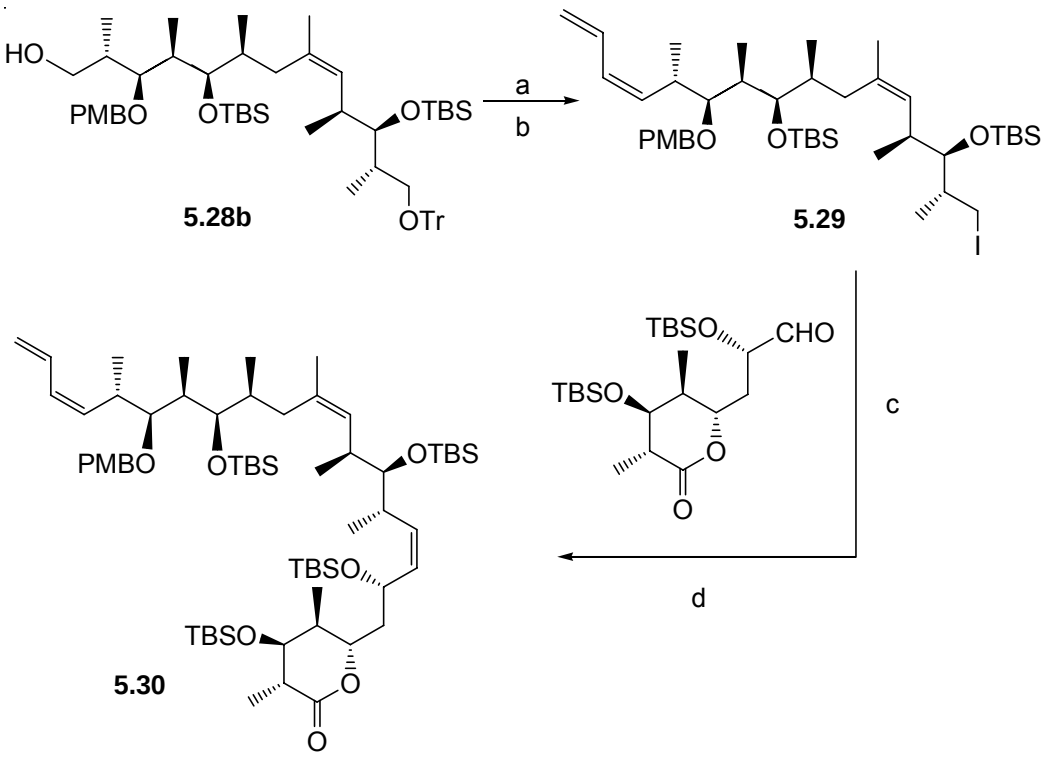

a) Dess-Martin, b)$Ph_3PCH_2CH{=}CH_2$ c)Ph_3P d) heat

Scheme 5.12

Relative to the Smith first-generation synthesis, the Smith second-generation approach dramatically reduced the number of steps, due to exploiting the common-precursor strategy. The Smith second-generation synthesis also exhibited improved stereoselectivity.

For instance, in the first generation, the C1-C8 segment thioacetal aldehyde **5.17** was prepared in 14 steps from **5.21**, including coupling of dithiane **5.31** with Sharpless epoxide **5.32** to give **5.33** (Scheme 5.13).

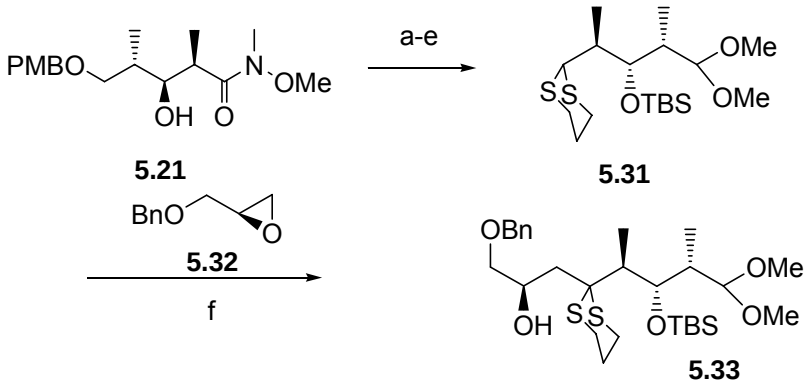

a) TBSCl b) H_2 c) DMP d) $TMSS(CH_2)_3STMS$ e) DIBAL f) BuLi

Scheme 5.13

Therefore, the second-generation synthesis process with 6% overall yield over 24 steps in the longest linear sequence, is considerably improved from the 2.2% overall yield over 28 steps (longest linear sequence) in the first generation synthesis.

However, the generation of the phosphonium salt of **5.29** was troublesome and required ultrahigh pressure for over 6 days in a specialized reactor, which considerably limited large-scale preparation. Recently, the Smith group has reported a third-generation synthesis to eliminate the requirement of ultrahigh pressure for formation of the Wittig salt of **5.29**. Surprisingly, replacement of the bulky TBS protecting group at C11 with the MOM group permitted the formation of the phosphonium salt of **5.30** under ambient pressure, albeit with the formation of some undesired cyclization by-products (Scheme 5.14).

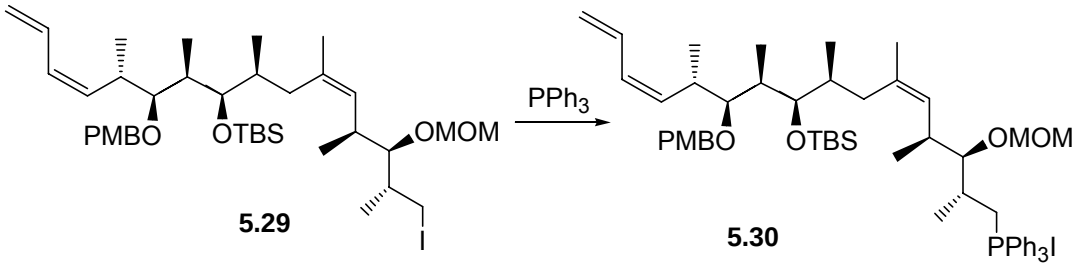

Scheme 5.14

Nevertheless, this approach made their synthetic route amenable for large-scale preparation. Moreover, the methyl group at C14 was eliminated to simplify the synthesis, leading to a discodermolide analog displaying similarly potent *in vivo* cytotoxicity.

5.4.3 Myles Synthesis of Discodermolide[33]

The synthetic plan adopted by Myles *et al.* for (-)discodermolide involved the three subunits **5.31** (C1-C7), **5.32** (C9-C15) and **5.33** (C16-C21), with key couplings performed at C7-C8 based on a Nozaki-Kishi addition and C15-C16 by a lithium enolate alkylation. Their retro synthesis of (-)discodermolide is shown in Scheme 5.15. Recently, they reported the synthesis of the natural antipode (+)discodermolide, using essentially the same route in the correct enantiomeric series.

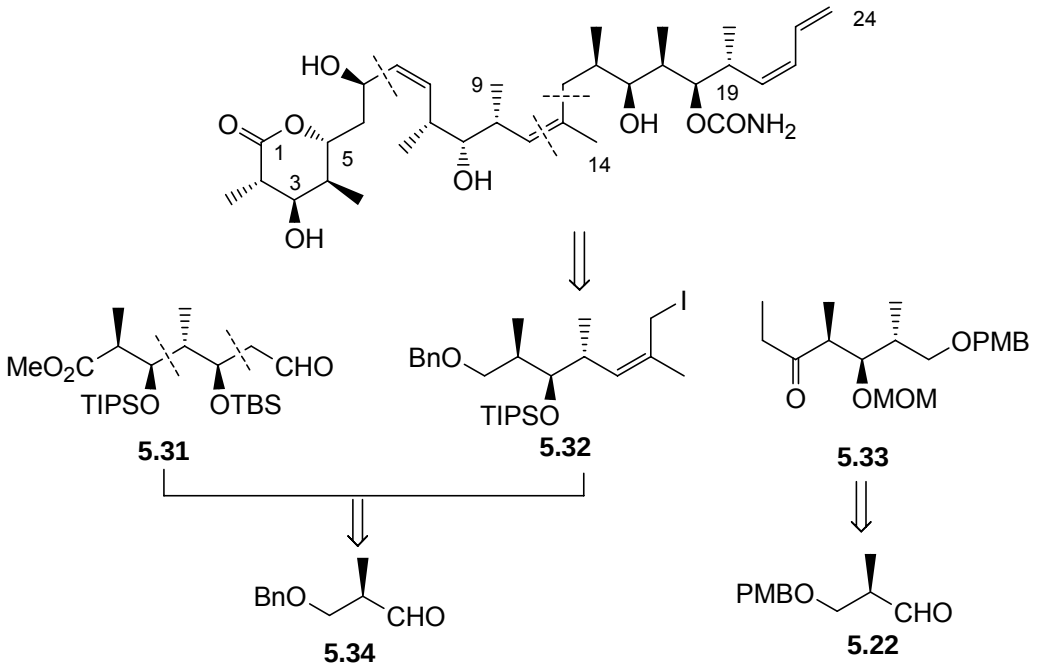

Scheme 5.15 Retrosynthesis of (-) discodermolide by Myles group

Synthesis of the C1-C7 subunit aldehyde **5.31** started with commercially available ester **5.17**, which was reduced to the alcohol and protected as its benzyl ether and then reduced to the corresponding alcohol. Oxidation to aldehyde, followed by the crotylboration methodology developed by the Brown group gave the homoallylic alcohol **5.35** (Scheme 5.16).

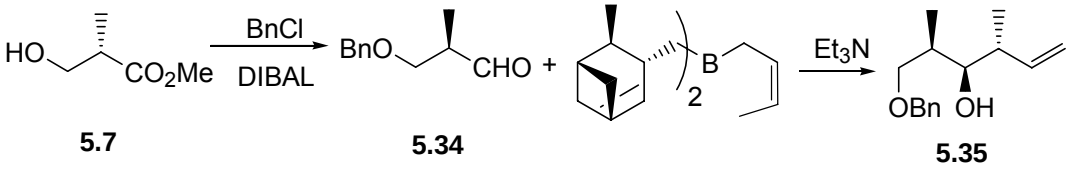

5.7 **5.34** **5.35**

Scheme 5.16

Subsequent protecting group manipulation and oxidative cleavage gave aldehyde **5.36**, which was then subjected to a second Brown crotylboration to give alcohol **5.37**. Compound **5.37** was converted into the C1-C7 fragment aldehyde **5.31** by a further five steps (Scheme 5.17).

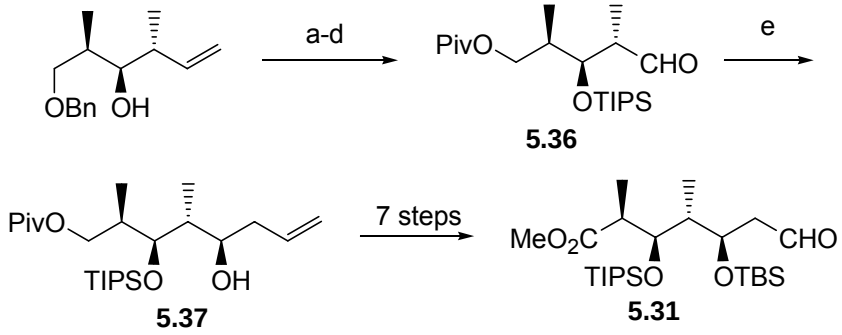

5.36

5.37 **5.31**

a) TIPSCl b) Li/NH_3, c) PivCl d) O_3 e) $BrCH_2CH{=}CH_2$

Scheme 5.17

The C-9 to C-15 synthon was prepared through a cyclic structure developed by Danishefsky (Scheme 5.17). Cyclocondensation of aldehyde **5.34** and diene **5.38** mediated by Lewis acid gave dihydropyrone **5.39**. Luche reduction and Ferrier

rearrangement gave the lactol **5.40**, which was then converted into the iodide **5.32** in a further five steps.

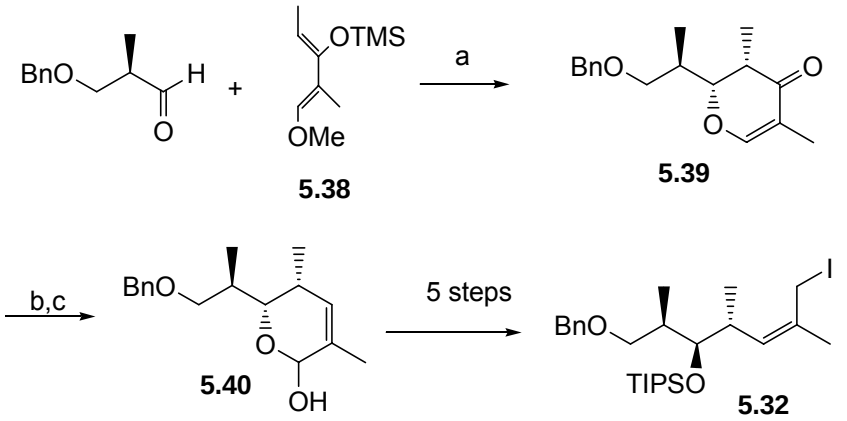

5.38 **5.39** **5.40** **5.32**

a $TiCl_4$ TsOH b) $NaBH_4$ c) TsOH

Scheme 5.18

Aldehyde **5.41**, derived from Roche ester **5.17** was subjected to a lithium-mediated aldol reaction with pentan-3-one, followed by MOM protection, and provided the C16-C21 fragment **5.33** (Scheme 5.19)

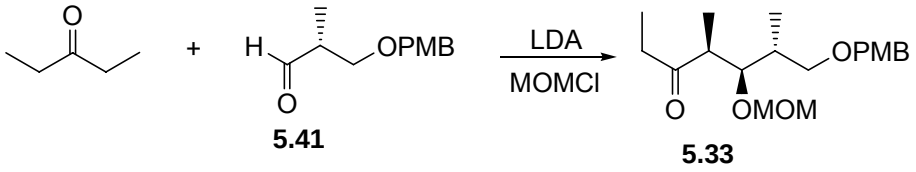

5.41 **5.33**

Scheme 5.19

According to the previous work done by both the Schreiber and Heathcock groups, formation of the C15-C16 bond with the desired stereochemistry had proven to be troublesome. Alkylation of the lithium (*Z*)-enolate of **5.33** with **5.32** gave the desired C9-C21 fragment **5.42** with *dr* = 6:1 using a specific protective group, lithium base and solvent system conditions. Selective reduction at C17 with *dr* = 8:1, followed by a Stork-Wittig olefination, gave the C8-C21 vinyl iodide **5.43**. The terminal diene unit was

introduced by PMB deprotection, followed by oxidation to the corresponding aldehyde and then Roush allylation and *syn* elimination. Deprotection of the MOM protecting group followd by carbamation gave **5.44**. Coupling of **5.44** with aldehyde **5.31** by means of a Nozaki-Kishi coupling gave **5.45**, with relatively low selectivity *dr* = 2:1 at C-7 (Scheme 5.20). Global deprotection and δ-lactonisation of **5.45** gave discodermolide in ca. 1.4% overall yield**.**

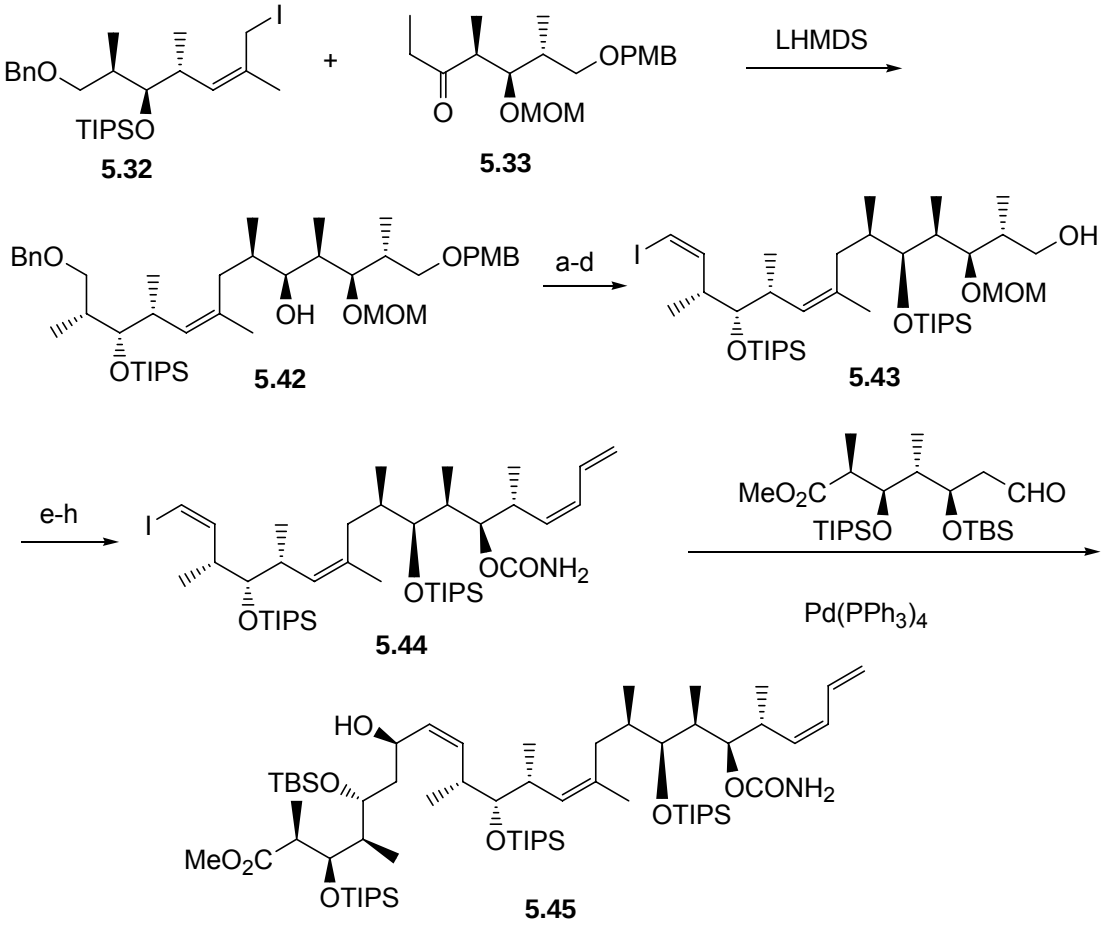

a) TIPSCl, b) H_2, c) Ph_3PCH_2I d) DDQ e) Dess-Martin, f)$Ph_3PCH_2CH{=}CH_2$ g) HCl h) $CCl_3CON{=}C{=}O$

Scheme 5.20

5.4.4 Marshall Synthesis of Discodermolide[34,35]

The total synthesis of discodermolide reported by Marshall *et al.* proceeded via the three segments **5.46** (C1-C7), **5.47** (C8-C13) and **5.48** (C15-C24). The key coupling steps were C7-C8 by lithium acetylide addition to an aldehyde and C14-C15 using a modified Suzuki cross-coupling reaction (Scheme 5.21), respectively.

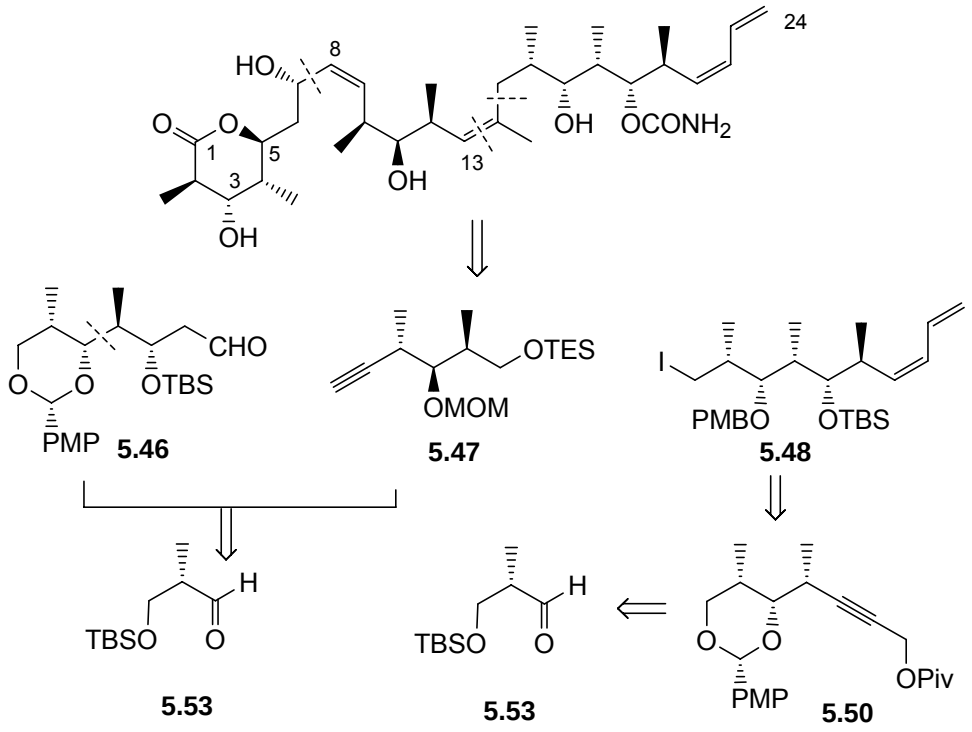

Scheme 5.21 Retrosynthesis of discodermolide by Marshall group

Addition of propargylic mesylate **5.52** to aldehyde **5.53** using Et_2Zn and $Pd(PPh_3)_4$ gave **5.54** with *dr* = 9:1, which serves as the building block for **5.46** (C1-C7) and **5.47** (C8-C13). MOM protection of **5.54** as its ether gave the C8-C13 segment **5.47** (Scheme 5.22).

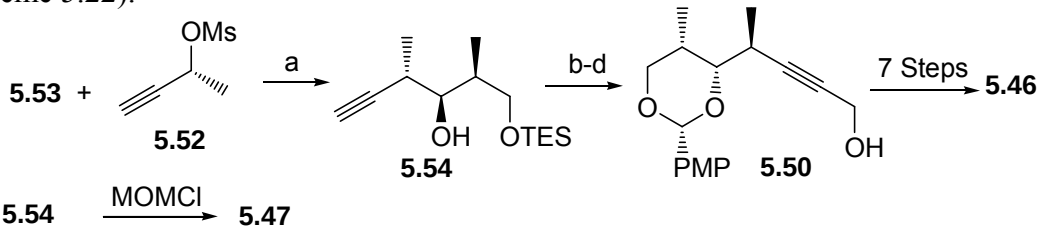

a), Et_2Zn, $Pd(PPh_3)_4$ b) HF c)$PMB(OMe)_2$ d) BuLi, CH_2O

Scheme 5.22

Addition of chiral allenylstannane **5.49** to the Roche ester derived aldehyde **5.53** gave **5.50** with *dr* = 20:1. Red-Al reduction, Sharpless epoxidation and methyl cuprate opening gave an epoxide, which was converted to diol **5.51**. The subsequent steps were the protection of the secondary hydroxyl group, oxidation to an aldehyde and conversion to the terminal diene unit by the Nozaki-Hiyama/Peterson protocol to give the C15-C24 segment iodide **5.48** (Scheme 5.23).

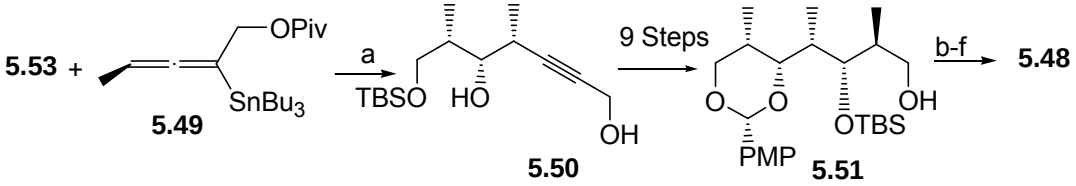

a) BF_3; b) TESCl; c) Dess- Martin, d) TMS BrCCH=CH_2, KH; e) DIBAL; f) I_2

Scheme 5.23

Subsequent coupling of the lithiated alkyne **5.47** with aldehyde **5.46** gave alcohol **5.55** with *dr* = 6:1 at C7. Lindlar hydrogenation and protecting group manipulations, followed by the Zhao-Wittig olefination protocol gave the (*Z*)-alkenyl iodide **5.57** with variable selectivity [(*Z*)/(*E*) = 1.3:1 to 9:1). Suzuki cross-coupling of **5.57** with boronate derivative of **5.48** gave C1-24 intermediate **5.58** (Scheme 5.24).

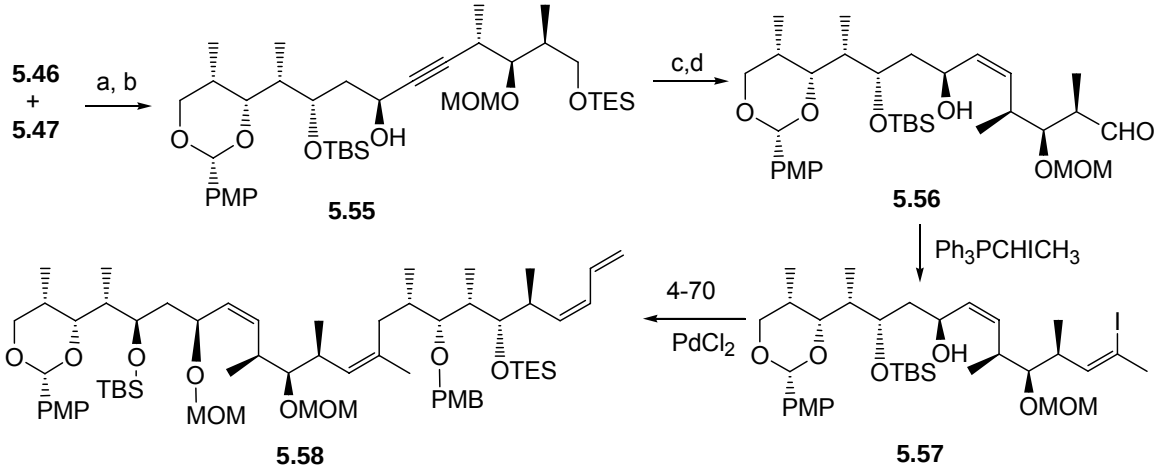

a) BuLi, b) 9BBNHMe c) H_2, Pd d)HF e) Dess-Marin

Scheme 5.24

Subsequent manipulations and deprotections were performed to complete the synthesis of discodermolide with a 2.2% overall yield over 29 steps (longest linear sequence).

5.4.5 Paterson Synthesis of Discodermolide[28,36-38]

In the synthetic strategy of Paterson *et al.*, three subunits **5.59** (C1-C6), **5.60** (C9-16) and **5.61** (C17-24) were employed with aldol couplings at C6-7 and a lithium-mediated aldol coupling at C16-17 (Scheme 5.25).

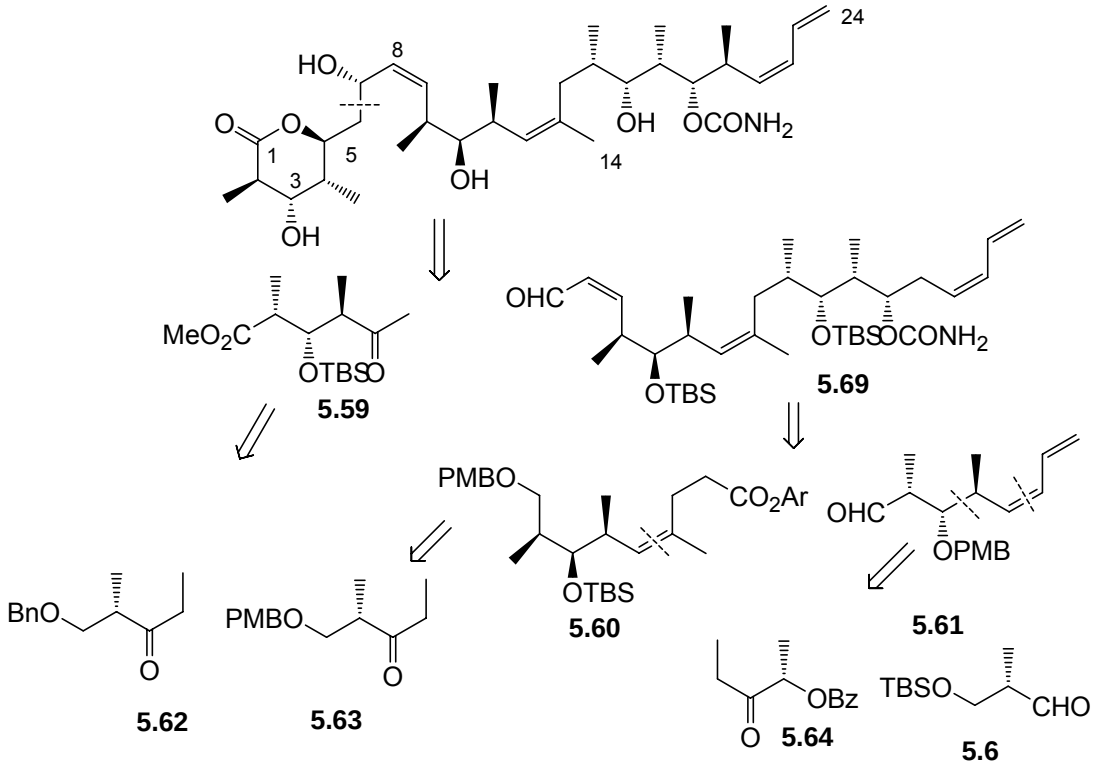

Scheme 5.25 Retrosynthesis of discodermolide by the Paterson group

Ethyl ketones **5.62**, **5.63** and **5.64** serve as building blocks. Roche ester **5.7** was protected by a Bn group and thence converted to the corresponding Weinreb amide, which was subjected to ethyl Grignard addition to give ethyl ketone **5.62**. *Anti*-aldol addition of **5.63** with acetaldehyde through a boron enolate, followed by *in situ* reduction

with $LiBH_4$ gave the 1,3-*syn* diol **5.65** with *dr* = 30:1 (Scheme 5.24). Protection of **5.65** as its bis-TBS ether and selective removal of the C5 TBS group followed by hydrogenolysis of the benzyl ether gave diol **5.66**. Subsequent methyl ester formation gave the C1-C6 methyl ketone **5.59** (Scheme 5.26). The same boron-mediated aldol reaction of PMB protected ethyl ketone **5.63** gave **5.67** (*dr* = 30:1), which was subjected to Evans anti reduction to give diol **5.68** (*dr* > 30:1).

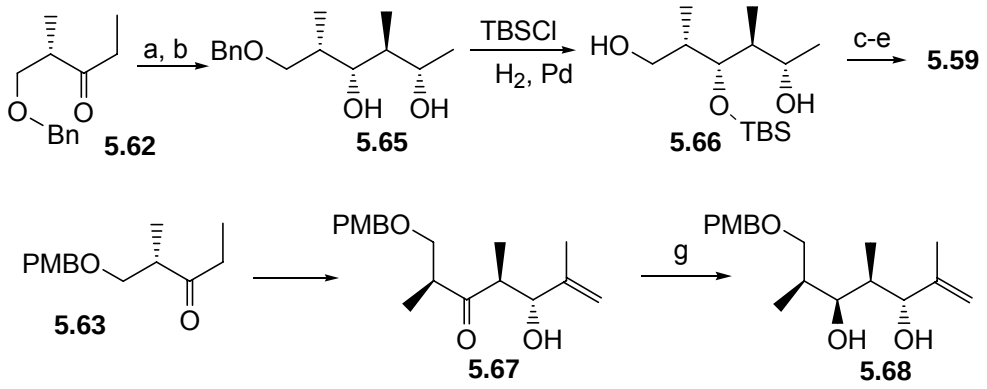

a) Cy_2BCl, MeCHO b) $LiBH_4$ c) Swern; d) $NaClO_2$ e) CH_2N_2, f) Cy_2BCl, CH_2=CMeCHO g) $Me_4NBH(OAc)_3$

Scheme 5.26

Transacetalisation of **5.68** with **5.77** gave acetal **5.78** (Scheme 5.27). Following a Holmes protocol, oxidation and elimination of the phenyl selenoxide and installation of a trisubstituted (*Z*)-alkene by a Claisen [3,3] rearrangement provided the lactone **5.79**. A further three steps were performed to complete the C9-C16 aryl ester **5.60**.

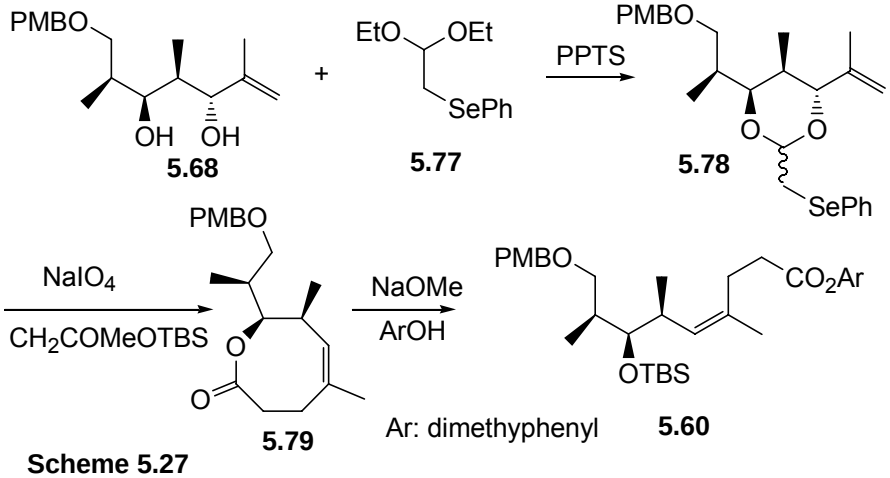

Scheme 5.27

Lactate derived ethyl ketone **5.64** was subjected to anti-aldol condensation with aldehyde **5.6** to give **5.67**. PMB protection of **5.67**, followed by oxidative cleavage, gave aldehyde **5.68**. Installation of the terminal (*Z*)-diene subunit by means of Zhao-Wittig olefination protocol gave the (*Z*)-diene **5.70**. Deprotection of TBS and oxidation gave the C17-C24 fragment aldehyde **5.61** as shown in Scheme 5.28.

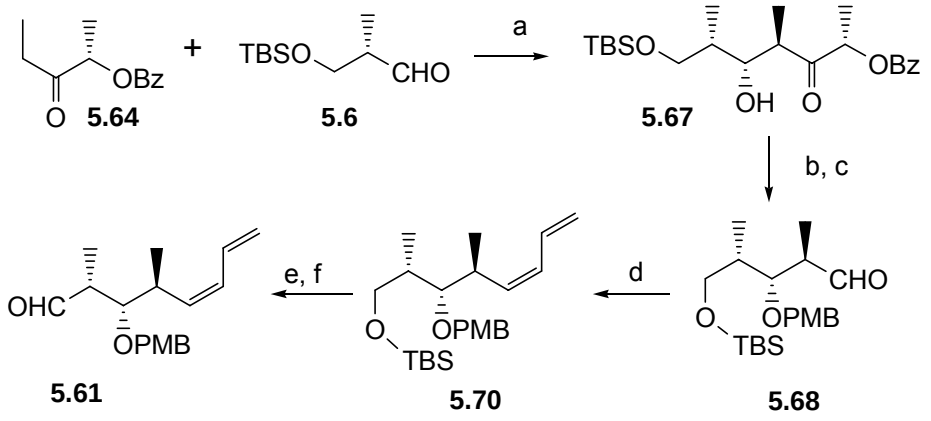

a) Cy_2BCl b) PMBBr, LAH c) $NaIO_4$ d) $Ph_3PCHCH{=}CH_2$ e)HF, f) Dess-Martin

Scheme 5.28

Subsequent lithium mediated anti-aldol condensation of aryl ester **5.60** with aldehyde **5.61** gave the intermediate **5.71** with *dr* = 30:1 based on Felkin-Anh selective addition. Reduction of the ester and deoxygenation at C16, followed by PMB deprotection at C9 gave **5.72**. Oxidation and reaction of the resulting aldehyde gave C8-C9 (*Z*)-olefin **5.73** with (*Z*)/(*E*) > 30:1 by the Still-Gennari HWE protocol. Carbamation at C19, reduction and oxidation at C7 gave enal **5.69**. Coupling **5.69** with C1-C6 methyl ketone **5.59** by means of a second boron-mediate aldol reaction gave **5.74** with dr = 5:1 at C7 (Scheme 5.29).

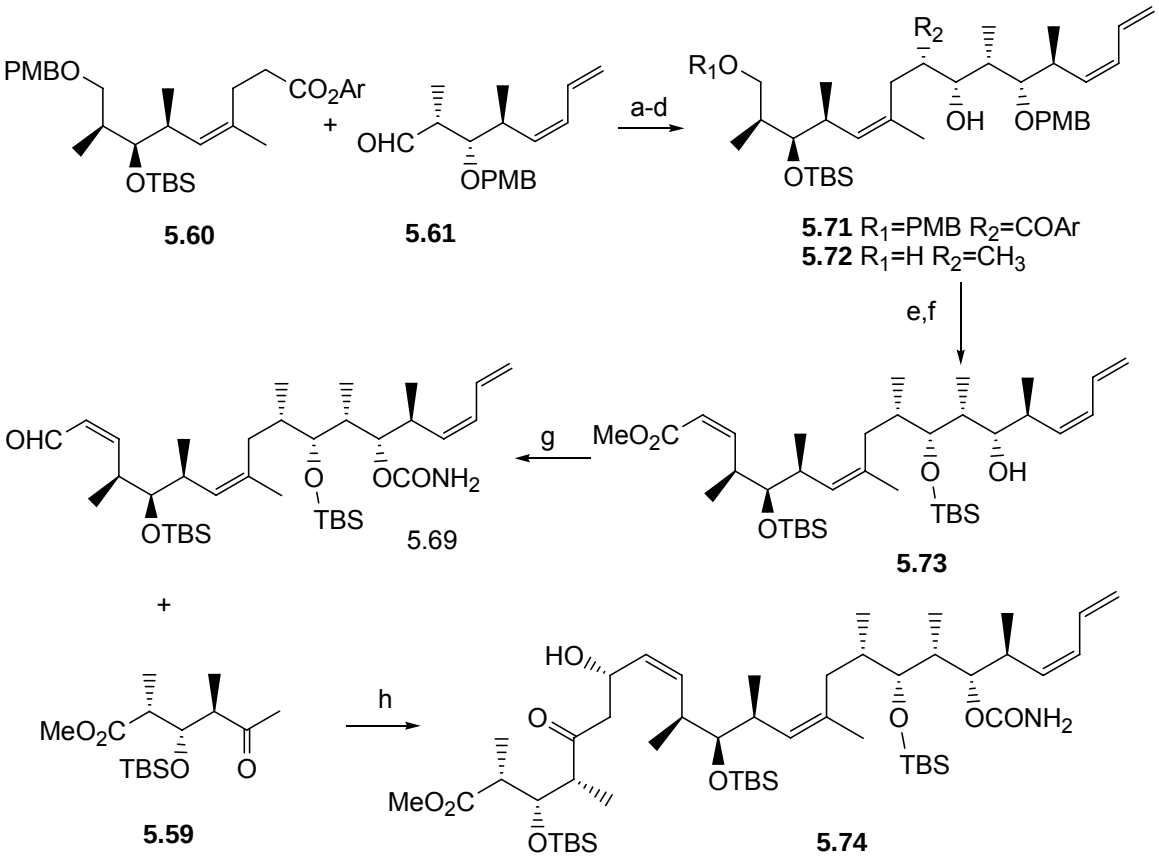

a) LiTMP, b) TsCl, LAH c) DDQ d) TBSCl, e) Dess-Martin, f) Ph_3PCHCO_2Me
g) DIBAL h) Cy_2BCl

Scheme 5.29

A second Evans 1,3-*anti* reduction performed on **5.74** gave a secondary alcohol at C5 with *dr* > 30:1. Subsequent global deprotection and δ-lactonisation were performed to complete the synthesis of discodermolide with 5.1 % overall yield (23 steps in longest sequence).

In their later work, a second generation synthesis was designed both to reduce the total number of steps by employing a common precursor and to eliminate the usage of chiral auxiliaries by substrate control. The retrosynthesis route is shown in Scheme 5.30.

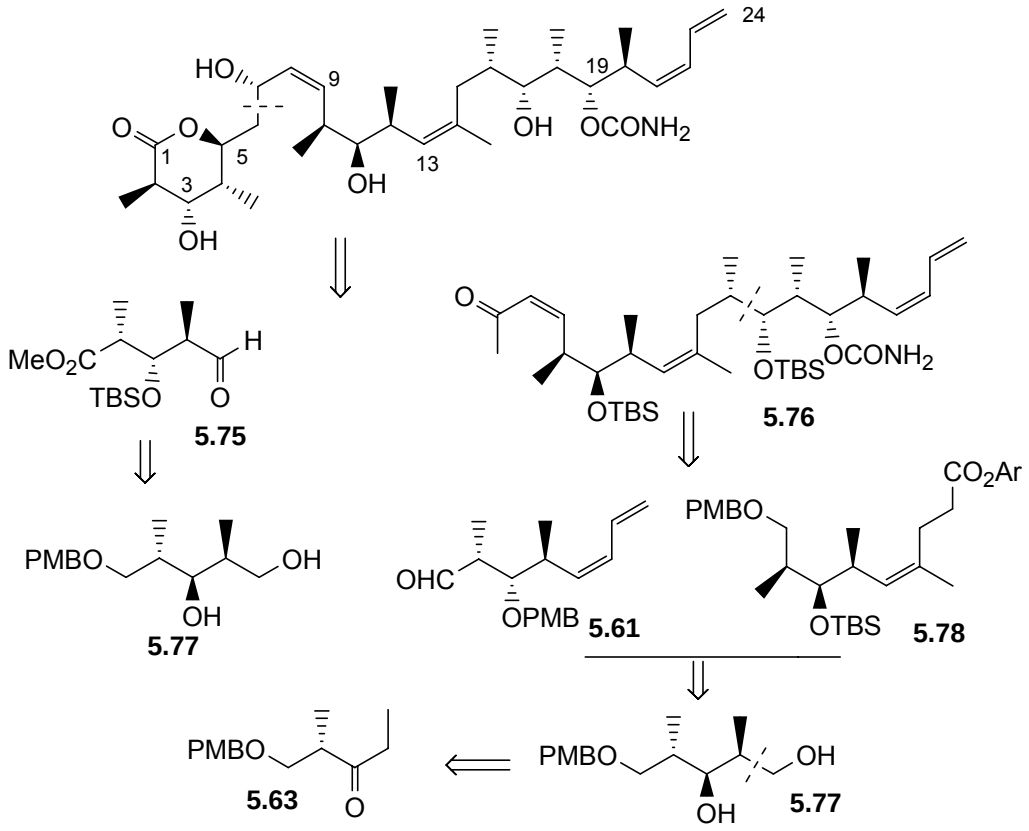

Scheme 5.30 Retrosynthesis of discodermolide in 2nd generation by Paterson group

In the common precursor strategy, three fragments **5.75** (C1-C5), **5.78** (C9-C16) and **5.61** (C17-C24) were employed with a key coupling at C5-C6 by boron aldol condensation and C16-C17 by a lithium-mediated aldol reaction. Coupling of ethyl ketone **5.63** with formaldehyde by means of a boron-mediated aldol reaction gave **5.79** with *dr* = 20:1. Hydroxyl-directed reduction and recrystallization gave common precursor **5.77** with *dr* = 10:1, which served as a building block for the synthesis (Scheme 5.31).

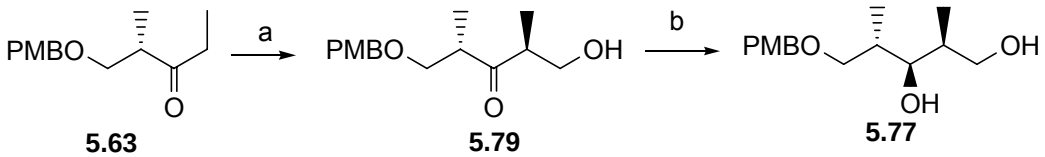

a) Cy_2BCl, CH_2O; b) $NaBH(OAc)_3$

Scheme 5.31

Selective oxidation of the common precursor **5.77** at C1 gave aldehyde **5.80,** and thence to the corresponding methyl ester **5.81**. Protection of **5.81** as its TBS ether, followed by selective removal of PMB with DDQ and oxidation to the aldehyde, gave the C1-C5 subunit **5.75**. Alternatively conversion of aldehyde **5.80** to the terminal (*Z*)-olefin unit by Still-Gennari HWE olefination protocol, followed by TBS protection gave **5.82**, which was converted to **5.83** by reduction and iodination (Scheme 5.32).

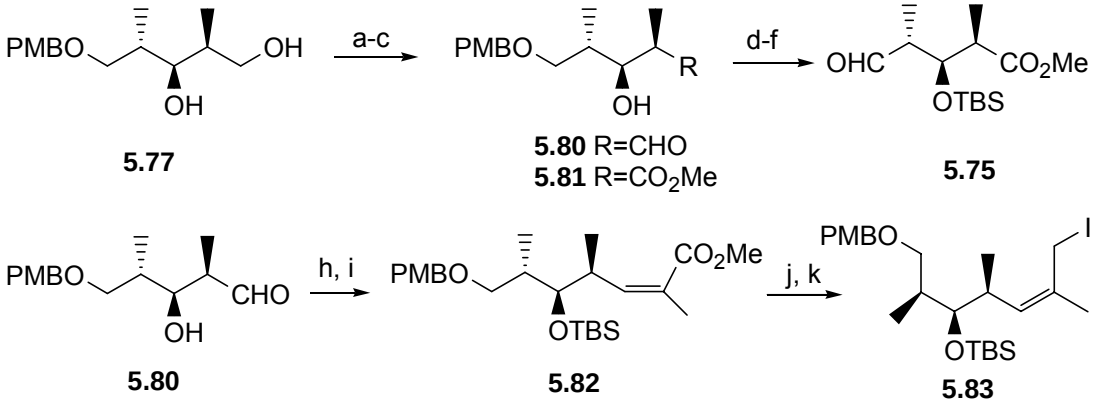

a) Swern; b) $NaClO_2$; c) CH_2N_2; d) TBSOTf; e) DDQ; f) Swern; h) $Ph_3PCMeCO_2Me$
i) TBSOTf; j) DIBAL; k) I_2, Ph_3P

Scheme 5.32

Alkylation of **5.83** with the lithium enolate of the novel aryl ester **5.84** gave the C9-C16 subunit **5.78** (Scheme 5.33). Protecting group manipulations of common precursor **5.77** to **5.85**, oxidation to aldehyde and thence conversion to terminal (*Z*)-diene unit gave **5.70**, which was converted to C17-C24 subunit **5.61** as in the first generation (Scheme 5.33).

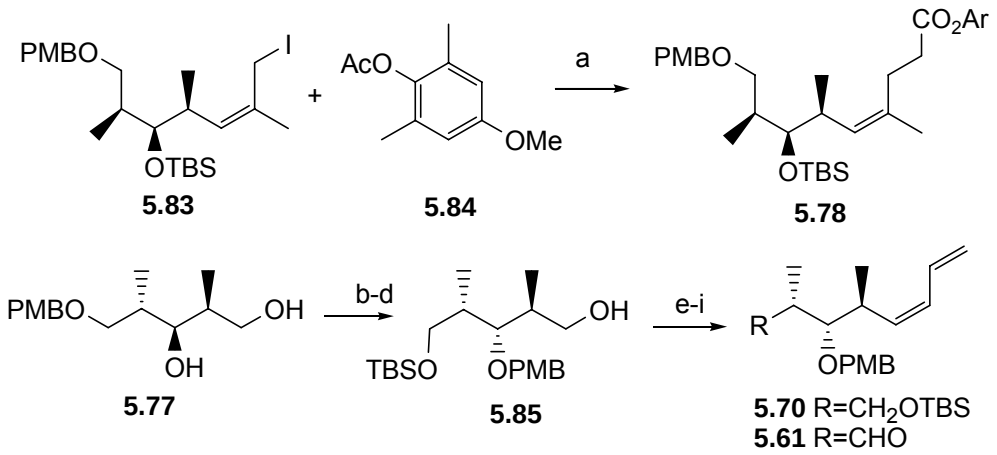

a) LiHMDS; b) TBSCl; c) DDQ; d) DIBAL; e) Swern; f) $CrCl_2$, TMS allylBr; g) KH; h) 10-CSA; i) Swern

Scheme 5.33

Coupling of **5.78** and **5.61** by means of a lithium-mediated aldol condensation gave **5.86** with *dr* = 6:1. Reduction and deoxygenation on C16, followed by deprotection with a PMB group gave alcohol **5.72**, similar to the first generation approach. Oxidation to the aldehyde, carbamation at C19 and thence conversion to the (*Z*)-olefin by Still-Gennari HWE olefination protocol gave (*Z*)-enone **5.76** with [(*Z*)/(*E*) = 12:1] (Scheme 5.34).

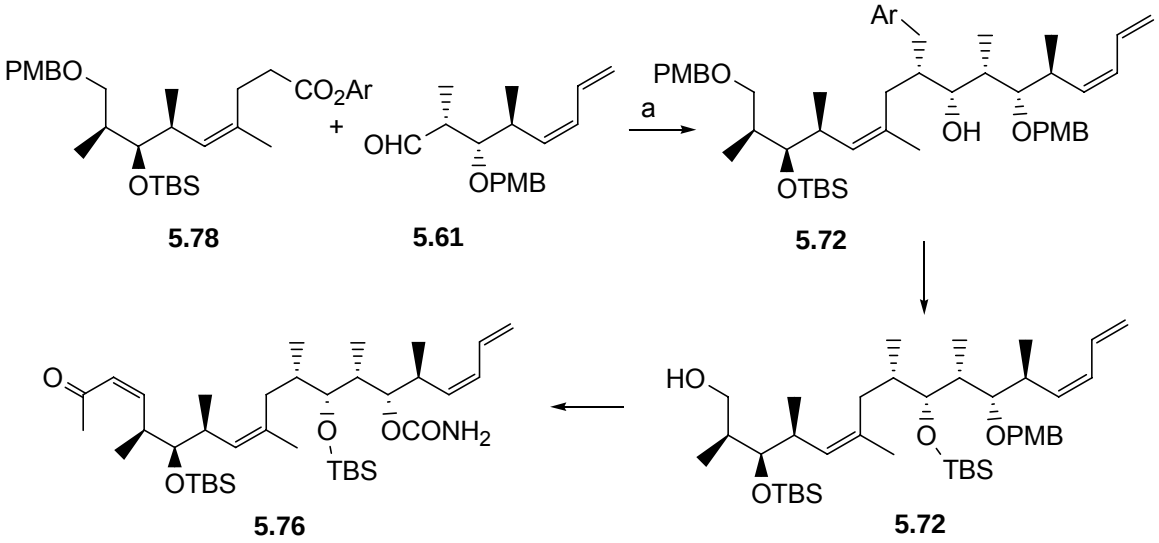

a) LiTMP, b) TsCl, LAH c) TBSOTf; d) DDQ, e) TEMPO, f) CCl_3NOCO; g) $Ph_3PCHCOMe$

Scheme 5.34

Coupling **5.76** with aldehyde **5.75** through a boron-mediated aldol reaction, relying on remote 1,6-asymmetric induction from C10, gave **5.87** with *dr* = 20:1 (Scheme 5.35).

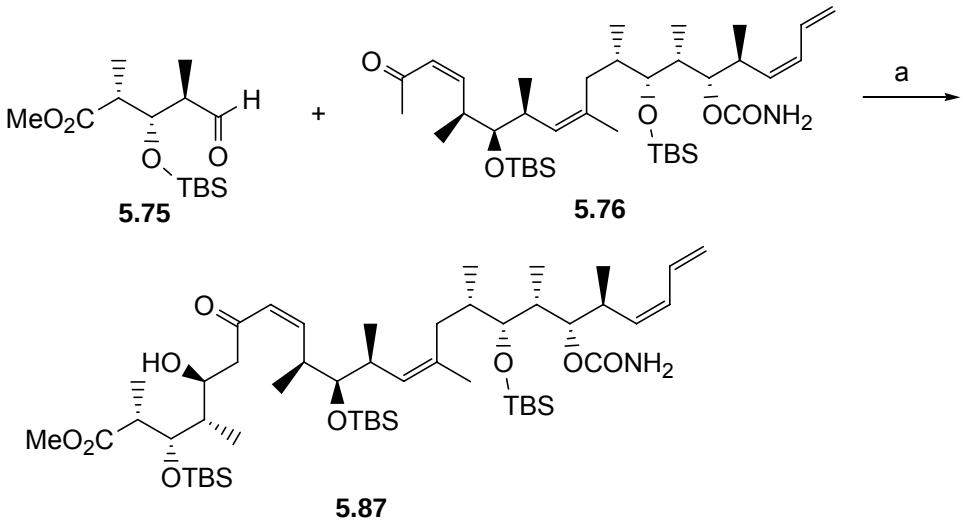

a) Cy_2BCl

Scheme 5.35

δ-Lactonisation of **5.87,** followed by K-Selectride reduction at C7 with *dr* = 30:1 and global deprotection completed the second-generation synthesis of discodermolide in 7.5% with overall yield over 24 steps in the longest linear sequence (35 total steps).

5.4.6 Summary

Among these synthetic approaches mentioned above, Smith and Paterson's synthetic routes are the best because both groups adopted a highly convergent common precursor strategy, which considerably simplified the synthetic routes and greatly improved the overall yield (5% in Smith, 7.5% in Paterson). SAR studies are severely hampered by problems with the supply of analogs. On the other hand, the conformation

of discodermolide on tubulin will provide valuable information on the SAR and its mechanism, and it will direct the synthesis of more efficient and simplified analogs. Unfortunately, this study largely lags behind the synthesis. Although NMR studies and computational modeling by Snyder[5] offered insights into the conformation of discodermolide in solution, this approach does not provide experimental data for the conformation on tubulin. The application of spectroscopic techniques by using labeled analogs is a promising approach to determining the binding conformation, as has been shown by previous work on paclitaxel.

References:

1. Gunasekera, S. P.; Granik, S.; Longley, R. E. Immunosuppressive compounds from a deep water marine sponge, *Agelas flabelliformis*. *J. Nat. Prod.* **1989,** *52*, 757-761.
2. Gunasekera, S. P.; Gunasekera, M.; Longley, R. E. Discodermolide: A new bioactive polyhydroxylated lactone from the marine sponge *Discodermia dissoluta*. *J. Org. Chem.* **1990,** *55*, 4912-4915
3. Gunasekera, S. P.; Paul, G. K.; Longley, R. E.; Isbrucker, R. A.; Pomponi, S. A. Five new discodermolide analogues from the marine sponge *Discodermia species*. *J. Nat. Prod.* **2002,** *65*, 1643-1648.
4. Smith A. B. III; Freeze, B. S.; Lamarche, M. J.; Hirose, T.; Brouard, I.; Rucker, P. V.; Xian, M.; Sundermann, K. F.; Shaw, S. J.; Burlingame, M. A.; Horwitz, S. B.; Myles, D. C. Design, synthesis, and evaluation of carbamate-substituted analogues of (+)-discodermolide. *Org. Lett.* **2005,** *7*, 311-314.

5. Monteagudo, E.; Cicero, D. O.; Cornett, B.; Myles, D. C.; Snyder, J. P. The conformations of discodermolide in DMSO. *J. Am. Chem. Soc.* **2001,** *123*, 6929 - 6930.

6. Hung, D. T.; Nerenberg, J. B.; Schreiber, S. L. Distinct binding and cellular properties of synthetic (+)- and (-)-discodermolides. *Chem. Biol.* **1994,** *1*, 67-71.

7. Longley, R. E.; Caddigan, D.; Harmody, D.; Gunasekera, M.; Gunasekera, S. P. Discodermolide: A new marine-derived immunosuppressive compound. I *in vitro* studies. *Transplantation* **1991,** *52*, 650-656.

8. Longley, R. E.; Caddigan, D.; Harmody, D.; Gunasekera, M.; Gunasekera, S. P. Discodermolide: A new marine-derived immunosuppressive compound. II *in vivo* studies. *Transplantation* **1991,** *52*, 656-661.

9. ter Haar, E.; Kowalski, R. J.; Hamel, E.; Lin, C. M.; Longley, R. E.; Gunasekera, S. P.; Rosenkranz, H. S.; Day, B. W. Discodermolide, a cytotoxic marine agent that stabilizes microtubules more potently than taxol. *Biochemistry* **1996,** *35*, 243.

10. Hung, D. T.; Nerenberg, J. B.; Schreiber, S. L. Syntheses of discodermolides useful for investigating microtubule binding and stabilization. *J. Am. Chem. Soc.* **1996,** *118*, 11054-11080.

11. Kowalski, R. J.; Giannakakou, P.; Gunasekera, S. P.; Longley, R. E.; Day, B. W.; Hamel, E. The microtubule-stabilizing agent discodermolide competitively inhibits the binding of paclitaxel (taxol) to tubulin polymers, enhances tubulin nucleation reactions more potently than paclitaxel, and inhibits the growth of paclitaxel-resistant cells. *Mol. Pharmacol.* **1997,** *52*, 613-622.

12. Martello, L. A.; McDaid, H. M.; Regl, D. L.; Yang, C. P. H.; Meng, D.; Pettus, T. R. R.; Kaufman, M. D.; Arimoto, H.; Danishefsky, S. J.; Smith, A. B. I.; Horwitz, S. B. Taxol and discodermolide represent a synergistic drug combination in human carcinoma cell lines. *Clin. Canc. Res.* **2000,** *6*, 1978-1987.

13. Honore, S.; Kamath, K.; Braguer, D.; Horwitz, S. B.; Wilson, L.; Briand, C.; Jordan, M. A. Synergistic suppression of microtubule dynamics by discodermolide and paclitaxel in non-small cell lung carcinoma cells. *Canc. Res.* **2004,** *64*, 4957-4964.

14. Smith III, A. B.; LaMarche, M. J.; Falcone-Hindley, M. The solution structure of (+)-discodermolide. *Org. Lett.* **2001,** *5*, 695-698.

15. Smith III, A. B.; Rucker, P. V.; Brouard, I.; Freeze, B. S.; Xia, S.; Horwitz, S. B. Design, synthesis, and biological evaluation of potent discodermolide fluorescent and photoaffinity molecular probes. *Org. Lett.* **2005,** *7*, 5199-5202.

16. Smith A. B. III; Rucker, P. V.; Brouard, I.; Freeze, B. S.; Xia, S.; Horwitz, S. B. Design, synthesis, and biological evaluation of potent discodermolide fluorescent and photoaffinity molecular probes. *Org. Lett.* **2005,** *7*, 5199-5202.

17. Xia, S.; Kenesky, C. S.; Rucker, P. V.; Smith A. B. III; Orr, G. A.; Horwitz, S. B. A photoaffinity analogue of discodermolide specifically labels a peptide in α-tubulin. *Biochemistry* **2006,** *45*, 11762-11775.

18. Smith A. B. III; Xian, M. Design, synthesis, and biological evaluation of simplified analogues of (+)-discodermolide. Additional insights on the

importance of the diene, the C(7) hydroxyl, and the lactone. *Org. Lett.* **2005,** *7*, 5229-5232.

19. Smith A. B. III; Xian, M.; Liu, F. Design, total synthesis, and evaluation of c(13)-c(14) cyclopropane analogues of (+)-discodermolide. *Org. Lett.* **2005,** *7*, 4613-4616.

20. Gunasekera, S. P.; Longley, R. E.; Isbrucker, R. A. Acetylated analogues of the microtubule-stabilizing agent discodermolide: Preparation and biological activity. *J. Nat. Prod.* **2001,** *64*, 171-174.

21. Smith III, A. B.; Freeze, B. S.; LaMarche, M. J.; Sager, J.; Kinzler, K. W.; Vogelstein, B. Discodermolide analogues as the chemical component of combination bacteriolytic therapy. *Bioorg. Med. Chem. Lett.* **2005,** *15*, 3623-3626.

22. Smith A. B. III; Freeze, B. S.; Lamarche, M. J.; Hirose, T.; Brouard, I.; Rucker, P. V.; Xian, M.; Sundermann, K. F.; Shaw, S. J.; Burlingame, M. A.; Horwitz, S. B.; Myles, D. C. Design, synthesis, and evaluation of carbamate-substituted analogues of (+)-discodermolide. *Org. Lett.* **2005,** *7*, 311-314.

23. Shaw, S. J.; Sundermann, K. F.; Burlingame, M. A.; Myles, D. C.; Freeze, B. S.; Xian, M.; Brouard, I.; III, S. A. B. Toward understanding how the lactone moiety of discodermolide affects activity. *J. Am. Chem. Soc.* **2005,** *127*, 6532-6533.

24. Burlingame, M. A.; Shaw, S. J.; Sundermann, K. F.; Zhang, D.; Petryka, J.; Mendoza, E.; Liu, F.; Myles, D. C.; LaMarche, M. J.; Hirose, T.; Freeze, B. S.;

Smith A. B. III Design, synthesis and cytotoxicity of 7-deoxy aryl discodermolide analogues. *Bioorg. Med. Chem. Lett.* **2004,** *14*, 2335-2338.

25. Mınguez, J. M.; Kim, S.-Y.; Giuliano, K. A.; Balachandran, R.; Madiraju, C.; Day, B. W.; Curran, D. P. Synthesis and biological assessment of simplified analogues of the potent microtubule stabilizer (+)-discodermolide. *Bioorg. Med. Chem.* **2003,** *11*, 3335-3357.

26. Choy, N.; Shin, Y.; Nguyen, P. Q.; Curran, D. P.; Balachandran, R.; Madiraju, C.; Day, B. W. Simplified discodermolide analogues: Synthesis and biological evaluation of 4-*epi*-7-dehydroxy-14,16-didemethyl-(+)-discodermolides as microtubule-stabilizing agents. *J. Med. Chem.* **2003,** *46*, 2846 - 2864.

27. Smith III, A. B.; Xian, M. Design, synthesis, and biological evaluation of simplified analogues of (+)-discodermolide. Additional insights on the importance of the diene, the C(7) hydroxyl, and the lactone. *Org. Lett.* **2005,** *7*, 5229-5232.

28. Paterson, I.; Florence, G. J.; Gerlach, K.; Scott, J. P.; Sereinig, N. A practical synthesis of (+)-discodermolide and analogues: Fragment union by complex aldol reactions. *J. Am. Chem. Soc.* **2001,** *123*, 9535-9544.

29. Nerenberg, J. B.; Hung, D. T.; Somers, P. K.; L., S. S. Total synthesis of the immunosuppressive agent (-)-discodermolide. *J. Am. Chem. Soc.* **1993,** *115*, 12621-12622.

30. Smith III, A. B.; Beauchamp, T. J.; LaMarche, M. J.; Kaufman, M. D.; Qiu, Y.; Arimoto, H.; Jones, D. R.; Kobayashi, K., Evolution of a gram-scale synthesis of (+)-discodermolide. *J. Am. Chem. Soc.* **2000,** *122*, 8654-8664.

31. Smith III, A. B.; Qiu, Y.; Jones, D. R.; Kobayashi, K. Total synthesis of (-)-discodermolide. *J. Am. Chem. Soc.* **1995,** *117*, 12011-12012.

32. Smith III, A. B.; Kaufman, M. D.; Beauchamp, T. J.; LaMarche, M. J.; Arimoto, H. Gram-scale synthesis of (+)-discodermolide. *Org. Lett.* **1999,** *1*, 1823-1826.

33. Haried, S. S.; Yang, G.; Strawn, M. A.; C., M. D. Total synthesis of (-)-discodermolide: An application of a chelation-controlled alkylation reaction. *J. Org. Chem.* **1997,** *62*, 6098-6099.

34. Marshall, J. A.; Lu, Z.-H.; Johns, B. A. Synthesis of discodermolide subunits by S_E2' addition of nonracemic allenylstannanes to aldehydes. *J. Org. Chem.* **1998,** *63*, 817-823.

35. Marshall, J. A.; Johns, B. A. Total synthesis of (+)-discodermolide. *J. Org. Chem.* **1998,** *63*, 7885-7892.

36. Paterson, I.; Florence, G. J.; Gerlach, K.; Scott, J. P. Total synthesis of the antimicrotubule agent (+)-discodermolide using boron-mediated aldol reactions of chiral ketones *Angew. Chem., Int. Ed.* **2000,** *39*, 377.

37. Paterson, I.; Delgado, O.; Florence, G. J.; Lyothier, I.; Scott, J. P.; Sereinig, N. 1,6-asymmetric induction in boron-mediated aldol reactions: Application to a practical total synthesis of (+)-discodermolide. *Org. Lett.* **2003,** *5*, 35-38.

38. Paterson, I.; Florence, G. J. The development of a practical total synthesis of discodermolide, a promising microtubule-stabilizing anticancer agent. *Eur. J. Org. Chem.* **2003**, 2193-2208.

Chapter 6. Synthesis of fluorescently labeled discodermolide analogs

6.1 Introduction

Understanding of the interaction of discodermolide and tubulin would be greatly enhanced by a knowledge of the 3D structure of the discodermolide tubulin complex. Unfortunately this complex has not been crystallized, so direct observation of this structure is not possible. However, it is possible to obtain indirect evidence of the position of the discodermolide binding site on tubulin by a study of the spectrum of a fluorescent discodermolide analog bound to microtubules. Fluorescence spectroscopy has been widely used in biological systems to investigate ligand–receptor interactions,[1] and fluorescent PTX derivatives have been used to probe the nature of PTX-tubulin interactions.[2] In our previous studies, a small environmentally sensitive fluorescent probe, such as an aminobenzoyl group, was successfully used to explore the local environment of the PTX binding site on the microtubule.[3-5] However, some characteristics of discodermolide hamper the use of fluorescent probes. First, discodermolide possesses no natural chromophore, which could be used as a probe. Second, the size of the parent molecule makes it difficult to add a fluorescent probe without making major structural changes. Third, the structural complexity of the molecule complicates synthetic efforts to create a wide range of derivatives. However, a series of 7-deoxy discodermolide analogs with the lactone fragment replaced by aryl substituents has been synthesized, and the products were found to have sub-micromolar cytotoxicity.[19] For our first fluorescent probe, we chose to replace the lactone ring of discodermolide with an aminobenzoate group. It was expected that this modification would not adversely interfere with the interaction of the analog with microtubules.

6.2 Design and synthesis of simplified fluorescently labeled discodermolide analogs

The synthesis of a simplified fluorescent discodermolide involved the coupling of a fluorescent probe with the known alcohol **6.1**, which was prepared from advanced intermediate **6.2** by using a Wittig olefination. Scheme 6.1 shows the restrosynthesis.

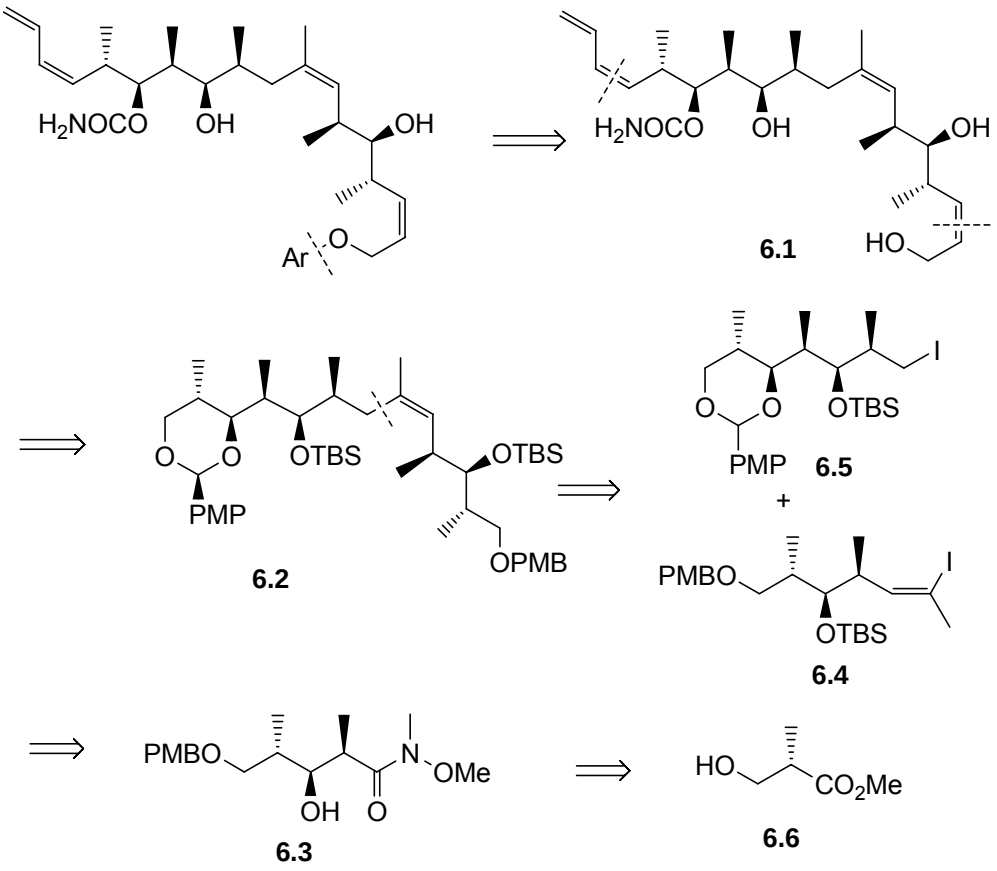

Scheme 6.1 Retrosynthesis of fluorescent discodermolide

The synthesis of known intermediate **6.2** has been extensively exploited. Smith's approach to this intermediate[6-8] was selected because it is highly convergent. Moreover all the fragments are derived from the same common precursor **6.3**, which incorporates the repeating stereotriad sequence of discodermolide. This synthetic route involved a key fragment coupling of iodides **6.4** and **6.5** using a Negishi cross-coupling reaction.

The synthesis started from the commercially available ester **6.6**, which was protected as its *p*-methoxybenzyl (PMB) ether by reaction with 4-methoxybenzyl-2,2,2-trichloroacetimidate. Reduction of the PMB derivative **6.7** with LAH, followed by Swern oxidation gave the corresponding aldehyde **6.8**. Aldehyde **6.8** was then subjected to Evans aldol *syn*-selective conditions with propionyl-(*R*)-oxazolidinone **6.9**, prepared from commercially available (*R*)-oxazolidinone, with dibutylboron triflate as the reagent. Conversion of the resulting oxazolidinone to the corresponding Weinreb amide gave the common precursor **6.3**, which served as the key building block of the synthesis (Scheme 6.2).

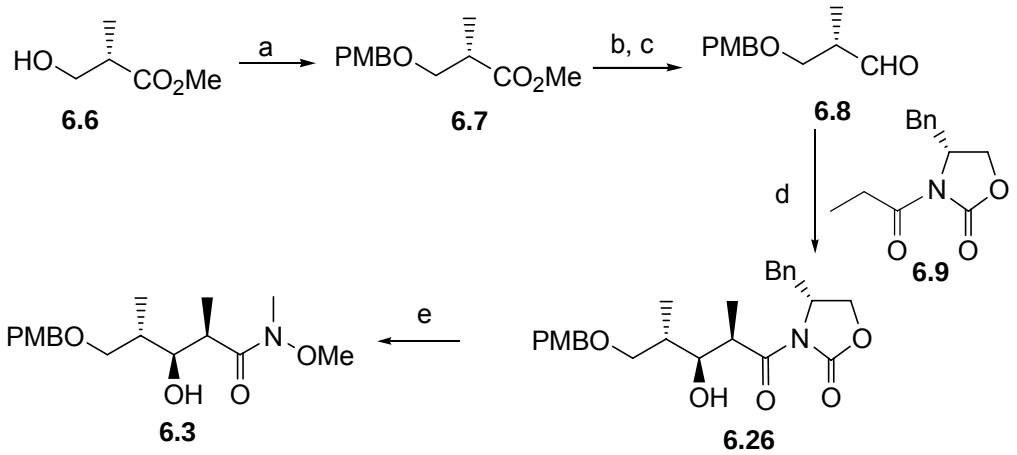

a) PMBOC(=NH)CCl_3 ; b) LAH, 90%; c) SO_3/Py, DMSO, 99% d) Bu_2BOTf, 91%
e) HNMe(OMe), $AlMe_3$, 93%

Scheme 6.2 Synthesis of common precursor **6.3**

Protection of **6.3** as its TBS ether, followed by reduction with DIBAL led to aldehyde **6.10**. The conversion of **6.10** to **6.4** by the Zhao-Wittig olefination protocol proved to be difficult, and the yield was only 30% (Scheme 6.3). The reaction described in the literature gave inconsistent results, and consistent results were only achieved when an alternate procedure was adopted (Scheme 6.4).

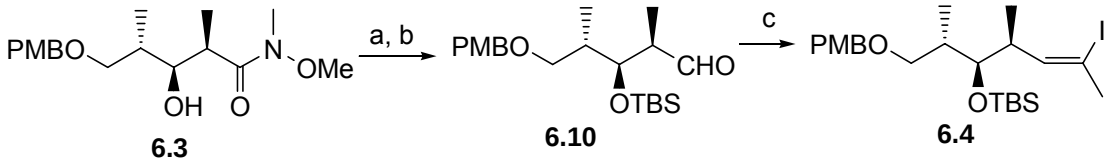

6.3 **6.10** **6.4**

a) TBSOTf, 98%; b) $LiBH_4$, Swern oxidation 85%; c) $Ph_3P^+Et\ I^-$, I_2, BuLi, 30%

Scheme 6.3 Synthesis of **6.4**

Oxidation of **6.3** with DDQ, followed by reduction with DIBAL, generated the acetal aldehyde **6.11b** (Scheme 6.4). Coupling of **6.11b** with **6.9** by means of a second Evans aldol syn-addition afforded **6.12**, which was converted to **6.5** by a sequence of TBS protection, reduction and iodination, as shown in Scheme 6.4. Iodide **6.5** was light-sensitive and it was thus made as it was needed.

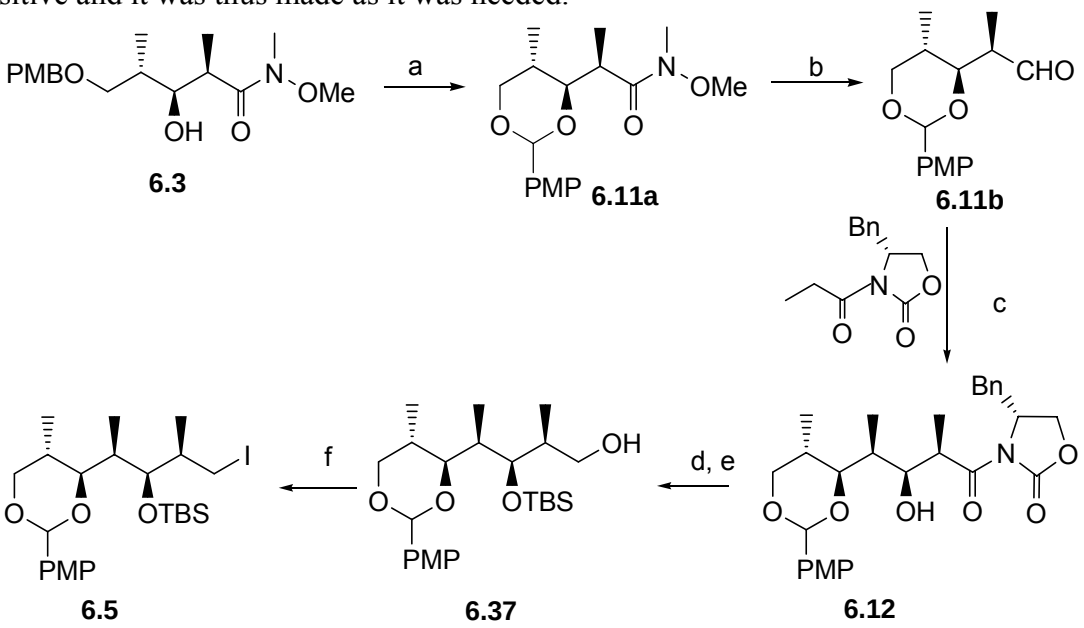

6.3 **6.11a** **6.11b** **6.12** **6.37** **6.5**

a) DDQ, 80%; b) DIBAL, 90%; c) Bu_2BOTf, Et_3N, 88%; d) TBSOTf, 95%;
e) $LiBH_4$, 93%; f) I_2, Ph_3P, 82%

Scheme 6.4 Synthesis of **6.5**

With compounds **6.4** and **6.5** in hand, the Negishi protocol coupling was the last challenge (Scheme 6.5). However, the task was very challenging. The coupling involves

the steps of insertion of palladium into the vinyl iodide, carbanion generation, and conversion of the anion to an organozinc species, which then reacts with the vinyl iodide-palladium complex. Several trial runs were performed based on the Smith procedure. Surprisingly, no desired product was obtained and only vinyl iodide was recovered. The reaction still did not occur under strictly anhydrous conditions with fresh reagents and a prolonged reaction time. By careful examination of the product, it was determined that the carbanion was generated. However, it was difficult to verify the formation of either the organozinc species or the vinyl iodide-palladium complex, and thus this approach was abandoned. An alternative methodology was developed by the Novartis group in which the Negishi coupling was replaced by the Suzuki coupling (Scheme 6.5). In contrast to the highly sensitive organozinc species, the boron species were more stable and easier to handle. The desired product **6.2** was thus obtained by using the Suzuki coupling procedure (Scheme 6.5).[9]

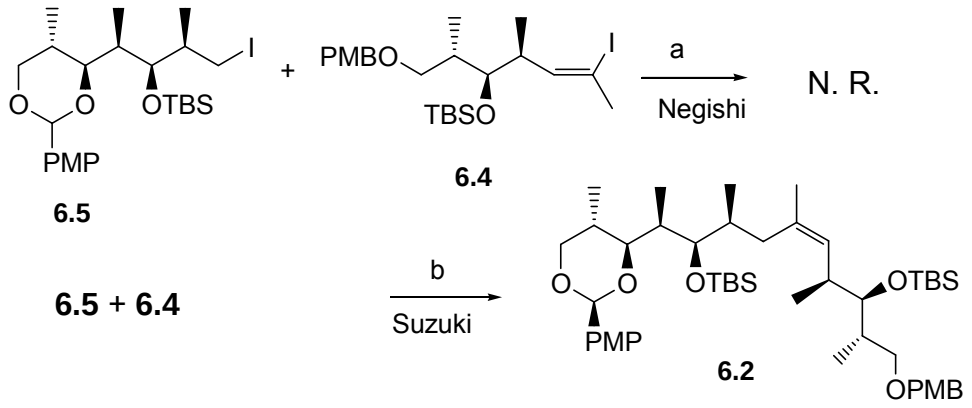

a) $ZnCl_2$, *t*-BuLi, $Pd(PPh_3)_4$, 0%; b) *t-B*uLi, 9-BBN, $Pd_2(dppf)_3$, 50%

Scheme 6.5 Coupling of **6.4** and **6.5**

Selective opening of the acetal ring of **6.2** by DIBAL, followed by oxidation gave aldehyde **6.13** (Scheme 6.6). Conversion of aldehyde **6.13** to the terminal diene **6.14** by a

Wittig olefination procedure resulted in the formation of a mixture of products. Formation of the terminal diene unit was thus carried out by the Paterson protocol.[10] Deprotection of both PMB groups in the resulting diene **6.14** by DDQ, followed by selective oxidation gave aldehyde **6.15**. Subsequent (*Z*)-selective Wittig coupling of **6.15** with the commercially available Wittig salt **6.16**, led to the (*Z*) ester **6.17** (Scheme 6.6).

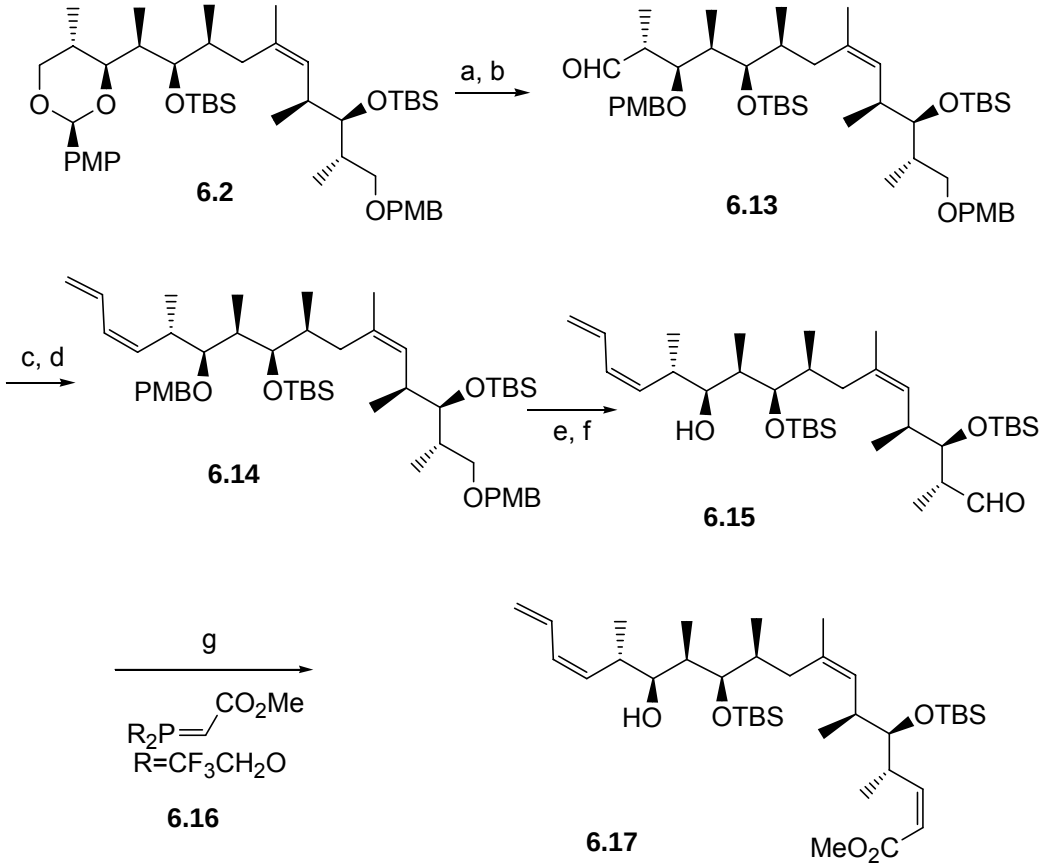

a) DIBAL, 88%; b) DMP, 95%; c) TMS allylbromide; d) KH, 87%;
e) DDQ, 60%; f) DMP, 90%; g) K_2CO_3, 85%

Scheme 6.6 Synthesis of **6.17**

The synthesis of the fluorescent discodermolide **6.1** was completed by carbamate formation and reduction. Reaction of **6.17** with trichloroacetylisocyanate gave the carbamate **6.18**, and reduction of **6.18** with DIBAL gave the alcohol **6.19** (Scheme 6.7).

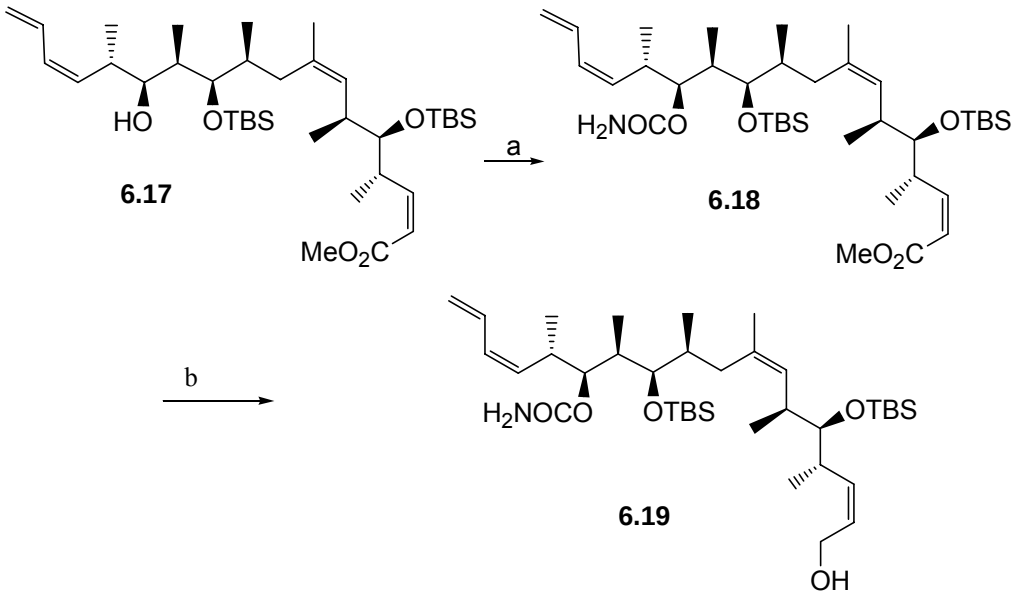

a)K_2CO_3, $Cl_3CCONCO$, 91% b)DIBAL, 87%

Scheme 6.7 Synthesis of **6.19**

Esterification of **6.19** with 3-dimethylaminobenzoic acid, employing the carbodiimide-based coupling protocol, yielded the corresponding ester, and subsequent removal of both silyl protecting groups gave the desired dimethylaminobenzoate **6.21a** (Scheme 6.8). The second analog **6.21b** was prepared from the **6.19** by esterification with a protected 3-aminobenzoic acid to give **6.20** followed by simultaneous removal of the protecting groups with TBAF to give the aminobenzoate **6.21b**.

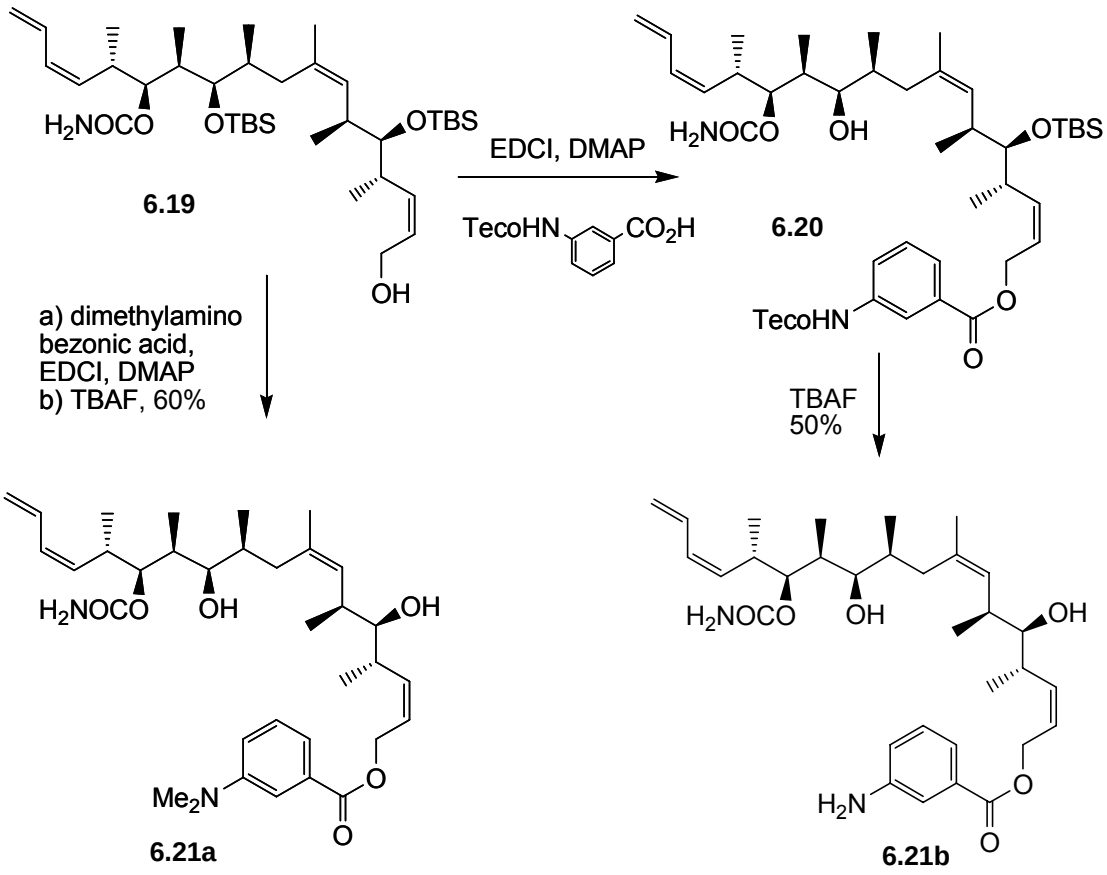

Scheme **6.8** Synthesis of **6.21a** and **6.21b**

6.3 Biological evaluation of simplified discodermolide analogs

Both fluorescent discodermolide analogues were tested against the A2780 ovarian cancer cell, with PTX as a control. The compounds were also evaluated by Dr. Susan Bane at SUNY Binghamton for tubulin-assembly activity, fluorescence and cytotoxity to PC-3 cells.

Table 1. Antiproliferative and tubulin-assembly activities of compounds **6.21a** and **6.21b**

Compounds	A2780 (nM)	PC3 (nM)	ED_{50} (μM)
PTX	11±0.34	20 ± 3.0	0.39 ± 0.03
6.21a	3400	780 ± 76.0	2.03 ± 0.21
6.21b	34000	ND	ND

Although a sample of natural discodermolide was not available, it has been reported as having an IC_{50} value of 0.7 nM against the P388 leukemia cell line, and 2.4 nM against the MCF-7 breast cancer cell line. It has also been reported to stabilize microtubules more potently than PTX. Compounds **6.21a** and especially **6.21b** are thus significantly less active than discodermolide, with **6.21a** having approximately 10-1000 fold lower antiproliferative activity than discodermolide.

6.4 Design and synthesis towards fluorescent labeled discodermolide analogs

Due to the considerable losses of activities noted above for compounds **6.21a** and **6.21b**, there is serious doubt as to whether these analogs would bind to microtubules in the same way as discodermolide. It was thus necessary to design and synthesize new fluorescently labeled discodermolides that would have a similar cytotoxicity to discodermolide. Based on the known SARs of discodermolide, modifications on the terminal diene unit would not significantly reduce the cytotoxicity. In a recent study of fluorescent discodermolides by Smith et al.,[11] fluorescent discodermolide analogs with fluorophore probes attached to the terminal diene exhibited remarkable antiproliferative and tubulin binding properties. In order to avoid duplication of this work, we initiated the synthesis of fluorescent discodermolide analogs with the fluorophore probes attached to a different position, which might provide additional information on the nature of the discodermide tubulin complex. Based on the known SAR of discodermolide, the C14 methyl group is not necessary for cytotoxicity. It is thus possible that fluorophore probes on the C14 methyl group might not induce loss of activity. Furthermore, no discodermolide analog with a bulky group at C14 has been reported so far. Therefore,

fluorescent discodermolide analogs with a fluorophore probe attached to the C14 methyl could serve not only for fluorescence studies, but also for extension of SARs. Due to these dual benefits, we designed **6.22** as a target. The retrosynthesis of **6.22** is shown in Scheme 6.9.

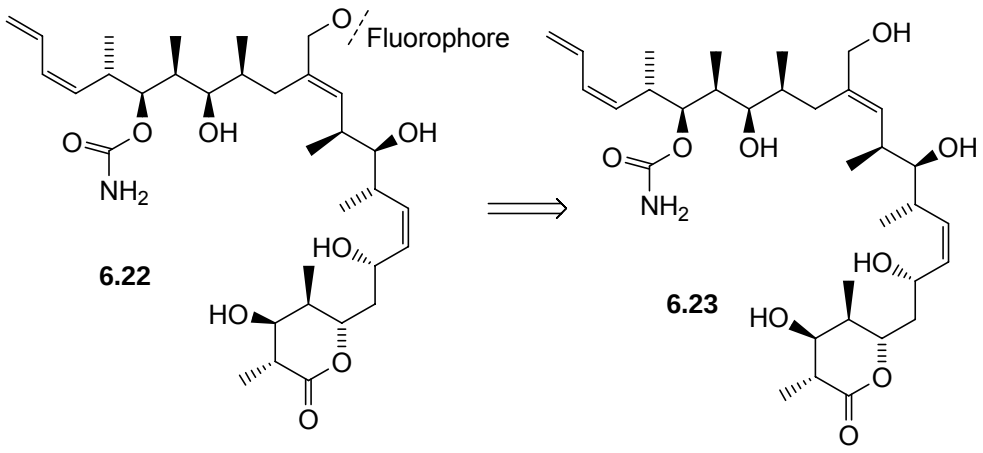

Scheme 6.9 Retrosynthesis of **6.22**

Coupling of a suitable fluorophore with the C14 hydroxy methyl discodermolide **6.23** will complete the synthesis. The retrosynthesis of **6.23** is shown in Scheme 6.10.

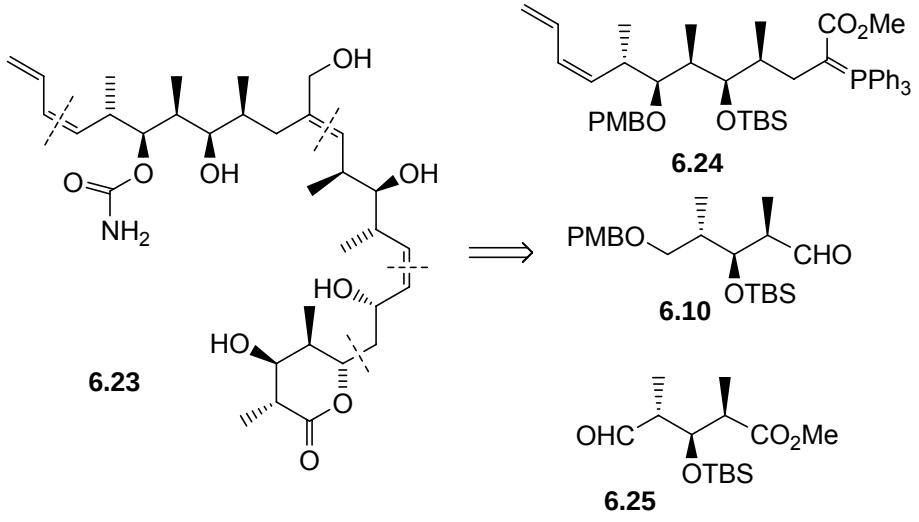

Scheme 6.10 Retrosynthesis of **6.23**

The synthesis adopts Smith's common precursor strategy, in which the three key fragments **6.24**, **6.10**, and **6.25** are all derived from the same precursor **6.9**. Compound **6.24** was coupled with **6.10** by using the Wittig protocol developed by Nicolaou in an epothilone synthesis.[12]

Evan's aldol reaction of **6.8** with **6.9** gave syn-aldol product **6.26**, in Scheme 6.2. Removal of the chiral auxiliary by LiOH in H_2O_2 gave the acid **6.27**, and methylation gave the methyl ester **6.28** (Scheme 6.11). Removal of the PMB protecting group by oxidation with DDQ, and oxidation of the resulting alcohol afforded the aldehyde **6.25**, as shown in Scheme 6.11.

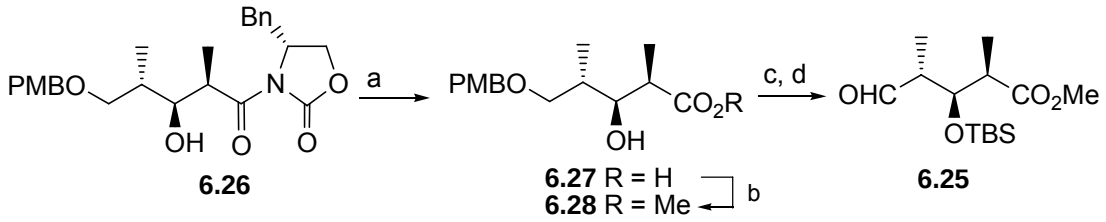

a) H_2O_2, LiOH, 96%; b) $TMSCH_2N_2$, 92%; c) TBSOTf, 91%; d) SO_3/Py, DMSO, 95%

Scheme 6.11 Synthesis of **6.25**

Beginning again with **6.26**, reductive removal of the chiral auxiliary, followed by selective protection of the primary hydroxyl group as TBS ether furnished **6.29** (Scheme 6.12). Formation of the PMP acetal with DDQ and selective opening of this acetal with DIBAL resulted in the primary alcohol **6.30**. The terminal diene unit was then introduced by the Paterson protocol to give **6.31**. Deprotection of TBS, followed by oxidation gave aldehyde **6.32**, which was used without purification in an Evans aldol condensation with **6.8** to afford aldol **6.33**. Protection of the secondary hydroxyl group as its TBS ether and reductive removal of the chiral auxiliary gave **6.34** (Scheme 6.12).

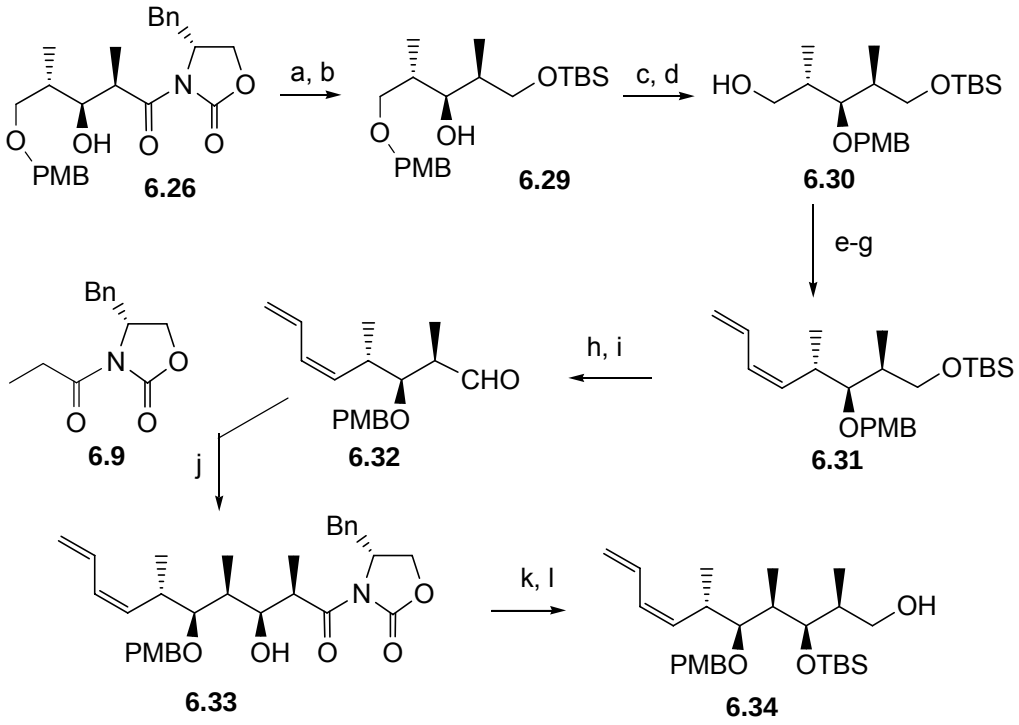

a) $LiBH_4$; 90%; b) TBSCl, imidazole, 92%; c) DDQ, 81%; d) DIBAL, 75%; e) SO_3/py, DMSO, 93%; f) 1-TMS allylbromide; g) KH, 87%; h) 10-CSA, 95%; i) SO_3/py, DMSO, 92% j) Bu_2BOTf, Et_3N, 86%; k) TBSOTf, 87%; l) $LiBH_4$, 91%

Scheme 6.12 Synthesis of **6.34**

Conversion of **6.34** to **6.35** was achieved through cyanide **6.36** (Scheme 6.13). An improved overall yield was achieved by tosylation of **6.34** to give the corresponding tosylate ester, which was easily converted to **6.36** in 98% yield by reaction with sodium cyanide. Reduction of **6.36** by DIBAL to the aldehyde, followed by reduction with $NaBH_4$ gave the corresponding alcohol, which was converted to iodide **6.35** (Scheme 6.13). Treatment of iodide **6.13** with molten PPh_3 generated the Wittig reagent **6.38**, as shown in Scheme 6.13. However, attempts to couple aldehyde **6.10** with ylide **6.24** prepared *in situ* from **6.38**, proved unsuccessful. Since ylide **6.24** decomposed during purification, little feedback was drawn from the reaction.

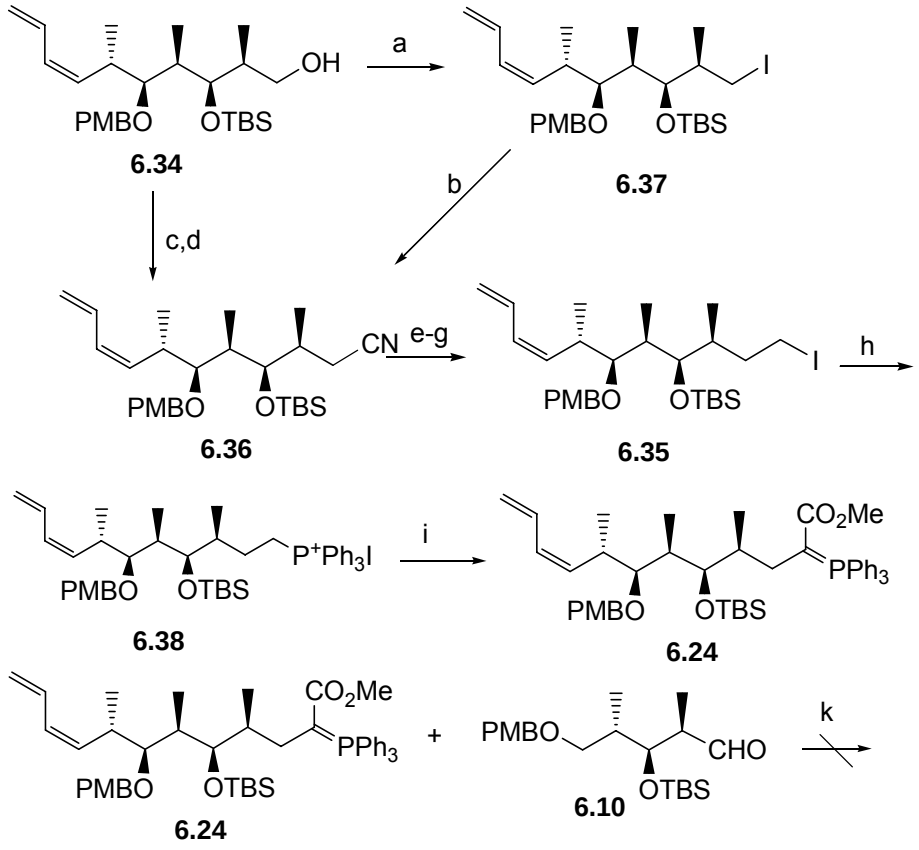

a) Ph_3P, I_2, 83%; b) KCN, 70%; c) TsCl, 95%; d) NaCN, 98%;e) DIBAL, 75%; f) $NaBH_4$, 92%; g) Ph_3P, I_2, 83%; h) Ph_3P, 95%; i) $ClCO_2Me$, BuLi; k) bezene, reflux

Scheme 6.13 Synthesis of **6.23**

To understand better the nature of this reaction, we turned to the model compound 2-phenylpropanal and its reaction with ylide **6.41** prepared from isopropyl triphenylphosphonium iodide (Scheme 6.14). The reaction of 2-phenylpropanal with **6.41** proceeded well, but coupling of aldehyde **6.10** with ylide **6.41** proved unsuccessful.

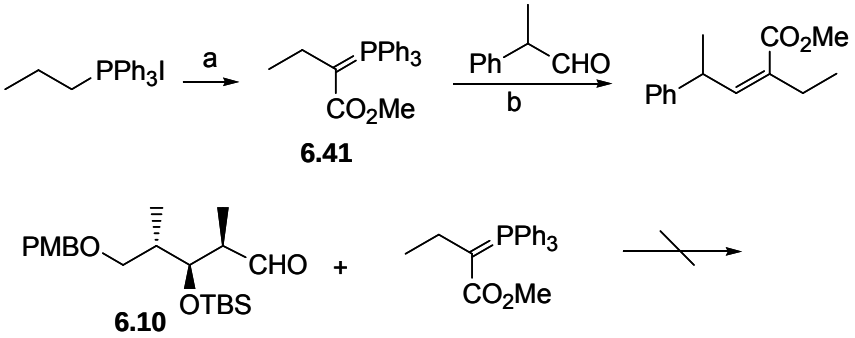

a) $ClCO_2Me$, BuLi; k) Bezene, reflux

Scheme 6.14 Model study of coupling of **6.24** with **6.10**

The decision was thus made to revise the synthetic pathway. The revised retrosynthesis is shown in Scheme 6.15. In the revised synthetic approach, the coupling of iodide **6.37** with vinyl iodide **6.42** was carried out by the Suzuki method. Iodide **6.37** was prepared as previously described (Scheme 6.15).

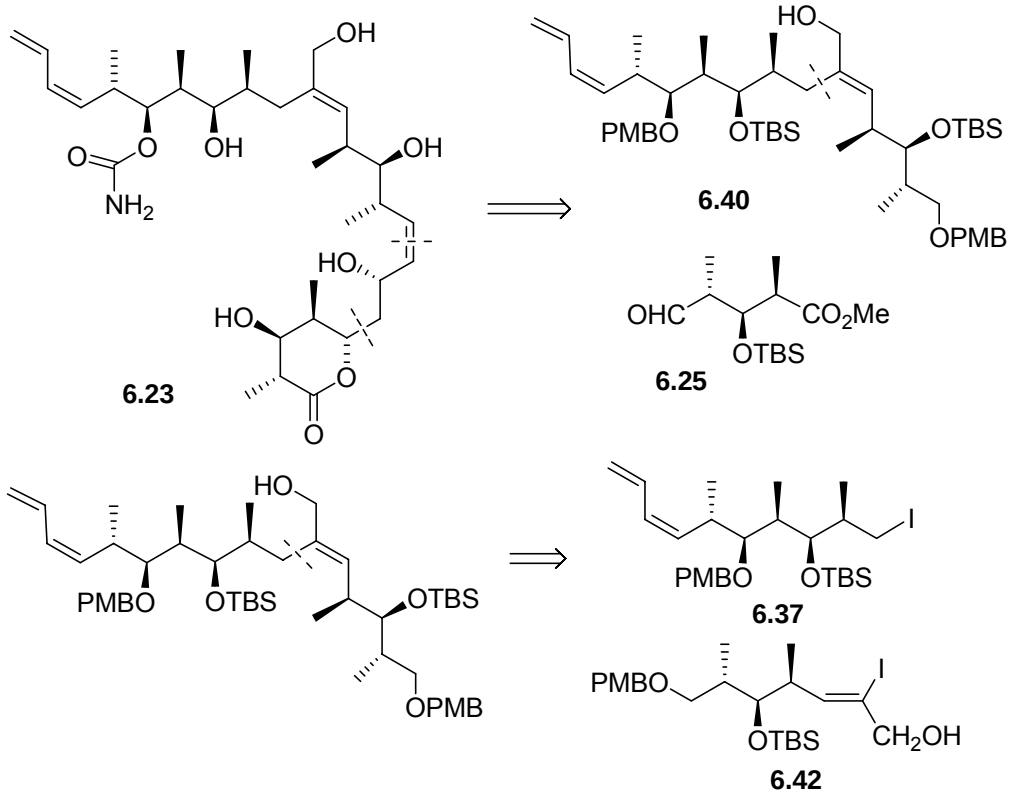

Scheme 6.15 Revised retrosynthesis of **6.23**

The vinyl iodide **6.42** can be prepared from alkyne ester **6.43**,[13] through radical hydrostannylation (Scheme 6.16).[14]

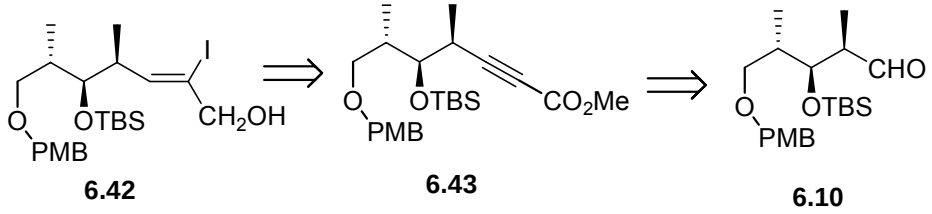

Scheme 6.16 Revised retrosynthesis of **6.42**

Aldehyde **6.10** was subjected to a Corey-Fuchs olefination[15] to obtain vinyl dibromide **6.44**.[16] Surprisingly, treatment of **6.44** with *n*-butyllithium followed by methyl chloroformate produced a complex mixture, instead of the desired alkyne ester **6.43** (Scheme 6.17). The model compound 2-phenylpropanal was successful converted to the corresponding alkyne ester following the same sequence. After extensive research in the literature, we found that other investigators had also encountered similar problems. The vinyl dibromide was converted to a vinyl anion, which is prone to a 1,5-silyl migration, producing by-products due to the 1,5 rearrangment.[17] The migration could be suppressed by the use of non-silyl protecting groups, such as the MOM group. Several other olefination reactions were also attempted, but unsuccessfully due to the instability of the iodide intermediates.

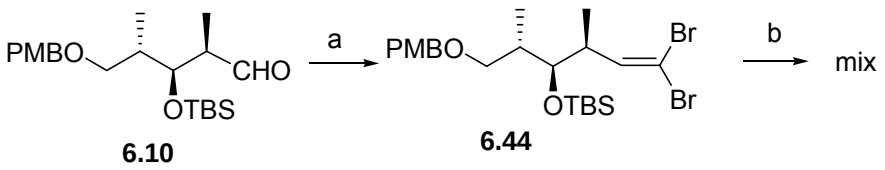

6.10 **6.44**

a) CBr_4, Ph_3P, 93%; b) BuLi, $ClCO_2Me$

Scheme 6.17 Synthesis of **6.43**

To circumvent this problem, a stepwise approach was adopted in which conversion of **6.10** to the α-bromo unsaturated ester **6.45** was followed by reduction to afford alcohol **6.46** (Scheme 6.18). Vinyl iodide **6.42** was then prepared via nickel-catalyzed bromine-iodine exchange, as shown in Scheme 6.18,[18] but it was obtained as a mixture with starting bromide, and this mixture could not be separated to give pure compound **6.42**.

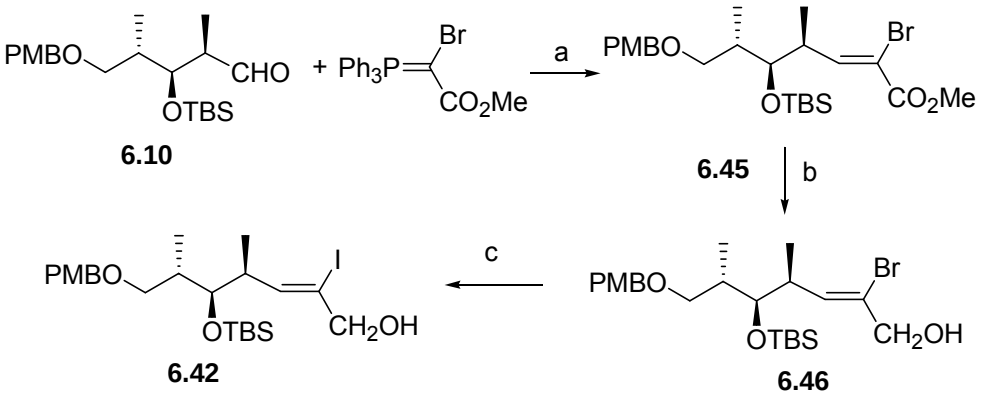

a) Toluene, 90 ^{o}C, 87%; b) DIBAL, 89%; c) Ni, ZnI_2, 67%

Scheme 6.18 Synthesis of **6.42**

Work to complete the total synthesis will be performed by other members of the Kingston group.

6.5 Experimental section

General Experimental Methods. All reagents and solvents received from commercial sources were used without further purification. ^{1}H and ^{13}C NMR spectra were obtained in $CDCl_3$ on Varian Unity or Varian Inova spectrometers at 400 MHz or a JEOL Eclipse spectrometer at 500 MHz. High-resolution FAB mass spectra were obtained on a JEOL HX-110 instrument. Compounds were purified by chromatography on silica gel using EtOAc/hexanes unless specified. Compounds (**6.2**-**6.5**, **6.7**-**6.19**, **6.25**-**6.34**, **6.37**, **6.44**-**6.46**) have all been prepared by other investigators.[6,7,9,10] These compounds were resynthesized as described below. All these compounds had NMR and mass spectra that matched the literature spectra, so these data are not reported here.

6.21a. At rt, a solution of **6.19** (22 mg, 0.033 mmol), DMAP (20 mg, 0.16 mmol), *m*-dimethylaminobenzoic acid (90 mg, 0.54 mmol) in DCM (2 mL) was treated with EDCI (20 mg, 0.10 mmol). After stirring overnight, the mixture was diluted with ether, quenched with water. The organic phase was separated, and the aqueous phase was extracted with ether. The combined organic layer was washed with water, brine, dried over Na_2SO_4, filtered and concentrated. Silica gel column chromatography provided **6.21a** (18 mg, 70%). ^{1}H NMR δ 7.42 (3H, m), 7.31-7.25 (1H, m), 6.94 (1H, br), 6.57 (1H, dt, *J* = 16.8, 7.2 Hz), 6.03 (1H, t, *J* = 6.8 Hz), 5.75 (1H, t, *J* = 10.0 Hz), 5.65-5.59 (1H, m), 5.36 (1H, t, *J* = 10.4 Hz), 5.22 (1H, d, *J* = 16.8 Hz), 5.13 (1H, d, *J* = 10.4 Hz), 4.96 (1H, d, *J* = 10.0 Hz), 4.80 (1H, dd, *J* = 12.8, 7.2 Hz), 4.73 (2H, m), 4.68 (2H, br s), 3.39 (1H, m), 3.32-3.29 (1H, m), 3.02-2.98 (1H, m), 2.98 (6 H, s), 2.74-2.70 (1H, m), 2.34-2.40 (1H, m), 2.09 (1H, dd, *J* = 12.8, 12.0 Hz), 1.89-1.82 (2H, m), 1.64-1.61 (1H, m), 1.61 (3H, s), 1.00-0.98 (6H, m), 0.92-0.87 (24H, m), 0.70 (3H, d, *J* = 6.4 Hz), 0.10-0.05 (12H, m); ^{13}C NMR δ 157.4, 137.5, 133.7, 132.8, 132.2, 131.3, 130.7, 129.9, 129.3, 129.2, 123.2, 118.2, 81.0, 78.9, 61.4, 38.3, 37.4, 37.1, 36.4, 35.0, 34.6, 26.4, 23.0, 19.2, 18.72, 18.66, 18.2, 17.7, 13.9, 10.3.

6.21b. At rt, a solution of **6.19** (20 mg, 0.03 mmol), DMAP (20 mg, 0.16 mmol), *m*-Teocaminobenzoic acid (20 mg) in DCM (3 mL) was treated with EDCI (30 mg, 0.15 mmol). After stirring overnight, the mixture was diluted with ether, quenched with water. The organic phase was separated, and the aqueous phase was extracted with ether. The combined organic layer was washed with water, brine, dried over Na_2SO_4, filtered and concentrated. The crude product was used directly in the next step. The crude product was dissolved in THF and treated with TBAF. After 2 days at rt, the mixture was

quenched with water, brine, dried over Na_2SO_4, filtered and concentrated. Silica gel column chromatography provided **6.21b** (6 mg, 50%), which was gradually decomposed under the light. ^{1}H NMR δ 7.42 (3H, m), 7.31-7.25 (1H, m), 7.06 (1H, br), 6.59 (1H, dt, *J* = 16.8, 7.2 Hz), 6.03 (1H, t, *J* = 6.8 Hz), 5.76 (1H, t, *J* = 10.0 Hz), 5.63-5.55 (1H, m), 5.36 (1H, t, *J* = 10.4 Hz), 5.22 (1H, d, *J* = 16.8 Hz), 5.13 (1H, d, *J* = 10.4 Hz), 4.96 (1H, d, *J* = 10.0 Hz), 4.83 (1H, dd, *J* = 12.8, 7.2 Hz), 4.71 (2H, m), 4.65 (2H, br s), 3.43 (1H, m), 3.32-3.29 (1H, dd, *J* = 7.5, 3.0 Hz), 3.03-2.92 (1H, m), 2.74-2.64 (1H, m), 2.42-2.31 (1H, m), 2.13 (1H, app t, *J* = 12.0 Hz), 1.93-1.79 (2H, m), 1.64-1.61 (1H, m), 1.61 (3H, s), 1.00-0.98 (6H, m), 0.92-0.87 (24H, m), 0.70 (3H, d, *J* = 6.4 Hz), 0.10-0.05 (12H, m); ^{13}C NMR δ 157.4, 138.5, 137.1, 133.8, 133.0, 132.3, 131.4, 130.6, 130.0, 129.4, 129.3, 124.8, 123.2, 118.2, 81.1, 79.0, 61.8, 38.4, 37.6, 37.0, 36.5, 35.3, 34.7, 26.4, 23.0, 19.2, 18.72, 18.66, 18.2, 17.7, 13.9, 10.3.

Aldol (6.33). At 0 ^{o}C, *n*-Bu_2BOTf (1M, 2.5 mL) was added to **6.9** (0.55 g, 2.4 mmol) in DCM (10 mL), followed by NEt_3 (0.5 mL, 3.7 mmol). The mixture was stirred for 0.5 h before cooling to -78 ^{o}C. A solution of **6.32** (0.59 g, 2 mmol) in DCM (6 mL) was added. After 2 h at -78 ^{o}C and 2 h at 0 ^{o}C, the mixture was quenched with water and 30% H_2O_2 in MeOH and was stirred overnight at rt The organic layer was separated and the aqueous phase was extracted with EtOAc. The combined organic layer was washed with $NaHCO_3$, water, brine, dried over Na_2SO_4, filtered and concentrated. Silica gel column chromatography provided oil **6.33** (0.9 g, 87%). ^{1}H NMR δ 7.35-7.26 (4H, m), 7.23-7.19 (3H, m), 6.82 (2H, d, *J* = 11.6 Hz), 6.67 (1H, dt, *J* = 16.8, 10.8 Hz), 6.06 (1H, t, *J* = 10.8 Hz), 5.51 (1H, t, *J* = 10.4 Hz), 5.22 (1H, d, *J* = 16.8 Hz), 5.14 (1H, d, *J* = 10.0 Hz), 4.69 (1H, d, *J* = 7.2 Hz), 4.58-4.64 (1H, m), 4.37 (1H, d, *J* = 7.2 Hz), 4.16 (2H, m), 3.99 (1H,

m), 3.84 (1H, dd, *J* = 6.4, 4.4 Hz), 3.77 (3H, s), 3.36 (1H, dd, *J* = 7.2, 3.6 Hz), 3.21 (2H, dd, *J* = 13.2, 3.6 Hz), 3.04 (1H, m), 2.75 (1H, dd, *J* = 13.2, 9.6 Hz), 1.80 (1H, m), 1.29 (3H, d, *J* = 7.2 Hz), 1.03 (3H, d, *J* = 7.2 Hz), 0.98 (3H, d, *J* = 6.8 Hz); ^{13}CNMR δ 177.1, 159.2, 152.9, 135.8, 135.3, 132.8, 131.0, 129.7, 129.6, 129.2, 127.7, 118.0, 113.9, 86.5, 74.6, 74.1, 66.2, 55.5, 55.2, 40.8, 38.0, 37.9, 36.0, 18.4, 13.5, 8.4; HRFABMS: found *m/z* 522.2856; Calcd. for $C_{31}H_{40}NO_6$ $(M+H)^+$ *m/z* 522.28265, Δ = 5.5 ppm.

TBS derivative of (6.33). At -20 °C, a solution of **6.33** (0.8 g, 1.5 mmol) and 2,6-lutidine (0.5 mL, 4.3 mmol) in DCM (6 mL) was treated with TBSOTf (0.8 mL, 3.1 mmol). After 4 h at 0 °C, the reaction was diluted with ether was washed with $NaHSO_4$, water, brine, dried over Na_2SO_4, filtered and concentrated. Silica gel column chromatography provided the TBS derivative of **6.33** (0.9 g). ^{1}H NMR δ 7.32-7.26 (4H, m), 7.23-7.18 (3H, m), 6.82 (2H, dd, *J* = 11.2, 2.4 Hz), 6.68 (1H, dt, *J* = 16.4, 10.4 Hz), 5.97 (1H, t, *J* = 11.2 Hz), 5.60 (1H, t, *J* = 10.4 Hz), 5.17 (1H, d, *J* = 8.8 Hz), 5.14 (1H, s), 4.48-4.54 (3H, m), 3.97-4.09 (4H, m), 3.79 (3H, s), 3.36 (1H, dd, *J* = 7.6, 2.8 Hz), 3.20 (1H, dd, *J* = 12.8, 3.2 Hz), 3.00 (1H, m), 2.69 (1H, dd, *J* = 13.2, 10.0 Hz), 1.60 (1H, m), 1.23 (3H, d, *J* = 6.8 Hz), 1.11 (3H, d, *J* = 7.2 Hz), 1.02 (3H, d, *J* = 7.2 Hz), 0.96 (9H, s), 0.15 (3H, s), 0.12 (3H, s); ^{13}C NMR δ 175.9, 159.2, 153.1, 135.6, 134.5, 133.3, 131.5, 129.7, 129.6, 129.2, 129.1, 127.5, 117.1, 113.8, 83.1, 77.5, 74.7, 73.8, 66.1, 55.7, 55.5, 43.3, 42.2, 37.9, 35.8, 26.5, 19.4, 18.8, 15.2, 10.5, -3.2, -3.4; HRFABMS: found *m/z* 636.3720; Calcd. for $C_{37}H_{54}NO_6Si$ $(M+H)^+$ *m/z* 636.37396, Δ = 3.1 ppm.

Alcohol (6.34). At -30 °C, $LiBH_4$ (2M, 1.5 mL) was added to a solution of the above TBS ether (0.9 g 1.4 mmol) in THF (18 mL). After 1 h at 0 °C and overnight at rt, the mixture was diluted with ether, quenched with NaOH, and stirred at rt for 3 h. The layer was

separated and the aqueous phase was extracted with EtOAc. The combined organic layer was washed with water, brine, dried over Na_2SO_4, filtered and concentrated. Silica gel column chromatography provided oil **6.34** (0.41 g, 85%). ^{1}H NMR δ 7.27 (2H, d, *J* = 9.6 Hz), 6.82 (2H, dd, *J* = 7.2, 2.4 Hz), 6.62 (1H, dt, *J* = 16.4, 10.4 Hz), 6.03 (1H, t, *J* = 10.8 Hz), 5.57 (1H, t, *J* = 10.4 Hz), 5.20 (1H, d, *J* = 16.8 Hz), 5.12 (1H, d, *J* = 10.0 Hz), 4.55 (1H, d, *J* = 10.4 Hz), 4.46 (1H, d, *J* = 10.8 Hz), 3.80 (3H, s), 3.70 (1H, t, *J* = 4.0 Hz), 3.51-3.56 (1H, m), 3.38-3.43 (1H, m), 3.20 (1H, dd, *J* = 6.4, 4.4 Hz), 3.00 (1H, m), 1.78-1.87 (2H, m), 1.63 (1H, brs), 1.08 (3H, d, *J* = 6.8 Hz), 1.02 (3H, d, *J* = 7.2 Hz), 0.93 (9H, s), 0.83 (3H, d, *J* = 7.6 Hz), 0.10 (6H, s); ^{13}C NMR δ 159.2, 135.0, 132.5, 131.3, 129.4, 129.3, 117.8, 113.8, 84.4, 75.0, 73.7, 66.1, 55.4, 40.6, 40.0, 35.8, 26.4, 18.9, 18.6, 12.4, 11.2, -3.4, -3.6; HRFABMS: found *m/z* 463.3266; Calcd. for $C_{27}H_{47}O_4Si$ $(M+H)^+$ *m/z* 463.3244, Δ = 4.8 ppm.

Nitrile (6.36). At 0 ^{o}C, a solution of alcohol **6.34** (0.41 g, 0.89 mmol) and DMAP (40 mg, 0.33 mmol) in DCM (10 mL) was treated with Et_3N (0.3 mL, 2.2 mmol) and TsCl (0.27 g, 0.97 mmol). After 1 day at rt, the mixture was diluted with ether washed with $NaHCO_3$, water, brine, dried over Na_2SO_4, filtered and concentrated. Silica gel column chromatography provided **6.34** tosylate (0.53 g, 97%). HRFABMS: found *m/z* 615.31818; Calcd. for $C_{34}H_{52}NO_6Si$ $(M+H)^+$ *m/z* 615.3176, Δ = 1.0 ppm. At 80 ^{o}C, a solution of the above tosylate (530 mg, 0.86 mmol) in DMSO (9 mL) was treated with NaCN (0.5 g, 10 mmol) and NaI (120 mg, 0.8 mmol). After 1 day at 80 ^{o}C, the mixture was cooled to rt, diluted with EtOAc and quenched by water. The layers were separated and the aqueous phase was extracted with EtOAc. The combined organic layer was washed with water, brine, dried over Na_2SO_4, filtered and concentrated. Silica gel column

chromatography provided oil **6.36** (0.37 g, 94%). ^{1}H NMR δ 7.27 (2H, d, *J* = 4.8 Hz), 6.82 (2H, dd, *J* = 10.8, 2.4 Hz), 6.63 (1H, dt, *J* = 16.8, 10.4 Hz), 6.05 (1H, t, *J* = 10.8 Hz), 5.53 (1H, t, *J* = 10.4 Hz), 5.23 (1H, d, *J* = 8.8 Hz), 5.15 (1H, d, *J* = 10.0 Hz), 4.58 (1H, d, *J* = 10.8 Hz), 4.41 (1H, d, *J* = 10.8 Hz), 3.81 (3H, s), 3.48 (1H, t, *J* = 4.4 Hz), 3.19 (1H, t, *J* = 5.2 Hz), 2.96-3.01 (1H, m), 2.19 (1H, dd, *J* = 8.4, 5.6 Hz), 2.19 (1H, dd, *J* = 8.4, 8.8 Hz), 1.95-2.00 (1H, m), 1.73-1.77 (1H, m), 1.06 (3H, d, *J* = 6.8 Hz), 0.983 (3H, d, *J* = 7.6 Hz), 0.98 (3H, d, *J* = 7.2 Hz), 0.92 (9H, s), 0.09 (3H, s), 0.06 (3H, s); ^{13}C NMR δ 159.3, 134.7, 132.4, 131.0, 129.6, 129.5, 119.8, 118.1, 113.9, 83.8, 74.7, 74.5, 55.4, 39.8, 35.7, 35.6, 26.3, 22.3, 18.7, 18.6, 14.5, 11.2, -3.3, -3.5; HRFABMS: found *m/z* 472.32581; Calcd. for $C_{28}H_{46}NO_3Si$ $(M+H)^+$ *m/z* 472.3247, Δ = 2.3 ppm.

Iodide (6.35). At -78 ^{o}C, a solution of nitrile **6.36** (0.35 g, 0.74 mmol) in toluene (4 mL) was treated with DIBAL (1M, 1.2 mL). After 2 h, the reaction was quenched with MeOH and aq. Rochelle's salt. After 3 h at rt, the layers were separated and the aqueous phase was extracted with Et_2O. The combined organic phase was washed with $NaHCO_3$, water, brine, dried over Na_2SO_4, filtered and concentrated. Silica gel column chromatography provided the oil aldehyde (0.33 g, 97%). HRFABMS: found *m/z* 477.34360; Calcd. for $C_{28}H_{49}NO_4Si$ $(M+H)^+$ *m/z* 477.3400, Δ = 7.5 ppm.

Compounds **6.35, 6.45** and **6.46** were prepared as described in the literature.[6,7]

References:

1. Stryer, L. Fluorescence energy transfer as a spectroscopic ruler. *Ann. Rev. Biochem.* **1978,** *47*, 819-846.

2. Souto, A. A.; Acuna, A. U.; Andrea, J. M.; Barasoain, I.; Abal, M.; Amat-Guerri, F. New fluorescent water-soluble taxol derivatives. *Angew. Chem., Int. Ed. Engl.* **1995,** *34*, 2710-2712.

3. Han, Y.; Malak, H.; Chaudhary, A. G.; Chordia, M. D.; Kingston, D. G. I.; Bane, S. Distances between the paclitaxel, colchicine, and exchangeable GTP binding sites on tubulin. *Biochemistry* **1998,** *37*, 6636-6644.

4. Han, Y.; Chaudhary, A. G.; Chordia, M. D.; Sackett, D. L.; Perez-Ramirez, B.; Kingston, D. G. I.; Bane, S. Interaction of a fluorescent derivative of paclitaxel (taxol) with microtubules and tubulin-colchicine. *Biochemistry* **1996,** *35*, 14173-14183.

5. Li, Y.; Poliks, B.; Cegelski, L.; Poliks, M.; Gryczynski, Z.; Piszczek, G.; Jagtap, P. G.; Studelska, D. R.; Kingston, D. G. I.; Schaefer, J.; Bane, S. Conformation of microtubule-bound paclitaxel determined by fluorescence spectroscopy and REDOR NMR. *Biochemistry* **2000,** *39*, 281-291.

6. Smith III, A. B.; Beauchamp, T. J.; LaMarche, M. J.; Kaufman, M. D.; Qiu, Y.; Arimoto, H.; Jones, D. R.; Kobayashi, K. Evolution of a gram-scale synthesis of (+)-discodermolide *J. Am. Chem. Soc.* **2000,** *122*, 8654-8664.

7. Smith III, A. B.; Qiu, Y.; Jones, D. R.; Kobayashi, K. Total synthesis of (-)-discodermolide. *J. Am. Chem. Soc.* **1995,** *117*, 12011-12012.

8. Smith III, A. B.; Kaufman, M. D.; Beauchamp, T. J.; LaMarche, M. J.; Arimoto, H. Gram-scale synthesis of (+)-discodermolide. *Org. Lett.* **1999,** *1*, 1823-1826.

9. Mickel, S. J.; Sedelmeier, G. H.; Niederer, D.; Schuerch, F.; Seger, M.; Schreiner, K.; Daeffler, R.; Osmani, A.; Bixel, D.; Loiseleur, O.; Cercus, J.; Stettler, H.;

Schaer, K.; Gamboni, R.; Bach, A.; Chen, G. P.; Chen, W.; Geng, P.; Lee, G. T.; Loeser, E.; McKenna, J.; Kinder, F. R.; Konigsberger, K.; Prasad, K.; Ramsey, T. M.; Reel, N.; Repic, O.; Rogers, L.; Shieh, W. C.; Wang, R. M.; Waykole, L.; Xue, S.; Florence, G.; Paterson, I. Large-scale synthesis of the anti-cancer marine natural product (+)-discodermolide. Part 4: Preparation of fragment C_7-C_{24}. *Org. Process Res. Dev.* **2004,** *8*, 113-121.

10. Paterson, I.; Florence, G. J.; Gerlach, K.; Scott, J. P.; Sereinig, N. A practical synthesis of (+)-discodermolide and analogues: Fragment union by complex aldol reactions. *J. Am. Chem. Soc.* **2001,** *123*, 9535-9544.

11. Smith III, A. B.; Rucker, P. V.; Brouard, I.; Freeze, B. S.; Xia, S.; Horwitz, S. B. Design, synthesis, and biological evaluation of potent discodermolide fluorescent and photoaffinity molecular probes *Org. Lett.* **2005,** *7*, 5199 -5202.

12. Nicolaou, K. C.; Ninkovic, S.; Sarabia, F.; Vourloumis, D.; He, Y.; Vallberg, H.; Finlay, M. R. V.; Yang, Z. Total syntheses of epothilones A and B via a macrolactonization-based strategy. *J. Am. Chem. Soc.* **1997,** *119*, 7974-7991.

13. Organ, M. G.; Bilokin, Y. V.; Bratovanov, S. Approach toward the total synthesis of orevactaene. 2. Convergent and stereoselective synthesis of the C18-C31 domain of orevactaene. Evidence for the relative configuration of the side chain. *J. Org. Chem.* **2002,** *67*, 5176 -5183.

14. Tatsuta, K.; Yamaguchi, T. The first stereoselective total synthesis of antiviral antibiotic, xanthocillin X dimethylether and its stereoisomer. *Tetrahedron Lett.* **2005,** *46*, 5017-5020.

15. Corey, E. J.; Fuchs, P. L. A synthesis method for the formyl to ethynyl conversion. *Tetrahedron Lett.* **1972,** *36*, 3769-3772.

16. Arefolov, A.; Panek, J. S. Crotylsilane reagents in the synthesis of complex polyketide natural products: Total synthesis of (+)-discodermolide *J. Am. Chem. Soc.* **2005,** *127*, 5596 -5603.

17. Marumoto, S.; Kuwajima, I. Regiochemically and stereochemically defined synthesis of allylsilanes. *J. Am. Chem. Soc.* **1993,** *115*, 9021-9024.

18. Takagi, K.; Hayama, N.; Inokawa, S. Synthesis of vinyl iodides from vinyl bromides and potassium iodide by means of nickel catalyst. *Chem. Lett.* **1978,** *7*, 1435-1436.

19. Shaw, S. J.; Sundermann, K. F.; Burlingame, M. A.; Myles, D. C.; Freeze, B. S.; Xian, M.; Brouard, I.; III, S. A. B. Toward understanding how the lactone moiety of discodermolide affects activity. *J. Am. Chem. Soc.* **2005,** *127*, 6532-6533.

Chapter 7 Approaches to the synthesis of isotopically labeled discodermolide analogs for REDOR NMR and bridged discodermolide analogs for bioevaluation

7.1 Design of isotopically labeled discodermolide analogs

Compared to fluorescent spectroscopic studies on discodermolide analogs, a study of isotopically labeled discodermolide analogs bound to microtubules could provide direct information of the conformation of the discodermolide on the tubulin complex. It has been suggested that discodermolide adopts a U-shaped conformation to minimize the strain and steric interactions, as shown in Figure 5.1.[1] To examine this hypothesis, it is important to determine the "head-tail"; also "head-middle" distance, is important. Isotopically labeled discodermolide derivative **7.2** was designed to determine the "head-middle" distance (Figure 7.1) and compound **7.3** was designed to determine the "head-tail" distance. Schemes 7.1 and 7.2 show the restrosynthesis of compounds **7.2** and **7.3**, respectively. Smith's approach[2] to these intermediates was selected because it is highly convergent.

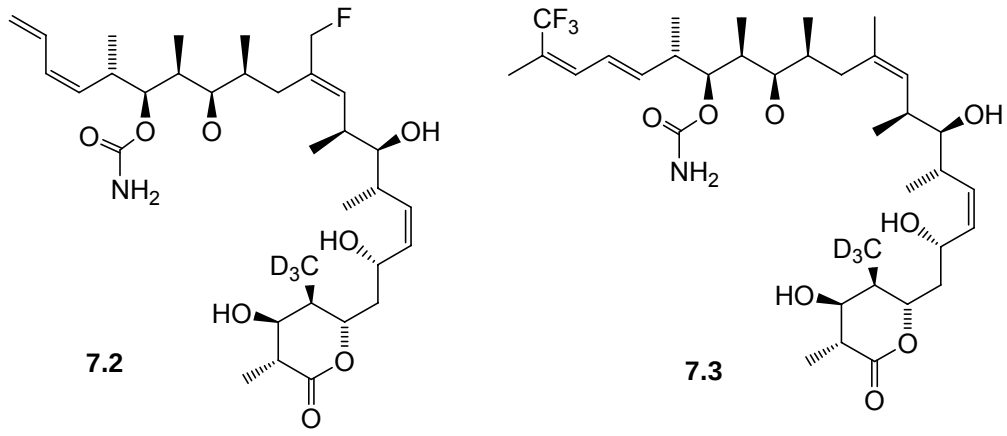

Fig. 7.1 Isotopically labeled discodermolide analogs

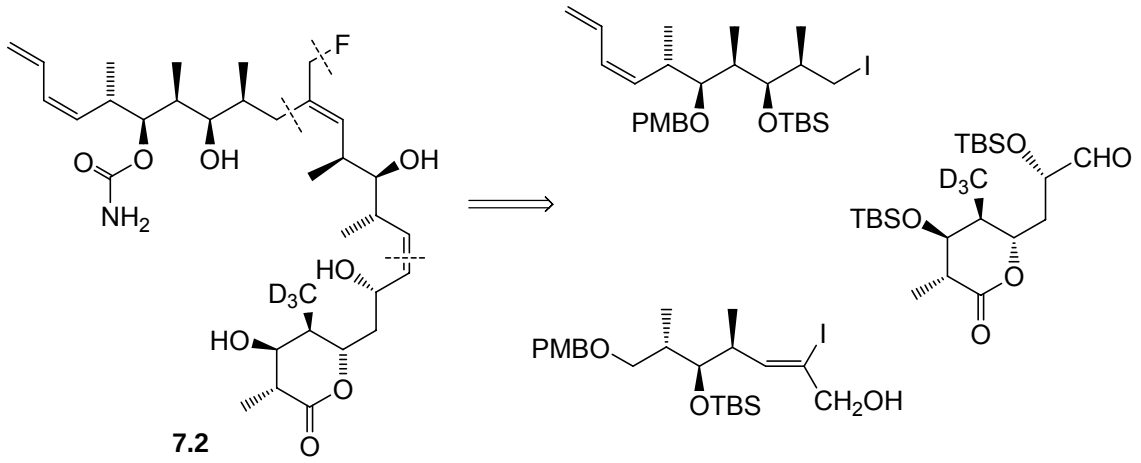

Scheme 7.1 Retrosynthesis of **7.2**

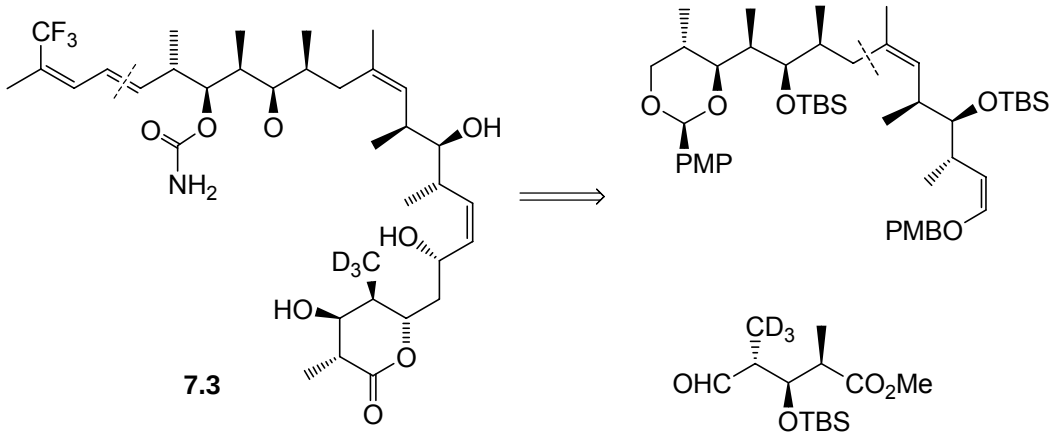

Scheme 7.2 Retrosynthesis of **7.3**

The synthesis of **7.2** started from the commercially available ester 1,3-propanediol, which was protected as its mono benzyl ether by reaction with benzyl chloride. Oxidation of the benzyl derivative **7.4** with Jones' reagent, followed by oxalyl chloride gave the corresponding acid chloride **7.5**. Acid chloride **7.5** was then coupled with (*R*)-benzyloxazolidinone to give alkyl-(*R*)-benzyl oxazolidinone **7.6**. It was reported that the methylation of this long chain alkyl-(*R*)-oxazolidinone gave good stereoselectivity in the epothilone synthesis.[3] Stereoselective methylation of the resulting

oxazolidinone was unsatisfactory, since methyl iodide gave a low yield while methyl triflate gave a higher yield but showed poor selectivity, as shown in Scheme 7.3.

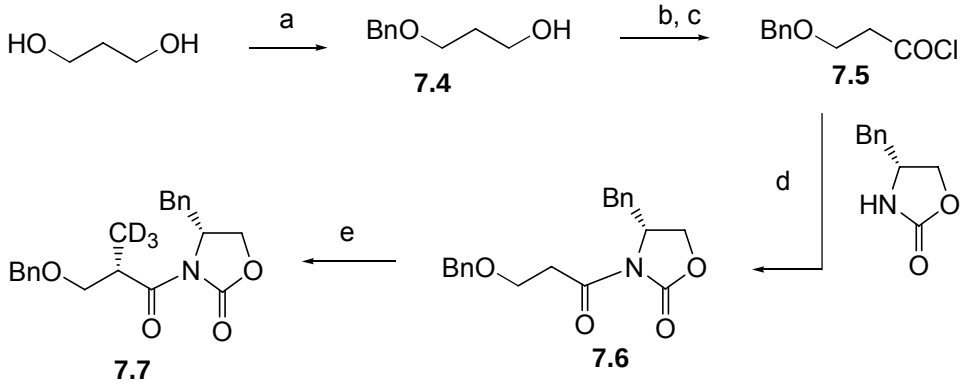

a) BnCl, NaH, 56%; b) Jone's reagent, 60%; c) oxazyl chloride; d) BuLi, 78%
e) CD_3I, NaH, 30%; f) CD_3OTf, NaH, 60% d.e.

Scheme 7.3 Synthesis of **7.7**

An alternative synthetic route was thus adopted. The synthesis started from the commercially available 3-d_3-propanic acid, which was converted to 3-d_3-propanoyl-(*R*)-benzyloxazolidinone **7.8** by reaction with commercially available (*R*)-oxazolidinone. Stereoselective conversion of **7.8** to **7.7** was carried out by the Evan's method[4] with a yield of 94%. Oxidative removal of the chiral auxiliary of **7.8** with H_2O_2, followed by amide formation gave the Weinreb amide **7.10** (Scheme 7.4).

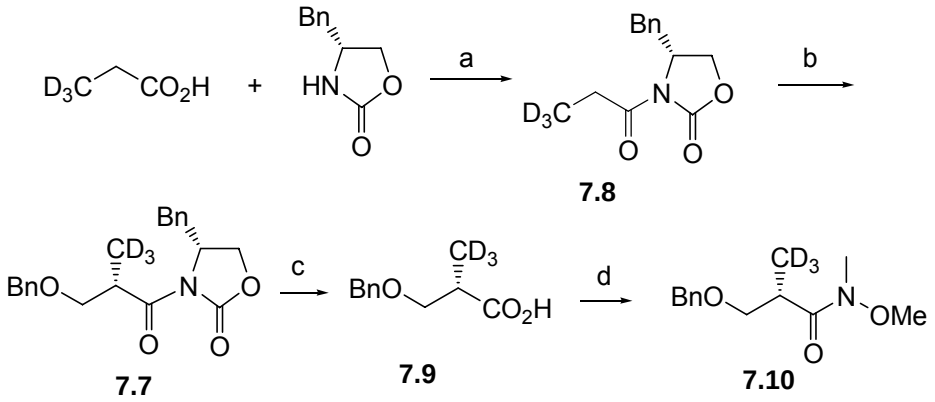

a) Me_3CCOCl, DMAP, Et_3N, 78%; b) $BnOCH_2Cl$, 94%; c) H_2O_2, LiOH, 89%;
d) EDCI, DMAP, 93%

Scheme 7.4 Synthesis of **7.10**

Reduction of the amide **7.10** with LAH, followed by Swern oxidation gave the corresponding aldehyde **7.12**. Aldehyde **7.12** was subjected to Evans aldol *syn*-selective conditions with propionyl-(*R*)-benzyloxazolidinone **6.9**, prepared from (*R*)-benzyloxazolidinone, using dibutylboron triflate as the reagent. Oxidative removal of the chiral auxiliary of **7.13** by H_2O_2, followed by methylation, gave the methyl ester **7.14** as shown in Scheme 7.5.

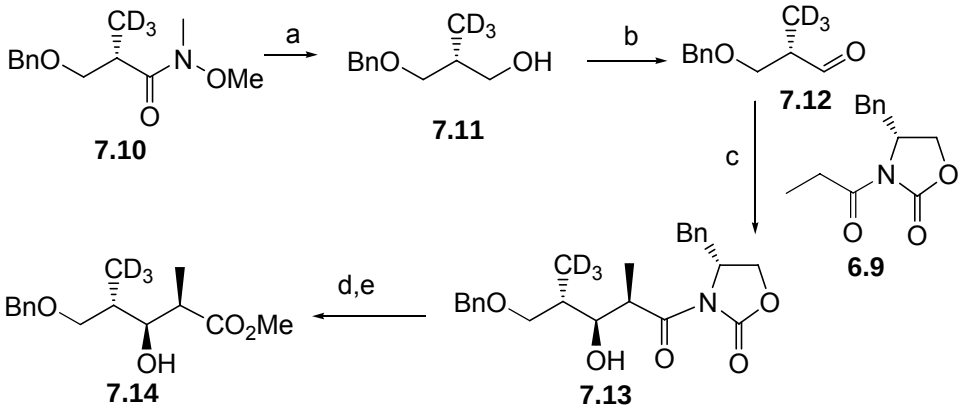

a) LAH, 89%; b) SO_3/py, DMSO, 98%; c) Bu_2BOTf, 89%; d) H_2O_2, LiOH, 96%; e) $TMSNNCH_2$, 89%

Scheme 7.5 Synthesis of **7.14**

The known compound **7.15** was used to test the designed synthetic route. Reductive deprotection of the *p*-methoxybenzyl (PMB) protecting group of **7.15** led to alcohol **7.16**, which was prone to form cyclic compound **7.19**. Oxidation of the alcohol **7.16** gave aldehyde **7.17**. The conversion of **7.17** to **7.18** by Smith protocol[2] proved to be difficult, and the yield was only 20% as shown in Scheme 7.6.

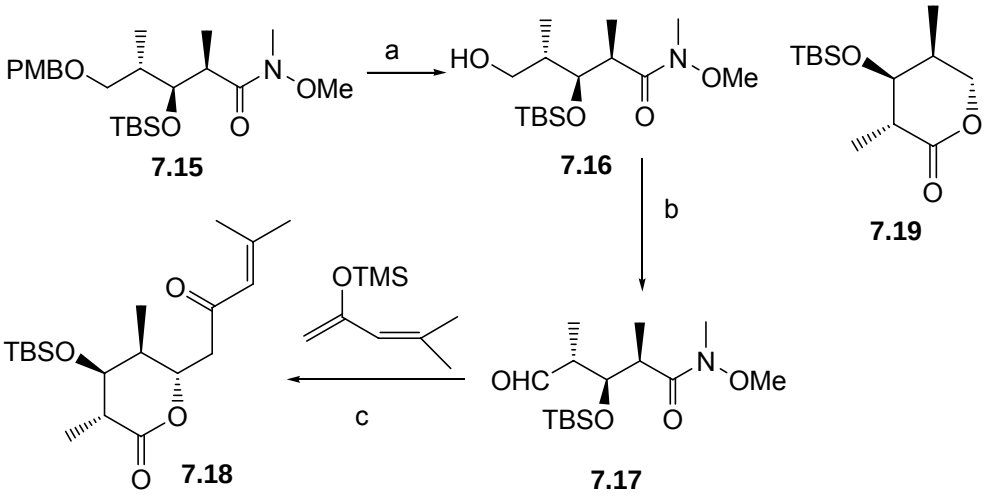

a) $Pd(OH)_2$, H_2, 90%; b) SO_3/py, DMSO, 95%; c) $TiCl_4$, 20%

Scheme 7.6 Synthesis of **7.17**

An alternative approach devised by Paterson[5] was adopted to circumvent this problem. The retrosynthesis is shown in Scheme 7.7.

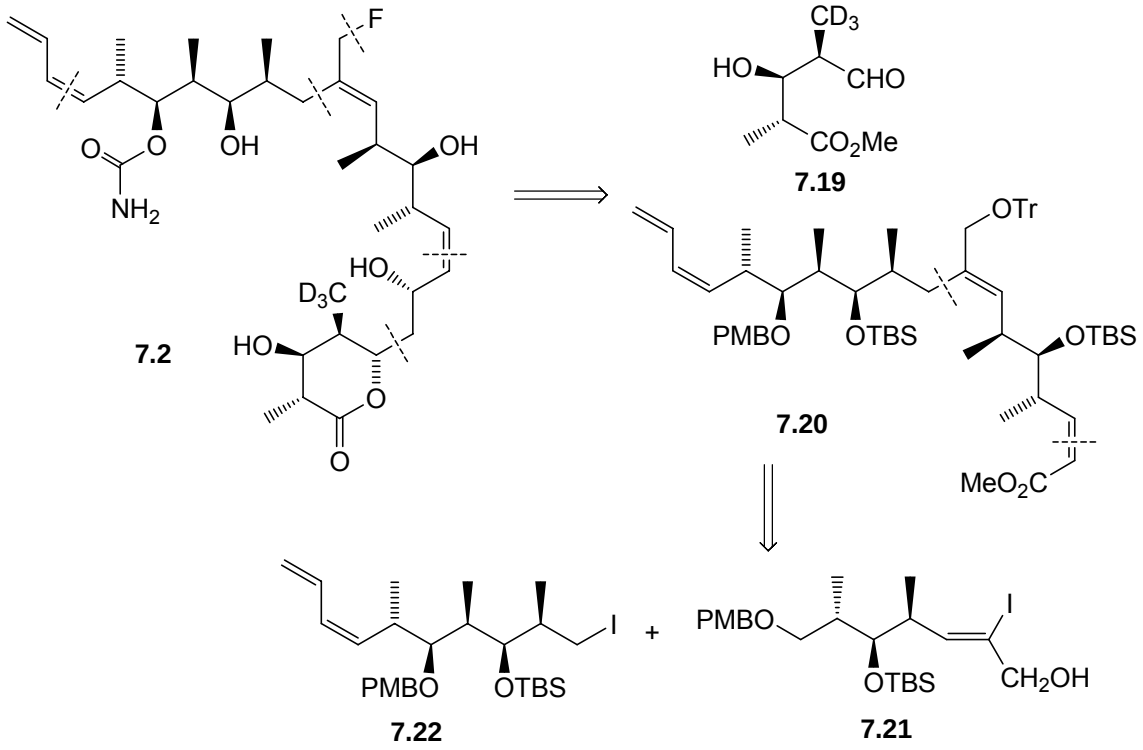

Scheme 7.7 Revised retrosynthesis of **7.2**

The synthesis of **7.3** involves the coupling of **7.19** and **7.20**. Deuterated compound **7.19** can be synthesized from previously prepared methyl ester **7.17** through a sequence of debenzylation and oxidation. Intermediate **7.20** can be synthesized by coupling of **7.21** with **7.22**. Synthesis of intermediate **7.21** has been described in Chapter 6.

The synthesis of intermediate **7.22** started from **6.3**, described in chapter 6. Reduction with $LiBH_4$, followed by selective protection as its TBS ether generated **7.23**. Oxidation of **7.23** with DDQ gave acetal **7.24** and selective opening of the acetal ring gave **7.25**. Swern oxidation of **7.25** gave aldehyde **7.26**. Formation of the terminal diene unit was thus carried out by the Paterson protocol[6] as described in Chapter 6, to give **7.27**. Deprotection of the TBS group in **7.27** in acid media, followed by Swern oxidation, gave aldehyde **7.28** (Scheme 7.8).

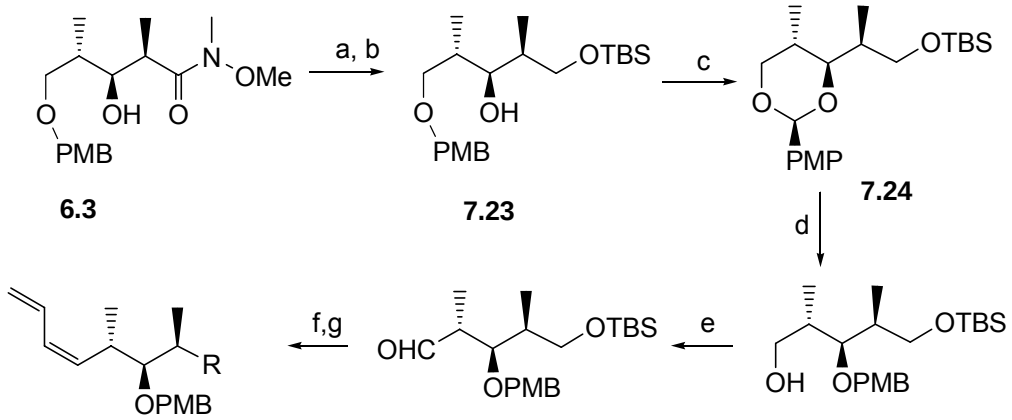

a) $LiBH_4$, THF, 90%; b) TBSCl, imidazole, 95%; c) DDQ, 81%; d) DIBAL, 75%; e) SO_3/py, 95%; f) $CrCl_2$, 1-TMS allylbromide, g) KH, 90%; h) SO_3/py

Scheme 7.8 Synthesis of **7.28**

Coupling of **7.28** with **6.9** by means of Evans aldol syn-addition[2] afforded **7.29**, which was converted to alcohol **7.31** by a sequence of TBS protection and reduction as

shown in Scheme 7.9. Iodination of alcohol **7.31** gave **7.22**, which was light-sensitive and was thus made as it was needed.

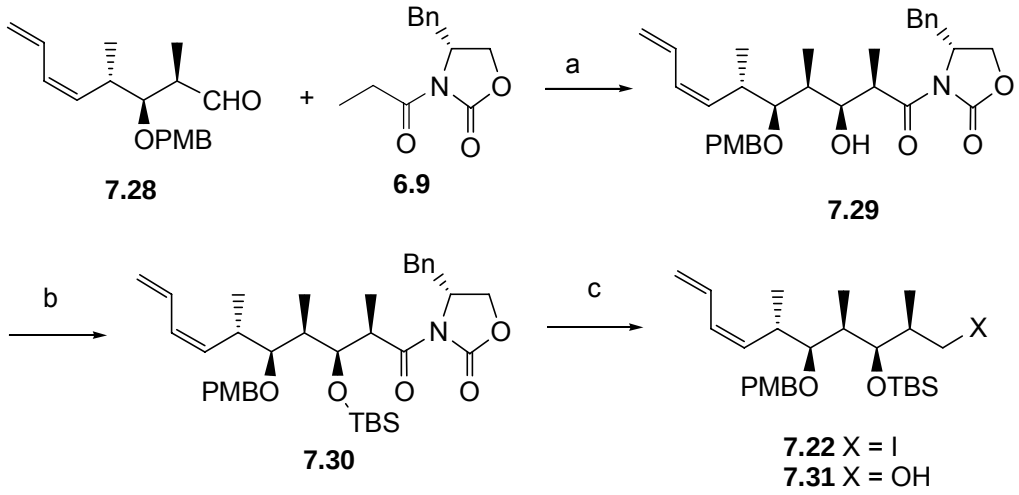

a) Bu_2BOTf, 85%; b) TBSOTf, 2,6-lutidine, 93%; c) $LiBH_4$, THF, 92%

Scheme 7.9 Synthesis of **7.31**

7.2 Summary of the synthesis of isotopically labeled discodermolide derivatives

This investigation has succeeded in preparing the key intermediates **7.19**, **7.21** and **7.22** required for the synthesis of the doubly labeled discodermolide analog **7.2** for REDOR NMR studies. The completion of the synthesis of **7.2** will be carried out by Dr. Q. H. Chen in the Kingston group.

7.3 Design of bridged discodermolide analogs

It has been suggested that discodermolide adopts a U-shaped conformation as the bioactive conformation.[1] Two bridged discodermolide analogs **7.32** and **7.33** were designed to minic the U-shaped conformation as shown in Figure 7.2. The modeling structure of discodermolide and compounds **7.32**, **7.33** are shown in Figure 7.3-7.5.

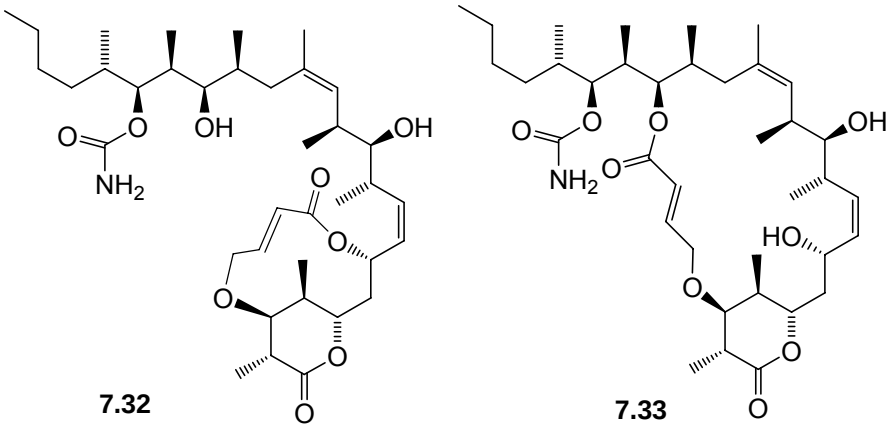

Fig. 7.2 Bridged discodermolide analogs

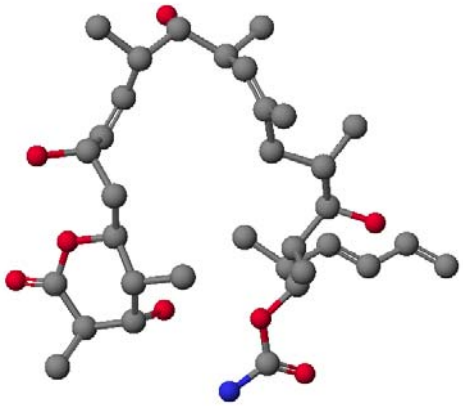

Fig. 7.3 Structure of discodermolide

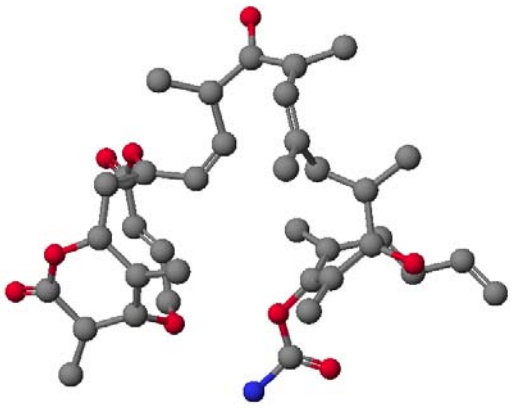

Fig. 7.4 Structure of **7.32**

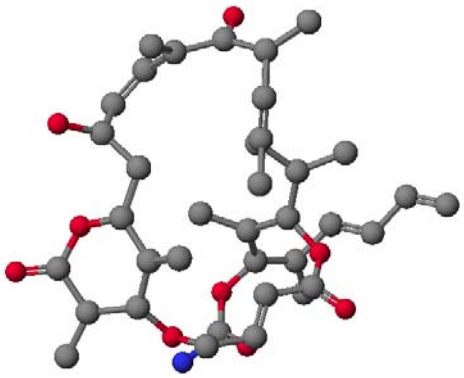

Fig. 7.5 Structure of **7.33**

The retrosynthesis of **7.32** is shown in Scheme 7.10. Synthesis of iodide **7.36** has been reported[7] and synthesis of vinyl iodide **6.4** was described in chapter 6.

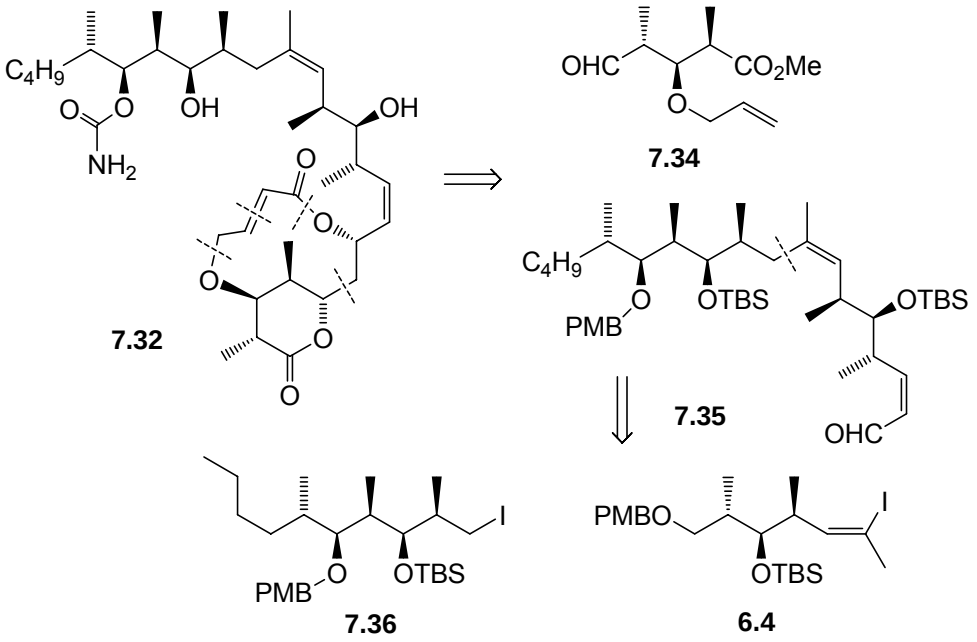

Scheme 7.10 Retrosynthesis of **7.32**

The synthesis of **7.34** started from the known compound **6.35** described in chapter 6. Direct allylation by allyl-2,2,2-trichloroacetimidate proved to be unsuccessful. Compound **7.37**, which served as precursor of **7.34**, was prepared from **7.23** by a sequence of allylation and deprotection (Scheme 7.11).

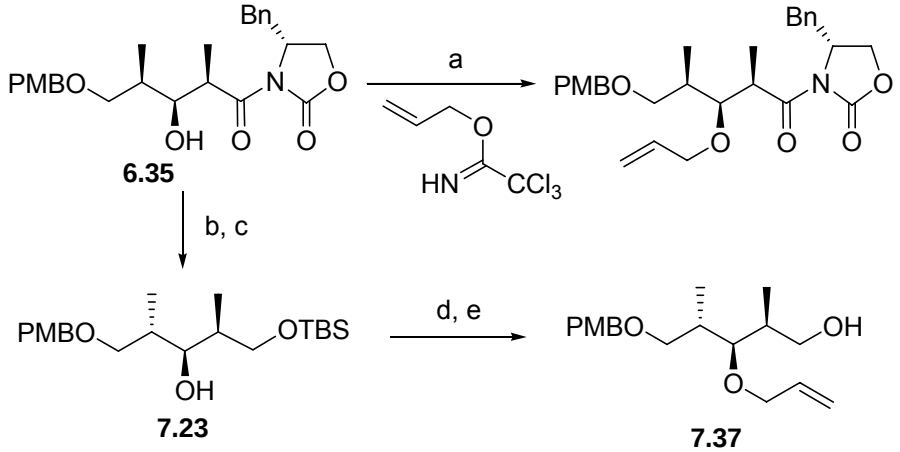

a) triflate acid, 0% b) LiBH4, 91%; c) TBSCl, imidazole, 90%; d) allyl bromide, NaH, 83%; e) 10-CSA

Scheme 7.11 Synthesis of **7.34**

Protection of compound **6.42** as its trityl ether, followed by selective opening of the acetal ring gave **7.38**. Oxidation of **7.38** to the aldehyde **7.39**, followed by a Wittig reaction, gave alkene **7.40**. Reduction of **7.38** to saturated compound **7.41**, followed by deprotection of the trityl group, gave known alcohol **7.42**, which can be converted to iodide **7.36**[7] as needed (Scheme 7.12).

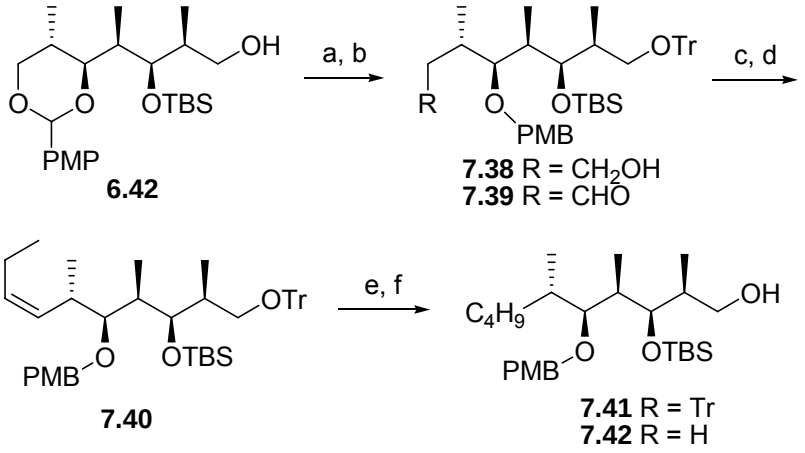

a) TrCl, py, 88% b) DIBAL, 82%; c) SO_3/Py, DMSO, 90%; d) allyl triphenyl phophonium bromide,; e) PtO_2, H_2 f) TFA

Scheme 7.12 Synthesis of **7.39**

The retrosynthesis of **7.33** is shown in Scheme 7.13.

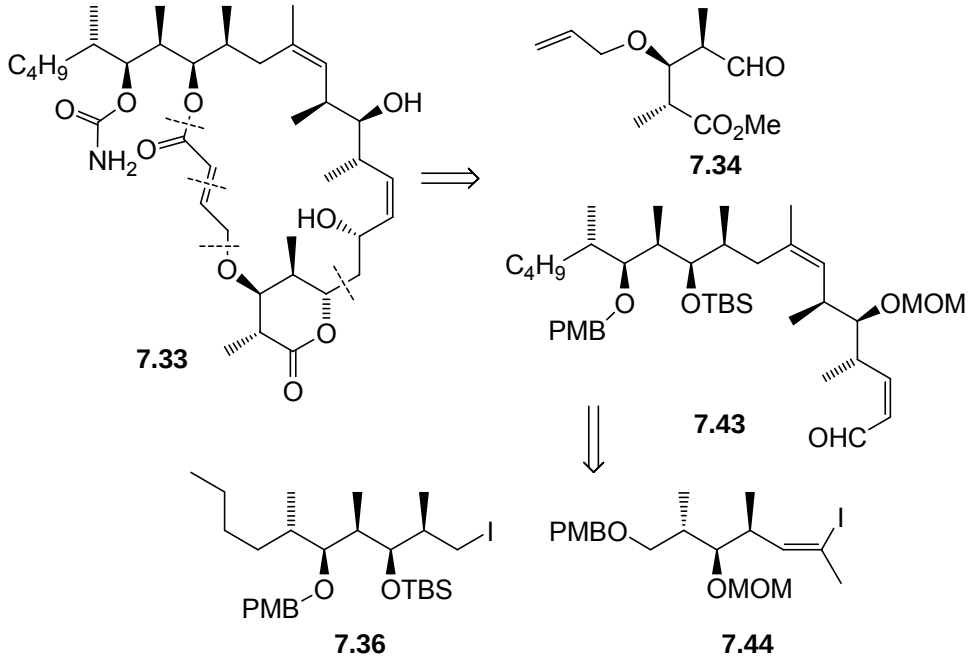

Scheme 7.13 Retrosynthesis of **7.33**

Synthesis of known vinyl iodide**7.44**[8] started from **6.3**, followed by a sequence of MOM protection, reduction and Wittig-Zhao olefination (Scheme 7.14).

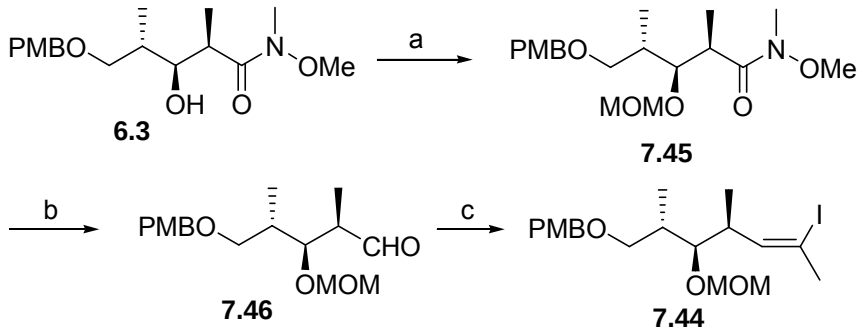

a) MOMCl, 89%; b) DIBAL, 85%, c)$Ph_3P^+Et\ I^-$, I_2, 32%

Scheme 7.14 Synthesis of **7.44**

7.4 Summary of progress on the synthesis of bridged discodermolide derivatives

This investigation has succeeded in preparing the key intermediates **7.19**, **7.21** and **7.22** required for the synthesis of the discodermolide analogs **7.32** and **7.33** for bioactivity evaluation. The completion of the synthesis of **7.32** and **7.33** will be carried out by Dr. Q. H. Chen in the Kingston group.

7.5 Experimental section

General Experimental Methods. All reagents and solvents received from commercial sources were used without further purification. ^1H and ^{13}C NMR spectra were obtained in $CDCl_3$ on Varian Unity or Varian Inova spectrometers at 400 MHz or a JEOL Eclipse spectrometer at 500 MHz. High-resolution FAB mass spectra were obtained on a JEOL HX-110 instrument. Compounds were purified by chromatograph on silica gel column using EtOAc/hexane unless specified. Compounds (**6.42**, **7.15-7.18**, **7.23-7.31**, **7.36**, **7.38-7.42**, **7.44-7.46**)[2,5,7,8] have all been prepared by other investigators.

These compounds were resynthesized as described below. All these compounds had NMR and mass spectra that matched the literature value, so these data are not reported here.

(*R*)-3-[3-*d*$_3$-propionyl]-4-benzyloxazolidin-2-one (7.8). At -78 ^{o}C, 3-*d*$_3$-propionic acid (3 mL, 40 mmol) in THF (30 mL) was treated with Et_3N (6.8 mL, 50 mmol), followed by pivaloyl chloride (5.2 mL). After an 1 h at 0 ^{o}C, the mixture was cooled to -78 ^{o}C and was treated with a solution of *R*-benzyloxazolidinone (7.35 g, 42 mmol), DMAP (0.28g, 2.3 mmol) and Et_3N (6.3 mL, 46 mmol) in THF (30 mL). After additional 2 days at rt, the mixture was concentrated, quenched with 1M NaOH and diluted with EtOAc. The organic layer was separated and the aqueous phase was extracted with EtOAc. The combined organic layer was washed with $NaHCO_3$, water, brine, dried over Na_2SO_4, filtered and concentrated. Silica gel column chromatography provided oil product **7.8** (7.8 g, 82%). ^{1}H NMR δ 7.3-7.4 (2H, m), 7.22-7.26 (1H, m), 7.18-7.20(2H, m), 4.70 (1H, m), 4.08 (2H, m), 3.30 (1H, dd, J = 14.2, 3.2 Hz), 2.94 (2H, Abq, J_{AB} = 17.6 Hz, $\Delta\nu_{AB}$ = 27.6 Hz), 2.77 (1H, dd, J = 14.2, 9.6 Hz). ^{13}C NMR δ 174.1, 153.6, 135.4, 129.4, 129.0, 127.3, 66.2, 55.2, 37.9, 29.0.

(*R*)-3-[(*S*)-3-benzyloxy-2-(*d*$_3$-methyl)propionyl]-4-benzyloxazolidin-2-one (7.7). At 0 ^{o}C, **7.8** (2.35 g, 10 mmol) in DCM (35 mL) was treated with 1M $TiCl_4$ (10 mL), followed *i*-$PrNEt_2$ (1.75 mL, 10 mmol). After 1 h at 0 ^{o}C, the mixture was was treated with 60% benzyl chloromethyl ether (8 mL). After additional 6 hours at 0 ^{o}C, the mixture was quenched by $NaHCO_3$ and diluted with EtOAc. The organic layer was separated and the aqueous phase was extracted with EtOAc. The combined organic layer was washed with $NaHCO_3$, water, brine, dried over Na_2SO_4, filtered and concentrated. Silica gel column

chromatography provided benzyl oxazolidinone oil product **7.7** (3.33 g, 94%).[1]H NMR δ 7.22-7.42 (10H, m), 4.60 (1H, m), 4.16-4.26 (3H, m), 3.86 (1H, dd, *J* = 9.2, 8.0 Hz), 3.63 (1H, dd, *J* = 8.0, 4.2 Hz), 3.27 (1H, dd, *J* = 13.6, 3.2 Hz), 2.76 (1H, dd, *J* = 13.6, 9.2 Hz). ^{13}C NMR δ 175.2, 153.5, 138.2, 133.5, 129.5, 128.9, 128.4, 127.7, 127.3, 127.0, 73.5, 72.3, 65.9, 55.2, 38.4

3-benzyloxy-2*S*-(*d*$_3$-methyl)propionic acid (7.9). At 0 ^{o}C, a solution of benzyl oxazolidinone (1.8 g, 7.5 mmol) in THF/H_2O (1:1) (30 mL) was treated with LiOH (0.4 g, 0.95 mmol), followed 30% H_2O_2 (3.5 mL). After 2 hours at 0 ^{o}C, the mixture was diluted with DCM. The organic layer was separated and the aqueous phase was extracted with DCM. The combined organic layer was washed with $NaHCO_3$, water, brine, dried over Na_2SO_4, filtered and concentrated. The residue oil, acid **7.9** (0.93 g, 93%), was used without purification.

3-benzyloxy-2*S*-(*d*$_3$-methyl)propionyl Weinreb amide (7.10). At rt, a solution of benzyl CD_3-propionic acid (0.356 g, 1.8 mmol) in DCM (5 mL) was treated with diimidazole carbonyl (0.36 g, 2.2 mmol), followed by N,O-dimethylhydroxylamine hydrochloride (0.32 g, 3.3 mmol). After 2 hours at 0 ^{o}C, the mixture was diluted with DCM. The organic layer was separated and the aqueous phase was extracted with DCM. The combined organic layer was washed with $NaHCO_3$, water, brine, dried over Na_2SO_4, filtered and concentrated. Silica gel column chromatography provided benzyl oxazolidinone oil product **7.10** (0.93 g, 93%). ^{1}H NMR δ 7.26-7.36 (5H, m), 4.41 (2H, bs), 3.68 (1H, dd, *J* = 8.2, 4.0 Hz), 3.65-3.70 (1H, m), 3.39 (1H, dd, *J* = 9.2, 6.4 Hz), 3.54 (1H, dd, *J* = 9.2, 6.4 Hz), 3.22-3.28 (1H, br), 3.20 (3H, s). ^{13}C NMR δ 159.3, 137.9, 128.6, 127.9, 127.8, 76.0, 74.8, 61.5, 55.2, 35.7.

Aldol ester (7.14). At 0 ^{o}C, a solution of adol **7.13** (1.9 g, 4.8 mmol) in THF/H_2O (1:1) (20 mL) was treated with LiOH (1.0 g, 24 mmol), followed by 30% H_2O_2 (5 mL). After 2 hours at 0 ^{o}C, the mixture was diluted with DCM. The organic layer was separated and the aqueous phase was extracted with DCM. The combined organic layer was washed with $NaHCO_3$, water, brine, dried over Na_2SO_4, filtered and concentrated to afford acid g. Silica column chromatography provided aldol acid **7.14** (0.97 g, 93%), which was used without purification. At rt, a solution of above acid in hexane (5.5 mL) and MeOH (0.8 mL) was treated with TMS diazomethane (2M) until the solution became yellow and no gas was released. After 10 minutes, the mixture was quenched with acetic acid and concentrated. Silica gel column chromatography purification gave oil methyl ester **7.14** (1g, 93%). ^{1}H NMR δ 7.26-7.36 (5H, m), 4.51 (2H, bs), 3.90 (1H, dd, *J* = 8.2, 4.0 Hz), 3.70 (3H, s), 3.64 (1H, dd, *J* = 9.2, 4.4 Hz), 3.54 (1H, dd, *J* = 9.2, 6.4 Hz), 2.61 (1H, dq, *J* = 4.0, 7.2 Hz) 1.85-1.90 (1H, m). ^{13}C NMR δ 176.3, 137.9, 128.6, 127.9, 127.8, 76.0, 74.8, 73.7, 52.0, 42.6, 35.7, 9.9.

The syntheses of compounds **7.24-7.31** were described in Chapter 6.

Compounds **7.23**, **7.37-7.39, 7.44** and **7.45** were prepared as described in the literature.[7]

Aldehyde (7.46). At -10 °C, a solution of **7.45** (140 mg, 0.38 mmol) in DCM (4 mL) was treated with DIBAL (1.0 M, 0.5 mL). After 3 h, the reaction was quenched with MeOH and Rochelle's salt, diluted with EtOAc, and stirred at rt for 3 h. The layers were separated and the aqueous phase was extracted with EtOAc. The organic layer was washed with $NaHCO_3$, water, brine, dried over $MgSO_4$, filtered, and concentrated to give oil aldehyde **7.46** (110 mg, 91%), which was used without further purification.

References:

1. Smith A. B. III; LaMarche, M. J.; Falcone-Hindley, M. Solution structure of (+)-discodermolide. *Org. Lett.* **2001,** *3*, 695-698.
2. Smith A. B. III; Beauchamp, T. J.; LaMarche, M. J.; Kaufman, M. D.; Qiu, Y.; Arimoto, H.; Jones, D. R.; Kobayashi, K. Evolution of a gram-scale synthesis of (+)-discodermolide. *J. Am. Chem. Soc.* **2000,** *122*, 8654-8664.
3. Koch, G.; Loiseleur, O.; Altmann, K.-H. Total synthesis of 26-fluoro-epothilone B. *Synlett* **2004**, 693-697.
4. Evans, D. A.; Urpi, F.; Somers, T. C.; Clark, J. S.; Bilodeau, M. T. New procedure for the direct generation of titanium enolates. Diastereoselective bond constructions with representative electrophiles. *J. Am. Chem. Soc.* **1990,** *112*, 8215-8216.
5. Paterson, I.; Delgado, O.; Florence, G. J.; Lyothier, I.; O'Brien, M.; Scott, J. P.; Sereinig, N. A second-generation total synthesis of (+)-discodermolide: The development of a practical route using solely substrate-based stereocontrol. *J. Org. Chem.* **2005,** *70*, 150-160.
6. Paterson, I.; Florence, G. J.; Gerlach, K.; Scott, J. P.; Sereinig, N. A practical synthesis of (+)-discodermolide and analogues: Fragment union by complex aldol reactions. *J. Am. Chem. Soc.* **2001,** *123*, 9535-9544.

7. Smith A. B. III; Xian, M. Design, synthesis, and biological evaluation of simplified analogues of (+)-discodermolide. Additional insights on the importance of the diene, the C(7) hydroxyl, and the lactone. *Org. Lett.* **2005,** *7*, 5229-5232.

8. Smith A. B. III; Freeze, B. S.; Brouard, I.; Hirose, T. A practical improvement, enhancing the large-scale synthesis of (+)-discodermolide: A third-generation approach. *Org. Lett.* **2003,** *5*, 4405-4408.

9. Smith A. B. III; Freeze, B. S.; Brouard, I.; Hirose, T. A practical improvement, enhancing the large-scale synthesis of (+)-discodermolide: a third-generation approach. *Org. Lett.* **2003,** *5*, 4405-4408.